ANNUAL REVIEW

INSTITUTE FOR MOLECULAR SCIENCE

1985

ANNUAL REVIEW

INSTITUTE FOR MOLECULAR SCIENCE

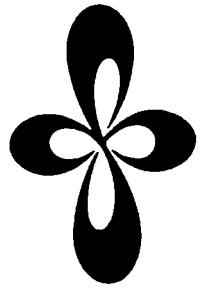

1985

Published by
Okazaki National Research Institutes
Institute for Molecular Science
Myodaiji, Okazaki 444, Japan
Phone 0564-54-1111
Telex 4537-475 KOKKEN J
December 00, 1985

IMS 1985

Ten years have passed since the Institute for Molecular Science (IMS) was established in April 1975. IMS celebrated the tenth anniversary last May, having a congratulatory ceremony, a commemorative lecture meeting, an exhibition, and the 23rd Okazaki Conference on "Ten Years in Molecular Science; Progress and Opportunities" in the presence of many guests including foreign distinguished scientists. It was a good opportunity for the staff of IMS to survey the progress in the past decade, to review the present activities, and also to discuss future progress and possibilities in molecular science. I feel that IMS has created an atmosphere full of an enthusiasm for scientific research and strongly hope that during coming decade its scientific activity will be in bloom on the basis of the high potentiality accumulated during the last ten years.

During the past year, several members of our staff have promoted to new positions outside. Concerning senior ones, Dr. S. Saito, Associate Professor of Molecular Structure Laboratory promoted to Professor of Nagoya University and Dr. T. Ito, Associate Professor of Applied Molecular Science I Laboratory to Professor of Tohoku University. We have had a number of new scientists joined us. Among them a senior member was Dr. M. Sato who moved from the Institute for Solid State Physics, the University of Tokyo to IMS as Associate Professor of Molecular Assemblies Dynamics Laboratory. The smooth flow of scientists is deemed essential for IMS to maintain the high research activity and desirable from the present situation as an interuniversity research institute.

Professor M. Kasha (Florida State University) completed his term of service as a foreign member of our Council at the end of last May. I would like to express my sincere gratitude for his excellent service to IMS. I am happy to announce that Professor K. Morokuma of Thoretical Chemistry Laboratory was elected last August a member of International Academy of Quantum Molecular Science.

February 1986

Saburo Nagakura
Director-General

CONTENTS

RESEARCH ACTIVITIES IV DEPARTMENT OF MOLECULAR ASSEMBLIES

ORGANIZATION AND STAFF
Organization

The Institute for Molecular Science comprises seventeen research laboratories – each staffed by a professor, and associate professor, two research associates and a few technical associates –, two research laboratories with foreign visiting professors, and six research facilities. The laboratories are grouped into five departments and one facility for coordination chemistry:

Department of Theoretical Studies	Theoretical Studies I
	Theoretical Studies II
	Theoretical Studies III[1)]
Department of Molecular Structure	Molecular Structure I
	Molecular Structure II[1)]
	Molecular Dynamics
Department of Electronic Structure	Excited State Chemistry
	Excited State Dynamics
	Electronic Structure[1)]
	Molecular Energy Conversion[2)]
Department of Molecular Assemblies	Solid State Chemistry
	Photochemistry
	Molecular Assemblies Dynamics
	Molecular Assemblies[1)]
	Synchrotron Radiation Research[2)]
Department of Applied Molecular Science	Applied Molecular Science I
	Applied Molecular Science II[1)]
Coordination Chemistry Laboratories	Synthetic Coordination Chemistry
	Complex Catalysis

Research Facilities are:	Computer Center
	Low-Temperature Center
	Instrument Center
	Chemical Materials Center
	Equipment Development Center
	Ultraviolet Synchrotron Orbital Radiation (UVSOR) Facility.

1) Professors and associate professors are adjunct professors from universities.

2) Research Laboratories with foreign visiting professors.

Scientific Staff

Saburo NAGAKURA	**Professor, Director-General**

Department of Theoretical Studies

Theoretical Studies I

Keiji MOROKUMA	Professor
Iwao OHMINE	Associate Professor
Koichi YAMASHITA	Research Associate
Chikatoshi SATOKO	Research Associate
Hideki TANAKA	Research Fellow (April '84–)
Shinichiro NAKAMURA	Visiting Research Fellow from Waseda Univ. (October 84'–March '85), JSPS Fellow (April '85–)
Nobuaki KOGA	Technical Associate
Jun KAWAI	Graduate Student from Univ. of Tokyo* (April '85–)
Susumu MIZUUCHI	Visiting Reserach Fellow from Nippon Soda Co. (April '84–)
Tadahiro OZAWA	Visiting Research Fellow from Kao Corp. (April '85–)

Theoretical Studies II

Hiroki NAKAMURA	Professor
Keiichiro NASU	Associate Professor
Kazuo TAKATSUKA	Research Associate
Hidemitsu HAYASHI	Research Associate
Akihiko OHSAKI	Technical Associate
Jun-ichi TAKIMOTO	Technical Associate (April '85–)
Keiji NAKAJIMA	Graduate Student from Kyushu Univ. (October '85–)

Teoretical Studies III

Kimio OHNO	Adjunct Professor from Hokkaido Univ. (April '83–March '85)
Kichisuke NISHIMOTO	Adjunct Professor from Osaka City Univ (April '85–)
Isao SHIMAMURA	Adjunct Associate Professor from Inst. of Phys. and Chem. Res. (April '84–)
Katsuhisa OHTA	Research Associate
Masaki SASAI	Research Associate (August '85–)
Katsunori SAKURAI	Granduate Student from Osaka City Univ. *(April '85–)

Department of Molecular Structure

Molecular Structure I

Eizi HIROTA	Professor
Shuji SAITO	Associate Professor (–March '85)[1]
Chikashi YAMADA	Research Associate
Yasuki ENDO	Research Associate
Tetsuo SUZUKI	Technical Associate
Hideto KANAMORI	Technical Associate
Tatsuya MINOWA	Research Fellow (April '83–March '85)[2]
Tsutomu SHINZAWA	Graduate Student from Tokyo Inst. Tech. *(April '85–)

Molecular Structure II

Soji TSUCHIYA	Adjunct Proferssor from Univ. of Tokyo (April '83–March '85)

Shuji SAITO	Adjunct Professor from Nagoya Univ. (April '85–)
Hiroo HAMAGUCHI	Adjunct Associate Professor from Univ. of Tokyo (April '84–)
Kentarou KAWAGUCHI	Research Associate

Molecular Dynamics

Teizo KITAGAWA	Professor
Yasuo UDAGAWA	Associate Professor
Keiji KAMOGAWA	Research Associate
Kazuyuki TOHJI	Technical Associate (–October '84) Research Associate (November '84–)
Takashi FUJII	Technical Assistant (January '85– March '85) Technical Associate (April '85–)
Hohi Lee	Technical Assistant (April '85–)
Takashi OGURA	Graduate Student from Osaka Univ.* (April '83–March '85)
Shinji HASHIMOTO	Graduate Student from Osaka Univ.* (April '83–)
Shoji KAMINAKA	Graduate Student from Hiroshima Univ.* (April '84–March '85)
Takashi IDA	Graduate Student from Toyohashi Univ. of Tech.* (April '84–March '85)
Takanori MIZUSHIMA	Graduate Student from Toyohashi Univ. of Tech.* (April '84–)
Mutsumi HARADA	Graduate Student from Toyohashi Univ. of Tech.* (April '85–)
Akira ENDO	Graduate Student from Tokyo Metropolitan Univ* (April '85–)

Department of Electronic Structure

Excited State Chemistry

Keitaro YOSHIHARA	Professor
Tadayoshi SAKATA	Associate Professor
Nobuaki NAKASHIMA	Research Associate
Kazuhito HASHIMOTO	Research Associate
Minoru SUMITANI	Technical Associate
Masahiro HIRAMOTO	Technical Associate (Sept. '84–)
Noriaki IKEDA	IMS Fellow (–March '85)[3]
Hrvoje PETEK	Visiting Scientist (August '85–)
Yoshizumi KAJII	Graduate Student from Tokyo Inst. of Tech.* (April '85–)
Kazushige SATO	Graduate Student from Toyohashi Univ. of Tech.* (April '85–)
Yasuhisa SAITO	Graduate Student from Nagoya Inst. of Tech.* ( )

Excited State Dynamics

Ichiro HANAZAKI	Professor
Nobuyuki NISHI	Associate Professor
Iwao NISHIYAMA	Research Associate
Hisanori SHINOHARA	Research Associate
Masaaki BABA	Technical Associate
Tohru OKUYAMA	Technical Associate (–Dec. '84)[4]
Kazunori YAMAMOTO	Technical Associate (March '85–)
Kanekazu SEKI	Graduate Student from Univ. of Tokyo* (October '83–)

Electronic Structure

Hisaharu HAYASHI	Adjunct Professor from Inst. of Phys. and Chem. Res. (April 84–)

Yoshifumi TANIMOTO	Adjunct Associate Professor from Kanazawa Univ. (April '83–March '85)
Hirochika SAKURAGI	Adjunct Associate Professor from Tsukuba Univ. (April '85–)
Ryoichi NAKAGAKI	Research Associate
Takashi IMAMURA	IMS Fellow (April '85–)
Takashi WATANABE	Technical Assistant (–March '85)[5]
Mitsuo HIRAMATSU	Visiting Research Fellow from Hamamatsu Photonics Co. (April '83–March '85)
Yoshio FUKUDA	Visiting Reserach Fellow from Inst. of Phys. and Chem Res. (April '84–)
Haruo ABE	Visiting Research Fellow from Inst. of Phys. and Chem. Res. (March '85–)

Molecular Energy Conversion

Jon T. HOUGEN	Visiting Professor from NBS, U.S.A. (July '84–December '84)
G.L. CLOSS	Visiting Professor from Univ. of Chicago (January 85–July '85)
H.D. BIST	Visiting Professor from Indian Institute of Technology (Aug. '85–)

Department of Molecular Assemblies

Solid State Chemistry

Hiroo INOKUCHI	Professor
Inosuke KOYANO	Associate Professor
Kenichiro TANAKA	Research Associate (–Sept. '85)[6]
Kazuhiko SEKI	Research Associate
Tatsuhisa KATO	Technical Associate (–Sept. '84)[7]
Shinzo SUZUKI	Technical Associate (April '85–)
Kenichi IMAEDA	Technical Associate (September '84–)
Mototada KOBAYASHI	IMS Fellow (–Match '85)
	Visiting Scientist (April '85–)
Shinya MAYAMA	Graduate Student from Tokyo Inst. of Tech.* (April '85–)
Hiromichi YAMAMOTO	Graduate Student from Nagoya Univ.* (April '83–)
Takae TAKEUCHI	Graduate Student from Nara Women's Univ.* (–March '85)
Naohisa OHYAMA	Visiting Research Fellow from Nippondenso Co,, Ltd. (April '84–March '85)
Munehisa MITSUYA	Visiting Research Fellow from Hitachi Ltd. (April '84–March '85)
Satoshi ASADA	Visiting Research Fellow from TOYOTA Motor Co., Ltd. (April '85–)

Photochemistry

Katsumi KIMURA	Professor
Kosuke SHOBATAKE	Associate Professor
Yohji ACHIBA	Research Associate
Kiyohiko TABAYASHI	Research Associate
Kenji SATO	Technical Associate
Atsunari HIRAYA	Technical Associate (Oct. '84–)
Haruo SHIROMARU	IMS Fellow (April '85–)
Yatsuhisa NAGANO	Graduate Student from Osaka Univ.* (–March '85)
Yoshiyasu MATSUMOTO	Visiting Research Fellow (Sept. 84–Jap. '85)
Marcus J.J. VRAKKING	Graduate Student from Eindhoven Univ. Tech. (Sept. '85–)

Molecular Assemblies Dynamics

Yusei MARUYAMA	Professor
Masatoshi SATO	Associate Professor (February '85–)
Tamotsu INABE	Research Associate
Masashige ONODA	Research Associate (July '85–)
Rumiko HORIGUCHI	Graduate Student from Ochanomizu Univ.* (–March '85)
Hatsumi URAYAMA	Graduate Student from Ochanomizu Univ.* (April '84–)
Yuji MATSUDA	Graduate Student from Tokyo Univ.* (April '85–)
Toshifumi NISHII	Visiting Research Fellow from Mitsubishi Petrochemical Co., Ltd. (June '84–)

Molecular Assemblies

Masahiko KOTANI	Adjunct Professor from Gakushuin Univ. (May '84–)
Nobuaki WASHIDA	Adjunct Associate Professor from National Inst. for Environmental Studies (April '85–)
Naohiko MIKAMI	Adjunct Associate Professor from Tohoku Univ. (–March '85)
Takehiko MORI	Research Associate
Shinichi NAGAOKA	Research Associate (Oct. '85–)

Synchrotron Radiation Research

Willis B. Person	Visiting Professor from Univ. of Florida (Aug. '84–Jan. '85)
Ernst Lippert	Visiting Professor from Technical Univ. of Berlin, West Germany (Jan. '85– July '85)

Department of Applied Molecular Science

Applied Molecular Science I

Hiizu IWAMURA	Professor
Tasuku ITO	Associate Professor (–Sept. '85)[8]
Tadashi SUGAWARA	Research Associate
Koshiro TORIUMI	Research Associate
Masako KATO	Technical Associate (–June '85)[9]
Shigeru MURATA	Technical Associate
Akira IZUOKA	Research Fellow (April '83–)
Yuji UMETSU	Graduate Student from Kumamoto Univ.* (April '84–March '85)
Katsuya ISHIGURO	Graduate Student from Nagoya Univ.* (April '85–)

Applied Molecular Science II

Akio YAMAMOTO	Adjunct Professor from Tokyo Inst. of Tech. (April '83–March '85)
Soichi MISUMI	Adjunct Professor from Osaka Univ. (April '85–)
Renji OKAZAKI	Adjunct Associate Professor from Univ. of Tokyo (April '84–)
Noboru KOGA	Research Associate
Hiroki OSHIO	Research Associate

Coordination Chemistry Laboratories

Kazuo SAITO	Director

Synthetic Coordination Chemistry

Humihiko TAKEI	Professor
Shozo TERO	Associate Professor
Shin TSUNEKAWA	Research Associate

Syoichi HOSOYA	Research Associate
Masahiro EBIHARA	Graduate Student from Tohoku Univ.* (April '84–)
Bateel WANG	Graduate Student from Tohoku Univ.* (April '85–)

Complex Catalysis

Kazuo SAITO	Professor
Akira NAKAMURA	Adjunct Professor from Osaka Univ. (April '84–)
Kazuo KASHIWABARA	Adjunct Associate Professor from Nagoya Univ. (April '84–)
Kiyohiko NAKAJIMA	Graduate Student from Nagoya Univ.* (April '84–)
Satoru UENO	Graduate Student from Osaka Univ.* (April '85–August '85)

Research Facilities

Computer Center

Kenji MOROKUMA	Director
Hiroshi KASHIWAGI	Associate Professor
Unpei NAGASHIMA	Research Associate
Shigeyoshi YAMAMOTO	Technical Associate

Low-Temperature Center

Hiroo INOKUCHI	Director
Toshiaki ENOKI	Research Associate

Instrument Center

Keitaro YOSHIHARA	Director
Iwao YAMAZAKI	Associate Professor
Keisaku KIMURA	Research Associate
Naoto TAMAI	Research Associate

Chemical Materials Center

Hiizu IWAMURA	Director
Hidemasa TAKAYA	Associate Professor
Kazushi MASHIMA	Research Associate
Tetsuo OHTA	Technical Associate

Equipment Development Center

Eizi HIROTA	Director
Tadaoki MITANI	Associate Professor
Yoshihiro TAKAGI	Reserach Associate
Yoshiki WADA	IMS Fellow (April '85–)

Ultraviolet Synchrotron Orbital Radiation Facility

Hiroo INOKUCHI	Director
Makoto WATANABE	Associate Professor
Toshio KASUGA	Associate Professor
Hideo NAKAGAWA	Adjunct Associate Professor from Fukui Univ. (April '84–)
Hiroto YONEHARA	Research Associate
Kazutoshi FUKUI	Research Associate (Sept. '85–)
Kaizo NAKAMURA	Visiting Scientist from Kyoto Univ. (JSPS, April '85–)
Teruo HOSOKAWA	Visiting Research Fellow from NTT (April '85–)

Technical Staff

Akira UCHIDA	Technical Division Head
Keiichi HAYASAKA	Technical Section Chief
Kusuo SAKAI	Technical Section Chief
Satoshi INA	Computer Center (Unit Chief)
Fumio NISHIMOTO	Computer Center
Takaya YAMANAKA	Instrument Center
Shunji BANDOW	Instrument Center
Kiyonori KATO	Low-Temperature Center
Kazuo HAYAKAWA	Equipment Development Center (Unit Subchief)
Hisashi YOSHIDA	Equipment Development Center
Masaaki NAGATA	Equipment Development Center
Toshio HORIGOME	Equipment Development Center (Unit Subchief)
Norio OKADA	Equipment Development Center
Mitsukazu SUZUI	Equipment Development Center
Nobuo MIZUTANI	Equipment Development Center
Shinji KATO	Equipment Development Center
Osamu MATSUDO	UVSOR Facility (Unit Chief)
Toshio KINOSHITA	UVSOR Facility
Masami HASUMOTO	UVSOR Facility
Jun-ichiro YAMAZAKI	UVSOR Facility
Eiken NAKAMURA	UVSOR Facility

* Carries out graduate research at IMS on the Cooperative Education Programs of IMS with graduate schools.
1) Present Address: Dept. of Astrophysics, Faculty of Science, Nagoya Univ. Chikusa, Nagoya 464
2) Present Address: Dept. of Physics, Faculty of Science, Toho Univ., Funabashi, Chiba 274
3) Present Address: Kyoto Univ. of Industrial Arts and Textile Fibers, Sakyo-ku, Kyoto 606
4) Present Address: Toyohashi Univ. of Technology, Tenpaku-cho, Toyohashi 440
5) Present Address: Toray Research Center, Sonoyama, Ohtsu 520
6) Present Address: National Laboratory for High Energy Physics, Oho-Machi, Tsukuba, Ibaraki 305
7) Present Address: Dept. of Chemistry, Faculty of Science, Kyoto Univ., Sakyo-ku Kyoto, 606
8) Present Address: Dept. of Chemistry, Faculty of Science, Tohoku Univ. Sendai, Miyagi 980
9) Present Address: Dept. of Chemistry, Faculty of Science, Kyoto Univ., Sakyo-ku Kyoto, 606

Foreign Visiting Staff

Kyoang Tai No	Soong Jun Univ., Korea	Dec. 8, 1984–Feb. 28, 1985
Yoon Sup Lee	KAIST, Korea	Dec. 14, 1984–Mar. 2, 1985
A. Robert W. McKellar	Herzberg Institute of Astrophysics, Canada	Mar. 22, –May 18, 1985
Pierre Laszio	Univ. of Liege, Belgium	April 3–May 15, 1985 Aug. 26–Oct. 6, 1985
David M. Hanson	State Univ. of New York at Stony Brook, U.S.A.	May 20–Aug. 20, 1985
Kyung-Hoon Jung	KAIST, Korea	June 25–Aug. 31, 1985
Man Chai Chang	Sun Cheon National Univ.,	July 1–Aug. 31, 1985
Bon Su Lee	Inha Univ., Korea	July 1–Aug. 31, 1985
Luigi Mario Venanzi	ETH, Switzerland	July 10–Aug. 15, 1985
Rong Chen	Dalian Institute of Chemical Physics, Chinese Academy of Science, China	Aug. 27–Nov. 26, 1985

COUNCIL
Saburo NAGAKURA Director-General
Councillors

Chairman	Kenichi FUKUI	President, Kyoto Institute of Technology
Vice-Chairman	Hiroaki BABA	Professor, The Research Institute of Applied Electricity, Hokkaido University
	Hideo AKAMATU	Professor Emeritus, The University of Tokyo and IMS
	Masao FUJIMAKI	President, Ochanomizu University
	Ryuichi HIRANO	Professor Emeritus, The University of Tokyo
	Namio HONDA	President, Toyohashi University of Technology
	Soichi IIJIMA	President, Nagoya University
	Shô Itô	Professor, Tohoku University
	Masao KAKUDO	President, Himeji Institute of Technology
	Tetsuji KAMETANI	President, Hoshi University
	Masatoshi MORITA	Chief Executive Officer, Toyota Central Research & Development Laboratories, INC
	Minoru ODA	Director-General, The Institute of Space and Astoronautical Science
	Yoshihiko SAITO	Professor, Keio University
	Susumu SUZUKI	Director, The Research Institute for Iron, Steel and other Metals, Tohoku University
	Ikuzo TANAKA	Professor, Tokyo Institute of Technology
	Yutaka TOYOZAWA	Director, The Institute for Solid State Physics, The University of Tokyo
	Yasutada UEMURA	Professor, Science University of Tokyo
	Per-Olov LOWDIN	Professor, University of Florida and Professor Emeritus, Uppsala University
	George Claude PIMENTEL	Professor, University of California, Barkley

The Council is the advisory board for the Director-General. Two of the councillors are selected among distinguished foreign scientists.

Professor Emeritus

Professor Hideo AKAMATU, *ex*-Director-General of IMS, was named the first professor Emeritus of this Institute in September, 1982.

Distinguished Research Consultants

Kenichi FUKUI	President, Kyoto Institute of Technology; Professor Emeritus, Kyoto University

Masao KOTANI	Professor Emeritus, The University of Tokyo
Yonezo MORINO	Professor Emeritus, The University of Tokyo; Director and Supreme Consultant, Sagami Chemical Research Center

Administration Bureau

Katsuhiko KURIOKA	Director-General, Administration Bureau
Minoru OKAMOTO	Director, General Affairs Department
Seigo MIUTA	Director, Finance and Facilities Department
Hideo ISHIKAWA	Head, General Affairs Division
Shigeyoshi ONO	Head, Personnel Division
Takeru YAMAKAWA	Head, Research Cooperation and International Affairs Division
Kaichi ONUMA	Head, Budget Division
Yasutaro NAGATA	Head, Accounts Division
Hirohiko URA	Head, Construction Division
Shoichi SATO	Head, Equipment Division

BUILDINGS AND CAMPUS

The IMS campus covering 62,561 m^2 is located on a low hill in the middle of Okazaki City. The inequality in the surface of the hill and growing trees are preserved as much as possible, and low-storied buildings are adopted for conservation of the environment. The buildings of IMS are separated according to their functions as shown in the map. The Research Office Building and all Research Facilities except for the Computer Center are linked organically to the Main Laboratory Building by corridors. Computer Center, Library, and Administration Buildings are situated between IMS and the neighboring National Institute for Basic Biology and National Institute for Physiological Sciences, because the latter two facilities are common to these three institutes.

The lodging facility of IMS called Yamate Lodge, located within 10 min walk, has sleeping accommodations for 20 guests. Since June 1, 1981 a new lodging facility called Mishima Lodge has been opened. Mishima Lodge, located within four minutes' walk east of IMS can accommodate 30 guests and ten families. Scientists who visit IMS as well as the two other institutes can make use of these facilities. Foreign visiting scientists can also live at these lodgings with their families during their stay.

The Institute for molecular Science

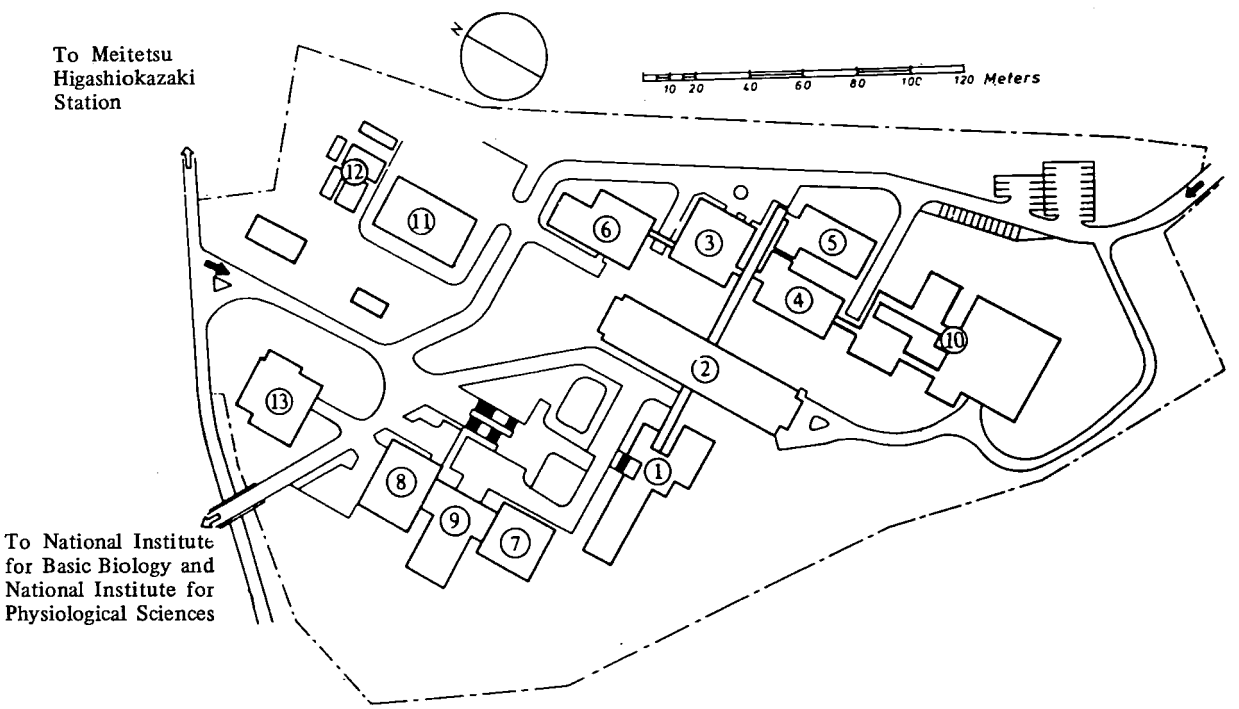

1. Research Office Building
2. Main Laboratory Building
3. Equipment Development Center
4. Instrument Center
5. Chemical Materials Center
6. Low-Temperature Center
7. Computer Center
8. Library
9. Central Administration
10. UVSOR Facility
11. Power Station
12. Waste-Water Disposition Facilities
13. Faculty Club

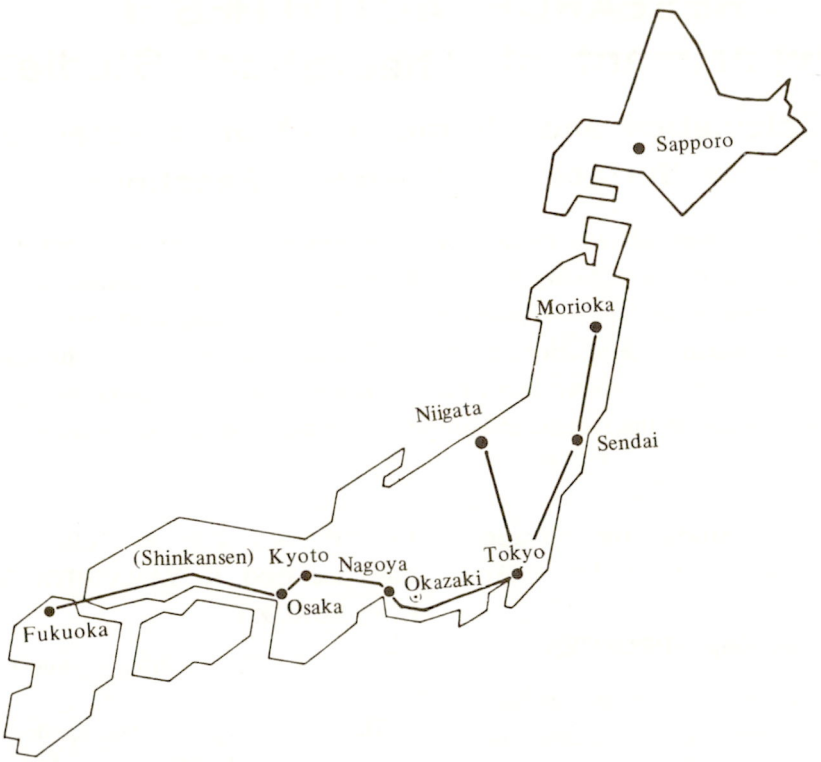

Okazaki (population 280,000) is 260 km southwest of Tokyo, and can be reached by train in about 3 hours from Tokyo via New Tokaido Line (Shinkansen) and Meitetsu Line.
The nearest large city Nagoya, about 40 km west of Okazaki.

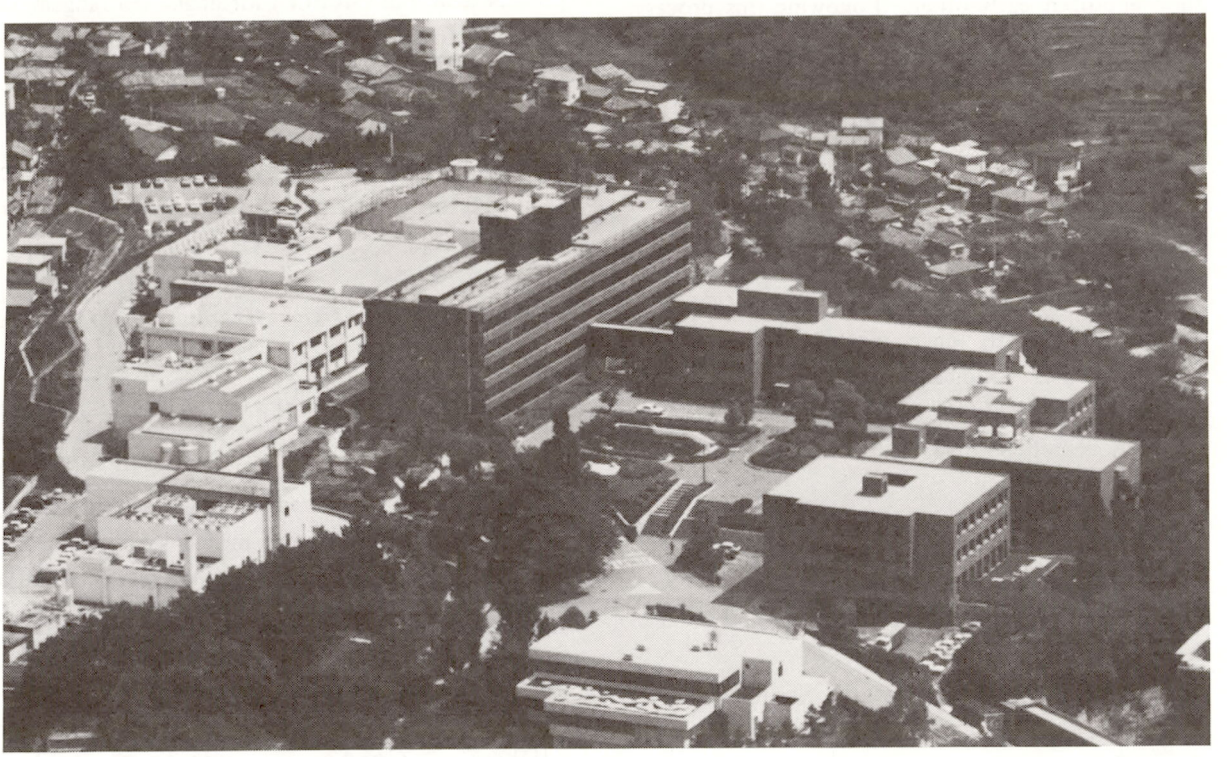

IMS, 1985

RESEARCH ACTIVITIES I
Department of Theoretical Studies

I—A Calculation and Characterization of Potential Energy Surfaces of Chemical Reactions

Dr. Shigeki Kato, Research Associate who has published many excellent papers on potential energy surfaces of chemical reactions, left our group in April, 1984. In his place, Dr. Koichi Yamashita jointed our group in October, 1984. With his new leadership, in addition to Dr. Ohta's continuing contribution, we have carried out theoretical studies on excited state reactions, reactions of ionic species, reactions in hydrated clusters and electron transfer reactions. Since last year we have had three Korean and three Chinese visiting scientists in our group. Some of their work appear in this section, and others will appear in the succeeding sections.

1-A-1 A Theoretical Study on Charge Transfer Reaction: $Ar^+ + CO \rightarrow CO^+ + Ar$

Koichi YAMASHITA and Keiji MOROKUMA

We have performed potential energy surface calculations for the charge transfer reaction of $Ar^+ + CO\ (^1\Sigma^+) \rightarrow Ar + CO^+\ (^2\Sigma^+)$ using the multi-reference configuration interaction method. The result suggests two distinct mechanisms, both involving potential surface crossing at a small Ar^+... CO distance. In both cases, a π-electron of the CO molecule is transferred to Ar^+ in an early stage, as they approach each other. Following this process, one of the resulting $Ar + CO^+\ (^2\Pi)$ surface ($2^2A'$) forms an avoided crossing with the product $Ar + CO^+\ (^2\Sigma^+)$ surface ($1^2A'$), and the transition between them is promoted by a radial coupling. The other $Ar + CO^+\ (^2\Pi)$ surface ($1^2A''$) crosses with the product $1^2A'$ surface and the ratational coupling induces a transition between them. These two transitions occur at a region where the CO bond length is significantly longer than that of the equilibrium $CO^+\ (^2\Sigma^+)$ molecule, and this explains qualitatively the vibrational excitation of the product CO^+ ion recently observed by Leone et al.[1)]

Reference

1) C.E. Hamilton, V.M. Bierbaum, S.R. Leone, *J. Chem. Phys.* 82, 5527 (1985).

1-A-2 Theoretical Study of Structure and Energy of $[HCOO]^+$ and $[COOH]^+$ and Their Rearrangement

J.G. YU*, X.Y. FU*, R.Z. LIU* (*Beijing Normal Univ. and IMS), K. YAMASHITA, N. KOGA, and K. MOROKUMA

[*Chem. Phys. Lett.*, in press]

The structures of the two isomers of protonated carbon dioxide, $[HCOO]^+$ and $[COOH]^+$, and the transition state on their rearrangement path are determined by the MCSCF gradient method with the 6-31G* bsis set. The results clearly show that $[HCOO]^+$ has a σ-σ biradical character and is a stable intermediate, with an calculated energy barrier of 12.4 kcal/mol (MCSCF) for singlet rearrangement. It is also found that the rearrangement is not likely to occur on the triplet path.

1-A-3 Potential Energy Surface and Reaction Mechanism of the Ion-Molecule Reaction: $CH_4 + CH_4^+ \rightarrow CH_3 + CH_5^+$

Kenshu KAMIYA (*Univ. of Tokyo and IMS*) and Keiji MOROKUMA

[*Chem. Phy. Lett.*, in press]

The potential energy surface for the reaction system has been calculated with the ab initio method to elucidate three different mechanisms of forming CH_5^+. A stable complex, responsible to the complex mechanism, has been found but is hard to reach during the reaction mainly due to the mass effect, making the complex mechanism of minor importance. The proton transfer mechanism has been found to consist of two steps: the hydrogen atom transfer and the exit-channel electron fransfer,

whereas the hydrogen atom transfer mechanism consists of the entrance-channel electron transfer and the hydrogen atom transfer, followed by exit-channel electron transfer.

1-A-4 Potential Energy Surface of S_N2 Reaction in Hydrated Gas Cluster

Kyoung Tai NO (*Soong Jun Univ., Korea, and IMS*), **Keiji MOROKUMA and Katsuhisa OHTA**

Dynamical study of the chemical reaction in hydrated gas clusters is one of our goals of the present project. Here we have been preparing for the dynamic study the potential energy surface of the S_N2 reaction $CH_3Cl + F^-$ with hydration. Ab initio calculations were performed in the neighborhood of the pseudo intrinsic reaction coordinate (IRC) which connects the reactant, the reactant complex, the transition state, the product complex, and the product. The calculated potential surface was fitted to an analytical form both for motion along IRC and for other degrees of freedom perpendicular to IRC. The interaction potential between the $(CH_3Cl + F^-)$ system and a water molecule has also been calculated and is being represented in a reasonable functional form.

1-A-5 Electron Transfer in Hydrated Gas Cluster $(H_2O)_nO_2^- + O_2 \rightarrow O_2 + O_2^-(H_2O)_n$

Katsuhisa OHTA and Keiji MOROKUMA

D.W. Fahey et al.[1] have investigated the electron transfer in hydrated anion of the oxygen molecule by the flowing afterglow technique. The observed rate of electron transfer from an oxygen molecule anion to a neutral oxygen molecule decreases as the hydration number increases. Here we studied this reaction with the ab initio method using UHF broken space-symmetry solutions as initial and final states of electron transfer. Preliminary results are as follows. (1) In the case without water molecule, O_4^- makes a stable complex where an excess electron is delocalized, and the electron transfer takes place via this complex. (2) Solvation causes the adiabatic energy barrier for the electron transfer reaction in $O_2^-(H_2O)$ .... O_2. (3) Electron transfer is faster through the A′ state than through the A″ state. (4) Electron transfer is faster through the quartet spin state than through the doublet state.

Reference

1) D.W. Fahey, H. Bohringer, F.C. Fehsenfeld, and E.E. Ferguson, *J. Chem. Phys.*, 76, 1977 (1982).

1-A-6 Stereo-Electronic Effects in Intramolecular Long-Distance Electron Transfer in Radical Anions as Predicted by Ab Initio MO Calculation

Katsuhisa OHTA, Gerhart L. CLOSS (*Univ. of Chicago, U.S.A., and IMS*), **and Keiji MOROKUMA**

[*J. Am. Chem. Soc.*, in press]

Ab initio calculations were carried out at the STO-3G and 4-31G level on trans and cis 1,4-dimethylenecyclohexane radical anion to evaluate the trans annular interaction matrix element as function of cyclohexane conformation and torsional angles of methylene groups. It was found that the magnitude of this interaction is highly dependent on geometry, conformation and methylene rotational angle. These calculations serve as models for experimental studies involving long distance electron transfer in related systems.

I—B Theoretical Studies of Molecular Structure and Molecular Interaction

As you see, this section contains very wide varieties of problems we have studied this year on molecular structure and molecular interactions. Most of the problems have been brought to our attention by experimentalist collaborators, who are working in the field ranging from higher energy physics to organic synthesis. We have enjoyed such an active collaboration.

1-B-1 Ab initio Calculations of Doublet States of NH^+

Isao KUSUNOKI (*Tohoku Univ.*), **Koichi YAMASHITA, and Keiji MOROKUMA**

[*Chem. Phys. Lett.*, in press]

The eight low-lying doublet states of the NH^+ ion are investigated by the MRSD-CI method with a DZP basis set, using full valence configurations as the reference configurations. The spectroscopic constants for the $X^2\Pi$, $A^2\Sigma^-$, $B^2\Delta$, and $C^2\Sigma^+$ states and the transition moments for $X^2\Pi$-$A^2\Sigma^-$ and $X^2\Pi$-$B^2\Delta$ are calculated. The results are compared with the recent experiment by Kusunoki and Ottinger.[1)]

Reference

1) I. Kusunoki and C. Ottinger, *J. Chem. Phys.* **80**, 1872 (1984).

1-B-2 Structure and Stability of Isomers of New Compounds RNS_2

Masaki TAKAHASHI (*Univ. of Tokyo*), **Shinichiro NAKAMURA, Keiji MOROKUMA and Renji OKAZAKI** (*Univ. of Tokyo and IMS*)

Ab initio calculations have been carried out on the new compound RNS_2, where R = H is used as a model. In order to compare the sructure and stability of various isomers, the full geometrical optimization has been performed at the HF level and the relative energy has been obtained at the MP3 level. Harmonic vibrational analysis has been carried out on some isomers. For comparison, corresponding calculations have been also performed for well-known compound HNO_2. In HNS_2, cis- and trans-HNSS and $HN<^{S}_{S}$ have a comparable stability with cis- and trans-HSNS only about 10 kcal/mol higher, while in HNO_2, as observed experimentally, only cis- and trans-HONO are stable, followed by $HN<^{O}_{O}$. The hypervalency of the sulfur atom has been attributed as the origin of this variety and difference. The relative stability has been discussed based on localized orbital and energy analysis.

1-B-3 Determination of the Lowest Energy Point on the Crossing Seam between Two Potential Surfaces Using Energy Gradient

Nobuaki KOGA and Keiji MOROKUMA

[*Chem. Phy. Lett.*, **119**, 371 (1985)]

A method is presented to search the energy minimum crossing point between two potential surfaces with the aid of the energy gradient and the optimization method with a constraint. The method has been applied for two low-lying triplet excited states of chlorobenzene with the ab initio UHF wavefunction.

1-B-4 Theoretical Studies of the Electronic Factor for Asymmetric Induction

Nobuaki KOGA, Susumu MIZUUCHI (*IMS and Nippon Soda Co.*), **Keiji MOROKUMA and Minoru ISOBE** (*Nagoya Univ.*)

The electronic factors of stereoselectivity in asymmetric induction were studied by the ab initio RHF method with the 3-21G basis set. Nucleophilic and electrophilic additions to olefin and carbonyl having a chiral center were chosen as model reactions. Nucleophiles and electrophiles used are H^- and H_2O and H^+ and BH_3, respectively, and model olefin and carbonyl are X = CHY–CHZ^1Z^2 (X = CH_2, O; Y = H, CH_3; (Z^1, Z^2) = (CH_3, OH), (SiH_3, CH_3), (SiH_3, OH). The difference of activation energies between the path leading to *R*-product and that to *S*-product is divided into two components. One of them originates from the difference of conformations (ΔE_{conf}) of model olefin and carbonyl, and the other is interaction energy difference (ΔE_{int}) between the substrate and the reagent. ΔE_{int} is further analyzed by using the energy decomposition method. In the reaction of olefin with an ionic reagent, the electrostatic factor often controls the stereoselectivity. When the substrate is olefin and the attacking reagent is neutral, the exchange repulsion is often dominant factor, with the orbital mixing terms (charge tranfer, polarization and coupling terms) making a minor but parallel contribution.

1-B-5 An Ab Initio Calculation of the Infrared Spectrum and Tautomerism of Guanine

Z. LATAJKA, W.B. PERSON, and K. MOROKUMA

[*J. Mol. Str.*, in press]

An ab initio molecular orbital calculation has been made for guanine to predict its equilibrium geometry, harmonic force constants, atomic polar tensor elements and vibrational frequencies and intensities. The predicted infrared spectrum, with the 3-21G basis set and further scaled, agrees well with the recent experimental study of guanine in an argon matrix for the in-plane modes. Further calculations indicate that complication of experimental spectrum is probably due to existence of tautomers other than the 9-H tautomer for which the spectrum was calculated.

1-B-6 Higher Order Molecular Effects on the Neutrino Mass Determination by Triton β Decay

Jiro ARAFUNE (*Univ. of Tokyo*), Nobuaki KOGA, Keiji MOROKUMA, and Tadashi WATANABE (*Kobe Univ.*)

The correction due to the Coulomb interaction of the ejected β ray with the residual charged particles is derived in a most general form for the β decay of tritium-containing molecules. The effect on final states is of $a/\beta O$ (10^{-4}) with β_e, the β-electron velocity, and the transition probabilities are modified by at most 0.2% from the usual sudden approximation. Further, the transition distributions of two alkanes are calculated for every excitation energy by ab initio SCF-MO methods; The basis set dependence of the distribution is examined for CH_3T using four types of basis sets of the double zeta quality with and without diffuse and polarization functions. For CH_3-CHT-CH_3, the transition probability to two-particle excited states amounts to 4.8%, the inclusion of which improves the unitarity of the probability to a large extent.

I—C Structure and Reaction of Transition Metal Complexes

Dr. Shinichiro Nakamura, new Postdoctoral Fellow, has joined us this year in our efforts in determining the structure and energy of intermediates and transition states of elementary reactions of organometallic compounds. Last few years we have studied several elementary reactions essential in homogeneous catalytic processes. With the arrival of a new supercomputer system in January, 1986, we hope to extend our studies toward the goal of theoretical design of effective catalysts.

1-C-1 Ab Initio MO Study of Carbonyl Insertion Reactions of Pd and Pt complexes.

Nobuaki KOGA and Keiji MOROKUMA

[*J. Am. Chem. Soc.*, **107**, 7230 (1985)]

The carbonyl insertion reactions M (CH_3) (H) (CO) (PH_3) → M ($COCH_3$) (H) (PH_3) (M = Pd, Pt) are investigated by the restricted Hartree-Fock (RHF) method and the frozen core second order Møller-Plesset perturbation method with the relativistic effective potential. The structures of the transition states as well as the reactants and the products is fully optimized at the RHF level. The three-center transition state obtained is unequivocally that of methyl migration. Carbonyl cannot migrate due to the repulsion between its lone pair electrons and metal d electrons. The reaction of the Pt complex is more exothermic and needs higher activation energy than that of the Pd complex. These differences can be explained by the differences of M-CO and M-CH_3 bond strengths between the Pd and the Pt complex. The effects of substituents on the migrating methyl group have also been dicussed.

I-C-2 A Theoretical Study on Insertion Reaction Rh (Cl) $(H)_2$ (C_2H_4) $(PH_3)_2$ → Rh (C_2H_5) (Cl) (H) $(PH_3)_2$ in the Ethylene Hydrogenation by Wilkinson Catalyst.

Jin HAN*, Xiao-Yuan FU* (*Beijing Normal Univ. and IMS), Nobuaki KOGA and Keiji MOROKUMA

One of the essential elementary processes in the Wilkinson catalysis is the insertion of ethylene into the cis hydride-Rh bond to form an ethyl complex, which will be followed by the reductive elimination in which the ethyl group couples with the second hydride. In the present study, the structure of intermediates and transition states in the insertion reaction has been optimized with the RHF method under the relativistic effective core potential approximation. The first transition state (TS1) obtained represents the hydride migration to ethylene with an RHF activation energy of 18 kcal/mol. The product of this step, Rh (C_2H_5) (Cl) (H) $(PH_3)_2$, with C_2H_5 and H trans to each other, isomerizes with a low barrier (3 kcal/mol at RHF) to the cis product through hydride migration. Electron correlation (MP2) makes the trans intermediate less stable than TSl, suggesting that two hydride migrations may take place in a single step.

I-C-3 Theoretical Prediction of Carbene Intermediate in Thermolysis of Transition-Metal Ketene Complex

Shinichiro NAKAMURA and Keiji MOROKUMA

The first theoretical prediction is presented as to the existence of carbene intermediate in thermolysis reaction of transition-metal ketene complex Pt $(PPh_3)_2$ $(CH_2 = C = O)$ → [Pt $(PPh_3)_2$ (CH_2) (CO)] → CH_2CH_2 + C_3H_6 + others. Structures of the ketene complex, the transition state and the carbene intermediate have been searched with full optimization at the RHF level. A square carbene complex with its CH_2 unit *in* the molecular plane has been found to be an intermediate. The transition state is *late* with the C – C bond completely broken and the CH_2 group half twisted. The roles of metal in this C –C cleavage are (i) the activation of the C = C bond through coordination and (ii) the stabilization of the resultant carbene through conjugation with vacant metal p orbital.

I—D Development and Application of the Local-density functional Methods

The local-density-functional (LDF) methods are quite convenient for the study of such systems as solids, surfaces, and large clusters. On the base of the electronic structures by the LDF methods we study the stable geometry and dynamical processes of surfaces, and the final state interaction effect on high energy spectra.

I-D-1 Strong electric field effects on surface atoms

Chikatoshi SATOKO

Desorption processes of surface atoms are observed in the field ion microscope in which the strong electric field is applied around the surface. The threshold of the desorption (evaporation field) depends on the surface electronic structure, the pressure of the image gas and the temperature. It is suggested by experiments that the bond positions broken by the strong field depend on the bonding properties between the surface atoms. A great many of theories were treated by the continuum models which could not discriminate the local chemical properties between the surface atoms. We calculate the force acting on the atoms in the electric field by the LCAO-Xα-force method and estimate the processes of the field desorption.

Here we discuss the results of the physisorption of a rare-gas atom and the chemisorption of a CO molecule on Ni surfaces. The rare-gas atom is physisorbed very weakly in no electric field. In the high electric field such as 1.0 V/A, however, the rare-gas atom is more strongly adsorbed like a chemisorbed bond because of the high polarization. On the other hand the CO molecule is chemisorbed on the

surface in no electric field. The high electric field induces high charge transfers between the surface atoms. These quantities depend on the orbital properties. The σ orbital of the CO molecule bonded with the Ni surface is depressed into the O atom direction. Therefore the bond of the CO molecule with the surface become weaker in the strong electric field.

I-D-2 Electronic Structure of the Pyramidal Cluster Model of the Si (111) 7 × 7 Surface

M. TSUKADA (*Univ. of Tokyo*) **and C. SATOKO**

[*Surface Science,* in press]

There have been proposed various microscopic structures of the Si (111) 7 × 7 surface from many experiments. Recently the Pyramidal cluster model of the Si 7 × 7 surface was proposed from the experiments of the impact collision ion scattering spectroscopy and the diffracted XPS by M. Aono et al and K. Higashiyama et al, independently. The experiments of the UPS and ELS show the existence of four occupied surface states and a empty surface state above the Fermi energy.

The purpose of the present paper is to elucidate special features of the electronic states of the pyramdal cluster model. The cluster model used is Si_7H_9 which has the main structure of the Si 7 × 7. Electronic structures and forces acting on the atoms are calculated for some distorted clusters in the neutral and ionic states by the LCAO-Xα force methods. The calculated results show that various peaks of the UPS and ELS can be explained by the transitons between the energy levels of the dangling bonds in the anionic pyramidal cluster. The position of the apex Si in the cluster moves outwardly from the pyramidal basal plane for the anionic charge state. The stability of the pyramidal cluster can be understood by the occupation of the electrons in the surface dangling bonds.

I-D-3 Applications of force analysis to interactions between oxygen atoms on the Al (111) and Mg (0001) surfaces.

Chikatoshi SATOKO

To understand chemisorption processes of the oxygen molecules on the Al and Mg surfaces, we calculate the force acting on the oxygen and metal atoms as a function of the oxygen positions. It sheds light on the difference, whether the dissociated oxygen atoms on the Al and Mg surfaces are absorbed or not and whether they are assembled in island or not.

The calculated results show that the interaction between the oxygen atoms at the nearest neighbor positions is repulsive for the Al surface. While on the Mg surface the oxygen atoms penetrate into the surface from the nearest neighbor sites. Whether the interaction between the nearest neighbor adatoms is repulsive or attractive is due to the following reasons. When the first adatom makes the surface metal-metal bonds weak, the second adatom is not chemisorbed at the nearest neighbor site of the first adatom because of the bond saturation of the metal atoms. In the case of the chemisorption of the oxygen atom on the Al (111) surface the interaction between the Al atoms is weakened because of the bonding between the oxygen and Al atoms. On the other hand the interaction between the Mg atoms is not so repulsive as to break the bond with the chemisorption of the oxygen atom. The interaction of the former case is repulsive, while the latter is not repulsive.

I-D-4 Theoretical Studies of Satellite Structure in X-Ray Emission Spectra as an Application of Xα Method

Jun KAWAI (*Univ. of Tokyo and IMS*), **Chikatoshi SATOKO, and Yohichi GOHSHI** (*Univ. of Tokyo*)

X-ray emission spectra have characteristics to reflect the electronic structure or chemical state of matter. Recently, sateilite structures in X-ray emission spectra have attracted considerable interest. This is because the electron correlation effects are not small. The use of transition state theorem within the framework of the Xα method is of advantage in calculating energy differences between initial and final states, particularly x-ray transitions. We applied the Xα method to the study of the mechanism of a chemical effect on x-ray emmision spectra. Shake-off probabilities are calculated for several

compounds as a function of the covalency parameter γ in the sudden approximation. It is concluded that some of unusual properties of shake-off satellites are due to the large relaxation of valence orbitals in the presence of an inner-shell hole. The relaxation is large when the valence orbital is localized around the position of the core hole.

I—E Photochemical Reaction in Gas and Liquid Phases

To understand the chemical reactions in gas and liquid phases, we need to know not only the electronic and dynamic properties of reacting molecules, but also the nature of reactant and solvent molecular interactions such as solvation mechanism. We have made the following three studies for this purpose; (i) Nonadiabatic coupling between the excited and ground states of polyenes, (ii) the energy dissipation mechanism of the excited molecules in liquid phases and (iii) the structure of the solvent and solute interactions (hydration structure).

I-E-1 Mechanisms of nonadiabatic transitions in photoisomerization processes of conjugated molecules: Role of hydrogen migrations

Iwao OHMINE

[*J. Chem. Phys.*, 83, 2348 (1985)]

Mechanism of nonadiabatic transition in the C = C torsional photoisomerization process of ethylene and polyenes is investigated by using the ab initio configuration interaction calculation method. We have calculated the low-lying singlet state potential energy surfaces and their nonadiabatic couplings. A multi-dimensional search for the molecular configurations yielding strong nonadiabatic couplins is performed to find the origin of very fast photoisomerization kinetics, which are experimentally observed to be typically in the order of a few or a few tens of picoseconds. It is found that the "pseudo" migration motion of a hydrogen adjacent to the twisted C = C bond causes a potential surface crossing of the low-lying excited and ground states and thus induces a sufficiently large nonadiabatic coupling to explain this experimental evidence. The hydrogen migration motion is facilitated by the so-called zwitterionic character of the low-lying excited states near the 90° C = C twisted conformation, proceeds almost without an energy barrier and involves large molecular conformational changes. The role of the "2^1Ag^-" state in the photoisomerization is also discussed.

I-E-2 Energy Dissipation of Excited Molecules in Liquid Phase

Iwao OHMINE

We are continuing to investigate on the energy dissipation mechanism of highly excited molecules in liquid phases. A ethylene in Ar or in water is choosen as a model system. The intra-ethylene molecular force is simulated by the MINDO/3 method and the Lennard-Jones potential is used for the solvent-solute and solvent-solvent interactions. A very large difference in energy dissipation mechanism is observed between Ar and water as solvents. The power spectrum of Force-Force correlation function and others shows that water makes a response to the ethylene vibrational motion even in very high frequency and large amplitude, whereas Ar does not. A simple model of an oscillator in the Ar solvent is used to find the dependence of decay rate on the excess vibrational energy and solvent-solvent interaction strength. The effects of so called sudden polarization in the polyene photoisomerization on the energy dissipation mechanism is also studied.

I-E-3 On the Hydrophobic Effect: Integral Equation Approach

Hideki TANAKA

The hydrophobic effects are investigated by integral equation in which the molecular anisotropy

and strong and long-ranged interaction can be taken into account. The microscopic structure and thermodynamic quantities are obtained by solving so-called RISM equation with HNC-like closure. The integral equation shows that the solvent separated association is dominant in water-like solvent even when attractive interaction is removed. This indicates that the hydration structure is determined principally by the geometrical factor of water molecule as in the case of simple liquid. The Coulomb part of hydrogen bond has small effects on it and only makes solute-solute pair correlation slightly higher. Thermodynamic quantities are, however, found to depend sensitively on the attractive force of Coulomb interaction.

I—F Studies of Chemical Reaction Dynamics

Our research activity in this area is pursued in two directions. One is a development and application of a new semiclassical theory in phase space. The other is the hyperspherical coordinate approach to atom transfer reactions.

I-F-1 Semiclassical Theory in Phase Space for Molecular Processes: Scattering Matrix as a Special Case of Phase Space Distribution Function

Kazuo TAKATSUKA and Hiroki NAKAMURA

[*J. Chem. Phys.* 83. 3491 (1985)]

The dynamical characteristic function (DCF) introduced previously[1] as a kind of phase space distribution function is generalized so as to give an overlap integral of two wave packets which are to be propagated on different potential energy hypersurfaces. The development of our new semiclassical theory is motivated by the fact that the scattering (S-) matrix is just one of this kind of overlap integrals. In this theory the semiclassical DCF is evolved in time by running a pair of classical trajectories, which are determined by two different Hamiltonians, total scattering Hamiltonian of the system and unperturbed final channel Hamiltonian. The DCF becomes an overlap integral of two wave packets, if these two trajectories coincide with each other in the exit region at $t = \infty$. The validity of this semiclassical theory is shown to be ensured, if the oscillatory wave packets are employed to construct the DCF. The S-matrix in the stationary state scattering theory is given as a superposition of the wave packet DCF's.

Reference

1) K. Takatsuka and H. Nakamura, *J. Chem. Phys.* 82, 2573 (1985).

I-F-2 Dynamics of Collinear Asymmetric Light Atom Transfer Reactions

Hiroki NAKAMURA and Akihiko OHSAKI

[*J. Chem. Phys.* 83, 1599 (1985)]

The Rosen-Zener formula in its sophisticated form is shown to be applicable to asymmetric collinear light atom transfer reactions with near degeneracy of asymptotic vibrational levels. The formula is applied to simple model systems and is demonstrated to work well over a wide range of energy for both systems with and without reaction barrier. It is also discussed that effects of surface topology and masses on reaction dynamics are effectively investigated by hyperspherical coordinates.

I—G Dynamic Processes of Electronically Highly Excited States of Simple Molecules

I-G-1 Dissociative Recombination of H_2^+ by Collisions with Slow Electrons

Hidekazu TAKAGI (*Kitasato Univ.*) **and Hiroki NAKAMURA**

[*J. Chem. Phys.*, in press]

The title process via the $^1\Sigma_g\ (2p\sigma_u)^2$ resonance state is investigated by the multichannel quantum defect theory (MQDT). Our analysis is different from the analysis by Giusti et al[1] mainly in two respects. The quantum defects employed here are different from those used by them. The procedure used to obtain the scattering matrix is that of Seaton, and is also different from theirs. The main purpose of this work is to investigate the effect of the difference of the quantum defects. The result is shown in Figure 1 in comparison with that of Giusti et al (chain line) and the experiment (dash line)[2]. The present result (solid line) agrees with the experiment better than that of Giusti et al in respect to the energy dependence at low energies. Especially the position of the first dip at $E \cong 0.1$ eV agrees well with that of experiment. In respect to the magnitude of the cross section there still remains a discrepancy between the present result and the experiment.

References

1) A. Gisti et al, *Phys. Rev.* A28, 682 (1983).
2) D. Auerbach et al, *J. Phys.* B10, 3797 (1977).

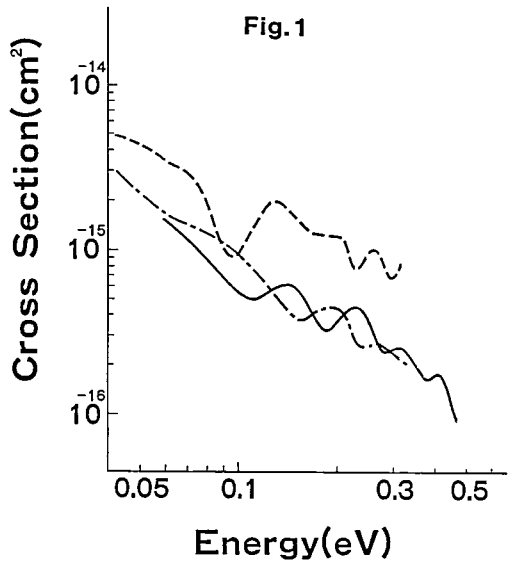

I—H Electron-Correlation and Electron-Phonon Coupling in One-Dimensional Many-Electron System

To understand optical, magnetic and electric properties of various newly synthesized one-dimensional materials from unified theoretical point of view, we are continuing to study the phase diagram, optical and magnetic excitations of a one-dimensional many-electron system with the electron-electron repulsion and the electron-phonon coupling.

I-H-1 Effect of Electron Correlation on the Ground State, Singlet and Triplet Excitons of Trans-Polyacetylene

Hidemitsu HAYASHI and Keiichiro NASU

[*Phys. Rev.* B. 32, 5295 (1985)]

In order to clarify various properties of trans-polyacetylene both in ground and optically excited states, we have studied a one-dimensional many-electron system with electron transfer (T), site-off-diagonal electron-lattice interaction (S_{od}), intra (U) and nearest-neighbour site (V) electron-electron repulsions. Its ground state is determined within unrestricted Hartree-Fock approximation, and the resultant phase diagram is shown to consist of five parts: BDW (bond density wave), SDW (spin density wave), CDW (charge density wave), BDW + CDW and BDW + CDW. The CDW phase originates from the nearest neighbour e-e repulsion and does not accompany the lattice displacement. According to the experimental results, polyacetylene occupies the BDW part of this phase diagram. Low-lying excited states such as singlet and triplet excitons in the BDW phase are also calculated within random phase approximation for the first time, and proved that they are very sensitive to the ratio between U and V. When $U > 2V$ the lowest state is the triplet exciton, while when $U < 2V$ it becomes singlet one, and the former case is concluded to be realized in trans-polyacetylene.

I-H-2 Periodic Kondo-Hubbard Model for Quasi One-Dimensional Organic Ferromagnet, m-Polydiphenylcarbene—Cooperation between Electron-Correlation and Topological Structure of Carbon Network—

Keiichiro NASU

Ferromagnetic properties of a new organic polymer m-polydiphenylcarbene is studied by the periodic Kondo-Hubbard model. This polymer is so designed that coplanar benzene-rings make a one-dimensional chain, through a bridge made of a single carbon atom with a π-electron and a nonbonding localized one. The antiferromagnetic correlation between π-electrons of benzenes and of bridging-carbons is taken into account by the Hubbard model as well as their itineracy, while the ferromagnetic correlation between the π-electrons and the non-bonding-ones at bridging-carbon atoms is taken into account by the context of negative Kondo model. Within the mean field theory, the ferromagnetic ground state is shown to be always stable, as the result of cooperation between the two kinds of correlations and the topological structure of carbon-network. This theoretical result agrees with the observed spin density of a finite chain. The ferromagnetic magnon is also studied within the RPA, and is shown to have a large exchange energy, indicating that this material has a quite exotic magnetism, as compared with the ordinary transition metals.

I—I Unified Theory for Resonant Raman, Hot Luminescence and Ordinary Luminescence with Nonradiative Process

To study the dynamics of lattice relaxation of optical excitations in solids and molecules, we derive an unified theory that can describe all components of the resonant secondary radiation: resonant Raman scattering, the hot luminescence and ordinary luminescence. We are especially interested to clarify how the nonradiative transition appears in the time resolved spectrum under pico-second pulse excitation.

I-I-1 Depolarization dynamics of hot luminescence in F centre—Time resolved spectrum under pico-second pulse excitation—

Shinji MURAMATSU (*Utsunomiya Univ.*), Masaki AIHARA (*Yamaguchi Univ.*), and Keiichiro NASU

A theory for the time-resolved secondary radiation from the F centre excited by a pico-second photon-pulse is formulated on the basis of a vibronic model. It includes 1s ground state, 2s and 2p excited states with a pseudo-Jahn-Teller type electron-phonon interaction. The transient behavior of intensity and polarization of the radiated photon, in a pico-second time region, is calculated as a function of time interval between the excitation and the detection. It is found that this transient behavior enables us to distinguish the hot luminescence from the ordinary one more clearly than our previously reported results. Especially, the depolarization due to hot luminescence becomes more prominent in the transient polarization spectrum than the case of stationary excitation, where the hot luminescence is usually masked by the tail part of the predominant ordinary luminescence.

I—J Theoretical Studies of Some Photochemical Reaction Mechanisms

I-J-1 Ab Initio Molecular Orbital Study on the Electronic Structure of Some Excited Hydrogen-Bonding Systems

Hidetsugu TANAKA (*Osaka City Univ.*) and Kichisuke Nishimoto (*Osaka City Univ. and IMS*)

[*J. Phys. Chem.* 88, 1052 (1984)]

The electronic structure of some excited hydrogen-bonding systems and their electronic structure changes associated with proton movement are investigated by ab initio MO-CI calculations. The present calculation shows that when both the proton donor

and the proton acceptor are π-electronic conjugated systems, e.g., phenol-pyridine or aniline-pyridine systems, slight movement of the proton in the neighborhood of the energy barrier brings about a large amount of charge transfer from proton donor to proton acceptor. Furthermore, hydrogen atom transfer might be expected via charge transfer followed by proton transfer in the case of donor excitation. On the other hand, neither charge transfer nor proton transfer occur when one of hydrogen-bonding system does not have conjugated π-electrons.

I-J-2 Ab Initio MO Study of the Redox Function of Flavin

Kichisuke NISHIMOTO (*Osaka City Univ. and IMS*)

[*Biomolecules-Electronic Aspects*, C. Nagata et al., Ed., Japan Sci. Soc. Press, Tokyo (1985)]

To understand the structure-function relationships of flavoproteins, we used a STO-3G minimal basis set for *ab initio* MO calculation[1] of lumiflavin in the oxidized and fully reduced forms. The hydrogen-bonding effect on the reactivity of flavin is important in understanding its catalytic ability, so we calculated the electronic structure of lumiflavin $\cdot (H_2O)_n$ complexes in both forms. In oxidized flavin, N (5) which is an electron accepting site, is activated by the hydrogen-bonding at O (12) and O (14), while in reduced flavin, C (4a) which is the most reactive site for molecular oxygen is activated by the hydrogen-bonding at N (3)-H.

References

1) K. Nishimoto, E.Kai, and K. Yagi, *Biochim. Biophys. Acta*, **802**, 311 (1984).

I-J-3 Theoretical Study of Electron Impact Mass Spectrometry. II. Ab Initio MO Study of the Fragmentation of Ionized 1-Propanol

Takae TAKEUCHI (*Nara Women's Univ.*), **Shoko UENO** (*Nara Women's Univ.*), **Masao YAMAMOTO** (*Nara Women's Univ.*), **Toshio MATSUSHITA** (*Osaka City Univ.*), **and Kichisuke NISHIMOTO** (*Osaka City Univ. and IMS*)

[*Int. J. Mass. Spectrom. Ion. Processes*, **64**, 33 (1985)]

In order to elucidate qualitatively the fragmentation mechanism of 1-propanol following low energy electron bombardment, the potential energy curves have been calculated using ab initio MO methods (4-31G/STO-3G). The present study indicates the H_2O elimination proceeds via the formation of a five-membered ring intermediate/transition state. A hydrogen atom of the methyl group is shifted to form H_2O, which is in line with the deuterium labelling experiment. In the simple bond cleavage process, it is mainly the C_α-C_β bond which is expected to be broken.

I-J-4 Partial Structure Analysis of Conjugated Systems I Benzene Character

Katsunori SAKURAI (*Osaka City Univ. and IMS*), **Kazuo KITAURA** (*Osaka City Univ.*), **and Kichisuke NISHIMOTO** (*Osaka City Univ. and IMS*)

A new method for analysing the partial structure of conjugated systems is proposed. The present method is applied to the most important partial structure, benzene, which is closely related to aromaticity. The calculated results are in accord with the previously proposed indices of aromaticity.

RESEARCH ACTIVITIES II
Department of Molecular Structure

II—A High Resolution Spectroscopy of Transient Molecules and Ions

During the course of chemical reactions many transient molecules and ions appear as intermediates. Because of their high reactivities, i.e. their short lifetimes, these transients have remained to be explored and some of them have even escaped detection. Many of these molecules have open-shell electronic structures, which characterize them as free radicals. Unpaired electrons in the molecule cause splittings in high resolution spectra of such species through fine and hyperfine interactions, and, when properly analyzed, these splittings provide us with information on the electronic properties of the molecule which is not obtainable for molecules without unpaired electrons. High resolution spectroscopy not only provides molecular constants of transient molecules at very high precision, but also allows us to unambiguously identify chemical species occuring in reaction systems and to unravel the details of reaction mechanisms. The present project will also be of some significance in related fields such as astrophysics and environmental sciences, and even in semiconductor fabrication.

II-A-1 Infrared Diode Laser and Microwave Spectroscopy of the NCl Radical: Breakdown of Born Oppenheimer Approximation

Chikashi YAMADA, Yasuki ENDO, and
Eizi HIROTA

We have previously reported the microwave spectrum of $^{14}N^{35}Cl$ in the ground vibronic state[1]. In order to examine the effect of the breakdown of Born-Oppenheimer approximation in detail, the measurement has been extended to $^{14}N^{35}Cl$ in $v = 1 - 3$, to $^{14}N^{37}Cl$ in $v = 0$ and 1,[2] and to $^{15}N^{35}Cl$ and $^{15}N^{37}Cl$ in $v = 0$. The infrared spectrum has also been observed for the $^{14}N^{35}Cl$ $v = 1 \leftarrow 0$ up to $4 \leftarrow 3$ transitions and for the $^{14}N^{37}Cl$ $v = 1 \leftarrow 0$ up to $3 \leftarrow 2$ transitions. All these observed spectral data have been analyzed by employing Watson's expression[3] for the Dunham coefficient including the effects of the breakdown of the Born-Oppenheimer separation:

$$Y_{k\ell} = \mu^{-(k+2\ell)/2} U_{k\ell} (1 + m_e \Delta_{k\ell}^{a}/M_a + m_e \Delta_{k\ell}^{b}/M_b)$$

and similar expressions for the spin-spin (λ) and spin-rotation (γ) interaction constants.[4] Some of the major molecular parameters thus obtained are given in Table I, where Born-Oppenheimer correction terms Δ are also listed. The Born-Oppenheimer

Table I. Molecular Constants of the $^{14}N^{35}Cl$ Radical in $X^3\Sigma^-$

Dunham coefficient[a]	Value[b]	Born-Oppenheimer correction[c]	Value[b]
Y_{10}	827.957 72 (71)	$\Delta^{Cl}(Y_{10})$	−1.59 (16)
Y_{20}	−5.300 18 (58)		
U_{01}	6.497 730 (16)	$\Delta^{Cl}(Y_{01})$	−1.964 (57)
Y_{11}	−0.006 414 42 (19)	$\Delta^{N}(Y_{01})$	−1.863 (39)
$U(\lambda)$	1.873 5 (23)	$\Delta^{Cl}(\lambda)$	221. (32)
α^{λ}	−0.017 678 (11)	$\Delta^{N}(\lambda)$	2.8 (24)
$U(\gamma)$	−0.067 84 (29)	$\Delta^{Cl}(\gamma)$	856. (108)
α^{γ}	0.000 129 63 (90)	$\Delta^{N}(\gamma)$	114. (61)

a. In cm^{-1}, except for U_{01} and $U(\gamma)$ which are given in amu cm^{-1} unit.
b. Values in parentheses denote one standard deviation and apply to the last digits of the constants.
c. Dimensionless.

equilibrium bond length was determined to be 1.610 710 (19) Å.

References

1) C. Yamada, Y. Endo, and E. Hirota, *J.Chem. Phys.*, 79, 4159 (1983).
2) C. Yamada, Y. Endo, and E. Hirota, *IMS Ann, Rev.*, 28 (1984).
3) J.K.G. Watson, *J. Mol. Spectrosc.*, **80**, 411 (1980).
4) E. Tiemann, *J. Mol. Spectrosc.*, **91**, 60 (1982).

II-A-2 The Microwave Spectrum of the CH_3S Radical

Yasuki ENDO, Shuji SAITO, and Eizi HIROTA

Symmetric tops in ^2E electronic states are interesting because Jahn-Teller effect might distort the molecules in unique ways. We have previously investigated CH_3O in $\tilde{X}^2E$ by microwave spectroscopy.[1] The present study is directed to a related molecule CH_3S. The J = 4.5-3.5, 5.5-4.5, and 6.5-5.5 transitions have been observed for both the $^2E_{1/2}$ and $^2E_{3/2}$ spin states, and have resulted in molecular parameters listed in Table I, where the corresponding data of CH_3O are included for comparison. As is expected from the larger spin-orbit coupling constant of CH_3S than that of CH_3O, the orbital angular momentum is less quenched in CH_3S than in CH_3O by Jahn-Teller effect. The observed A and B rotational constants lead to the C-S distance of about 1.79Å, where C-H is transferred from CH_3SH. This distance is shorter than C-S in CH_3SH, but not as much as the difference between C-O in CH_3O and C-O in CH_3OH. The hyperfine structure is discussed in II-A-9.

Table I. Molecular Constants of CH_3S and CH_3O in $\tilde{X}^2E$[a]

Constant	CH_3S	CH_3O
a (cm^{-1})		−145.6 (15)
$a\zeta_e d$ (cm^{-1})	−221.0 (10)	−62.24 (17)
$A\zeta_t$ (MHz)	76 002. (600)	54 330. (270)
A (MHz)	[160 000.][b]	154 960. (570)
B (MHz)	13 477.882 3 (12)	27 931. 14 (46)

a. Values in parentheses denote 2.5 standard deviations and apply to the last digits of the constants.
b. Estimated.

Reference

1) Y. Endo, S. Saito, and E. Hirota, *J. Chem. Phys.*, **81**, 122 (1984).

II-A-3 The Microwave Spectrum of the PF_2 Radical

Shuji SAITO, Yasuki ENDO, and Eizi HIROTA

Little has been known on the PF_2 radical; no spectroscopic studies have so far been reported on this molecule in the gas phase. We have previously investigated the PF radical by microwave spectroscopy.[1] In this experiment the radical was generated by a DC discharge in a mixture of PH_3 and CF_4. Additional paramagnetic lines were observed, which we assigned to PF_2. The optimum condition for the generation was not much different for the two radicals, but a slightly smaller discharge current was preferred for PF_2 than for PF.

The observed transitions include $^rR_0$ ($N = 6 - 10$), $^pR_1$ ($N = 5 - 9$), $^rQ_0$ ($N = 10 - 13$), $^rR_1$ ($N = 5 - 8$), $^pR_2$ ($N = 8 - 11$), $^rQ_1$ ($N = 9 - 13$), $^rQ_2$ ($N = 7 - 11$), and $^rQ_2$ ($N = 7 - 11$), which are split into 261 fine and hyperfine components. The analysis was performed using the $\mathbf{J} = \mathbf{N} + \mathbf{S}$, $\mathbf{F}_1 = \mathbf{J} + \mathbf{I}_P$, and $\mathbf{F} = \mathbf{F}_1 + \mathbf{I}_F$ coupling scheme. Table I lists the rotational, the spin-rotation coupling, and the hyperfine coupling constants derived by the least-squares analysis.

The structure parameters calculated from the observed rotational constants are r_0 (P − F) = 1.5792 (18) Å and θ_0 (FPF) = 98.48 (21)°, where the values in parentheses reflect merely an internal consistency of the result. The vibrational frequencies have been calculated from the observed centrifugal distortion constants to be ω_1 = 864 ± 10, ω_2 = 365.2 ± 1, and ω_3 = 844 ± 22, in cm^{-1}. It is interresting to note that ϵ_{aa} is very small. The observed Fermi term of the phosphorus nucleus σ (P) leads to the s-character of the unpaired electron orbital to be 1.64%, which may be compared with 2.57% of NF_2. The dipole-dipole hyperfine interaction terms of P corresponds to the spin density of 93.7%, to be compared with 90.8% in NF_2.

Reference

1) S, Saito, Y. Endo, and E. Hirota, *J. Chem. Phys.*, **82**, 2947 (1985).

Table I. Molecular Constants of the PF_2 Radical in the Ground Vibronic State[a]

Constant	Value	Constant	Value
A	27 958.3263 (98)	σ(P)	218.20 (14)
B	9 306.1134 (20)	T_{aa} (P)	−322.80 (43)
C	6 963.7443 (15)	T_{bb} (P)	−352.96 (23)
ϵ_{aa}	−30.08 (19)	σ(F)	93.83 (12)
ϵ_{bb}	138.369 (48)	T_{aa} (F)	−138.24 (24)
ϵ_{cc}	0.463 (38)	T_{bb} (F)	−147.28 (11)

a. In MHz. Values in parentheses denote 2.5 standard deviations and apply to the last digits of the constants.

II-A-4 CCCO: Generation by dc Glow Discharge in Carbon Suboxide, and Microwave Spectrum

Tong B. TANG, Hiroo INOKUCHI, Shuji SAITO, Chikashi YAMADA, and Eizi HIROTA

[*Chem. Phys. Lett.*, **116**, 83 (1985)]

Generation of the CCCO molecule was observed through its microwave spectrum in a dc glow discharge of carbon suboxide. Thirteen rotational transitions J = 7–6 to 19–18 were measured in the frequency region 67–183 GHz with the use of a source-modulation microwave spectrometer. A least-squares analysis of 19 observed spectral lines, including the six previously reported by Brown et al., yielded the following revised molecular constants for CCCO: B_0 = 4810.886 24 (65) MHz and D_0 = 0.000 777 07 (130) MHz, with 3σ in parentheses. The concentrations of CCO as well as CCCO produced in the glow discharge are estimated to be about 11 ppm.

II-A-5 Direct Observation of the Fine Structure Transitions in the Ne^+ and Ar^+ Ions with Diode Lasers

Chikashi YAMADA, Hideto KANAMORI, and Eizi HIROTA

[*J. Chem. Phys.*, **83**, 552 (1985)]

The $^2P_{1/2}$–$^2P_{3/2}$ fine structure transitions in the ground (np^5) state of the neon (n = 2) and argon (n = 3) atomic ions have been observed in absorption in the positive column of a liquid-nitrogen cooled discharge cell, by employing tunable infrared diode lasers as sources. The transition frequencies were measured to be 780.4240 ± 0.0011 and 1432.5831 ± 0.0007 cm^{-1} for Ne^+ and Ar^+, respectively. A few transitions have also been observed for the neutral Ne and Ar atoms.

II-A-6 Doppler-Limited Dye Laser Excitation Spectroscopy of the $\tilde{A}^1A''$ (000)–$\tilde{X}^1A'$ (000) Band of HSiF

Tetsuo SUZUKI, Kohzo HAKUTA (*Univ. of Electro-Commun.*), Shuji SAITO, and Eizi HIROTA

[*J. Chem. Phys.*, **82**, 3580 (1985)]

The $\tilde{A}^1A''$ (000)-$\tilde{X}^1A'$ (000) band of HSiF was observed by Doppler-limited dye laser excitation spectroscopy. The HSiF molecule was produced by the reaction of SiH_3F with microwave discharge products of CF_4. The observed spectrum was found to be almost free of perturabations and was readily assigned to about 1300 transitions of K_a'-K_a'' = 5-6, 4-5, 3-4, 2-3, 1-2, 0-1, 1-0, 2-1, 3-2, 4-3, 5-4, 0-0, 1-1, and 2-0. A least-squares analysis of the observed spectrum yielded the rotational constants and the centrifugal distortion constants for both the $\tilde{A}$ and $\tilde{X}$ states. The molecular structure was discussed using the observed rotational constants.

II-A-7 Microwave/Radio-frequency Optical Double Resonance Spectroscopy of the CCN Radical

Tetsuo SUZUKI, Shuji SAITO, and Eizi HIROTA

Microwave/rf-optical double resonance (MODR) spectroscopy allows us to observe fine and/or hyperfine structures in excited electronic states. We have applied this technique to the CCN radical, whereby the $\tilde{A}^2\Delta$ (000)-$\tilde{X}^2\Pi$ (000) transition at 470 nm was pumped by a dye laser.

A total of 12 transitions were observed between hyperfine components in the $\tilde{A}^2\Delta$ (000) state, in addition to the lowest rotational transition J = 2.5-1.5, Ω = 1.5-1.5. The observed double-resonance signals were analyzed to determine four hyperfine

parameters and the rotational constant, as listed in Table I. An attempt was made to observe Λ-doubling transitions and rotational transitions in the $\tilde{X}^2\Pi$ (000) state without success. This failure is ascribed to the small dipole moment in the ground electronic state; it is probably less than 0.5 D, in contrast with an ab initio estimate of 1.3 ± 0.2 D.[1)]

The $\tilde{A}$ state is derived from an electronic configuration which is obtained by promoting one electron from 4σ to 2π in the lowest configuration, i.e. . . . $(4\sigma)^1$ $(2\pi)^2$. Therefore, two electrons in 2π with their spins antiparallel do not contribute to the spin-dependent hyperfine parameters b and c, but do to the orbital-dependent constant a. A comparison with the atomic value indicates that the 2π electrons stay about 36% at the nitrogen nucleus. On the other hand, the unpaired electron in 4σ contributes to b and c, but does not to a. Again, by comparing with the atomic value, the spin density is estimated to be 4.7% at the nitrogen atom, suggesting that 4σ is quite localized at the end carbon atom.

Reference

1) S. Green, *Astrophys. J.*, **240**, 962 (1980).

Table I. Hyperfine Coupling Constants of CCN in $\tilde{A}^2\Delta$ (000)[a]

a	50.22 (19)	c	7.8 (20)
b	−5.9 (12)	eQq	0.75 (54)

a. In NHz. Values in parentheses denote one standard deviation and apply to the last digits of the constants. The effective B constant is 12 402.902 (72) MHz.

II-A-8 The Microwave Spectrum of the Acetyl Radical

Yasuki ENDO, Shuji SAITO, and Eizi HIROTA

The CH_3CO radical is an interesting species; it has often been postulated as an intermediate in many organic reactions. This molecule may be regarded as a CH_3 derivative of the HCO radical; HCO is bent in the ground electronic state as a result of Renner-Teller interaction, whereas Jahn-Teller interaction causes CH_3CO to have a bent CCO skeleton. Almost nothing has so far been reported on its spectrum in the gas phase.

We have generated CH_3CO by the reaction of CF_4 microwave discharge products with acetaldehyde. This reaction system is essentially identical to that employed for producing the vinoxy radical. We have found that addition of a small amount of O_2 increased the signal intensity of acetyl by a factor of 2 to 3. The use of a 0.5 m long cell pumped by a turbo pump and the insertion of a tube with multiple holes in the cell, which served as an inlet of fluorine atoms, have contributed another factor of 2 to 3 to the improvement of the S/N ratio. In subsequent stages Hg-sensitized reaction was employed with biacetyl as a precursor, as described in II-B-4.

The N = 6–5 through 8–7 and 17–16 through 19–18 transitions have been observed, each consisting of many components ascribed to K structure, internal-rotation, and fine and hyperfine components. The observed spectrum is being analyzed using a Hamiltonian including the internal-rotation term.

II-A-9 Hyperfine Interactions in CH_3O and CH_3S

Yasuki ENDO and Eizi HIROTA

In a previous paper[1)] we reported hyperfine interaction constants of CH_3O in $\tilde{X}^2E$. We noticed that one of the dipolar coupling constants T_0^2 $(C_\pm)$ is anomalously large. Because the anisotropic Fermi term $\sigma_\pm$, which was also found to be large, contributes to the hyperfine doubling of K = 0 lines as the T_0^2 $(C_\pm)$ term does, the two observed constants may be susceptible to contributions of terms which have not been taken into account. This is really the case; the Fermi terms and dipolar coupling terms are derived primarily from the spin-orbit coupling (L-S) and the electron-orbital and nuclear-spin interaction (L-I) through second-order perturbation. In other words, they originate from a product of I and S. When the product is scalar, it reduces to the Fermi term. The second-rank tensor product corresponds to the dipolar interaction. The first-rank tensor, which has not been paid attention, may give rise to pseudo dipolar interaction terms. The interaction may be expressed in terms of the tensor T_q^1 (P_α) where P denotes an antisymmetic 3 × 3 matrix:

$$P = \begin{pmatrix} 0 & xy & zx \\ -xy & 0 & yz \\ -zx & -yz & 0 \end{pmatrix}$$

For a molecule of C_s symmetry, there are four non-vanishing interaction terms, $T^1_{\pm 1}$ ($P_{\mp 1}$), T^1_0 ($P_{\mp 1}$), $T^1_{\mp 1}$ (P_0), and $T^1_{\pm 1}$ ($P_\pm$), of which the second one is important in the present problem. The hyperfine structure of CH_3O has been reanalyzed including this term, and the reault is shown in Table I. The new term is more essential for CH_3S; without it no reasonable set of hyperfine coupling constants could have been derived.

Reference

1) Y. Endo, S. Saito, and E. Hirota, *J. Chem. Phys.*, 81, 122 (1984).

Table I. Hyperfine Coupling Constants of CH_3O and CH_3S[a]

Hyperfine coupling constant	CH_3O		CH_3S
	Ref. 1)	present	present
a_L	2.346	2.345	2.512
σ_0	119.00	119.01	41.84
$\sigma_\pm$	153.60	98.048	47.56
T^2_0 (C_0)	4.343	4.336	8.78
$T^2_{\pm 2}$ (C_0)	0.279	0.279	−0.293
T^2_0 ($C_\pm$)	55.55	—	—
$T^2_{\mp 2}$ ($C_\pm$)	1.466	1.446	1.227
T^1_0 ($P_\pm$)	—	3.626	4.94

a. In MHz.

II-A-10 Diode Laser Spectroscopy of CF^+

Kentarou KAWAGUCHI and Eizi HIROTA

[*J. Chem. Phys.*, 83, 1437 (1985)]

The fundamental band of CF^+ in the $X^1\Sigma^+$ state has been observed by infrared diode laser spectroscopy with magnetic field modulation of the dc discharge plasma. The CF^+ ion was generated by a hollow cathode discharge in a mixture of CF_4 and H_2. From an analysis of the observed spectra, the following molecular constants were obtained: ν_0 = 1766.3589 (9), B_e = 1.720 366 (81), α_e = 0.018 947 (96), D_e = 6.179 (17) × 10^{-6} in cm^{-1} unit and r_e = 1.154 272 (35) Å, with three standard errors in parentheses.

II-A-11 The NH_2 Radical Generation by the 193 nm Photolysis of NH_3

Hideto KANAMORI and Eizi HIROTA

The 193 nm laser pumps the NH_3 molecule to (a) highly excited vibrational state(s) associated with the $\tilde{A}^1A_2''$ electronic state; according to the result of Vaida et al.[1] on NH_3 cooled by supersonic jet expansion, the peak of the pumping radiation is close to the $6\nu_2'$ state. Douglas[2] has shown that NH_3 in $\tilde{A}$ is predissociated. There are two dissociative channels energetically possible: (1) NH_2 ($\tilde{X}^2B_1$) + H (^2S) + 16 000 cm^{-1} and (2) NH_2 ($\tilde{A}^2A_1$) + H (^2S) + 6 100 cm^{-1}. The $\tilde{A}$ state of NH_3 is primarily correlated with (1), while the $\tilde{X}$ state potential curve is connected with (2). Therefore, there must be a crossing of the two potential curves, and avoidance, if any, is likely to be small. In fact, Donnelly et al.[3] have found that only 2.5% NH_2 are prepared in the $\tilde{A}$ state by the 193 nm photolysis of NH_3.

In order to obtain more detailed information on the photolysis, we have diagnosed nascent NH_2 molecules through the observation of the ν_2 band in $\tilde{X}$ with diode laser spectroscopy. We have observed 26 spin pairs, of which 7 belong to ν = 1–0, 2 to ν = 2–1, 3 to ν = 3–2, leaving 14 unidentified, because spectroscopic data for higher overtones are incomplete, prohibitng us from assigning the observed lines. Figure 1 shows the time profiles of three spin pair lines. It is seen that they appear as emissions right after the photolysis and then turn to absorptions. The time scale seems to be shorter for higher overtones.

References

1) V. Vaida, W. Hess, and J.L. Roebber, *J. Phys. Chem.*, 88, 3397 (1984).
2) A.E. Douglas, *Discuss, Faraday Soc.*, 35, 158 (1963).
3) V.M. Donnelly, A.P. Baronavsky, and J.R. McDonald, *Chem. Phys.*, 43, 271 (1979).

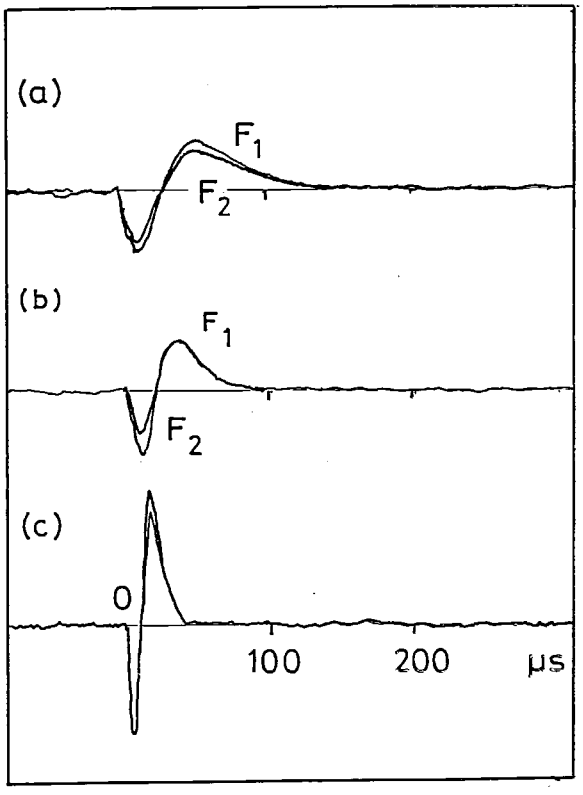

Figure 1. Time profiles of three vibration-rotation transitions of NH_2 in $\tilde{X}^2B_1$ generated by the 193 nm photolysis of NH_3. (a) $v = 2-1$ 5_{15}-6_{06}, (b) $v = 3-2$ 5_{15}-6_{06}, (c) unidentified spin pair. The NH_3 pressure is 0.05 for (a), 0.08 for (b), and 0.1 mTorr for (c), all diluted with 1 Torr of He.

II-A-12 Time-Resolved Diode Laser Spectroscopy for the 193 nm Photolysis of CS_2

Hideto KANAMORI and Eizi HITOTA

It has been recognized that CS_2 excited by the 193 nm laser to the $\tilde{C}^1B_2$ state [1] is predissociated through two channels: (1) CS $(X^1\Sigma^+)$ + S (^3P) + 15 700 cm^{-1} and (2) CS $(X^1\Sigma^+)$ + S (^1D) + 6 600 cm^{-1}. There has been controversy about the branching ratio.[2,3] In order to obtain the details of this photolysis reaction, we have examined the nascent distribution of CS fragments over vibrational-rotational levels in the ground-state manifold, by using time-resolved infrared diode laser kinetic spectroscopy described in II-B-1.

The vibration-rotation transition of CS has been observed for nearly entire region compatible with the available energy of channel (1), i.e. v up to 12 and J more than 100. Figure 1 shows a typical example of the observed spectrum. By assuming a spatially isotropic distribution of photofragments, the line profile has been analyzed to yield the nascent populatons in the upper and lower levels separately. Although a few lines appear as emissions at the central part of the Doppler profile for one to two μs after the photolysis, the majority of the observed lines are essentially absorptions, implying that there is no inversion in the vibrational population, in contradiction with the previous results.[2,4]

References

1) Heretofore referred to as $\tilde{A}$. However, since there are two lower-lying singlet states known (called V and T), the $\tilde{A}$ state must be renamed as $\tilde{C}$, in accordance with the spectroscopy convention.
2) S.C. Yang, A. Freedman, M. Kawasaki, and R. Bersohn, *J. Chem. Phys.*, **72**, 4058 (1980).
3) M.C. Addison, R.J. Donovan, and C. Fotakis, *Chem. Phys. Lett.*, 74, 58 (1980).
4) J.E. Butler, W.S. Drozdoski, and J.R. McDonald, *Chem. Phys.*, **50**, 413 (1980).

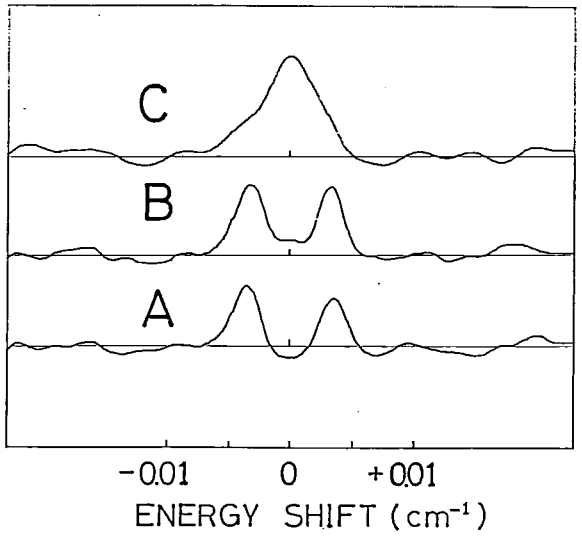

Figure 1. The $v = 4-3$ R (98) transition of CS generated by the 193 nm photolysis of CS_2. The gate width was chosen to be (a) 1 μs with no delay, (b) 1 μs with 1 μs delay, and (c) 10 μs with 2 μs delay.

II-A-13 Magnetic Field Modulated Infrared Laser Spectroscopy of Molecular Ions: The ν_1 Band of DCO^+

Kentarou KAWAGUCHI, A.R.W. McKELLAR (*NRC and IMS*), and Eizi HIROTA

The HCO^+ ion is one of the most typical molecular ions; it has been well established that this ion

plays an important role for molecular formation in interstellar space. A number of spectroscopic investigations have therefore been carried out in laboratory using microwave and infared laser as sources, and molecular parameters have already been determined precisely for HCO^+ not only in the ground vibrational state, but also in all the three fundamental vibrational states. For DCO^+, however, the ν_1 and ν_2 bands have not been observed. The former ν_1 band was investigated in the present study.

The DCO^+ ion was generated by a DC discharge (300 mA) in a D_2 (170 mTorr) and CO (130 mTorr) mixture. The modulation magnetic field consisted of a 1.74 kHz DC field of about 150 G superimposed on a DC field of about 75 G. The cell was cooled by liquid nitrogen. A total of eight lines were measured, and their analysis yielded the ν_1 band origin and the rotational constant in the ν_1 state, as listed in TableI. The change in rotational constant α_1 is relatively small as compared to theory and to the isoelectronic molecules DN_2^+ and DCN. This observation suggests the possibility of mixing the $(\nu_1, \nu_2, \nu_3) = (10^00)$ and (04^00) vibrational states.

Table I. Molecular Parameters of DCO^+[a]

Constant	$\nu_3 = 1$	$\nu = 0$
B (MHz)	35 793.47 (105)	[36 019.776]
D (kHz)	[55.87]	[55.87]
ν_0 (cm^{-1})	2584.5618 (14)	

a. Values in parentheses denote three standard errors and apply to the last digits of the constants. Values in square brackets are fixed in the fitting.

II-A-14 The Microwave Spectrum of the BO Radical

Mitsutoshi TANIMOTO (*Sagami Chem. Res. Center*), **Shuji SAITO, and Eizi HIROTA**

Because of its high reactivity, spectroscopic studies on the BO radical have been rather fragmentary. We have recently succeeded in generating BO to a concentration sufficient for the observation of the microwave spectrum. The reactions employed are a discharge in a BCl_3 and NO mixture, the reaction of nitrogen discharge products with NO and then with BCl_3, and a discharge in a ternary mixture, BCl_3, NO, and N_2. In the last system, BCl_3 may be replaced by B_2H_6, which results in a somewhat better efficiency for BO production.

The two rotational transitions $N = 1-0$ and $3-2$ have been observed for both $^{11}B^{16}O$ and $^{10}B^{16}O$, and have been analyzed by the least-squares method. Because the Fermi contact interaction is large, as in $^{13}CO^+$, Hund's case $b_{\beta S}$ was employed, namely the $\mathbf{I} + \mathbf{S} = \mathbf{F}_2$, $\mathbf{N} + \mathbf{F}_2 = \mathbf{F}$ coupling was used with $|ISF_2FM_FN\Lambda\rangle$ as a basis function. The molecular constants derived are listed in Table I with those obtained from optical spectroscopy[1] and ESR.[2]

The observed value of the Fermi term $b + c/3$ leads to the s-character of the unpaired electron orbital on the B atom of 40.3%. When corrected for this s-character, the spin density on the B atom is estimated to be 83%.

References

1) J.A. Coxon, S.C. Foster, and S. Naxakis, *J. Mol. Spectrosc.*, **105**, 465 (1984).
2) L.B. Knight, Jr., M.B. Wise, E.R. Davidson, and L.E. McMurchie, *J. Chem. Phys.*, 76, 126 (1982).

Table I. Molecular Constants of the BO Radical in $X^2\Sigma^+$[a]

	$^{11}B^{16}O$		$^{10}B^{16}O$	
Constant	Present	Refs. 1), 2)	Present	Refs. 1), 2)
B	53 165.5156 (46)	53 159.3 (14)	56 291.2073 (67)	56 280.3 (30)
D	0.191 48 (26)	0.1889 (11)	0.215 81 (37)	0.2045 (36)
γ	177.604 (10)	147.2 (48)	188.033 (14)	151 (13)
$b + c/3$	1 027.40 (31)	1 025 (1)	343.94 (57)	343 (1)
c	81.382 (32)	18.9 (18)	27.146 (39)	6.0 (18)

a. In MHz. Values in parentheses denote one standard deviation and apply to the last digits of the constants.

II-A-15 The Microwave Spectrum of the SiF_3 Radical

Mitsutoshi TANIMOTO (*Sagami Chem. Res. Center*), **Shuji SAITO, and Eizi HIROTA**

In sharp contrast with SiF_2 which is of long life and has been investigated in detail, almost no structural studies have been carried out on the SiF_3 radical in the gas phase. Milligan et al.[1] generated SiF_3 by photodecomposing $SiHF_3$ trapped in low temperature Ar, N_2, and CO matrices using ultraviolet light. They have observed four fundamental vibrational bands to establish a pyramidal structure for the molecule and have estimated the angle between the Si-F bond and the C_3 axis to be 71°. Wang et al.[2] observed an emission spectrum in 210-260 nm from a microwave discharge plasma of SiF_4 and ascribed it to the $^2B_1 \rightarrow \tilde{X}^2A_1$ transition of SiF_3.

We have recently succeeded in observing a number of paramagnetic lines around 330 GHz region, by passing Si_2F_6 through glow discharge. The lines were found to be spread over 200 MHz. If these lines were due to the $N = 22-21$ transition of SiF_3, we would observe similar clusters of paramagnetic lines at 345, 360, and 375 GHz. In fact, we have observed such lines in the latter two regions, each extending over 200 to 300 MHz. A preliminary analysis has been carried out to confirm the above assignment.

References

1) D.E. Milligan, M.E. Jacox, and W.A. Guillory, *J. Chem. Phys.*, 49, 5330 (1968).
2) J. L-F. Wang, C.N. Krishnan, and J.L. Margrave, *J. Mol. Spectrosc.*, 48, 346 (1973).

II-A-16 Infrared Diode Laser Spectroscopy of the PF Radical

Chikashi YAMADA, Man Chai CHANG (*Sun Cheon Natl. Univ. and IMS*), **and Eizi HIROTA**

The PF radical is the simplest of molecules involving P and F atoms. It plays important roles in many reactions such as fluorination reactions of P-containing molecules. However, only a few high-resolution spectroscopic investigations have been carried out; Douglas and Frackowiak[1] and Colin et al.[2] have reported the electronic spectra of PF in emission and absorption, respectively, and, more recently, Saito et al.[3] succeeded in observing the rotational spectrum by microwave spectroscopy.

We have observed ten vibration-rotation-fine structure transitions of the PF radical by infrared diode laser spectroscopy. The radical was generated by a DC discharge in a CF_4 and PH_3 mixture, as in the case of the microwave investigation.[3] The observed spectrum, all P-branch transitions, were analyzed, by fixing ground-state parameters to the values of Ref. 3. The results are summarized in Table I.

References

1) A.E. Douglas and M. Frackowiak, *Can. J. Phys.*, 40, 832 (1962).
2) R. Colin, J. Devillers, and F. Prevot, *J. Mol. Spectrosc.*, 44, 230 (1972).
3) S. Saito, Y. Endo, and E. Hirota, *J. Chem. Phys.*, 82, 2947 (1985).

Table I. Molecular Constants of the PF Radical[a]

Constant	$v = 0$[b]	$v = 1$
B	0.564 423 015	0.559 783 6 (70)
D	$0.101\ 35 \times 10^{-5}$	[$0.101\ 35 \times 10^{-5}$]
λ	2.948 237 277	2.943 19 (91)
λ_D	0.934×10^{-6}	[0.934×10^{-6}]
γ	0.15×10^{-2}	[0.15×10^{-2}]
T_v	0	837.816 36 (70)

a. In cm^{-1}. Values in parentheses denote one standard error and apply to the last digits of the constants. Values in square brackets are fixed.
b. Ref. 3.

II-A-17 The Microwave Spectrum of the HCCO Radical

Yasuki ENDO, Shuji SAITO, and Eizi HIROTA

It has been suspected that HCCO plays important roles in many organic reactions, however almost no spectroscopic information has been obtained on it. We have recently examined the reaction system of ketene and CF_4 microwave discharge products by microwave spectroscopy. When the partial pressure was 4 ~ 5 mTorr and 2 mTorr for H_2CCO and CF_4, respectively, we observed groups of lines in three frequency regions, 321.6-328.6, 342.6-

349.5, and 365.9-370.8 GHz, in addition to very strong spectral lines of H_2CF, whereas no CCO lines were detected for this condition. We have assigned the three groups of lines to a-type R-branch transitions of $J = 15 \leftarrow 14$, $16 \leftarrow 15$, and $17 \leftarrow 16$ of HCCO. This assignment readily gives us preliminary values of B + C and A to be 21 663 MHz and 900 GHz, respectively. These values are of reasonable magnitudes for the HCCO radical. The assignment of individual line has, however, been hampered by some perturbations. We have noticed that the spinrotation splitting is likely to be anomalously large and perhaps depends on the K_a value. These observations may indicate that there is a low-lying electronic state interacting with the ground state.

II-A-18 Dye Laser Excitation Spectrum of the DSO $\tilde{A}^2A'$ (012)-$\tilde{X}^2A''$ (000) Band

Nobukimi OHASHI (*Kanazawa Univ.*), **Shuji SAITO, Tetsuo SUZUKI, and Eizi HIROTA**

We have previously calculated a harmonic force field of HSO/DSO in the $\tilde{A}^2A'$ state from the observed spectroscopic data.[1,2] The results are, however, not as satisfactory as those on the ground electronic state. In order to obtain further information, the $\tilde{A}^2A'$ (012)-$\tilde{X}^2A''$ (000) band has been observed and rotationally analyzed. Table I lists molecular constants determined for the upper state. The ν_2' frequency is estimated to be 570 cm^{-1} in the $\tilde{A}$ state.

By using ν_2' (DSO), ν_3' (HSO, DSO), and the inertia defects Δ_{003} (HSO), Δ_{004} (HSO), Δ_{003} (DSO), and Δ_{012} (DSO) as input data, the force field was recalculated, where the F_{11} constant was fixed to a value estimated by Badger's rule and F_{12} and F_{13} were neglected. The force field thus derived reproduces the input data quite well, except Δ_{003} (DSO) and Δ_{012} (DSO), although the calculated difference between these two inertia defects fits well to the observed value. The discrepancy may be eliminated by reassigning the (003) and (012) bands of DSO to the (012) and (021) bands, respectively.

References

1) M. Kakimoto, S. Saito, and E. Hirota, *J. Mol. Spectrosc.*, 80, 334 (1980).
2) N. Ohashi, M. Kakimoto, S. Saito, and E. Hirota, *J. Mol. Spectrosc.*, 84, 204 (1980).

Table I. Molecular Constants of DSO in $\tilde{A}^2A'$ (012)[a]

A	154 749 (16)	ϵ_{aa}	8 840 (115)
B	16 995.1 (11)	ϵ_{bb}	106 (11)
C	14 972.8 (13)	ϵ_{cc}	−333 (12)
	ν_0	16 281.5541 (43) cm^{-1}	

a. In MHz, except for ν_0. Values in parentheses denote 2.5 standard deviations and apply to the last digits of the constants.

II-A-19 Infrared Diode Laser Spectroscopy of the HBF^+ Ion

Kentarou KAWAGUCHI and Eizi HIROTA

The HBF^+ ion is isoelectronic with HCO^+ and is expected to be linear. However, in contrast with HCO^+ for which a number of spectroscopic studies have been reported (cf. II-A-13), no observations have been performed on HBF^+ using spectroscopic techniques of any kind. We have recently succeeded in generating this ion by a DC discharge (400 mA) in a BF_3 (150 mTorr) and H_2 (25 mTorr) mixture and in observing the ν_3 band at 1635 cm^{-1}. Some 21 lines were identified in the 1547 to 1709 cm^{-1} region and were assigned to $H^{11}BF^+$. A few lines were also observed for $H^{10}BF^+$. Table I lists molecular constants derived from the observed spectrum. DeFrees et al.[1] have calculated the rotational constant to be 1.2025 (67) cm^{-1} using ab initio MO methods, which is in fair agreement with the present result. We have also observed five lines in the region of 700 to 760 cm^{-1}, which are assigned to the ν_2 band.

Reference

1) D.J. DeFrees, J.S. Binkley, and A.D. McLean, *J. Chem. Phys.*, 80, 3720 (1984).

Table I. Molecular Constants of HBF^+[a]

Constant	$\nu_3 = 1$	$\nu = 0$
B	1.203 006 (43)	1.211 623 (42)
D	2.574 (27) × 10^{-6}	2.634 (28) × 10^{-6}
ν_0	1633.2241 (12)	

a. In cm^{-1}. Values in parentheses denote three standard deviations and apply to the last digits of the constants.

II-A-20 The Ethylene and Atomic Oxygen Reaction Studied by Time-Resolved Microwave Spectroscopy

Yasuki ENDO, Seiichiro KODA (*Univ. Tokyo*), **Soji TSUCHIYA** (*Univ. Tokyo and IMS*), **Chikashi YAMADA, and Eizi HIROTA**

The C_2H_4 + O reaction had been thought to proceed as $C_2H_4 + O \rightarrow CH_3 + CHO$ (1). However, Buss et al.[1] have demonstrated by a crossed beam experiment that the $C_2H_4 + O \rightarrow CH_2CHO + H$ (2) mechanism is the major channel under single collision conditions. In a bulk sample, the CH_2CHO radical formed by (2) will further react with O: $CH_2CHO + O \rightarrow CH_2O + CHO$ (3). Because the microwave spectrum has been examined in detail not only for CH_2O, but also for CHO and CH_2CHO,[2] we have applied microwave spectroscopy to the C_2H_4 + O reaction to get further information on the mechanism, in particular, on the branching ratio of (1) and (2).

The spectrometer employed is described in II-B-4. Oxygen atoms were generated by Hg-sensitized photodecomposition of N_2O. The partial pressures of C_2H_4 and N_2O were 10 and 20 mTorr, respectively. Figure 1 shows the time profiles of the absorption signals of CH_2CHO, HCO, and CH_2O, after converted to the concentrations. It is seen that the CH_2CHO and CHO signals increase with nearly equal rates, but considerably faster than the CH_2O signal, and CHO is generated approximately twice as much as CH_2CHO. It is interesting to note that the present result with the pressure in the range of 0.01 ~ 0.1 Torr agrees well with that of Hunziker et al.[3] for several hundred Torr.

References

1) R.J. Buss, R.J. Baseman, G. He, and Y.T. Lee, *J. Photochem.*, 17, 389 (1981).
2) Y. Endo, S. Saito, and E. Hirota, *J.Chem. Phys.*, 83, 2026 (1985).
3) H.E. Hunziker, H. Kneppe, and H.R. Wendt, *J. Photochem.*, 17, 377 (1981).

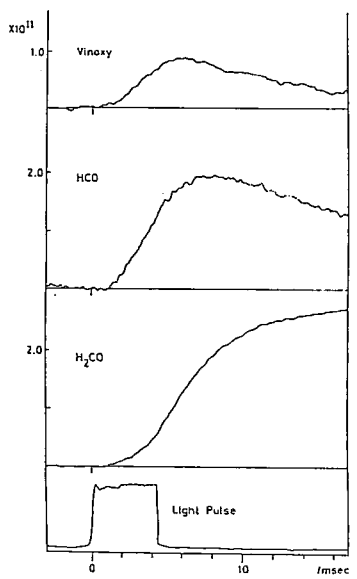

Figure 1. Time profiles of the CH_2CHO $17_{0,17}$-$16_{0,16}$ (342 311.5 MHz), CHO $4_{0,4}$-$3_{0,3}$ (346 708.5 MHz), and CH_2O $5_{1,5}$-$4_{1,4}$ (351 768.6 MHz) transitions; the ordinate has been converted to the concentrations of the three species. The lowest trace shows the Hg-lamp light pulse used to photodecompose N_2O.

II—B Development of New Instruments and New Experimental Methods for High Resolution Spectroscopy

The scope of a research is limited by the techniques and the capabilities of instruments available to a researcher. This is particularly true for spectroscopic investigations of simple molecules, radicals, and ions, which are main research themes this Department is interested in. The high precision with which we determine molecular parameters often unravels new features of molecular structure which have previously escaped experimental observation. The diversity of molecular systems which we can detect and analyze is often limited by the sensitivity of the spectrometer employed. It is thus imperative for us to steadily improve our research facilities and to develop equipments of radically new conceptual designs. The rewards of these efforts will include not only the detailed knowledge of the molecules under investigation, but also contributions to related fields. Various technical problems need to be solved to attain these goals. In this respect the collaboration of the Equipment Development Center is indispensable. New instruments developed in this program promise to open new research areas in the field of molecular science.

II-B-1 Infrared Diode Laser Spectroscopic System for the Study of Excimer Laser Photolysis

Hideto KANAMORI and Eizi HIROTA

Infrared diode laser kinetic spectroscopy has proved to be useful in unraveling photochemical reaction mechanisms through the determination of the nascent distributions of photofragments (II-A-11, II-A-12).[1,2] We have recently made two improvements for our spectroscopic system.

(1) Stabilized scanning of the source diode. Some diodes are often unstable in oscillation frequency and are difficult to scan slowly. This sort of instability must be eliminated to record the lineshape precisely, as is necessary in the present experiment. This has been achieved by exploiting the fact that the refraction index of the air is changed in the infrared region by 0.000 26 in going from the atmospheric pressure to the vacuum. We have been using a vacuum-spaced etalon of the free spectral range of about 0.01 cm^{-1} as an interpolation device. The source diode is locked to a fringe of this etalon and is scanned for about 0.3 cm^{-1} while introducing dry air into the etalon up to one atmosphere.

(2) Three gated integrators. Transient signals are collected for three gates of time: (a) 1 μs width with no delay, (b) 1 μs width with 1 μs delay, and (c) 10 μs width with 2 μs delay. The corresponding three signals reflect the time variation of the infrared absorption or emission lineshape. This system has been employed for CS photofragments generated by the 193 nm photolysis of CS_2, as described in II-A-12.

References

1) H. Kanamori, J.E. Butler, K. Kawaguchi, C. Yamada, and E. Hirota, *J. Chem. Phys.*, 83, 611 (1985).
2) H. Kanamori, J.E. Butler, T. Minowa, K. Kawaguchi, C. Yamada, and E. Hirota, Seventh Int. Conf. Laser Spectrosc. (SEICOLS '85), Maui, Hawaii, June 1985.

II-B-2 Infrared Diode Laser Spectroscopic System with Multiphoton Ionization

Tatsuya MINOWA, Kentarou KAWAGUCHI, Hideto KANAMORI, Chikashi YAMADA, and Eizi HIROTA

An MPI technique has been incorporated with an infrared diode laser spectroscopic system to improve the sensitivity of infrared spectroscopy. The effect of infrared pumping was observed for MPI signals of NO contained in a cell.

In order to apply this technique to chemically reactive species, a pulsed beam apparatus was constructed. It has two windows; one consists of a CaF_2 lens with f = 10 cm which focusses the infrared beam at a point in the molecular beam 10 cm downstream from the nozzle and the other is equipped with a glass lens with f = 10 cm for focussing the dye laser beam 2 to 3 mm further downstream. Ionic species produced by MPI were detected by a ceratron. The performance of the apparatus was tested using CD_3I. First, the direct absorption of the infrared beam was observed, although the S/N ratio did not exceed 10. Then MPI signals were observed which were induced by 3 + 2 or 2 + 2 processes. It was noticed that hot bands from excited vibrational states were induced by the Raman process. A double resonance signal was clearly observed for CD_3I when irradiated by the 10μ P(16) line of a CO_2 laser.

II-B-3 Submillimeter-Wave Spectrometer

Shuji SAITO, Yasuki ENDO, and Eizi HIROTA

As is well known, the absorption coefficient of the rotational transition is proportional to the square or the cube of the transition frequency. An obvious way of increasing the effective sensitivity is to extend the frequency region to higher frequency. There are, however, three difficulties to be overcome for millimeter-wave and submillimeter-wave spectroscopy: generation, transmission, and detection of the microwave. We have eliminated the second difficulty by using a free space cell and the third difficulty by introducing an InSb far-infrared detector.[1] The spectrometer we have been using is equipped with a series of klystrons which continuously cover the region up to 200 GHz. Klystrons beyond this limit often show poor performance, and in view of their high costs, it is no more practical to cover the region above 200 GHz with klystrons. Instead we have introduced a multiplier, Millitech Model MU4-2T, as a part of the IMS Special Research Project, which delivers the output of 100 to 650

μW in the region from 320 to 410 GHz, when we input 80-100 GHz radiation with the power up to 50 mW. We have confirmed that the effective sensitivity has been improved by an order of magnitude, by observing spectral lines of linear molecules. This new source has been employed for spectroscopy of BO (II-A-14), SiF_3 (II-A-15), and CH_3CO (II-A-8), and also used in the spectroscopic system designed for studying chemical reactions (II-B-4).

Reference

1) Y. Endo, S. Saito, and E. Hirota, *J. Chem. Phys.*, 75, 4379 (1981).

II-B-4 Microwave Spectroscopic System for the Study of Mercury-Sensitized Reaction

Yasuki ENDO, Seiichiro KODA (*Univ. of Tokyo*), **Soji TSUCHIYA** (*Univ. of Tokyo and IMS*), **Chikashi YAMADA, and Eizi HIROTA**

Almost no attempts have been made to explore reaction mechanisms through the time-resolved observation of microwave spectra. Recently, however, the microwave spectrum has been observed for quite a large number of transient molecules and ions including those which are difficult to detect by other spectroscopic techniques. The sensitivity of the microwave spectrometer has also been much improved in past ten years, and it is worth designing a microwave spectrometer for the time-resolved study of chemical reactions.

In the present study we have modified our microwave spectrometer to study Hg-sensitized reactions. Figure 1 shows a block diagram of the system. The central part of the absorption cell is made of a quartz tube 1 m long and 9 cm in diameter and is surrounded by 15 low-pressure 30 W Hg lamps, which are lighted for a few ms with the repetition rate of several Hz. The microwave signal, after detected by an InSb detector and amplified, is fed to a transient digitizer to follow the time variation of the signal. In order to eliminate low-frequency noises of baseline fluctuations, the signals at 1.5 MHz higher and lower than the center frequency are also recorded and subtracted from the main signal. This system has been applied to the determination of the branching ratio for the C_2H_4 + O reaction (II-A-20), and also employed for spectroscopy of the acetyl radical (II-A-8).

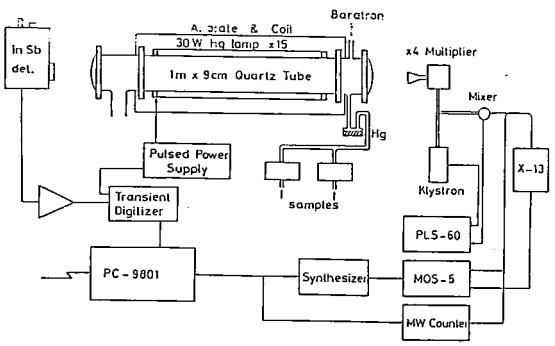

Figure 1. Block diagram of a microwave spectrometer for the study of Hg-sensitized reactions.

II-B-5 Spectroscopic System for Microwave-Optical Double Resonance

Tetsuo SUZUKI, Shuji SAITO, and Eizi HIROTA

A microwave-optical double-resonance (MODR) spectroscopic system with a Fabry-Perot cevity cell has been developed to observe rotational and fine/hyperfine transitions of transient molecules in excited electronic states. The cavity cell has a few advantages over the waveguide cell: (1) we need smaller microwave power to saturate microwave transitions, (2) the effective pumping speed is higher, and (3) the ratio of volume to inside wall area is larger, reducing chances of deteriorating transient molecules on metal surfaces.

Figure 1 shows a block diagram of the spectroscopic system. The Fabry-Perot cavity consists of two concave mirrors made of brass with the radius of curvature R = 90 mm and the diameter D = 70 mm. One of the mirrors was soldered to an end of a waveguide, and the coupling was made through an iris of 2 mm in diameter drilled at the center of the mirror. The other mirror was connected to a micrometer to tune the resonance frequency of the cavity. The Q value of the cavity was about 34 500 at 69 GHz. The klystron was frequency-modulated by 10 kHz square wave; during half cycle its frequency was locked to the center frequency of the cavity by an AFC loop, whereas for the other

half cycle it oscillates well outside the resonance dip of the cavity. The resonance frequency was scanned slowly by displacing the second mirror by a variable speed motor. The system has been employed to observe hyperfine structures of CCN in the $\tilde{A}^2\Delta$ (000) state (II-A-7).

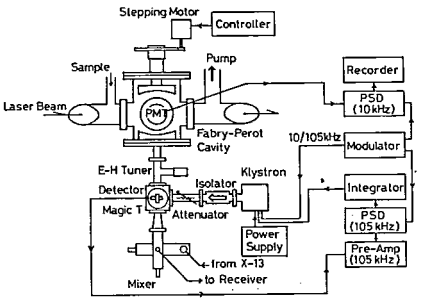

Figure 1. Block diagram of the spectroscopic system for the observation of MODR signals in the millimeter-wave region.

II—C High Resolution Spectroscopy of Molecules of Fundamental Importance

The need for high quality spectroscopic data has recently been increasing, especially for molecules of fundamental importance. Perhaps such spectroscopic data have been accumulated in the past because of interest in precise molecular structure determination. However, research activities in other related fields such as reaction kinetics, evvironmental sciences, plasma chemistry and physics, astronomy, and semiconductor technology have recently been advanced such that precise spectroscopic data are indispensable as a means of monitoring molecules. Spectroscopic data which are available at present are not necessarily good enough and must often be replaced by new data that meet necessary requirements. Such spectroscopic data on chemically stable molecules of fundamental importance will be presented in this section.

II-C-1 The Microwave Spectra of Deuterated Silanes

Keiichi OHNO (*Hiroshima Univ.*), **Hiroatsu MATSUURA** (*Hiroshima Univ.*), **Yasuki ENDO, and Eizi HIROTA**

As described in II-B-3, we have recently extended the frequency region covered by our microwave spectrometer to 320 to 410 GHz. We are thus able to observe the $J = 3$–2 transitions for the two symmetric-top deuterated species of silane, SiH_3D and $SiHD_3$, and to add a few R branch transitions for SiH_2D_2. These observations have allowed us to determine some of the centrifugal distortion constants without making assumptions. Table I summarizes molecular constants thus obtained, which replace those reported previously.[1] Recent high-resolution infrared studies[2,3] have yielded the results which agree remarkably well with the present results.

References

1) K. Ohno, H. Matsuura, Y. Endo, and E. Hirota, *J. Mol. Spectrosc.*, **111**, 73 (1985).
2) H. Bürger, A. Rahner, and J. Kauppinen, *Z. Naturforsch.*, **40a**, 386 (1985).
3) R.W. Lovejoy, R.D. Schaeffer, and W.B. Olson, 40th Symposium on Mol. Spectrosc., Columbus, Ohio, 1985.

Table I. Rotational Constants and Centrifugal Distortion Constants of Deuterated Silanes[a]

Species	B_0	D_J	D_{JK}
$^{28}SiH_3D$	62 943.615 (3)	0.477 69 (32)	1.613 06 (28)
$^{29}SiH_3D$	62 928.617 (4)	0.477 10 (51)	1.616 69 (44)
$^{30}SiH_3D$	62 914.508 (35)	0.476 4 (40)	1.618 8 (35)
$^{28}SiHD_3$	53 287.530 (33)	0.490 0 (37)	−0.352 8 (33)
$^{29}SiHD_3$	53 278.169 (15)	0.489 4 (18)	−0.352 8 (16)
$^{30}SiHD_3$	53 269.349 (1)	0.490 2 (1)	−0.352 3 (1)
Constant	$^{28}SiH_2D_2$	$^{29}SiH_2D_2$	$^{30}SiH_2D_2$
A_0	69 585.406 (23)	69 562.485 (48)	69 540.934 (41)
B_0	57 305.296 (55)	57 305.804 (20)	57 306.254 (18)
C_0	49 487.457 (50)	49 475.822 (21)	49 464.835 (18)
Δ_J	0.474 2 (22)	[0.474 2]	[0.474 2]
Δ_{JK}	−0.300 88 (82)	−0.303 3 (21)	−0.304 0 (18)
Δ_K	0.930 8 (36)	[0.933 4]	[0.935 9]
δ_J	0.109 90 (12)	[0.109 99]	[0.110 08]
δ_K	−0.183 12 (98)	[−0.184 87]	[−0.186 50]

a. In MHz. Values in parentheses denote 2.5 standard errors of the least-squares fitting and apply to the last digits of the constants. Values in square brackets are assumed values.

II-C-2 The Microwave Spectra of Deuterated Germanes

Keiichi OHNO (*Hiroshima Univ.*), **Hiroatsu MATSUURA** (*Hiroshima Univ.*), **Yasuki Endo, and Eizi HIROTA**

As an extension of our study on silance (II-C-1), we have investigated deuterated germanes by microwave spectroscopy. A number of spectroscopic observations have been carried out on GeH_4 and, to much less extent, on GeD_4, but very few high-resolution spectroscopic studies have been directed to GeH_3D and $GeHD_3$, except for a recent result by Anttila and Bürger[1] on $^{70}GeH_3D$, and almost nothing has been reported on GeH_2D_2.

Samples of GeH_3D, GeH_2D_2, and $GeHD_3$ were obtained by reducing GeH_3Cl, GeH_2Br_2, and $GeHCl_3$, respectively, with $LiAlD_4$ in butyl ether. The microwave spectrometer previously reported[2] was employed with the frequency region extended as described in II-B-3. The $J = 1-0$ and $3-2$ transitions were observed for GeH_3D and the $J = 1-0$ and $4-3$ transitions for $GeHD_3$. For GeH_2D_2 22 transitions have been measured. As in the case of SiH_2D_2, [3] the intensities of rotational transitions of GeH_2D_2 were found to be affected by the centrifugal distortion. The least-squares analysis of the observed spectrum has yielded rotational and centrifugal distortion constants with high precision, as shown in Table I. Anttila and Bürger's result[1] agrees remarkably well with the present result.

References

1) R. Anttila and H. Bürger, *J. Mol. Spectrosc.*, **111**, 201 (1985).
2) Y. Endo, S. Saito, and E. Hirota, *J. Chem. Phys.*, **75**, 4379 (1981).
3) K. Ohno, H. Matsuura, Y. Endo, and E. Hirota, *J. Mol. Spectrosc.*, **111**, 73 (1985).

Table I. Rotational Constants and Centrifugal Distortion Constants of Deuterated Germanes[a]

Species	B_0	D_J	D_{JK}
$^{70}GeH_3D$	59 072.190 (20)	0.421 5 (23)	1.572 5 (21)
$^{72}GeH_3D$	59 066.693 (20)	0.421 2 (23)	1.572 8 (20)
$^{73}GeH_3D$	59 064.04 (11)	0.421 (13)	1.573 (11)
$^{74}GeH_3D$	59 061.467 (11)	0.420 6 (13)	1.573 7 (11)
$^{76}GeH_3D$	59 056.506 (68)	0.420 6 (78)	1.574 8 (68)
$^{70}GeHD_3$	50 068.987 (23)	0.453 8 (14)	−0.361 36 (76)
$^{72}GeHD_3$	50 065.306 (12)	0.453 87 (74)	−0.361 00 (39)
$^{74}GeHD_3$	50 061.811 (11)	0.454 27 (67)	−0.361 72 (36)

Constant	$^{70}GeH_2D_2$	$^{72}GeH_2D_2$	$^{74}GeH_2D_2$
A_0	65 197.578 (19)	65 188.967 (9)	65 180.792 (9)
B_0	54 033.734 (13)	54 033.863 (6)	54 033.994 (6)
C_0	46 442.239 (13)	46 437.811 (6)	46 433.612 (6)
Δ_J	0.426 59 (40)	0.426 36 (20)	0.426 55 (19)
Δ_{JK}	−0.294 0 (12)	−0.294 13 (58)	−0.293 59 (55)
Δ_K	0.930 3 (14)	0.931 21 (69)	0.931 39 (65)
δ_J	0.102 663 (64)	0.102 726 (32)	0.102 768 (31)
δ_K	−0.222 00 (25)	−0.222 68 (12)	−0.223 21 (12)

a. See footnote a of Table I of II-C-1.

II-C-3 The Microwave Spectra of Deuterated Stannanes

Keiichi OHNO (*Hiroshima Univ.*), **Hiroatsu MATSUURA** (*Hiroshima Univ.*), **Yasuki ENDO, and Eizi HIROTA**

The studies on deuterated silanes (II-C-1) and germanes (II-C-2) have further been extended to deuterated stannanes by using the microwave spectrometer mentioned in II-B-3. Almost no high-resolution spectroscopic studies have been reported on deuterated stannanes. Deuterated stannanes were

synthesized by reducing stannic chloride with a mixture of $LiAlH_4$ and $LiAlD_4$; the mixing ratio was appropriately chosen so as to concentrate a particular isotopic species.

The $J = 1–0$ and $4–3$ transitions were observed for SnH_3D, although $J = 1–0$ and/or $J = 4–3$, $K = 3$ could not be detected for species with less abundnant Sn isotopes. For $SnHD_3$, the $J = 1–0$, $2–1$, and $4–3$ transitions were observed for the three main Sn isotopic species. Similarly for SnH_2D_2 the measurements have been limited to 11 to 12 transitions of the main Sn isotopes. Table I lists rotational constants and centrifugal distortion constants derived from the observed spectrum.

Table I. Rotational Constants and Centrifugal Distortion Constants of Deuterated Stannanes[a]

Species	B_0	D_J	D_{JK}
$^{116}SnH_3D$	47 316.411 (9)	0.283 2 (6)	1.265 2 (3)
$^{117}SnH_3D$	47 315.546 (77)	[0.283 3]	1.266 2 (17)
$^{118}SnH_3D$	47 314.696 (38)	0.283 4 (24)	1.265 7 (13)
$^{119}SnH_3D$	47 313.849 (78)	[0.283 3]	1.265 5 (25)
$^{120}SnH_3D$	47 313.023 (17)	0.283 2 (11)	1.265 7 (6)
$^{122}SnH_3D$	47 311.411 (77)	[0.283 3]	1.265 6 (29)
$^{124}SnH_3D$	47 309.846 (77)	[0.283 3]	1.266 2 (10)
$^{116}SnHD_3$	40 110.276 (34)	0.326 3 (26)	−0.259 5 (34)
$^{118}SnHD_3$	40 109.090 (17)	0.326 2 (12)	−0.259 4 (14)
$^{120}SnHD_3$	40 107.946 (7)	0.326 3 (5)	−0.259 3 (11)
Constant	$^{116}SnH_2D_2$	$^{118}SnH_2D_2$	$^{120}SnH_2D_2$
A_0	52 193.532 (16)	52 190.761 (59)	52 188.123 (13)
B_0	43 338.060 (12)	43 338.056 (40)	43 338.080 (9)
C_0	37 193.418 (5)	37 192.014 (17)	37 190.668 (4)
ΔJ	0.307 31 (23)	0.307 02 (72)	0.306 98 (17)
ΔJk	−0.261 90 (80)	−0.263 0 (30)	−0.262 61 (83)
ΔK	0.744 7 (12)	0.743 7 (21)	0.743 21 (60)
δJ	0.081 32 (13)	0.081 13 (40)	0.081 014 (92)
δK	−0.180 62 (89)	−0.180 31 (24)	−0.180 47 (56)

a. See footnote a of Table I of II-C-1.

II—D Raman Spectroscopy and Its Application

Raman scattering reveals a vibrational spectrum of molecules which is sensitive to a molecular structure and interatomic potential. We apply this technique to investigate the following three problems; 1) Structure-function relationship of biological molecules and their model compounds. 2) Structure of short lived molecules, 3) Solution structure. The first project utilizes the resonance enhancement of Raman intensity, which enables us to observe the vibrational spectra of chromophores selectively for a small amount of a dilute solution. Various kinds of heme proteins, flavoproteins, retinoid proteins and pyridoxal proteins are currently investigated. The second project aims to determine resonance Raman spectra of transient molecules, that is, reaction intermediates and excited molecules, by using two-color delayed laser pulses and optical multichannel detection system. The mixed flow apparatus is also used. The third project intends to evaluate a relative size of solute/solvent and solvent/solvent interactions for a binary mixtures of liquids and elucidate a structure of local assembly of molecules. For this purpose a system to measure Raman difference spectrum with high sensitivity was constructed.

II-D-1 Resonance Raman Study on Photoreduction of Cytochrome *c* Oxidase; Distinction of Cytochromes *a* and a_3 in the Intermediate Oxidation States.

T. OGURA, S. YOSHIKAWA (*Konan Univ.*), and T. KITAGAWA

[*Biochemistry* in press.]

Occurrence of photoreduction of bovine cytochrome *c* oxidase was confirmed with the difference absorption spectra and oxygen consumption measurements for the enzyme irradiated with laser light at 406.7, 441.6, and 590 nm. The resonance Raman spectra were obtained under the same experimental conditions as those adopted for the measurements of oxygen consumption and difference absorption spectra. The photoreduction was more effective upon irradiation at shorter wavelengths, and was irreversible under anaerobic conditions. However, upon aeration into the cell, the original oxidized form was restored. It was found that aerobic laser irradiation produces a photosteady state of the catalytic dioxygen reduction, and that the Raman scattering from this photosteady state probes cytochrome a^{2+} and cytochrome $a_3{}^{3+}$ separately upon excitations at 441.6 and 406.7 nm, respectively. The enzyme was apparently protected from the photoreduction in the spinning cell with the spinning speed between 1 and 1500 rpm. These results were explained satisfactorily with the reported rate constant for the electron transfer from cytochrome *a* to cytochrome a_3 (0.58 s^{-1}) and a comparable photoreduction rate of cytochrome *a*. The anaerobic photoreduction did give Raman lines at 1666 and 214 cm^{-1}, which are characteristic of the ferrous high spin cytochrome $a_3{}^{2+}$, but they were absent under aerobic photoreduction. The formyl CH = 0 stretching mode of the a_3 heme was observed at 1671 cm^{-1} for $a^{2+}a_3{}^{2+}CO$ but at 1664 cm^{-1} for $a^{2+}a_3{}^{2+}CN^-$, indicating that the CH = 0 stretching frequency reflects the π back donation to the axial ligand similar to the oxidation state maker line (ν_4).

II-D-2 Resonance Raman Study on Cytochrome *c* Peroxidase and Its Intermediate; Presence of the $Fe^{IV}=0$ Bond in Compound ES and Heme-Linked Ionization

S. HASHIMOTO, J. TERAOKA (*Osaka City Univ.*), T. INUBUSHI (*Univ. of Pennsylvania*), T. YONETANI (*Univ. of Pennsylvania*), and T. KITAGAWA

[*J. Biol. Chem*, in press]

Resonance Raman spectra of ferrous and ferric cytochrome *c* peroxidase and its peroxide complex, Compound ES, were investigated in resonance with the Soret band . The $Fe^{IV}=0$ stretching Raman line of Compound ES was assigned to a broad line around 765 cm^{-1} for the first time. This line was shifted to ca. 730 cm^{-1} with the ^{18}O derivative. The isotopic frequency shift was recognized upon formation of Compound ES with $H_2{}^{18}O_2$ in $H_2{}^{18}O$, but not with $H_2{}^{18}O_2$ in $H_2{}^{16}O$. This clearly indicated the occurrence of an exchange reaction between the heme-bound oxygen and bulk water. The $Fe^{IV}=0$ stretching frequency was unaltered between pH 4 and pH 11 in contrast with the case of Compound II of HRP. The Fe^{II}-histidine stretching Raman line was assigned on the basis of the frequency shift observed for ^{54}Fe isotopic substitution. This led us to a general conclusion that the strong hydrogen bonding of the proximal histidine and thus partial anionic character of the coordinated imidazole is a unique property of all peroxidases. The pK_a of the heme-linked ionization of ferroCcP was determined to be 7.3 from the intensity analysis of the Fe^{II}-His stretching Raman line. The Raman spectrum of ferriCcP strongly suggested that the heme is placed under an equilibrium between the five- and six-coordinate high-spin structures. At neutral pH it is biased to the five coordinate structure, but at acidic side of the transition of pK_a = 5.5 the six coordinate heme becomes dominant. F^- was bound to the heme iron at pH 6 but Cl^- was bound only at acidic pH. Acidification by HNO_3, H_2SO_4, CH_3COOH, HBr, or HI resulted in somewhat different populations of the five- and six-coordinate forms when they were compared at pH 4.3. Accordingly, it is inferred that a water molecule occupying the sixth coordination position of the heme iron is hydrogen bonded to a distal residue but is not coordinated to the heme iron at pH 6, and that protonation of the pK_a = 5.5 residue induces an appreciable structural change, allowing the coordination of the water molecule to the heme iron.

II-D-3 Iron-Histidine Stretching Raman Line and Enzymic Activities of Beef- and Bacterium Cytochrome *c* Oxidases

N. SONE (*Jichi Medical School*), T. OGURA and T. KITAGAWA

[Biochim. Biophys. Acta in press]

Resonance Raman spectra of the reduced form of cytochrome *c* oxidase isolated from beef heart and the thermophilic bacterium PS3 were investigated in relation to their H^+ pumping- and cytochrome *c* oxidizing activities, which were varied by incubating the enzyme at raised temperatures or at alkaline pH at room temperature. For both the beef heart and PS3 enzymes, the intensity of the Fe-histidine stretching Raman line of the ferrous a_3 heme (214 cm^{-1}) exhibited an incubation temperature-dependent change, which fell between the similar curves of the H^+ pumping and cytochrome *c* oxidizing activities. The intensities of the formyl CH = O stretching Raman line of the ferrous a_3 heme (1665 cm^{-1}) as well as of other lines were insensitive to the heat-treatment. The Fe-histidine stretching Raman line of both enzymes showed pH-dependent intensity change which was very close to the pH dependence of cytochrome *c* oxidizing activity. Therefore, deprotonation affecting the 214 cm^{-1} Raman line is responsible for the decrease of activity. This limited alkaline treatment to the PS3 enzyme was reversible, and the recovered enzyme exhibited Raman intensities and enzymic activities similar to the native one. However, the neutralized beef enzyme with a similar intensity of the 214 cm^{-1} line showed increased cytochrome *c* oxidizing activity and null H^+ pumping activity.

II-D-4 Resonance Raman Characterization of Iron-Chlorin Complexes Having Various Spin-, Oxidation-, and Ligation-States. I. Comparative Study with Analogous Porphyrin Derivatives.

Y. OZAKI, K. IRIYAMA, (*Jikei Medical Univ.*), H. OGOSHI, T. OCHIAI (*Tech. Univ. Nagaoka*) T. KITAGAWA

Resonance Raman (RR) spectra of octaethylchlorinato iron [Fe(OEC)] having various spin-, oxidation-, and ligation-states have been measured and compared with those of similar complexes of octaethyl-porphyrinato iron [Fe(OEP)]. Regarding the methine bridge stretching modes, the ν_{19} frequencies are different between the two kinds of complexes while the ν_{10} and ν_3 frequencies are close between them. For two $C_\beta C_\beta$ stretching modes designated as ν_2 and ν_{11} for Fe(OEP), their frequency separation became larger for Fe(OEC). The ν_4 band has been used as an oxidation state marker for Fe(OEP), but a change of the ν_4 frequency upon the redox change was much smaller for Fe (OEC) than for Fe(OEP), suggesting smaller π back donation. When the frequencies of Raman lines above 1450 cm^{-1} are plotted against the center-to pyrrole distance, both Fe(OEP) and Fe(OEC) gave generally straight lines, and their inclinations are nearly proportional to the contribution of the methine bridge stretching coordinate. The deviation from the straight line recognized for some ferrous low spin complexes of Fe(OEP) has been ascribed to larger π back donation, but such deviation was appreciably smaller for Fe(II)(OEC) derivatives, suggesting again smaller π back donation. It is presumably due to this feature that the ν_{10}, ν_{11}, and ν_4 frequencies of Fe(OEC) are less sensitive to nature of an axial ligand than those of Fe(OEP). It was noticed from this study that Fe(OEC) is more flexible and accordingly a ligand with a bulky group is easier of access to Fe of Fe(OEC) than of Fe (OEP).

II-D-5 Resonance Raman Spectra of Catalytic Intermediates of Cytochrome *c* Oxidase Detected with a Mixed-Flow Transient Apparatus.

Takashi OGURA, Shinya YOSHIKAWA (*Konan Univ.*) and Teizo KITAGAWA

[*Biochim. Biophys. Acta* in press]

Studies on a catalytic mechanism of cytochrome *c* oxidase is currently focused on identification of the oxygenated intermediate. We investigated the resonance Raman (RR) spectrum of an intermediate formed in the first 450 μs of reaction of the reduced enzyme with molecular oxygen using a new-built

mixed-flow transient Raman apparatus. The CO-bound enzyme and O_2-saturated buffer are mixed through a jet flow mixer just before the Raman flow cell. When the mixed solution comes to the laser beam, the CO-bound enzyme is first photo-dissociated and then reacts with oxygen. The RR spectrum arises from intermediates produced while the photo-dissociated enzyme remains in the laser beam. Although a few intermediates might be formed during this period, only the species whose Soret maximum is closest to the excitation wavelength is probably probed by the present technique. The observed transient RR spectrum excited at 416 nm (60 mW) is distinctly different from that of the resting, fully reduced, photoreduced, or carbonmonoxy form of the enzyme, and its S/N ratio is markedly improved in comparison with that of the CO-bound form, suggesting that the Soret maximum of the intermediate is located slightly shorter wavelength than the CO-bound form. When the same intermediate was excited at 425 nm, the ν_4 line was identified at 1355 cm^{-1}, indicating that cytochrome *a* of the intermediate is retained in the ferrous state. Since photoreduction of cytochrome *a* does not occur in this time scale, and also a prominent RR band observed at 1575 cm^{-1} for the "pulsed" form is absent, the intermediate cannot be the 420-nm or 428-nm "pulsed" form. On the other hand, the ν_4 frequency of the intermediate is higher than that of the CO-bound form like oxygenated hemoglobin. Consequently, the most likely candidate responsible for the intermediate is a transient oxygenated species having the Fe^{2+}–O_2 or Fe^{4+}= 0 heme in cytochrome a_3 and the Fe^{2+} heme in cytochrome *a*.

II-D-6 Resonance Raman Evidence for Oxygen Exchange between the $Fe^{IV}=0$ Heme and Bulk Water during Enzymic Catalysis of Horseradish Peroxidase and Its Relation with the Heme-Linked Ionizaton

S. HASHIMOTO, Y. TATSUNO (*Osaka Univ.*), and T. KITAGAWA

[Proc. Natl. Acad. Sci. USA in press]

The Raman line due to the $Fe^{IV}=0$ stretching vibration ($\nu_{Fe=O}$) of HRP Compound II was observed for various isotope combinations of H_2O_2 and H_2O at various pH. This mode exhibited a frequency shift from 787 cm^{-1} to 753 cm^{-1} when $H_2{}^{18}O_2$ was used instead of $H_2{}^{16}O_2$ at alkaline pH, but such a shift was not recognized at neutral pH. However, when $H_2{}^{16}O_2$ was made to react with HRP in $H_2{}^{18}O$ at neutral pH, the Raman line at 774 cm^{-1} was shifted to 740 cm^{-1}. This indicated that the bound oxygen of the $Fe^{IV}=0$ heme is exchanged with that of bulk water at neutral pH but not at alkaline pH. The $\nu_{Fe=O}$ mode of the neutral form, but not of the alkaline form, showed a small frequency shift (2 cm^{-1}) to higher frequency upon deuteration of the protein, and was appreciably intensified, indicating the absence of an exchangeable proton attached to the heme-bound oxygen. The RR spectrum of Compound II in the lower frequency region (below 450 cm^{-1}) was not largely altered by alkalization. Therefore, the slightly lower $\nu_{Fe=O}$ frequency at neutral pH than at alkaline pH was attributed to the presence of weak hydrogen bond between the heme-bound oxygen and an amino acid residue. The deuteration shift of the $\nu_{Fe=O}$ mode suggested that the hydrogen bond is slightly stronger in ^1H_2O than in ^2H_2O. The pH dependent intensity change of the $\nu_{Fe=O}$ mode allowed to determine the midpoint pH for the dissociation of the hydrogen-bonded proton to be 8.8, which is in good agreement with the pK_a value (8.6) of the heme-linked ionization of Compound II determined by other methods. Therefore, it became clear that the hydrogen-bonded proton plays an essential role in the acid/base catalysis of this enzyme as well as in the oxygen exchange, and that alkaline deactivation of this enzyme is attributed to lack of the hydrogen bonded proton.

II-D-7 Raman Difference Spectroscopy of the C-H Stretching Vibrations: Frequency Shifts and Excess Quantities for Acetone/Water and Acetonitrile/Water Solutions.

K. KAMOGAWA and T. KITAGAWA

[*J. Phys. Chem.* in press]

Frequency shifts of the C-H stretching vibrations of acetone and acetonitrile upon mixing with water were observed with a Raman difference spectrometer constructed using an optical multichannel analyser. From the observed shifts, homogeneous ($\Delta\nu_{AA}$) and heterogeneous ($\Delta\nu_{AB}$) interaction factors were

obtained as a function of concentration (X_A). For both acetone and acetonitrile, $\Delta\nu_{AA}$ decreased monotonously as X_A becomes smaller. The $\Delta\nu_{AA}$-vs-X_A curve is similar to the partial molar volume of the organic molecule versus X_A curve, and accordingly it is suggested that the frequency shift is related to the fragility of the liquid structure of the organic molecule. The $\Delta\nu_{AB}$-vs-X_A curve of the acetonitrile/water solution resembles the concentration dependence of the partial molar volume of water. The difference between the structures of the present solutions and that of methanol/water is discussed. Frequency shifts of a few organic molecules upon mixing with their deuterated analogues also were observed. For all the cases examined, $\Delta\nu_{AA}$ was zero, while $\Delta\nu_{AB}$ was constant, being around 2 and 0.7 cm^{-1} for the aliphatic and aromatic C-H groups, respectively. Implications of variations in $\Delta\nu_{AA}$ and $\Delta\nu_{AB}$ is discussed in terms of an empirical rule.

II-D-8 Resonance Raman Study on the Proton-Dissociated Bacteriorhodopsin: Stabilization of L-like Intermediate Having the All-trans Chromophore.

Akio MAEDA (*Kyoto Univ.*) **Takashi OGURA, and Teizo KITAGAWA**

[Biochemistry in press]

Resonance Raman (RR) spectra of light adapted bacteriorhodopsin (bR) in purple membrane were investigated at alkaline pH in the presence of 0.2 M KCl. The RR spectrum of alkaline bR (pH 10.5) under rapid flow, which was excited at 514.5 nm and detected with an OMA system (PAR 1215), remained unaltered from that of neutral bR when laser power was low, but additional bands appeared as the laser power was raised. When RR spectra were measured with a spinning cell (dia. 2 cm, 1800 rpm), neutral bR gave the RR spectrum of unphotolyzed bR, but alkaline bR exhibited distinct features, and it was ascribed to formation of a long-lived intermediate. The RR characteristics of the long-lived intermediate are as follows; 1) small shift or disappearance of the N-H (or N-D) bending line of the protonated Schiff base, 2) appearance of new Raman lines at 1188 and 1159 cm^{-1}, and 3) disappearance of the 1456 cm^{-1} line with appearance of several lines at 1380, 1447, and 1470 cm^{-1} . These features are quite similar to those of the neutral L intermediate. However, the C=C, C–C, and C=N stretching frequencies were the same as original ones. The L-like intermediate appears with a midpoint pH of conversion around 9 in parallel with the absorbance change at 296 nm, which is due to ionization of a residue in the vicinity of tryptophan. This residue cannot be cystein, histidine, tyrosine, and a free amino terminus. Lysine is also excluded from the experiments of chemical modification. Hence, the residue responsible for the ionization at pH 9 is tentatively assigned to a carboxylate with an unusually high pK_a and the all-trans chromophore is stabilized by its ionization.

II-D-9 Construction of a Multi-channel Spectrometer for Time-resolved Resonance Raman Spectroscopy

Hiro-o HAMAGUCHI (*Univ. of Tokyo and IMS*), **Chihiro KATO**, (*Univ. of Tokyo*), **Tahei TAHARA** (*Univ. of Tokyo*), **and Koichi IWATA** (*Univ, of Tokyo*)

A micro-computer (NEC PC-9801E) controlled multi-channel Raman spectrometer has been constructed to facilitate sub-nanosecond time-resolved measurements with a mode-locked Q-switched Nd: YAG laser and a synchronously pumped dye laser (Spectra Physics Series 3000).

Preliminary experiments performed with this system include the observation of the laser power dependence of the resonance Raman band profiles. The example of the C=C stretching band of spirilloxanthin (a kind of carotenoids having strong absorption at 532 nm, 7×10^4 molar extinction coefficient) is shown in Figure 1. As the laser power (532 nm, 3 ~ 300 KW peak power, the estimated rate of $S_1 \leftarrow S_0$ photoexcitation $10^9 \sim 10^{11}$ sec^{-1}) is increased, the band becomes broader. It is highly likely that this band broadening is caused by the contribution from the vibrationally excited molecules which are produced by the photoexcitation (and the subsequent internal conversion) and which are subject to further optical excitation before relaxing.

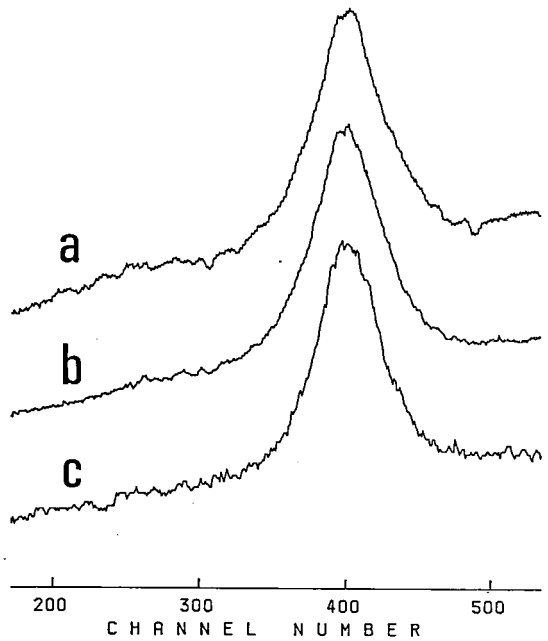

Figure 1. Laser power dependence of the C=C stretching band profile of spirilloxanthin in 1,2-dichloroethane. The second harmonic of a mode-locked Q-switched Nd:YAG laser was used for the excitation; a: 300 KW, b: 30 KW, d: 3 KW peak power.

II-D-10 Development of a Convenient Line-elimination Optical Filter for Multi-channel Raman Spectroscopy

Hiro-o HAMAGUCHI (*Univ. of Tokyo and IMS*) **and Keiji KAMOGAWA**

[*Appl. Spectrosc.* in press]

In multi-channel Raman spectroscopy, especially in time-resolved measurements with ultra-high sensitivities, the interference from Rayleigh and other elastic scattering causes a serious problem. We make use of, as a Rayleigh-line elimination filter, a sharp and strong absorption of the J-aggregate of a cyanine dye (5, 5′, 6, 6′-tetrachloro-1, 1′-diethyl-3, 3′-bis-(4-sulfobutyl)-benzimidazolocarbocyanine sodium salt in an alkaline aqueous solution, absorption maximum 585 nm, molar extinction coefficient 8.5×10^5, FWHM 8 nm). By placing a solution of this dye (concentration 3×10^{-5}, thickness 1 mm) in front of the entrance slit of a single spectrograph, more than one order of magnitude reduction of the stray-light level was achieved at 200 cm^{-1} from the exciting line (an Ar^+ pumped dye laser tuned at 585 nm). A systematic search is now being made for suitable dye molecules which can be used with fixed-frequency laser sources.

II-D-11 Transient Resonance Raman Band Profiles and the Dynamics of Electronically and/or Vibrationally Excited Molecules in Solution

Hiro-o HAMAGUCHI (*Univ. of Tokyo and IMS*)

[*Chem. Phys. Lett.* Submitted]

In the course of our previous studies of transient resonance Raman spectra of electronically excited molecules, it has been noticed that some observed bands exhibit characteristic band profiles which are not expected from the ordinary rotational-reorientation model.

The lowest excited triplet state of all-trans retinal gives a C=C stretching band having a narrower width than that of the ground state. It is possible that a dynamic process similar to motional narrowing is taking place.

In the case of the lowest excited singlet state of trans-stilbene, the olefinic C=C stretching band is much broader than its counterpart in the ground state. The band shape shows a marked dependence on the power of the probing laser. The competition between the vibrational relaxation and the $S_n \leftarrow S_1$ photoexcitation of hot S_1 stilbene (which are photolytically produced through $S_1 \leftarrow S_0$ with excess energies) is the most probable mechanism of this phenomenon.

Further studies, both theoretical and experimental, are needed to understand these characteristic band profiles and to elucidate the dynamics of electronically and/or vibrationally excited molecules in solution.

II—E Structure of Noncrystalline Materials

The structures of noncrystalline solids and liquids still largely remain to be determined. Since the majority

of chemical reactions takes place in the liquid state and amorphous solids exhibit interesting and important properties such as conductivity and catalytic activity, it is necessary to determine their structure from molecular viewpoint in order to understand their functions.

EXAFS (Extended X-ray Absorption Fine Structure) is best suited for the determination of local structures around a central metal atom in disordered systems such as liquid and amorphous materials. Among amorphous solids supported catalysts have been chosen as a primarily object because of the importance in chemistry and scare knowledge about their structure. In addition to the structural changes during the catalyst preparation procedures, effects of ambient gases and temperature to the catalyst structure have been studied by the use of an *in-situ* cell. Studies on the local structures around metals in aqueous solutions and in glassy materials also have been continued by joint studies program.

Improvements in the experimental conditions in the past year have made it possible to extend the EXAFS measurement to heavier metals such as Ru, Rh, and Pd, all of which have absorption over 20 keV. For this purpose higher order reflections of the monochromator crystals such as Ge (666) and Ge (933) are employed, with an SSD as a detector. A possibility of optical Raman spectroscopy was tested to probe the structure of adsorbed species on metal surface.

II-E-1 The Structure of the Cu/ZnO Catalyst by an *in-situ* EXAFS Study

Kazuyuki TOHJI, Yasuo UDAGAWA, Takanori MIZUSHIMA*, and Akifumi UENO** (**Graduate Student form Toyohashi Univ. of Technology, **Toyohashi Univ. of Technology*)

[*J. Phys. Chem.* in press]

By the use of an in-situ cell EXAFS measurements have been made on the Cu/ZnO catalyst under reacting conditions at elevated as well as at ambient temperature. It was found that the local structure around the Cu atoms, which have been believed to be the active atomic species, changes reversibly with heating/cooling cycles in a H_2 stream. Between about 400 K and 550 K highly dispersed Cu metal clusters appear, while metal clusters with metal-oxygen bonding exist below 400 K as is shown in Figure 1. Since this catalyst is used industrially at around 550 K, the former should be regarded to be the carrier of the catalytic activity of the system. However, once this catalyst is heated above its active region, the Cu clusters coalesce into large crystalline particles and the change with heating/cooling cycles ceases to be reversible. This provides rationale for a well known loss of activity when this catalyst is operated at higher temperatures. The results presented here emphasizes an importance to characterize catalysts at working conditions.

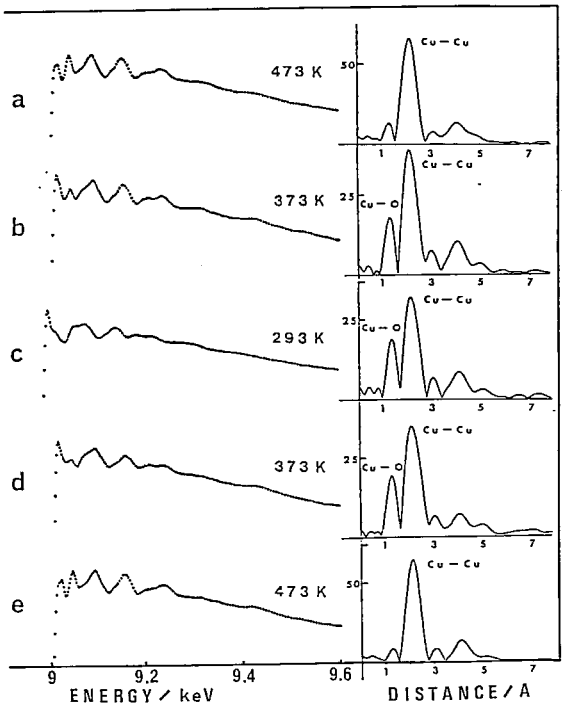

Figure 1. Observed changes in EXAFS spectra and associated Fourier transforms with temperature.

II-E-2 The Chemistry of Acetylene Exposed to Alumina and Alumina Supported Rhodium Catalysts

David M. Hanson (*SUNY at Stony Brook and IMS*), **Yasuo UDAGAWA, and Kazuyoshi TOHJI**

[Submitted to *J. Am. Chem. Soc.*]

The interaction between hydrocarbons and metals and metal oxides is important in many processes of heterogeneous catalysis. We have used Raman spectroscopy and mass analysis of desorption products to obtain information about the chemistry of acetylene exposed to alumina and alumina supported rhodium catalysts. Several Raman bands were observed and their intensity correlates with the desorption products having masses at 39, 52, and 78. An identification of the species which give Raman signal is discussed.

II-E-3 Structure of Ni (II)- and Zn (II)-Glycinato Complexes in Aqueous Solution Determined by EXAFS Spectroscopy

Kazuhiko OZUTSUMI*, Toshio YAMAGUCHI*, Hitoshi OHTAKI*, Kazuyuki TOHJI, and Yasuo UDAGAWA (**Tokyo Institute of Technology*)

[*Bull. Chem. Soc. Jpn.* **58**, 2786 (1985)]

The EXAFS spectroscopy has been used to determine the structure of the bis (glycinato) complexes of nickel (II) and zinc (II) ions of low solubility (0.1 – 0.3 mol dm^{-3}) in aqueous solution. The structural parameters were evaluated by the least squares analysis both in the reciprocal and in the real spaces on the basis of various standard samples of known structures. Analysis of the EXAFS spectra of aqueous solutions containing the bis (glycinato) complexes of nickel (II) and zinc (II) ions has revealed that the both complexes have two additional water molecules bound to the central metal ions to complete the octahedral structure. The structure of the nickel (II) complex is similar both in crystals and in solution, whereas the bis (glycinato) zinc (II) in solution is coordinated with two water molecules instead of two neighboring glycinato carbonyl oxygen atoms in the solid state.

II-E-4 Changes in Zr Coordination Number During Pyrolysis of a SiO_2-ZrO_2 Gel

Takuo OSUKA*, Hideki MORIKAWA*, Fumiyuki MARUMO*, Kazuyuki TOHJI, Yasuo UDAGAWA, and M. YAMANE* (**Tokyo Institute of Technology*)

[Submitted to *J. Noncrystal. Solid*]

An SiO_2-ZrO_2 gel containing 20 wt% ZrO_2 was prepared with the mixed solution of Si $(OCH_3)_4$ and ZrO $(NO_3)_2$. The Zr-EXAFS (extended X-ray absorption fine structure) above its K-absorption edge was measured for the gel treated at elevated temperatures up to 750 C. The estimated Zr-O distances indicated that Zr^{4+} ions were introduced into six-coordinated sites in the gel or glass structure by the pyrolysis above 400 C although Zr^{4+} ions loosely bonded to OH^-, H_2O, NO_3^- or framework silicates at the initial stage of the pyrolysis.

RESEARCH ACTIVITIES III
Department of Electronic Structure

III—A The Role of Hot Molecules in the Photochemistry of UV and VUV Laser Irradiation

Irradiation of molecules with UV or VUV light often induces photodissociation. Besides direct photodissociation and predissociation, we have recently been investigating another type of photodissociation, which consecutively involves excitation of electronically excited state, efficient internal conversion to the ground electronic state, and dissociation. The ground electronic state thus produced has a very high vibrational energy, in other words, it is vibrationally very hot. Since the internal energy of this state is determined by photon energy and is unique, we can directly obtain the specific rate constants of unimolecular dissociation. We firstly describe photodissociation of olefines to allylic radials and of alkyl benzenes to benzyl radical. We secondly describe a competition between pressure-dependent and independent photodissociations. We thirdly describe collisional relaxation times of hot molecules and finally some technical aspect of transient absorption studies.

III-A-1 Direct Measurements of Dissociation Rate from Hot Olefins and Alkylbenzenes.

Nobuaki NAKASHIMA, Noriaki IKEDA, and Keitaro YOSHIHARA

Rhotodissociation dynamics of olefins and alkylbenzenes were studied by nanosecond laser (ArF: 193 nm) flash photolysis. The primary intermediates were postulated to be hot molecules (S_0^{**}: highly excited vibrational states in the electronic ground state).[1] The dissociation rates from S_0^{**} have been measured for the first time for the following series of molecules.

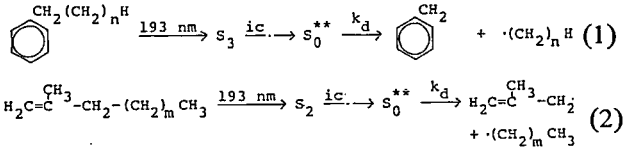

The dissociation rates under collision free conditions decrease with an increase in the number of n and m (Table I). They can be explained in terms of a thermal reaction (RRKM) theory.

Table I. Dissociation Rates of Hot Molecules ($10^6 s^{-1}$)

n,m in Scheme 1, 2.	0	1	2	3	4	5
Olefins	>300	150	19	4.5	1.25	<0.5
Benzens	2.4	22	7.6	2.0	–	–

References

1) N. Nakashima, N. Shimo, N. Ikeda, and K. Yoshihara, *J. Chem. Phys.*, **81**, 3738 (1984); N. Ikeda, N. Nakashima, and K. Yoshihara, *J. Chem. Phys.*, **82**, 5285 (1985).

III-A-2 Two Pathways for Photodissociation of Olefins

Nobuaki NAKASHIMA, Noriaki IKEDA, Nobuo SHIMO, and Keitaro YOSHIHARA

The major photodissociation route of olefins have clearly been explained in terms of the hot molecule mechanism.[1] The intermediate is hot molecule and is readily quenched by foreign gases. Therefore, this route must be completely quenched in solution and in a polymer chain. On the other hand, allyl radicals are known to be formed in a condensed phase. This means other rapid processes

exist. A pressure independent process was actually detected in this paper.

Figure 1 shows that the Stern-Volmer plots of the relative radical yield vs. the pressure of the foreign gases. The relative yield reaches a plateau. The yield at the high pressure limit is about 10% of that under a low pressure for the case of 2, 3-dimethyl-2-pentene. The Stern-Volmer plots indicate existence of a pressure independent process. Propane as a foreign gas is about 4 times effective than nitrogen.

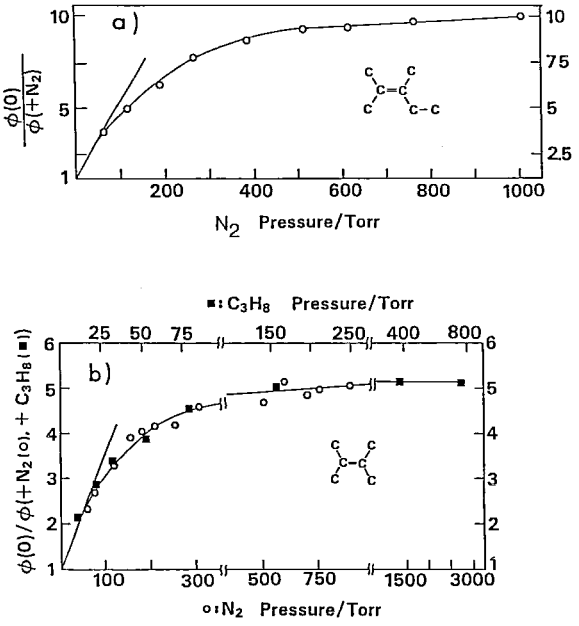

Figure 1. Stern-Volmer plots of the relative radical yield vs. the pressure of the foreign gases; a) 2, 3-dimethyl-2-pentene and b) 2,3-dimethyl-2-butene.

Reference

1) N. Nakashima, H. Shimo, N. Ikeda, and K. Yoshihara, *J. Chem. Phys.*, 81, 3738 (1984).

III-A-3 Collisional Relaxation Times of Hot Radicals

Nobuaki NAKASHIMA and Keitaro YOSHIHARA

During the course of studies of photochemistries of benzenes and olefins, we have directly detected absorption spectra of hot species (a highly excited vibrational state). These molecules and radicals carry more than 3 ev as an available energy, when the parent molecule absorbes a photon of the ArF laser light. In the presence of a foreign gas, the internal energy, collisionally transfers to the foreign gas and equilibrate with the bath. We can measure the relaxation times on the basis of the changes of the absorbances as shown for benzyl radical.[1)]

Table I summarizes apparent relaxation times of hot radicals and molecules by nitrogen. In the third column, relaxation times in the presence of 760 Torr of nitrogen are evaluated by using these rates. Larger radical gives faster relaxation time. The relaxation rate probably depends on vibrational modes, because hot benzyl and hot benzene show relatively slow relaxation times.

Table I. Collisional Relaxation Times of Hot Radicals and Molecules by Nitrogen.

Hot Radical	K_r/s^{-1} Torr^{-1}	τ_r (760 Torr)/ns
CH_3	1.3×10^4	100
C=C–C•	2.1 〃	65
C=C(C•)C	7.5 〃	18
C(C)C=C(C•)C	25 〃	5
⬡–$\dot{C}H_2$	8 〃	16[a)]
⬡••	1.75	75[b)]
Ⓕ••	7.4	18[c)]

a) Ref. 1, b) N. Nakashima and K. Yoshihara, *J. Chem. Phys.*, 79, 2727 (1983), c) T. Ichimura, Y. Mori, N. Nakashima, and K. Yoshihara, *J. Chem. Phys.*, 83, 117 (1985).

Reference

1) N. Ikeda, N. Nakashima, and K. Yoshihara, *J. Phys. Chem.*, 88, 5803 (1984).

III-A-4 Actionometry of ArF Laser Power and Measurements of Molar Extinction Coefficients of Transient Species

Nobuaki NAKASHIMA and Keitaro YOSHIHARA

In order to obtain absolute quantities in a photochemical process, we have to measure an out-put power of the laser light with a high accuracy. We can easily measure it by a commercially available power meter calibrated in the visible and near UV regions. For the deep UV and VUV regions, however, we need to calibrate a power meter. If we know a number of the photon, we can determine molar extinction coefficients of transient species detected

by nanosecond laser flash photolysis.

A power meter was calibrated on the basis of the photochemical reaction of nitrous oxide.[1] Then the extinction coefficients of the intermediate of benzene (hot benzene) and of methyl radical have been determined as shown in Table I. For methyl radical, 9 independent results have been published. The present value is in very good agreement with the recent and accurate measurement ($1.08 \pm 0.02 \times 10^4$ $M^{-1}cm^{-1}$, Ref. 2). The present results can be good references to determine molar extinction coefficients of transient species in the deep UV region.

Table I. Molar extinction coefficients

	$\epsilon/10^4 M^{-1} cm^{-1}$	Wavelength/nm	$\Delta\lambda$/nm
Hot benzene	0,35	230	1 ~ 5
Methyl radical	1.1	216.4	0.4

References

1) N. Nakashima and K. Yoshihara, *J. Chem. Phys.*, 79, 2727 (1983).
2) M.T. Macpherson, M.J. Pilling, and M.J.C. Smith, *J. Phys. Chem.*, 89, 2268 (1985).

III—B Radiationless Processes in Large Molecules ——Internal Conversion Directly Observed as a Dark Process

We are interested in the photochemical properties of benzene, a prototype of aromatic hydrocarbons. The nonradiative pathways are strongly depending on exciting wavelengths and suddenly opens a new pathway, called channel three, by which vibrational evergy in excess of about 2800 cm^{-1} is lost at an anomalously rapid rate. Excitation was made above the channel three threshold with a recently developed high power, picosecond, narrow bandwidth laser continuously tunable from 214 to 252 nm. The dramatic channel three effect was indeed observed in both quantum yields and lifetimes and three orders of magnitude change in radiationless process was found upon exciation at all vibrational levels. The most of energy goes radiationlessly to "hot" state, i.e., vibrationally highly excited state in the ground electronic manifold. We were able to observe, for the first time, the internal conversion rate as a dark process by detecting the formation rate of hot molecules by picosecond pump and probe method.

III-B-1 Formation Rates of Hot Benzene Following After Excitation in the Channel Three Region

Minoru SUMITANI and Keitaro YOSHIHARA

Formation rates of "hot" benzene are measured directly following after excitation of several single vibronic levels. These correspond to the horizontal internal conversion rates and are observed for the first time in the isolated molecule condition.[1] After excitation to the level of $6_0^1 10_0^2 1_0^1$, which is located below the channel three threshold, the rise curve was simulated with a single exponential and this corresponds to the fluorescence decay time. However, above the threshold, the rise curve have the double exponential rise. These curves were simulated with the following kinetic model which involves either an isomeric form of benzene or hidden singlet electronic state.

$S_1 \rightleftharpoons X \rightarrow S_0^{**}$

$\updownarrow$

S_0

S_1: singlet vibronic level or levels of benzene.
X: isomer or hidden electronic state.
S_0^{**}: hot benzene.

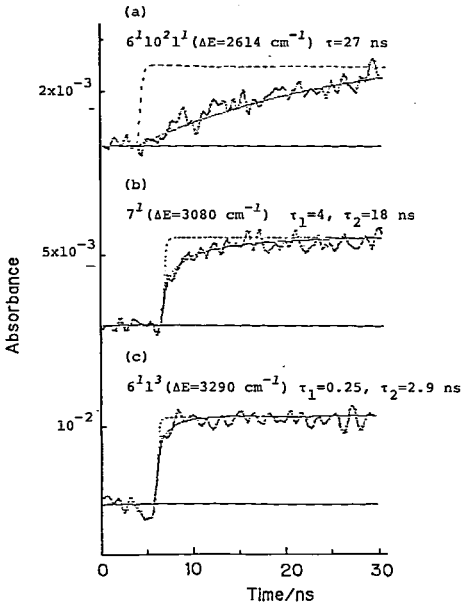

Figure 1. The rise curves of hot benzene formation resulting from excitation of (a) $6_0^1 10_0^2 1_0^1$, (b) 7_0^1, and (c) $6_0^1 1_0^3$. ΔE's indicate the excess vibrational evergy above the 0-0 level and τ_i's the single-vibronic-level fluorescence lifetimes of the corresponding states.[2)]

Reference

1) We observed a part of the rise process upon excitation of the $6^1 1^2$ (248 nm) band with KrF-laser nanosecond flash photolysis. N. Nakashima and K. Yoshihara, *J. Chem. Phys.*, 77, 6040 (1982).
2) M. Sumitani, D.V. O'Connor, Y. Takagi, N. Nakashima, K. Kamogawa, Y. Udagawa and K. Yoshihara, *Chem. Phys.*, 93, 359 (1985).

III—C Dynamic Behavior of Excited States

Optical excitation of molecules to electronic excited states causes a variety of dynamical behavior, depending on electronic structures and environments, such as energy transfer, proton transfer, chemical reaction, radiationless transition, ionization and others. Most of these processes fall into the picosecond time scale. Firstly we describe an intramolecular charge transfer in the excited state of phenyldisilane. Secondly, tautomerization via double proton switching has been studied in the excited state of indazole in acetic acid. Thirdly, aqualigand dissociation of $[Ce(CH_2)_9]^{3+}$ in the 5d←4f excited state has been studied in detail, and fourthly a water soluble quinone, 9,10-anthraquinone-2,6-disultonate, has been studied by observation of transient absorption and five different chemical intermediates has been recognized. Finally, cis-trans photochemical isomerization of 1, 2-bispyrazylethylene has been studied and the role of the triplet state on such chemical reaction has been clarified.

III-C-1 Intramolecular $2p\pi^* \rightarrow 3d\pi$ Charge Transfer in the Excited State of Phenyldisilane Studied by Picosecond and Nanosecond Laser Spectroscopy

Haruo SHIZUKA, Katsuhiko OKAZAKI, Masayuki TANAKA (*Gunma Univ.*), **Mitsuo ISHIKAWA** (*Kyoto Univ.*) **Minoru SUMITANI, and Keitaro YOSHIHARA**

[*Chem. Phys. Lett.*, **113**, 89 (1985)]

Intramolecular $2p\pi^* \rightarrow 3d\pi$ charge transfer in the excited state of phenyldisilane occurs very rapidly (< 10 ps) both in MP at 293 K and in EPA glass at 77 K. At room temperature a long-lived 425 nm transient (which is assigned to a rearranged intermediate) is produced with the rise time 30 ps, showing that the transient formation proceeds via the $^1(2p\pi, 3d\pi)$ CT state. Some of the time-resolved spectra in the picosecond timescale are shown in Figure 1.

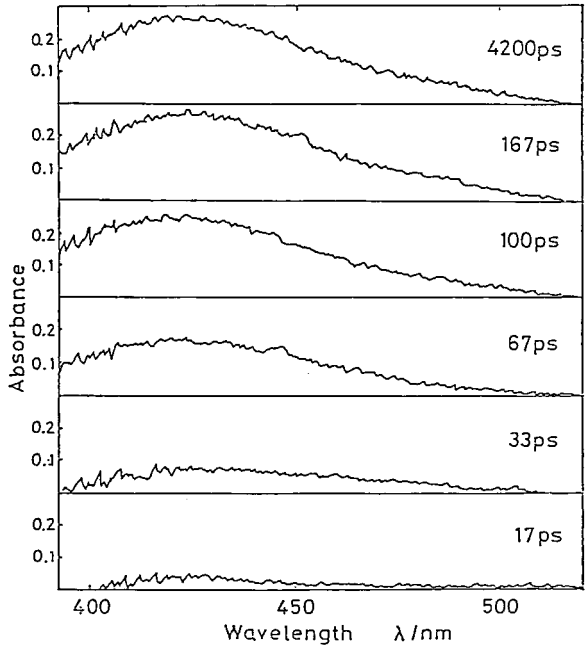

Figure 1. The buildup profile of the 425 nm transient absorption spectra measured by picosecond laser flash photolysis of phenyldisilane in MP at 293 K, where the times refer to the delay times.

II-C-2 Proton Transfer Tautomerism in the Excited State of Indazole in Acetic Acid: Tautomerization via Double Proton Switching

Masao NODA (*Tokai Women's College*), **Noboru HIROTA** (*Kyoto Univ.*), **Minoru SUMITANI, and Keitaro YOSHIHARA**

[*J. Phys. Chem.*, 89, 399 (1985)]

It is shown that the S_1 state of 1*H*-indazole in acetic acid undergoes double proton transfer along the hydrogen bonds in the indazole-acetic acid complex. The proton transfer converts 1*H*-indazole into 2*H*-indazole. The rate of proton transfer is estimated to be $2.7 \times 10^9 s^{-1}$ from transient fluorescence measurements. The proton transfer scheme is shown in Figure 1.

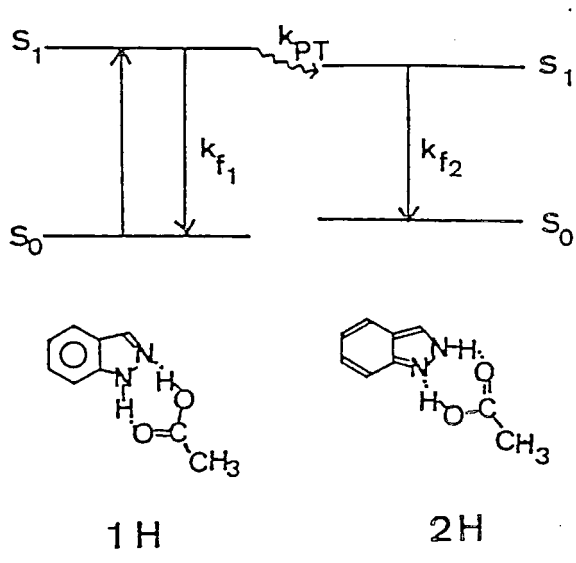

Figure 1. The proton transfer scheme of indazole in acetic acid.

III-C-3 Aqualigand Dissociation of $[Ce(OH_2)_9]^{3+}$ in the 5d ← 4f Excited State

Youkoh KAIZU, Koji MIYAKAWA, Keiko OKADA, Hiroshi KOBAYASHI (*Tokyo Inst. Tech.*), **Minoru SUMITANI, and Keitaro YOSHIHARA**

[*J. Am. Chem. Soc.*, **107**, 2622 (1985)]

Hydrated Ce^{3+} ions in aqueous solution are predominantly in a tricapped trigonal structure of $[Ce(OH_2)_9]^{3+}$. However an equilibrium between $[Ce(OH_2)_9]^{3+}$ and $[Ce(OH_2)_8]^{3+}$ exists in solution. Upon the 5d ← 4f excitaion, one of the aqualigands of $[Ce(OH_2)_9]^{3+}$ dissociates in the excited state. In ethylene glycol, however the emissions not only of the long-lived excited species $*[Ce(OH_2)_8]^{3+}$ (48 ns) but also of the short-lived excited species $*[Ce(OH_2)_9]^{3+}$ (430 ps) were detected. The rise transient which indicates an increase of $[Ce(OH_2)_8]^{3+}$ immediately after excitation was also observed in ethylene glycol as shown in Figure 1. The lifetime of $*[Ce(OH_2)_9]^{3+}$ in solution is controlled by the rate of aqualigand dissociation.

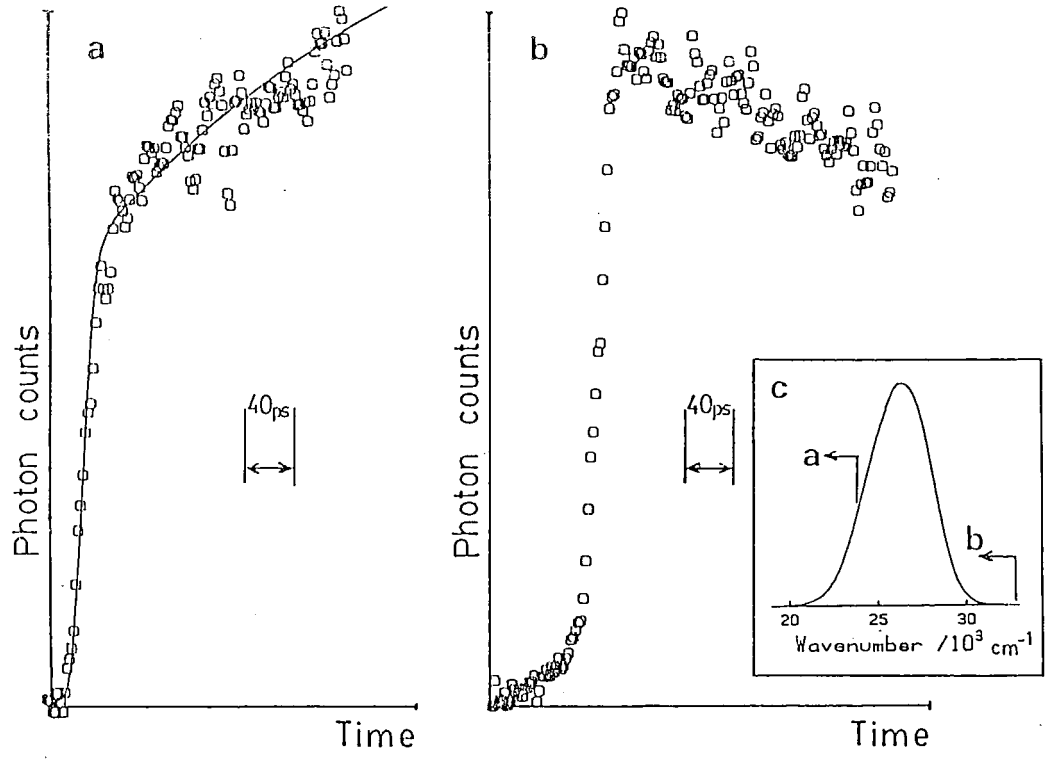

Figure 1. Emission rise transients of hydrated Ce^{3+} ion in ethylene glycol. The emission was detected with the monitoring wavelengths varied by means of cut-off filters (a: > 420 nm; b: > 300 nm). —: the best fit.

III-C-4 Photochemistry of 9, 10-Anthraquinone-2, 6-disulphonate

John N. MOORE, David PHILLIPS (*Royal Institution*), **Mobuaki NAKASHIMA, and Keitaro YOSHIHARA**

The photochemistry of 9, 10-anthraquinone-2, 6-disulphonate (AQ26DS) has been studied by observation of the transient emission and absorption following nanosecond laser excitation. Spectra and kinetics are reported for five different transient species as shown in Figure 1; the triplet, the semiquinoe radical anion and neutral radical, and two complexes formed by reaction of the triplet with water. Despite problems due to spectral overlap and the presence of up to three transients at the same time following excitation, spectra assignable to each species have been obtained by suitable choice of the chemical conditions.

A study is presented of the effect of pH, and anthraquinone and oxygen concentrations on the yields and kinetics of the transients and this allows correlation to be made between the species observed immediately after excitation and the hydroxylated

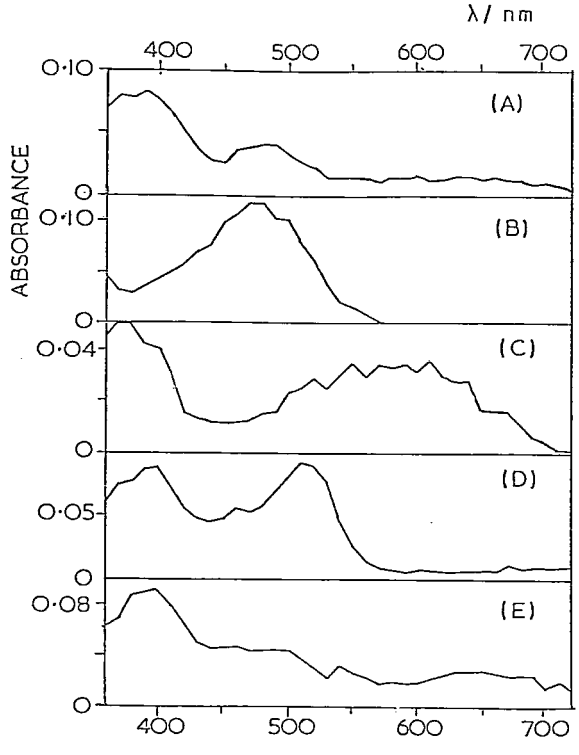

Figure 1. A summary of the five different transient spectra obtained on photolysis of AQ26DS. (a) ^{3}AQ26DS, (b) transient B, (c) transient C, (d) AQ26DS at 500 ns, and (e) AQ26DSH.

derivatives formed as permanent products. A mechanism is proposed which accounts for the observations in aqueous solution.

III-C-5 Nanosecond Laser Flash Photolysis Study of 1, 2-Bispyrazylethylene

Pill-Hoon BONG, Kyo Ho CHAE, Sang Chul SHIM, (*Korea Adv. Inst. Sci. Tec.*), **Nobuaki NAKASHIMA, and Keitaro YOSHIHARA**

Nanosecond laser flash photolysis results of 1, 2-bispyrazylethylene indicate an efficient intersystem crossing on direct excitation. The triplet energy level of trans isomer lies close to 39.0 kcal mol^{-1} and that of cis isomer lies between 35.1 to 39.0 kcal mol^{-1}. The triplet-triplet absorption maxima of trans isomer is blue shifted and the absorption spectra show fine structures because of the change of the energy gap between the $^3(n, \pi^*)$ and the lowest $^3(\pi, \pi^*)$ state as the polarity of the medium increases as shown in Figure 1. The directly measured triplet lifetime of trans isomer, 160 nsec, by laser flash photolysis also indicates that the direct photoisomerization of this compound proceeds through the triplet manifold in contrast to stilbene.

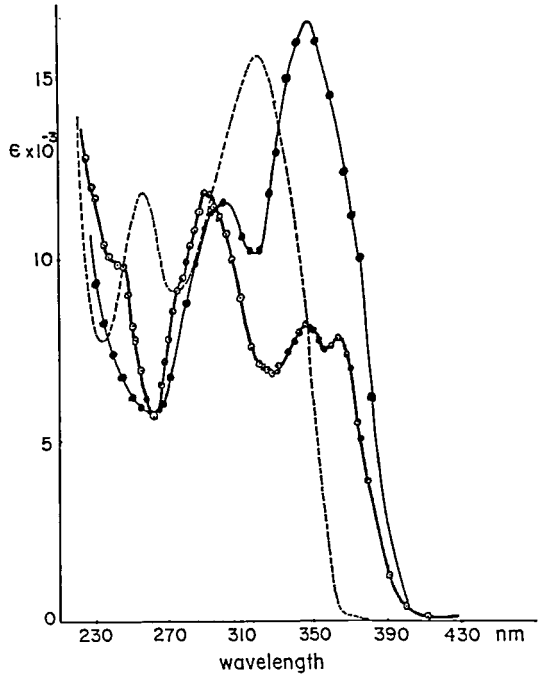

Figure 1. UV absorption spectrum (------) and triplet-triplet absorption spectrum of trans-BPE in n-hexane (•——•) and in methanol (o——o).

III-C-6 Photochemical *trans* ⇌ *cis* isomerization of 1, 2-Bispyrazylethylene

Pill-Hoon BONG, Hyeong Jin KIM, Sang Chul SHIM (*Korea Adv. Inst. Sci. Tec.*), **Kyu Ho CHAE** (*Chonnam National Univ.*), **Nobuaki NAKASHIMA, and Keitaro YOSHIHARA**

The direct and sensitized *trans* ⇌ *cis* photoisomerization of 1, 2-bispyrazylethylene (BPE) is investigated in various conditions. Quantum yields of the direct *trans* → *cis* photoisomerization increase with increasing solvent polarity because of the proximity of the lowest $^1(n, \pi^*)$ and $^1(\pi, \pi^*)$ states. pH and salt effects on the energy levels of these two states lead to opposing changes in photoisomerization and fluorescence quantum yields. Azulene qsuenches the direct and sensitized photoisomerization giving the same Stern-Volmer constant indicating that the triplet state is the reactive state in both cases. The directly measured triplet lifetime of *trans*-BPE by laser flash photolysis is the same as the lifetime calculated from the azulene quenching studies. Laser spectroscopy also indicates efficient intersystem crossing following direct irradiation. Decays of the triplet states (~ 160 ns) is accompanied by depletion of the ground states as shown in Figure 1. From these results, it is concluded that the direct photoisomerization of BPE proceeds through the triplet manifold in contrast to stilbene which undergoes direct *trans* ⇌ *cis* photoisomerization through the singlet manifold.

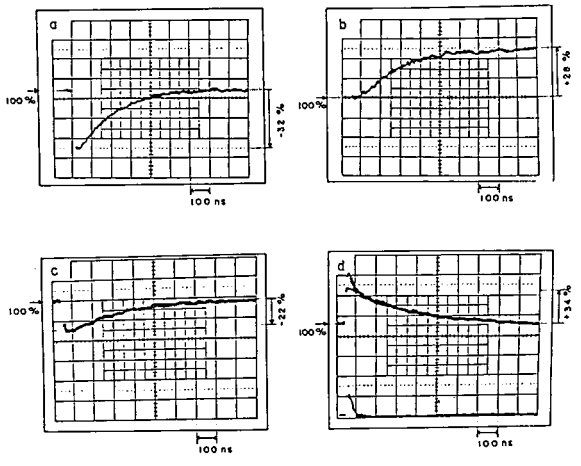

Figure 1. Nanosecond laser spectroscopy of BPE in methanol at room temperature; a, the triplet decay curve of trans-BPE at 376 nm; b, the trans-BPE depletion curve; c, the triplet decay curve of cis-BPE at 676 nm; d, the cis-BPE depletion curve.

III—D Solar Energy Conversion by Using Photocatalytic Effects of Semiconductors and Dyes

Essential roles are played by semiconductors and dyes in the photocatalytic effects to which a particular attention has been paid in connection to the direct conversion of solar energy to chemical energy. One of the most important applications is the water splitting reaction. Photocatalytic reactions of water with various organic compounds are also interesting not only from the view point of hydrogen production but also from that of the application to organic synthesis. In order to elucidate the mechanism of these photocatalytic reactions, we need detailed knowledges on the electronic structures of adsorbed molecules, the fundamental processes of photoinduced electron transfer at the semiconductor-liquid interface and catalysis on the surface. Work on the following topics is in progress with the purpose of clarifying the photocatalytic effects of semiconductors and dyes from the view point of solar energy conversion.

III-D-1 Visible-Light Induced Water Splitting on New Semiconductor Electrodes Made by Photolithography

Masahiro HIRAMOTO, Kazuhito HASHIMOTO, and Tadayoshi SAKATA

The photocorrosion of small bandgap semiconductors has been a difficult barrier to the stable and efficient decomposition of water with visible light. Here we report a new type of semiconductor electrode and its application to water splitting, especially concerning oxygen evolution. The surface of an electrode is partially coated with thick metal films (nickel) and the rest of it is coated with a transparent metal oxide film (silicon oxide) by making use of a photolithography technique. By applying this new coating method to several kinds of semiconductors, we have succeeded in an efficient oxygen evolution on Si electrodes with a p-n junction (p^+n-Si) or an MIS junction (MIS-Si) in concentrated alkaline solutions. This method can also be applied to *n*-CdS/*p*-CdTe hetero-junction photoanodes. Figure 1 shows photocurrent density (j)–potential (U) curves for p^+n-Si coated with SiO and Ni. Although a weak photocurrent was observed in a dilute alkaline solution (curve a), it increased dramatically in a concentrated alkaline solution (curve b). The quantum yield of oxygen evolution is about 45% over the whole visible region (from 600 to 800 nm). The electrode was stabilized for more than 100 hours and a photocurrent of 20 $mAcm^{-2}$ was continuously flowed. For *n*-Si with an MIS structure, microscopic photolithography was found to improve the efficiency. These results have important implications regarding photoelectrochemical energy conversion, since the present method is possibly a general solution for the stabilization of semiconductors.

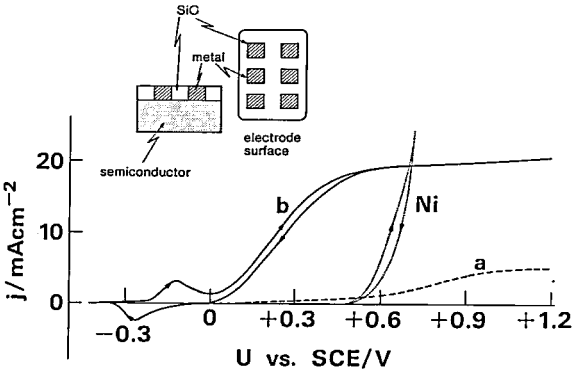

Figure 1. Photocurrent density (j)–potential (U) curves for a p^+n-Si electrode and for a Ni electrode (dotted curve). The electrolytes are 20% NaOH aqueous (curve b and Ni) and Na_2SO_4 aqueous solutions which were adjusted to pH 12.8 with NaOH (curve a).

III-D-2 Effect of Semiconductor on Photocatalytic and Photoanodic Decomposition of Lactic Acid

Hisashi HARADA*, Tadayoshi SAKATA, and Toyotoshi UEDA* (**Meisai Univ.*)

[*J. Am. Chem. Soc.*, **107**, 1773 (1985)]

The specificity of the semiconductor to a given reaction is important to control the reaction. We

have reported the dependence of the photocatalytic reaction of lactic acid on the kind of semiconductor. In that paper, the following reactions are proposed,

for Pt/TiO_2: $CH_3CH(OH)COOH \rightarrow CH_3CHO + H_2 + CO_2$

for Pt/CdS: $CH_3CH(OH)COOH \rightarrow CH_3COCOOH + H_2$

Similar results were obtained also from other photoelectrode reactions, as seen in Table 1.

These clear differences in the reaction might be explained by the following three factors; they are the difference in oxidation power of the hole in the valence band, the difference in ability of current doubling effect arising from different energy levels at the conduction band edge, and the difference in adsorption property of the lactic acid to the surface of semiconductors. We measured and discussed photoanodic and potentiostatic (dark) reactions for several electrodes in order to confirm the main factor controlling the reaction. First, potentiostatic oxidation of lactic acid was carried out using a glassy carbon electrode at 1.3 V, 1.5 V and 1.6 V vs. SCE. However, as shown in Table 1, pyruvic acid could not be detected even at 1.3 V which corresponded to the weakest oxidation power. Second, current doubling effect was observed not only on TiO_2 but also on CdS photoanode, when lactic acid was added to an electrolyte. Thus threre was no evident diffrence in the level effects of either valence band or conduction band edge. Therefore, the third factor might be the main reason for controlling the reaction. This interpretation was examined by the photocatalytic reaction products using ZnS and also by the photo-reaction products of Fe (III) complex with lactic acid.

Table I. Photoanodic and Potentiostatic Oxidation Products from Lactic acid Solution

Electrode	TiO_2	CdS	$SrTiO_3$	ZnO	Glassy carbon*			Pt*		Au*
Potential (V vs. SCE)	0	0	+1.0	+0.6	+1.3	+1.5	+1.6	+1.7	+2.0	+1.7
Quantity of electricity (C)	9.65	9.65	9.65	9.65	16.2	9.65	19	21	29	19
Product (μmol)										
CH_3OH	4.5	–	–	–	–	–	–	2.5		10
CH_3CHO	58	trace	40	36	67	47	181	55	55	94
$CH_3COCOOH$	–	45	5	trace	–	–	–	–	–	–

Irradiated with 500 W Xe lamp. Electrolyte was lactic acid–0.1 M K_2SO_4 solution (1:10 in volume).
* Dark reaction for metal electrodes.

III-D-3 Photocatalytic Reactions and the Polymorphology of Semiconductor

Tadayoshi SAKATA, Kazuhito HASHIMOTO, and Masahiro HIRAMOTO

The control of photocatalytic organic reactions is one of the important problems. Concerning this problem, we report here the dependence of photocatalytic reaction on the morphology of a semiconductor photocatalyst. In the decomposition of lactic acid and alanine synthesis from lactic acid and ammonia, the reaction depends strongly on the kind of CdS as a photocatalyst. Table 1 shows the result in the case of bare CdS photocatalysts under the same experimental condition. As shown in this table, CdS (Furuuchi, hexagonal) showed a high activity of hydrogen production both for reaction (1) and (2). On the other hand, for CdS (Mitsuwa, amorphous), hydrogen production is suppressed in the presence of NH_3, while alanine is produced efficiently. In this case, electrons excited into the conduction band are used mainly for the reduction of hydrogen ion (hydrogen production). This clear difference in photocatalytic activity is possibly brought about by the difference in the band structure and catalytic properties which depend on the morphology of CdS.

Table I.

$CH_3CH(OH)COOH \rightarrow CH_3COCOOH + H_2$ (1)

$CH_3CH(OH)COOH + NH_3 \rightarrow CH_3CH(NH_2)COOH + H_2O$ (2)

Photocatalyst	cryst. struct.	React. (1)	React (2)	
		H_2 (μmol/h)	Ala (μmol/h)	H_2 (μmol/h)
CdS (Furuuchi)	Hexa.	235	23	54
CdS (Mitsuwa)	Amor.	101	120	2
CdS (Kojundo)	Cub.	24	12	5

III-D-4 The Role of Excited Dyes as a Photocatalyst in the Photocatalytic Amino Acid Synthesis.

Tadayoshi SAKATA, Kazuhito HASHIMOTO, and Masahiro HIRAMOTO

Various amino acids were produced efficiently with visible light from keto- and hydroxy carboxylic acids in ammonia water through photocatalytic reactions with dyes and semiconductors.[1-3] The quantum yield of these reactions amounts to 40%. Moreover the reactions are selective and depend on the reducing power of excited dyes or semiconductors. Table 1 shows the correlation between reducing power of the excited dyes, photopotential of the galvanic cell < glassy carbon (light) | dye, NH_3, keto-carboxylic acid, TEOA | SCE >, and the production rate of valine. As seen in this table, ZnTPPS and acridine yellow whose oxidation potentials at the excited state are quite negative work as good photocatalysts, while methylene blue, whose oxidation potential at the excited state is not so negative, shows no photocatalytic activity. Since the imino acids were found to be reduced at ca. $-1.1 \sim -1.2$ V vs SCE at Hg electrode, this result seems to be reasonable.

References

1) T. Sakata, *Denki Kagaku*, 53, 15 (1985).
2) T. Sakata, *J. Photochemistry*, 29, 205 (1985).
3) T. Sakata and K. Hashimoto, *Nouv. J. Chim.*, in press.

Table I.

Dye	Oxidation potential of the lowest excited singlet state E° (D*) (V vs SCE)	Reduction potential at pH 7 (Vvs SCE)	Electrode potential of glassy carbon (V vs SCE)		Photo-potential (V)	Rate of Val formation (μmol/10h)
			under irradiation	at dark		
ZnTPPS	−1.30 V	−1.32 V	−1.01 V	−0.21 V	0.80 V	350
Acridine Yellow	−1.69	−0.97	−1.13	−0.22	0.91	286
Erythrosin	−1.01	−0.53	−1.09	−0.26	0.83	72
methylene blue	−0.71	−0.25	−0.52	−0.23	0.29	0

III-D-5 The Effects of Water Vapor and Temperature on the Electron Transfer from Adsorbed Ru $(bpy)_3^{2+}$ to TiO_2 Powder.

Kazuhito HASHIMOTO, Masahiro HIRAMOTO, and Tadayoshi SAKATA

The electron transfer from adsorbed dye to semiconductor substrate is one of the fundamental processes in the dye sensitization of semiconductor. We have been studing this process by measureing luminescence decay curves and time resolved spectra (TRS) of Ru $(bpy)_3^{2+}$ adsorbed on TiO_2 powders in vacuo.[1] We found strong electron transfer rate dependence on water vapor pressure in this system. As shown in Figure 1, introduction of water vapor to the system reduces the initial luminescence decay rate. Because the decay profile is mainly determined by the electron transfer rate,[1] this result

implies that the electron transfer rate becomes slower in the presence of water. Moreover, spectral blue shift of the fast decay component, which is caused by the strong interaction of the dye molecule with the surface, is reduced by water vapor. These phenomena are explained as follows. Because of the hydrogen bond, water molecules adsorb more tightly on the oxide semiconductor surface than Ru $(bpy)_3^{2+}$ moleculs; this reduces the interaction between the dye molecules and the surface. We also measured the luminescence decay curves in vacuo in the temperature range of room temperature and liquid nitrogen temperature. The electron transfer activation energy of about 0.01 eV is estimated from these results.

Reference

1) T. Kajiwara, K. Hashimoto, T. Kawai and T. Sakata, *J. Phys. Chem.*, 86, 4516 (1982).

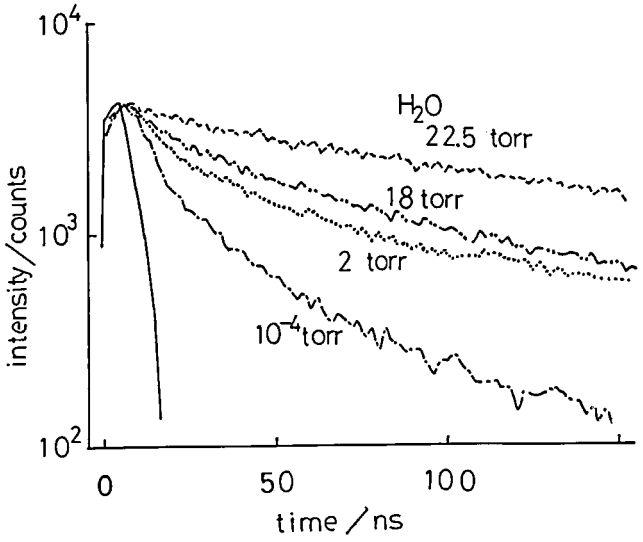

Figure 1. The effect of water vapor on the luminescence initial decay curve.

III-D-6 Luminescence Dynamics of Ru Complexes Chemically or Physically Immobilized on Semiconductor Particles in Water

Hirofumi TAKEMURA*, Tetsuo SAJI*, Masamichi FUJIHIRA*, Shigeru AOYAGI*, Kazuhito HASHIMOTO, and Tadayoshi SAKATA (**Tokyo Inst. Tech*)

The luminescence decay curves are recorded for ruthemium (II) complexes in water and in some organic solvents which are: i) chemically bound (covalently linked) to TiO_2 and SiO_2 particles, or ii) physically adsorbed on TiO_2, SnO_2, SiO_2, and Al_2O_3 particles. In both chemically and physically immibolized forms, the excited complexes on the semiconductors, i.e. TiO_2 and SnO_2, had significantly shorter lifetimes than those on the insulators, i.e. SiO_2 and Al_2O_3 as shown in Figure 1. The rate constants for electron transfer from the surface confined excited Ru (II) complexes to the semiconductor particles in contact with CH_2Cl_2 and H_2O are estimated from these curves. The effects of solvent and pH on the rate constants are also investigated.

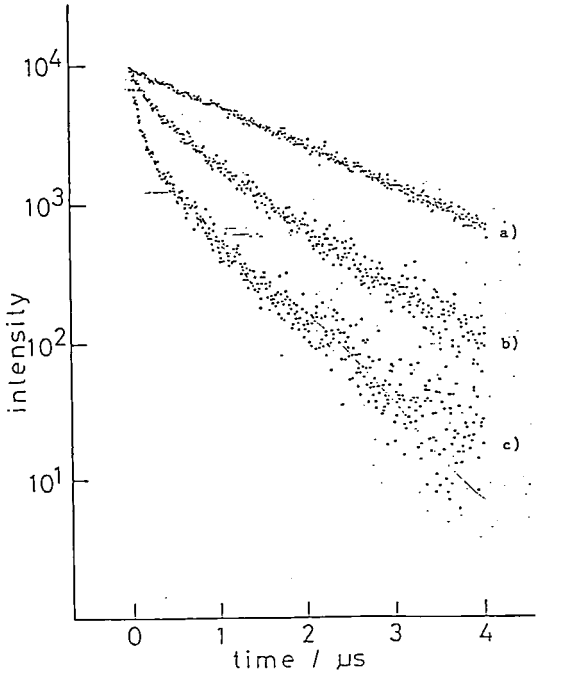

Figure 1. Luminescence decays of (a) 1-ester-SiO_2, (b) 1-amide-TiO_2, and (c) 1-ester TiO_2 in CH_2Cl_2.

III-D-7 Electron Transfer Rates from Adsorbed Organic Dyes to Various Semiconductors

Kazuhito HASHIMOTO, Masahiro HIRAMOTO, and Tadayoshi SAKATA

We have measured the luminescence decay curves of rose bengal (RB) and rhodamine B (Rh B) adsorbed on various semiconductors such as TiO_2, ZnO, and SnO_2. The energy diagrams for these systems are shown in Figure 1. The decay curves for RB

and Rh B adsorbed on quartz plate are also measured as references. The electron transfer rates from excited singlet states of these dyes to the conduction band of the semiconductors are determined from these decay curves. The rates show material dependence on both the dyes and semiconductor substrates. For example, the electron transfer rates from RB to TiO_2 and ZnO are slower than $10^9 s^{-1}$, however, the rate to SnO_2 is about $10^{10} s^{-1}$. Similar results are obtained for Rh B, but the electron transfer rate to each semiconductor is slower than that of RB. These results could be explained by the difference of the energy levels excited states of both dyes and conduction bands of semiconductors. Moreover it is found that the excited states of monomers of these dyes are easily quenched by the energy transfer to dimers. These results lead the conclusion that in the dye sensitized semiconductor electrochemical cell with these dyes, in which the dye concentration is in the order of 10^{-5}M, the light energy absorbed by monomer dye is transfered to dimer dye followed by the electron transfer to the semiconductor.

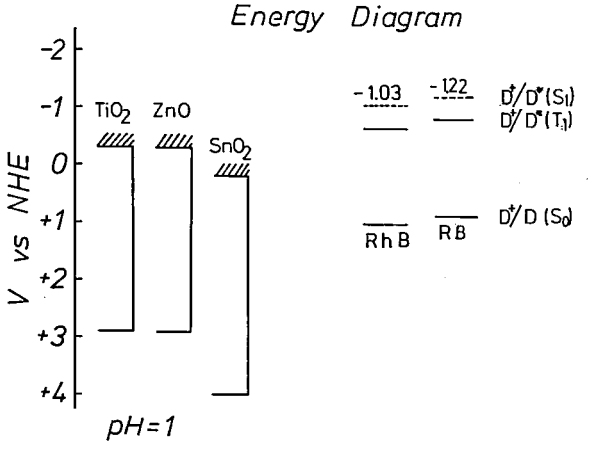

III-D-8 Transient Photocurrent and Luminescence Lifetime in the Photodiode of Merocyanine Dye Thin Flim

Kazuhito HASHIMOTO, Tadayoshi SAKATA, Yukihiro OZAKI*, Masahiko YOSHIURA*, and Keiji IRIYAMA* (**Jikei Univ.*).

[*Nippon Kagaku Kaishi*, 1178, 1985]

The mechanism of photocurrent generation in organic dye photodiode was studied by measuring both transient photocurrents and luminescence lifetimes following pulsed laser irradiation. The photodiode consists of an evaporated merocyanine dye film sandwiched between Al and Ag metal films. The singlet excition lifetime in the dye film was determined to be about 200 ps. A simple analytical model of transient photocurrent was proposed. This model treats the system as an RC circuit with a response time that is the rate constant for a recombination of charge carrier in the dye film. From the analysis of the risetimes, it is concluded that the transient photocurrent rise is determined by the diffusion process of an exciton in the bulk of the dye film. From these results it is inferred that the charge carrier is generated from an intermediate species with a lifetime of more than several hundred nanoseconds. Moreover, it is proposed that the charge separation occurs not only at the dye film-metal interface but also in the dye film bulk. The decay time of the transient photocurrent is determined by the RC constant of the circuit. The values of internal capacitance and internal resistance of the photodiodes are obtained. The rate constant of the recombination of charge carriers is also estimated to be about $5 \times 10^3 s^{-1}$.

III-D-9 Relaxation Processes of Excited States of H_2TPP on a Silver Surface

Shigeru OHSHIMA*, Takashi KAJIWARA*, Masahiro HIRAMOTO, Kazuhito HASHIMOTO, and Tadayoshi SAKATA, (**Toho Univ.*).

In order to investigate the relaxation processes of excited states of a dye molecule adsorbed on a metal surface, the following molecule-metal system was prepared by vacuum evaporation; a layer of tetraphenylporphine (H_2TPP) (10 Å in thickness) was separated from a silver surface by a layer of hexatriacontane (HTC). The thickness of the HTC layer (L Å) was varied in the range of 0 Å through 600 Å. For this system, the fluorescence spectrum and lifetime of the H_2TPP were measured with an excitation wavelength of 570 nm as a function of distance to the surface (L). The relative quantum yield (ϕ) was determined from both measurements independently and plotted in Figure 1. A significant

difference can be seen between them; when L is decreased, ϕ obtained from the spectrum data falls rapidly toward zero for L < 600 Å, while ϕ calculated from the lifetime data keeps almost constant for L > 100 Å and then drops gradually to the value at L = 0 Å. The latter is remarkably different from the previous experimental results and theoretical predictions. The following explanations are possible: (1) A stading wave generated at the metal surface causes the fluorescence intensity to decrease due to small amplitude of the excitation wave near surface, but it gives no effects to the lifetime. (2) The rate of energy transfer is slower than that previously expected, and competition processes such as intermolecular relaxation or charge injection into the metal can occur considerably.

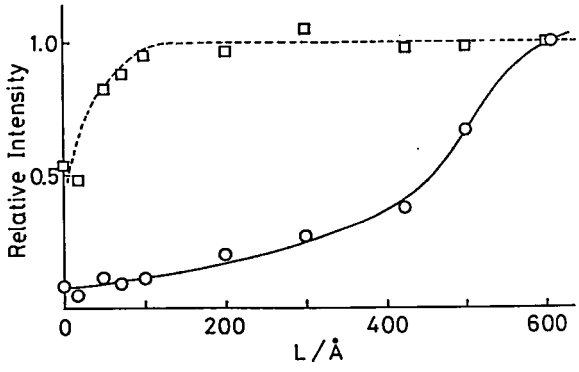

Figure 1. The relative quantum yields of fluorescence as a function of distance from a silver surface.
○: determined from the spectrum data
□: determined from the lifetime data

III—E Dynamical Processes in Electronically and/or Vibrationally Excited Molecules

III-E-1 Orientational Site Splitting of Methyl C-H Overtones in Acetone and Acetaldehyde

Ichiro HANAZAKI, Masaaki BABA and Umpei NAGASHIMA

[*J. Phys. Chem.*, in press]

Gas phase absorption spectra have been measured by an FTIR spectrometer for the C–H stretching overtones in acetone and acetaldehyde in the region $\Delta\nu = 1 \sim 4$. Measurements have also been made for the $\Delta\nu = 1$, 2 and 3 transitions of CD_3COCD_2H, which exhibits pure local mode transitions due to the in-plane and out-of-plane oriented C–H bonds (Figure 1). These data, together with the theoretical expression developed to describe the interaction in the methyl group with orientationally inequivalent C–H bonds, have shown that the Birge-Sponer relation holds down to the fundamental transition even for the methyl C–H stretching modes in $(CH_3)_2CO$ and CH_3CHO which are not "isolated" as in the case of benzene or CD_3H.

Origin of the splitting into the in-plane and out-of-plane bands is discussed on the basis of *ab initio* SCF calculations with a 6–31G** basis set. Analysis of the "group" overlap population between the methyl group and the rest of the molecule has shown that the splitting is determined by stabilization of the out-of-plane stretched conformation due to hyperconjugation and by the difference of the through-bond σ-interaction between the out-of-plane and in-plane stretched conformations.

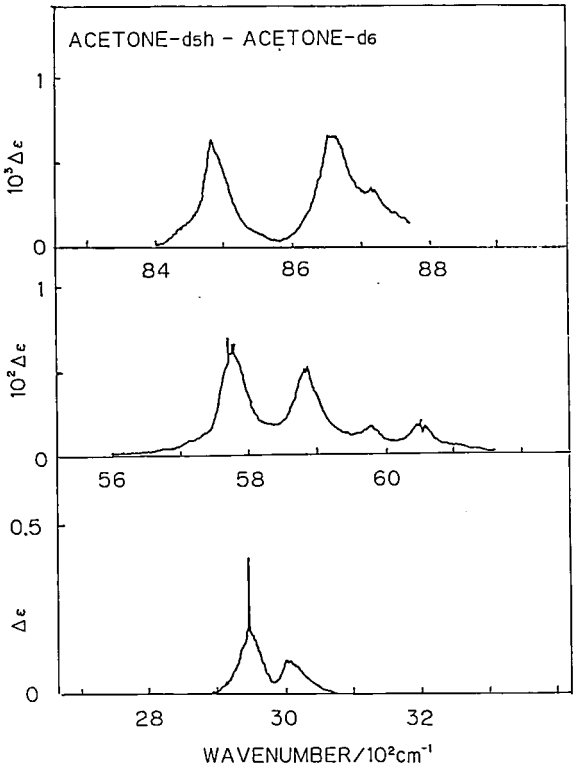

Figure 1. Absorption spectrum of gaseous $(CD_3)CO$ (CD_2H) for the $\Delta\nu = 1$, 2 and 3 transitions.

III-E-2 *Ab initio* Study of Methyl Internal Rotation of Acetaldehyde in the S_1 (n,π^*) State

Masaaki BABA, Umpei NAGASHIMA, and Ichiro HANAZAKI

[*J. Chem. Phys.*, **83**, 3514 (1985)]

Ab initio SCF calculations have been performed on the methyl internal rotation of acetaldehyde in the S_1 (n, π^*) state as well as in the ground state. The Gaussian-type basis set of Dunning and Fuzinaga was used with p or d type polarization functions. The calculated barrier heights to methyl internal rotation are shown in Figure 1. They are in good agreement with the experimental values which have been determined by the microwave absorption or the fluorescence excitation spectra[1]. The Mulliken population analysis has revealed that the π-bonding between the methyl and formyl groups (hyperconjugation) is important in determining the barrier. The change of the stable conformation from the H eclipsing O type in the ground state to the "H anti-eclipsing O" conformation in the S_1 state is shown to be due to the presence of an antibonding π^* electron in the latter.

Reference

1) M. Baba, I. Hanazaki, and U. Nagashima, *J. Chem. Phys.* 82, 3938 (1985)

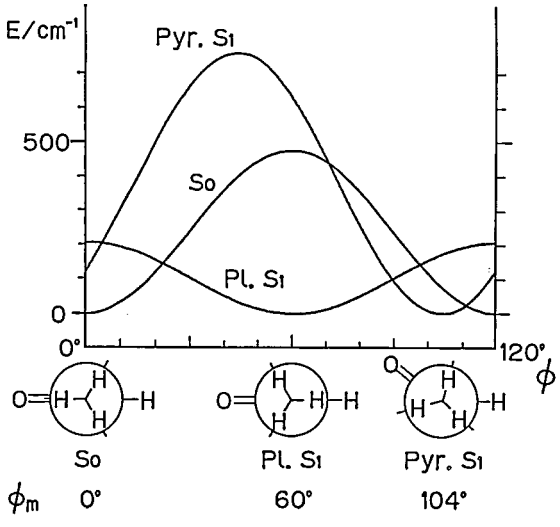

Figure 1. Calculated potential curves for the methyl internal rotation of acetaldehyde in the S_0, planar S_1 and pyramidal S_1 states.

III-E-3 Spectroscopic Study of 2-Indanone; The T_1 (n, π^*) and S_1 (n, π^*) States

Masaaki BABA, Ichiro HANAZAKI, and Noboru HIROTA* (*IMS and Kyoto Univ.**)

[*J. Chem. Phys.*, **83**, 3318 (1985)]

Phosphorescence excitation spectrum of 2-indanone single crystal has been observed at 1.5 K (Figure 1 (a)). The lowest triplet state T_1 is of $\pi^* \leftarrow n$ character which is localized in the carbonyl moiety. The very weak 0–0 band is located at 28853 cm^{-1}. The molecule is pyramidally distorted like formaldehyde and has an active out-of-plane C=O wagging mode. The barrier height to inversion (V) and the C=O bond angle at the potential minimum (θ_m) have been determined to be 883 cm^{-1} and 37°, respectively.

This distortion is consistent with the previous

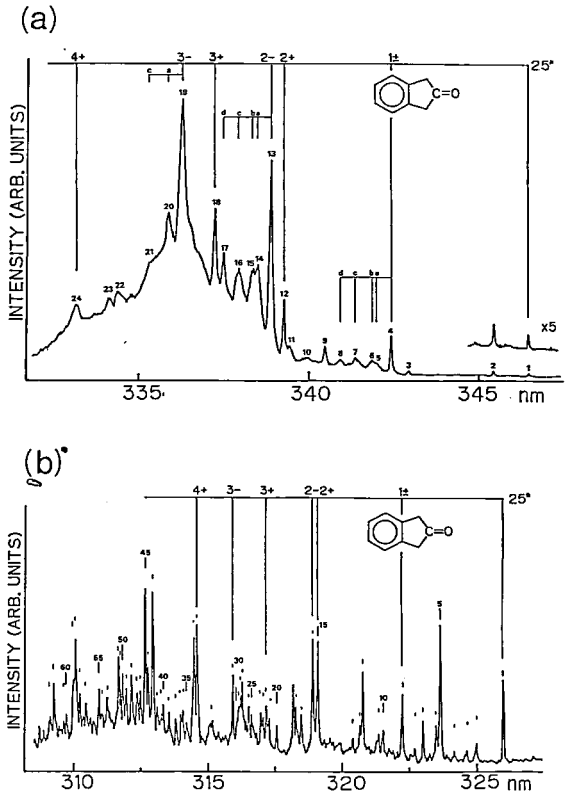

Figure 1.
(a) Phosphorescence excitation spectrum of 2-indanone single crystal at 1.5 K.
(b) Fluorescence excitation spectrum of 2-indanone in an Ar supersonic nozzle beam.

ODMR results. Fluorescence excitation spectrum of 2-indanone has also been observed using a pulsed supersonic nozzle beam technique (Figure 1 (b)). The lowest excited singlet state is also of $\pi^* \leftarrow n$ character localized in the carbonyl moiety. The 0–0 band is relatively intense and located at 30664 cm^{-1}. We obtained $\nu = 1006$ cm^{-1} and $\theta_m = 37°$ for the S_1 state. The spectroscopic results and *ab initio* calculation show that the S_1 and T_1 states of 2-indanone are very similar to those of cyclopentanone.

The S_1 spectrum is much more complicated than the T_1 spectrum. The difference of the spectral features of these two states is explained by the symmetry lowering of the molecule and by the vibronic coupling with higher excited states.

III-E-4 The S_1 States of Intramolecularly Hydrogen-bonded Molecules in a Supersonic Beam and in a Mixed Crystal

Teruhiko NISHIYA*, Noboru HIROTA*, Masaaki BABA, and Ichiro HANAZAKI (*Kyoto Univ.* and IMS*)

Intramolecularly hydrogen-bonded molecules such as *o*-hydroxyacetophenone (OHAP) and salicylamide (SAM) are of great interest in view of the possibilities of a four-level proton transfer laser and of an information storage device at molecular level. We have measured fluorescence excitation and emission spectra of those compounds in a durene mixed crystal as well as in a He supersonic nozzle beam.

The fluorescence emission spectra of OHAP and SAM in mixed crystals have maxima at 470 and 420 nm, respectively. Sharp vibronic bands observed near the 0–0 transitions are assigned to the C=O bending, C–OH stretching and O–H bending vibrations. We also observed intense broad bands in the crystal excitation spectra at ~ 320 nm. The Franck-Condon envelope of the excitation spectra suggests a single minimum, strongly distorted potential with respect to the proton transfer. A number of sharp bands are also seen in the excitation spectra of SAM in crystal (Figure 1 (a)) and in a He supersonic jet (Figure 1 (b)). Prominent vibronic bands are also associated with the O–H···O vibration. However, the more intense 0–0 band in the latter indicates smaller distortion of the potential in the gas phase.

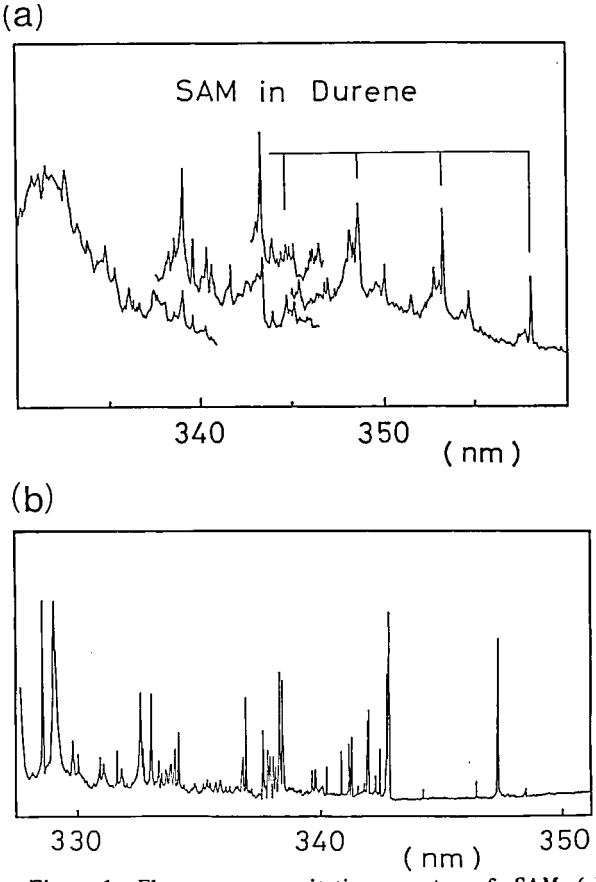

Figure 1. Fluorescence excitation spectra of SAM (a) in a durene mixed crystal at 4.2 K and (b) in a He supersonic jet.

III-E-5 Electronic Spectra of Hydrogen-bonded Indazoles in a Supersonic Nozzle Beam

Masayo N. TERAJIMA$^+$, Noboru HIROTA*, Masaaki BABA, and Ichiro HANAZAKI ($^+$*Tokai Women's Junior College, *Kyoto Univ. and IMS*)

It is known that indazole shows the excited state proton transfer in some carboxylic acids solutions. We observed fluorescence excitation and emission spectra of indazole and its complexes with water, ethanol, formic acid and acetic acid (Figure 1). The 0–0 band of the S_1 state of free indazole is located at 34473 cm^{-1}. The energies of observed vibronic bands are in good agreement with those of the absorption spectrum of indazole vapour. The 0–0 band of complex is red shifted. The values of red shifts are 272 (water), 201 (ethanol), 243 (formic acid) and 256 cm^{-1} (acetic acid). The

fluorescence emission spectra of complexes are very similar to that of free indazole and we could not observe emission from the proton-transfered state in a supersonic beam. It is suggested that the proton transfer observed in solution is due to the solvent effect.

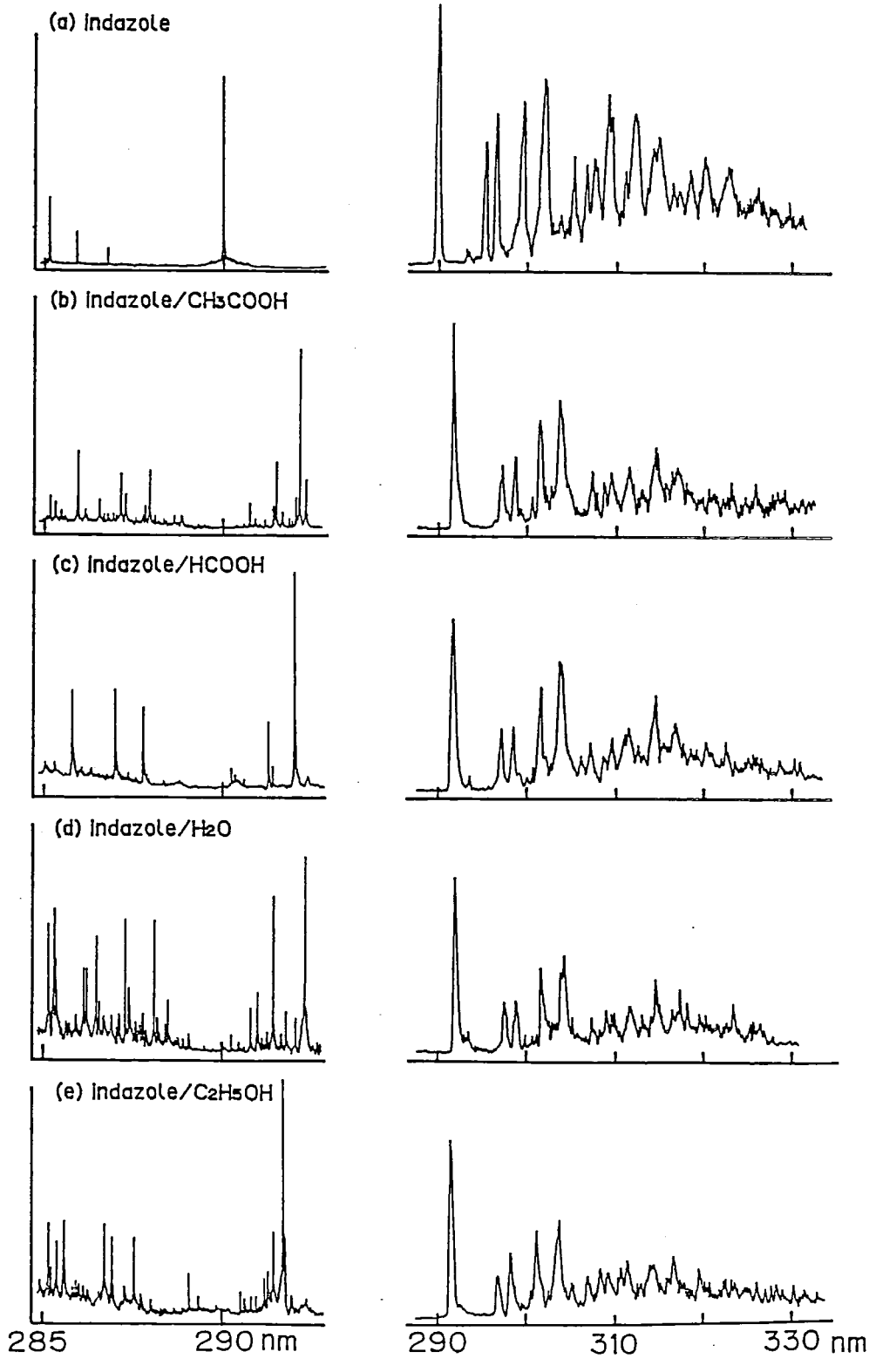

Figure 1. Fluorescence excitation (left) and emission (right) spectra of indazole and its complexes in a He supersonic nozzle beam.

III—F Study of Molecular Association in Liquid and Gas Phases

Molecular association is one of the most important and interesting phenomena in nature, particularly, in its roles in chemical evolution and molecular activities in living cells. Theoretical approaches, such as *ab initio* calculation analysis of intermolecular interaction of small and large molecular systems, have currently made progress and given reliable knowledge on intermolecular forces. On the other hand, astrophysically, icy dust formation processes are highly related to intermolecular forces which act in collision complexes of interestellar molecules. At such a very low temperature phase transition of molecular condensates hardly occurs, and this results in the accretion of various molecules on amorphous ices. It is not known how those molecules form stable structures. This problem is also studied in section III-H.

Structure of solute-solute or solute-solvent associates has been the subject studied theoretically and experimentally in somewhat detail. Here, we show a new mass spectrometric approach coupled with our original liquid expansion technique, which enables us to study various kinds of molecular associates more directly.

III-F-1 Generation of Cluster Beams from Liquid Jet

Nobuyuki NISHI, Kazunori YAMAMOTO, Toshio HORIGOME, and Tohru OKUYAMA

Usually, molecular beams of molecular complexes have been generated by the expansion of high pressure gas mixture into vacuum through a small nozzle. The method developed here is just the opposite. Liquid jet produced by pressing the solution through a 20 μm hole is smashed into small droplets and clusters by the collision with outer cylindrical hot gas flow. Because of sudden pressure change evapolation of molecules occurs from the surface of these droplets and clusters. This adiabatic expansion cools the molecular clusters quite rapidly leaving much smaller frozen clusters composed of stronger intermolecular bindings.

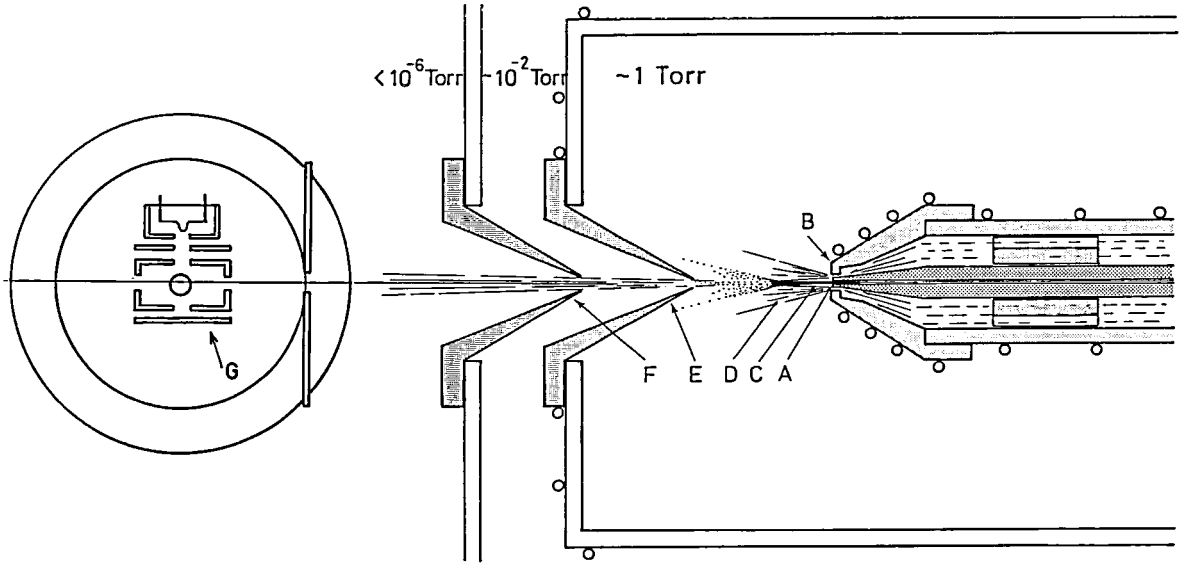

Figure 1. Main part of the apparatus generating molecular beams from liquid jet. A liquid chromatograph pumping unit is used to press out the solution in a stainless steel pipe (i.d. = 0.1 mm, o.d. = 1.59 mm) at a flow rate of 0.1–0.3 ml/min. Outside of the nozzle is surrounded by hot gas flow (N_2 or Ar) which is produced from a cyrindrical gap. The temperature at the top of the outer gas nozzle was controlled to be 100–250°C depending on the solution emitted.
A: liquid jet nozzle, B: gas nozzle cap forming a cyrindrical gap, C: liquid jet, D: gas flow, E and F: skimmers in tandem, G: ionizer.

Mass spectrometric detection requires the ionization of the surviving clusters by applying energy higher than the ionization potentials. This causes subsequent fragmentation of the clusters in most cases. Although mass spectroscopic detection posseses this problem, one can obtain information on the composition of clusters by threshold photoionization as well as low energy electron bombardment ionization.

Figure 1 schematically shows the essential part of the apparatus. Detailed explanation is given in the caption. One must note that the ionization is done at a distance sufficiently down the stream so that the vacuum of the ionization chamber is maintained lower than 2×10^{-6} Torr. For multiphoton ionization or resonance lamp ionization it is possible to locate the ionization point much closer to the nozzle.

III-F-2 A Mass Spectrometric Study of Water Association in Acetonitrile by a New Liquid Expansion Method

Nobuyuki NISHI, Kazunori YAMAMOTO, Hisanori SHINOHARA, Umpei NAGASHIMA, and Tohru OKUYAMA

[*Chem. Phys. Letters*, in press]

Liquid acetonitrile containing water was expanded into vacuum by using a coaxial dual nozzle. Figure 1 displays the electron impact mass spectrum of CH_3CN solution containing 2% of H_2O (top) and neat CH_3CN liquid which usually contains of the order of 0.2% H_2O (bottom). One can see that the addition of 2% H_2O in neat CH_3CN changes the spectral pattern quite drastically. Main sequence is constructed by the cluster $H^+ (CH_3CN)_2 (CH_3CN - H_2O)_n$ and there is a sub-sequence composed of $H^+ CH_3CN (CH_3CN-H_2O)_n$. In the CD_3CN + 2% H_2O system, the water containing cluster ions exhibit doublet peaks of $H^+ (CD_3CN)_n (H_2O)_m$ and $D^+ (CD_3CN)_n (H_2O)_m$ with an intensity ratio of 7:3. Based on these results and the concentration dependence of the spectrum, the origin of the main and the subsequences is attributed to the water chains coordinated by acetonitriles in the following form:

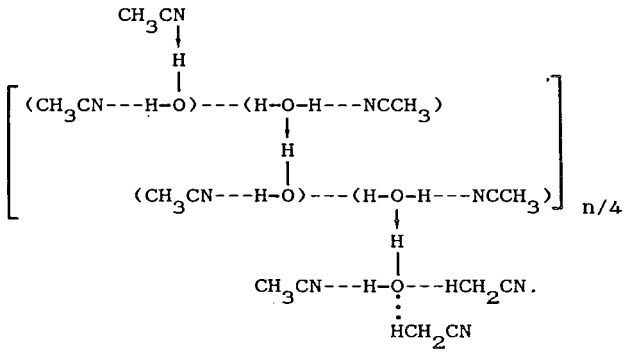

This cluster was not seen in the water concentratation more than 10% where water forms clusters similar to pure liquid water.

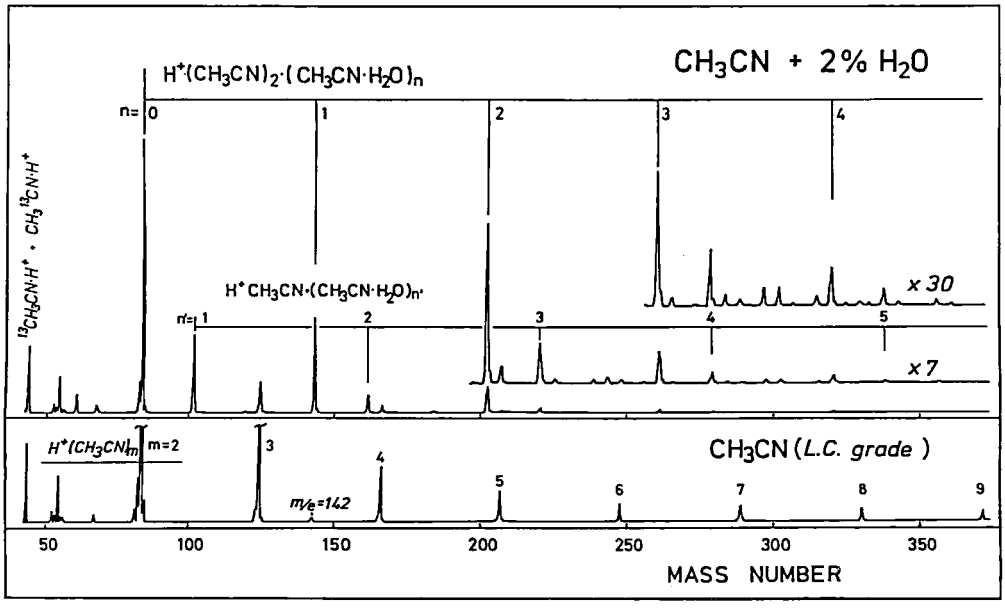

Figure 1. Mass spectra of CH_3CN solution containing 2% of H_2O (top) and neat CH_3CN (bottom; liquid chromatograhp grade). Ionization electron energy: 19 eV.

III-F-3 Mass Spectrometric Study of [Carboxylic Acid - Amine] Complexes produced by the Expansion of Aqueous Solution

Kazunori YAMAMOTO, Yoshiya TAKENOSHITA (*Kitakyushy Univ.*), **and Nobuyuki NISHI**

Carboxylic acid and amine molecules dissolved in water solution are surrounded independently by H_2O molecules in diluted solution and the formation of acid-base complexes (including salt form) is quite rare. Mass-spectrometrically, $H^+ \cdot HCOOH\text{-}CH_3NH_2$ complex was observed for solute concentrations higher than 0.5%. At the 20% solute concentration with an equivalent acid and base composition, the intensity of this one-one complex is comparable to the ion signals of $H^+ \cdot CH_3NH_2 \cdot H_2O$ and $H^+ \cdot HCOOH \cdot H_2O$. All of those signals are followed by the additional H_2O sequence. At much higher solute concentrations, pure water clusters were observed very weakly and the spectrum is dominated by the acid-base complex signals. Figure 1 shows a typical spectrum taken for a concentration ratio of 2.6 (H_2O) : 1 (HCOOH) : 1 (CH_3NH_2). The original neutral clusters of the strong signals (observed at the mass region higher than m/e = 60 (were attributed to HCOOH $(HCOOH\text{-}CH_3NH_2)_n$, $H_2O \cdot (HCOOH\text{-}CH_3NH_2)_n$, $CH_3NH_2 \cdot (HCOOH\text{-}CH_3NH_2)_n$, and $H_2O\text{-}CH_3NH_2 \cdot (HCOOH\text{-}CH_3NH_2)_n$ on the basis of the proton affinities, the ionization potentials, and the relative concentration.

The structure of these complexes is a matter of controversy. What is the nature of the intermolecular bindings ? Mass spectrometric observation can provide little information on that problem. Application of the repeller potential less than 20 ev did not give any signal in the absence of impact electrons. One-photon or two-photon resonant multiphoton ionization method with the exciting laser energy scanning and mass spectrometric detection gives us the electronic spectra of neutral clusters which may contain information on the structure of the neutral clusters.

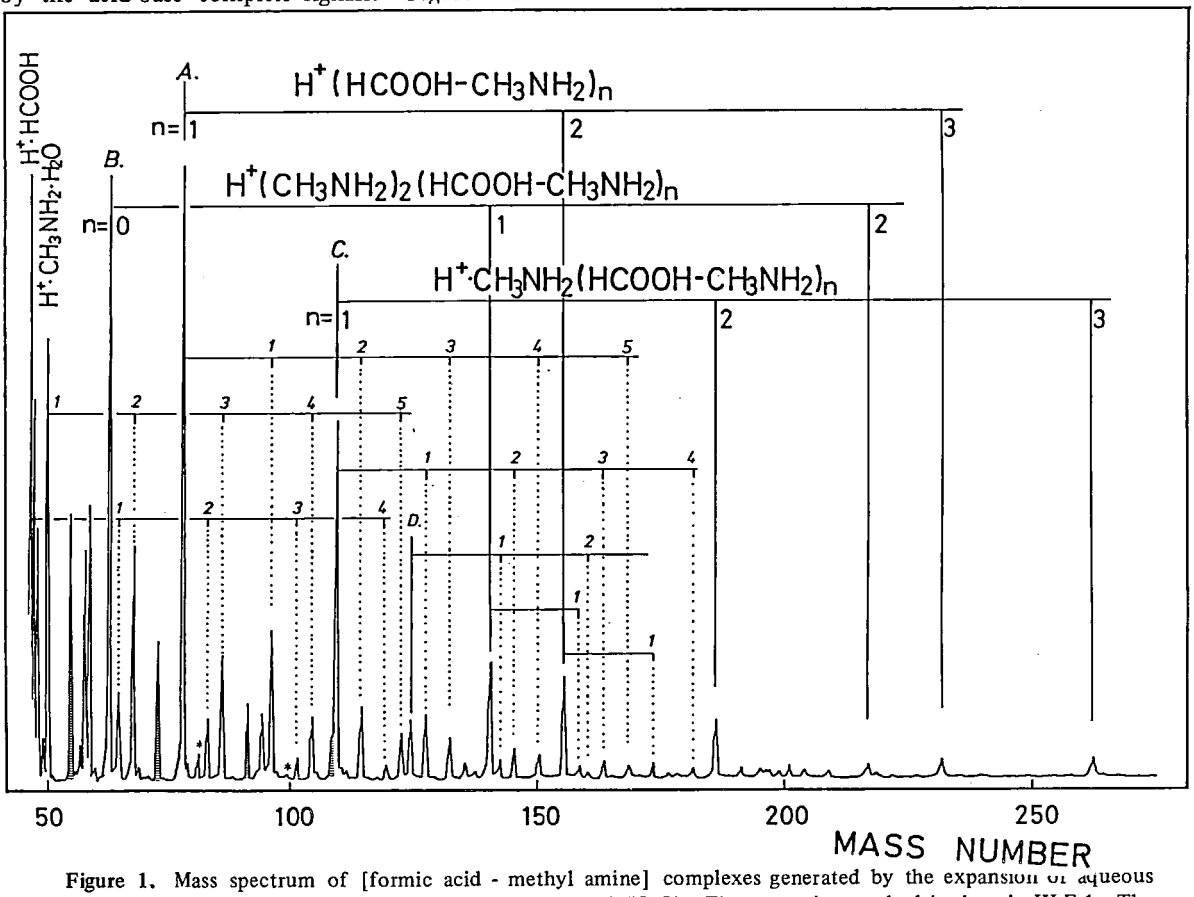

Figure 1. Mass spectrum of [formic acid - methyl amine] complexes generated by the expansion of aqueous solution with a ratio of 1 (HCOOH) : 1 (CH_3NH_2) : 2.6 (H_2O). The expansion method is given in III-F-1. The strong ion signals were observed for $H^+ \cdot [HCOOH\text{-}CH_3NH_2]$ and $H^+ \cdot [CH_3NH_2]_2$. The former accampanies the H_2O association sequence as shown by dotted lines but the water associated cluster signal of $H^+ \cdot [CH_3NH_2]_2$ ion (as indicated by *) are extremely weak suggesting that this ion is a daughter ion, most probably produced from the HCOOH $[CH_3NH_2]_2$ neutral cluster. The shaded signals are pure H_2O cluster ions $H^+ \cdot (H_2O)_n$.

III—G Photodissociation of Isolated Molecules and Surface Molecules

III-G-1 Photodissociation of surface CS_2 on CO_2 solid: Fragment translational energy and its momentum

Nobuyuki NISHI, Masahiro KAWASAKI (*Mie Univ.*), and Tohru OKUYAMA

Dynamics of photoexcited surface CS_2 molecules has been studied through the direct detection of dissociation fragments and their kinetic energy measurement using a mass spectrometer and a pulsed UV laser coupled with an ultra-high-vacuum system. Time-of-flight spectra of both fragments S and CS were measured for 193 nm laser pulse irradiation (< 10 mJ/cm^2). The observed translational energy distribution is quite different from that of molecular beam. The surface fragments showed higher energy component and the distribution is reproduced by two Boltzmann-distribution components. The low energy one was attributed to slow fragments which lost the primary kinetic energy by the collision at rough surface. Highest energy limit converges at 49 ± 2 kcal/mol for both fragments S and CS_2. Since this value is close to the total available energy of free molecule for the 193 nm dissociation, the surface fragments are considered to carry all of the total available energy for the dissociation in the extreme case (highest energy limit). This phenomena cannot seen in gas phase molecules and total available energy is devided by two fragments by keeping the momentum conservation law. Table 1 shows the mean fragment translational evergy and fragment momentum observed in various systems. In spite of the extension toward the high energy limit, the mean energies of the fragments are relatively smaller than those seen in the gas phase photodissociation. Namely, the dissociation of the surface molecules are strongly coupled with solid lattice motion dissipating excess energy.

Table I. Mean fragment translational energy and momentum

System	fragment	$\bar{E}_t$/kcal·mol^{-1}	$\bar{P}$/10^{-18}g·cm·sec^{-1}
Neat CS_2	S	10.3 ± 0.5	8.7 ± 0.2
	CS	7.7 ± 0.4	8.8 ± 0.2
CS_2 in CO_2 (1.4%)	S	10.9 ± 0.4	9.0 ± 0.2
	CS	8.0 ± 0.4	9.0 ± 0.2
CS_2 in CO_2 Annealed	S	15.5 ± 1.2	10.7 ± 0.4
	CS	12.7 ± 1.0	11.3 ± 0.4

Gas Phase E_t^{max} ($S(^3P)$) = 17 kcal/mol
E_t^{max} (CS_{high}) = 13 kcal/mol

III-G-2 Time-of-flight Photofragmentation Study of IBr

R.J. Donovan (*Univ. of Edinburg*), and N. NISHI

[*Chem, Phys. Letters*, **117**, 286, (1985)]

Photofragmentation of IBr has been studied, using time-of-flight techniques, following excitation in the region of the first Rydberg and ion-pair state transition (193 nm, ArF laser). A time-of-flight spectrum was observed for ^{81}Br from IBr and its transformation into the energy domain is illustrated in Figure 1, where it can be seen that three sets of products are formed. Thus, the photodissociation of IBr at 193 nm results in the formation of three sets of atomic products; I ($^2P_{3/2}$) + Br ($^2P_{3/2}$) (E = 435 ± 15kJ/mol), I ($^2P_{3/2}$) + Br ($^2P_{1/2}$) (E = 395 ± 10kJ/mol), and I ($^2P_{1/2}$) + Br ($^2P_{3/2}$) (E = 356 ± 10kJ/mol). The absorption spectrum of IBr in the region of 193 nm is dominated by a strong Rydberg system, while for I_2 only an extensive

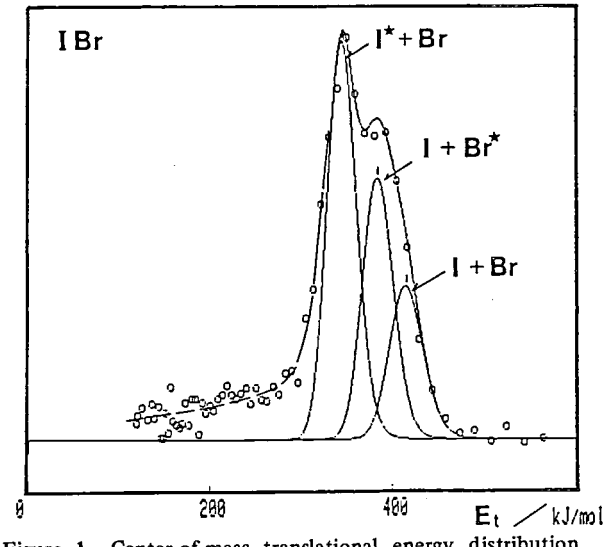

Figure 1. Center-of-mass translational energy distribution of the photofragments following excitation of IBr at 193 nm. The asterisk denotes spin-orbit excitation (i.e. X* = X ($^2P_{1/2}$); X = X ($^2P_{3/2}$).

ion-pair system is observed. Rydberg states of I_2 also lie in this region. However they are gerade states and are not observed by single photon absorption. This is not the case for IBr where the inversion symmetry is lost. Polarization studies showed that the absorption at 193 nm can be assigned as $1 - 0^+$. The identity of the states causing predissociation is more difficult to establish but we note that several states having the correct symmetry and correlating with the appropriate atomic fragments are expected to lie close to the repulsive wall of the minimum that has predominantly Rydberg character.

III-G-3 Photodissociation of Molecular Beams of Chlorinated Benzene Derivatives at 193 nm

Teijiro ICHIMURA (*Tokyo Inst. Tech,*), **Yuji MORI** (*Tokyo Inst. Tech,*), **Hisanori SHINOHARA and Nobuyuki NISHI**

[*Chem. Phys. Lett.* in press]

Molecular beams of chlorobenzene, isomers of o-, m-, p- chlorotoluene and dichlorobenzene were photodissociated using an excimer laser at 193 nm to measure the time-of-flight distributions of the photofragment (Cl, m/e = 35) in order to investigate the primary processes and the photodissociation dynamics.

Three peaks are apparent in fragment translational energy (E_T) distributions obtained (Fig. 1). A small sharp peak with an average E_T value of 30 kcal/mol is attributed to direct photodissociation of the C-Cl repulsive state. Very similar values of E_T attributable to direct dissociation are observed for these compounds. The primary process of direct photodissociation should occur very quickly after the (n, σ^*) excitation localized in the C-Cl bond.

A major broad peak with E_T = 10 kcal/mol is also observed for all the compounds studied. This distribution of the relatively slow photofragment can not be represented by a statistical model, which suggests the excitation energy is not completely randomized. These relatively slow dissociation processes of chlorinated benzene derivatives take place through a triplet (π, π^*) state, whose lifetime depends upon molecular structure.

The slowest fragment of 3 kcal/mol peak energy, whose distribution can be simulated by a Boltzmann function, should result from photodecomposition of the thermalized state. The most probable state is a vibrationally highly excited ground state.

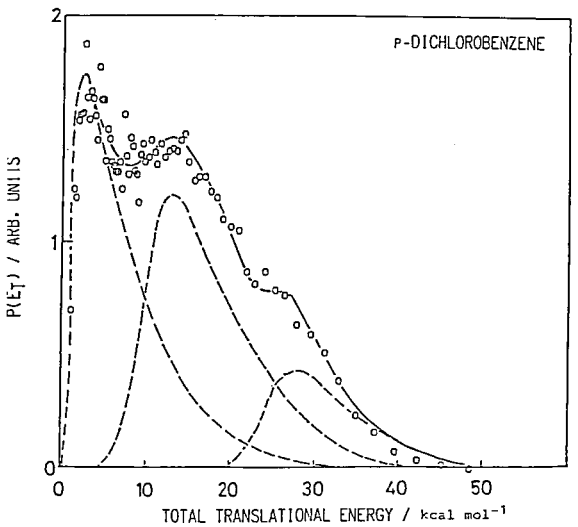

Figure 1. Total center-of-mass translational energy distribution P (E_T) obtained from Cl photofragments in the photolysis of p-dichlorobenzene at 193 nm. P (E_T) are simulated by superposition of three components using a Maxwell-Boltzmann function and two Gaussian functions. The simulated line is shown by a solid line and the best fit functions are drawn by broken lines.

III-G-4 UV Photodissociation of Chlorine Molecules Adsorbed on an Si Wafer

Masahiro KAWASAKI* (**Mie Univ.*), **Kazuo KASATANI*, Hiroyasu SATO*, Nobuyuki NISHI, and Gen INOUE** (*Nat. Inst. for Environmental Studies*)

Gaseous chlorine molecule has a weak continuum absorption in the region 300–400 nm. This repulsive $^1\Pi_u$ state is correlated to two ground state Cl atoms. When Cl_2 deposited on an n-type Si (100) wafer was photodissociated, Cl, SiCl, and $SiCl_2$ were detected by 193 and 248 nm irradiation.

Neutral photofragments were detected by a quadrupole mass filter with an ion bombardment ionizer. At 352 nm, the signal intensity of Cl was weak although gaseous Cl_2 has its absorption maximum at 340 nm. When the laser irradiated Cl_2 on a quartz plate and in a CO_2 matrix, the signal intensity was still weak. Since the Si wafer has strong absorption at $\lambda < 290$ nm, the photoexcited Si surface enhances Cl_2 dissociation on the surface.

This enhancement has been reported in halogen photoetching of Si surfaces.

Concerning the ablation of Si surface by laser irradiation, LIF signals of Si atoms but no Si_2 molecules were detected as ablation products when the laser beam was focused. Without focusing, no signals were detected. The formation of SiCl and $SiCl_2$ in the Cl_2 photodissociation on the Si surface is due to the Cl reaction with Si surface. The translational energy E_T is obtained by fitting TOF spectra with Maxwell-Boltzmann distributions characterized by temperature T. E_T is defined by 3RT/2. Results are tabulated in Table I. Small E_T (~ 1 kcal/mol) for SiCl and $SiCl_2$ is due to the desorption of the products from the surface. Concerning the large E_T of Cl atoms, the Cl atoms from the quartz surface have large E_T than from the Si surface. The incident energy for the quartz experiment is $h\omega$ (6.4 eV). For the Si (100) experiment it is the band gap energy (~ 4 eV) because the photoexcited Si surface enhances Cl_2 dissociation.

Table I. Solid Cl_2 photolysis on an Si wafer and a quartz plate at 100 K

Products	substrate	laser	E_T^*/kcal·mol^{-1}
Cl	Si	193 nm	10/3/0.7
	SiO_2		17
	Si	248 nm	7/0.6
SiCl	Si	193 nm	1.3
		248 nm	1.2
$SiCl_2$	Si		1.3

* Averaged translational evergy 3RT/2. For two (three) E_T values, two (three) Maxwell-Boltzmann distributions are assumed to fit with experimental data.

III—H Formation and Properties of Hydrogen-bonded Molecular Clusters

III-H-1 Photoionization of Ammonia Clusters: Detection and Distribution of Unprotonated Cluster Ions $(NH_3)_n^+$, n = 2–25

Hisanori SHINOHARA, Nobuyuki NISHI, and Nobuaki WASHIDA (*Nat. Inst. for Environmental Studies*)

[*J. Chem. Phys.*, **83**, 1939 (1985)]

Unprotonated ammonia cluster ions $(NH_3)_n^+$ of various sizes (n = 2 – 25) are detected for the first time, in addition to normally observed protonated ions $(NH_3)_{n-1}H^+$, via the molecular-beam VUV photoionization by using Ar (11.83, 11.62 eV), Kr (10.64, 10.03 eV), and Xe (9.57 eV) resonance lamps. The observation of the species indicates that there exist potential minima for the various $(NH_3)_n^+$ cluster ions along the proton-transfer reaction coordinates. Considerations based on intracluster ion-molecule reactions reveal that the unprotonated cluster ions have the proton-transferred structures of $(NH_3)_{n-2}NH_4^+\cdots NH_2$ rather than $(NH_3)_n^+$ which usually lead to the dissociated protonated products $(NH_3)_{n-1}H^+$. Figure 1 shows semilogarithmic plots of reduced intensity $(NH_3)_n^+/(NH_3)_{n-1}H^+$ distributions, which is a measure of the intracluster ion-molecule reactions as a function of n. The figure reveals that the so-called "magic numbers" found in the intensity distributions of both the protonated $(NH_3)_4NH_4^+$ and unprotonated $(NH_3)_5^+$ cluster ions suggest the special stability of the ions.

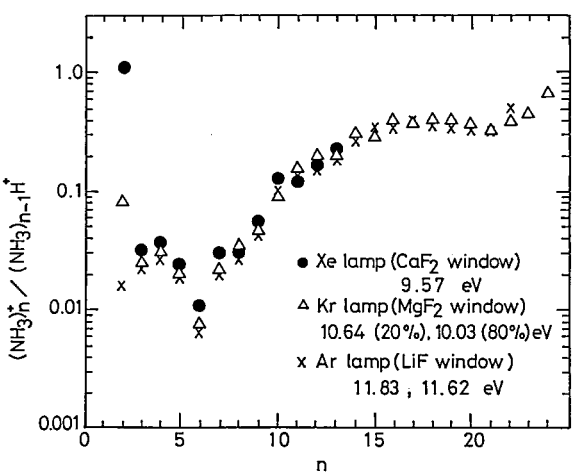

Figure 1. Semilogarithmic plots of reduced intensity $(NH_3)_n^+/(NH_3)_{n-1}H^+$ distributions as a function of cluster size n. The results obtained by the three photoionizations (Ar, Kr, and Xe lamps) are given. Aside from the excitation energy, all experimental conditions are kept constant.

III-H-2 Magic Numbers for Water-Ammonia Binary Clusters: Enhanced Stability of Ion Clathrate Structures

Hisanori SHINOHARA, Umpei NAGASHIMA, Hideki TANAKA, and Nobuyuki NISHI

[*J. Chem. Phys.*, **83**, 4183 (1985)]

The formation of water-ammonia binary clusters, $(H_2O)_n\,(NH_3)_mH^+$ ($q < 40$, $q = n + m$), have been investigated employing a neutral supersonic nozzle expansion of premixed water-ammonia gas with molecular-beam-mass spectrometry. Mass spectroscopic evidence for the existence of enhanced structural stabilities ("magic numbers") has been found[1] at the protonated clusters $(H_2O)_{20}(NH_3)_mH^+$ ($m = 1 - 6$) and $(H_2O)_{27}NH_4^+$. Considerations for the magic number stabilities are presented within the framework of ion clathrate (ion-centered cage) structures (see Figure 1). Monte Carlo simulations are also presented for the ionized clusters around $n = 20$ and $n = 27$ with $m = 1$. The clusters $(H_2O)_{20}NH_4^+$ and $(H_2O)_{27}NH_4^+$ have greater binding energies per molecule than their neighbors, in agreement with the mass spectroscopic observations. The calculated structure for $(H_2O)_{20}NH_4^+$ also indicates the stability of pentagonal rings of water molecules and deformed dodecahedral structure with an NH_4^+ ion trapped inside.

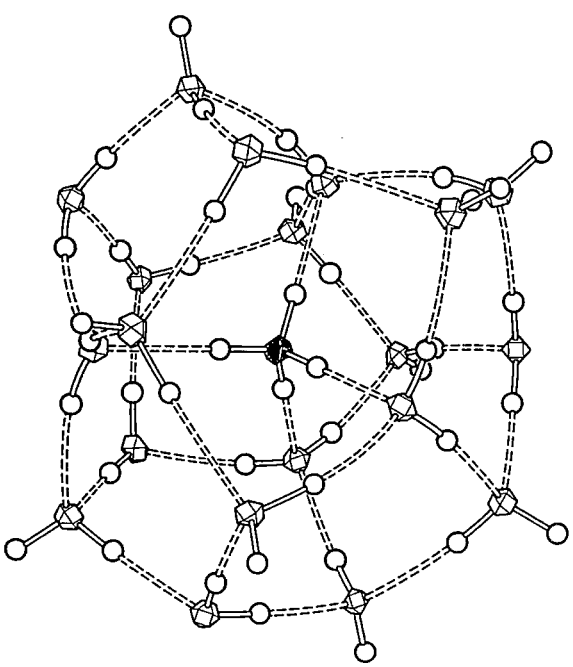

Figure 1. A model for the proposed ion clathrate structure for the magic number ion $(H_2O)_{20}NH_4^+$. The black polygon in the center represents N atom, whereas the white ones stand for O atoms. Hydrogen bond network is shown by dotted lines.

Reference

1) H. Shinohara, U. Nagashima, and N. Nishi, *Chem. Phys. Lett.*, **111**, 511 (1984).

III-H-3 Enhanced Stability of Ion-Clathrate Structures for Magic Number Water Clusters

Umpei NAGASHIMA, Hisanori SHINOHARA, Nobuyuki NISHI, and Hideki TANAKA

[*J. Chem. Phys.* in press]

The near threshold vacuum-UV photoionization of water clusters has performed by using a resonance line emission of argon at 11.83 eV. The well-known intensity anomaly at the cluster ion $(H_2O)_{21}H^+$ is observed even in this threshold photoionization, for the first time, with very small excess energy. Structures for the water cluster ions $(H_2O)_{21}H^+$ and $(H_2O)_{28}H^+$ which exhibit enhanced structural stabilities (magic number), are presented based on Monte Carlo simulations as well as on the analogy of our previous study on the stability of the $(H_2O)_{20}NH_4^+$ ion[1]. The calculation suggests that the clusters $(H_2O)_{21}H^+$ and $(H_2O)_{28}H^+$ have greater

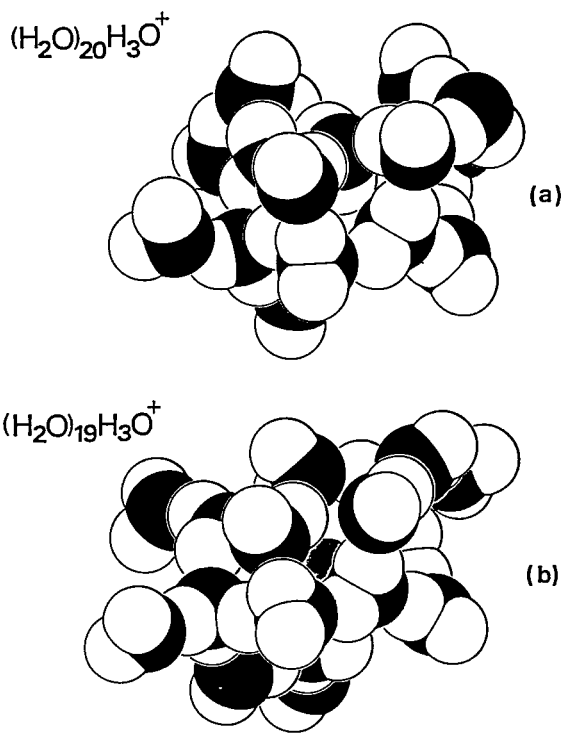

Figure 1. The results of the Monte Carlo calculations at 50 K in space-filling representation for the ionized water clusters. Black and white balls represent O and H atoms, respectively; (a) $(H_2O)_{20}H_3O^+$, (b) $(H_2O)_{19}H_3O^+$; the shaded ball represents H_3O^+.

binding energies per molecule than their neighbors although the enhancement of the latter is somewhat temperature dependent. The calculation also suggests that the stable structures for $(H_2O)_{21}H^+$ and $(H_2O)_{28}H^+$ are represented by the ion-clathrate configurations with either an H_3O^+ or $(H_2O \cdot H_3O)^+$ ion trapped inside the cage, respectively (see Figure 1).

Reference

1) H. Shinohara, U. Nagashima, T. Tanaka, and N, Nishi, *J. Chem. Phys.*, 83, 4183 (1985).

III-H-4 Photoionization of Water Clusters at 11.83 eV: Observation of Unprotonated Cluster Ions $(H_2O)_n^+$ $(2 \leqq n \leqq 10)$

Hisanori SHINOHARA, Nobuyuki NISHI, and Nobuaki WASHIDA [*Nat. Inst. for Environmental studies*]

Unprotonated cluster ions $(H_2O)_n^+$ $(2 \leqq n \leqq 10)$ and $(Ar)_m$ $(H_2O)_n^+$ $(1 \leqq m \leqq 3;\ 2 \leqq n \leqq 7)$ are detected in the mass spectra, for the first time, in addition to normally observed protonated ions $(H_2O)_{n-1}H^+$ when supersonic cluster beams of water-argon mixtures ($P \simeq 2$ atm) are photoionized with vacuumUV resonance lines at 11.83 and 11.62 eV (see Figure 1). The protonated and unprotonated cluster ions are generated, respectively, via the following reactions (i) and (ii):

$$(H_2O)_n + h\nu \rightarrow [(H_2O)_n^+]^*_{vip} + e^- \rightarrow (H_2O)_{n-1}H^+ + OH + e^-, \qquad \text{(i)}$$

$$(Ar)_m\,(H_2O)_n + h\nu \rightarrow [(Ar)_m\,(H_2O)_n^+]^*_{vip} + e^- \rightarrow$$

$$\rightarrow (Ar)_k\,(H_2O)_n^+ + (m-k)\,Ar + e^-;\ k \neq 0 \qquad \text{(ii-a)}$$

$$\rightarrow (H_2O)_n^+ + mAr + e^-;\ k = 0, \qquad \text{(ii-b)}$$

where vip represents virtically ionized points. The excess energies on ionization can be randamized within the $[(Ar)_m(H_2O)_n^+]^*_{vip}$ clusters ("intracluster excess energy dissipation") and are finally converted to the decomposition of the argon atoms, giving rise to the stable $(H_2O)_n^+$ and the various $(Ar)_k$ $(H_2O)_n^+$ cluster ions.

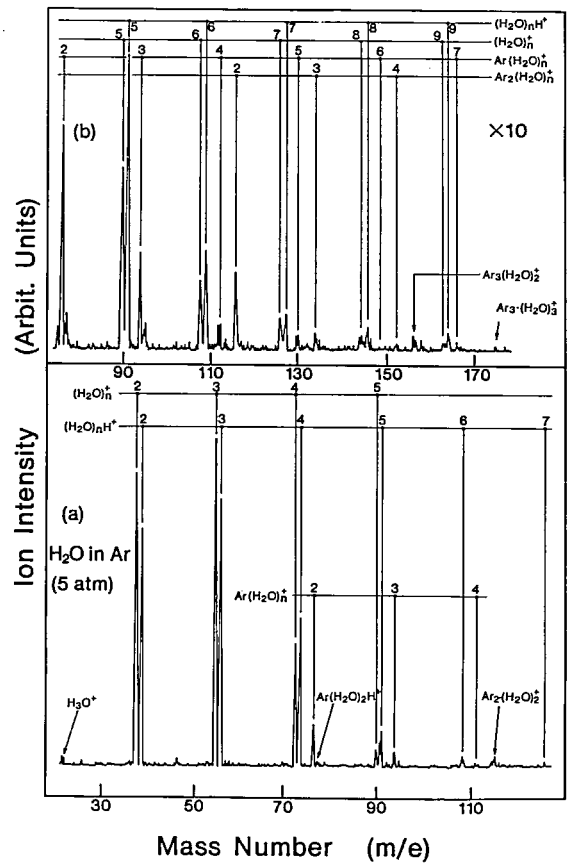

Figure 1. Photoionization (11.83, 11.62 eV) mass spectrum of Ar-seeded supersonic water beam with unit mass resolution. In figure (b) the vertical scale has been changed in order to obtain a better display of the higher masses. Spectral assignments are given on top of the spectrum. The conditions: 5 atm total stagnation pressure (seeded in Ar); 25° C nozzle temperature; 500 accumulations.

III-H-5 Identification of Ammonia Clusters in Low-Temperature Matrices Using the FTIR Short-Pulsed Matrix Isolation Technique

Teruhiko NISHIYA (*Kyoto Univ.*), **Noboru HIROTA** (*Kyoto Univ.*), **Hisanori SHINOHARA, and Nobuyuki NISHI**

[*J. Phys. Chem.*, 89, 2260 (1985)]

The clustering of ammonia in rare gas matrices at 15 K has been studied by Fourier-transform infrared (FTIR) matrix isolation spectroscopy. The experimental technique is based on trapping of short-pulsed (~ 1.4 ms) supersonic beam molecules into the matrices where the trapped ammonia molecules are allowed to self-associate. The method is

shown to be a sensitive technique for quantitative identification of the hydrogen-bonded clusters. Detailed studies of the concentration and nozzle stagnation dependences enable us to identify the bands due to dimer, trimer, and higher clusters. Considerations in terms of an extended quenched reaction model reveal strong evidence for stepwise association of NH_3 to give $(NH_3)_2$, $(NH_3)_3$, and a number of different $(NH_3)_n$ species. It is shown that these matrix infrared studies are complementary to the gas-phase infrared studies of the ammonia clusters.

III—I Effects of External Magnetic Field upon Chemical Reactions

Magnetic field effects on chemical reactions provide us with not only new methods for studying reaction mechanisms but also new techniques based on new principles. In these several years, we have been studying the effects on photochemical and electrochemical reactions in solution. Recently, we have extended the study of the effects to reactions in the gas phase, constructing an apparatus for afterglows using a microwave discharge.

III-I-1 External Magnetic Field Effects on the Emission Intensities of the NO ($B^2\Pi_r$-$X^2\Pi_r$) Bands in an Afterglow Produced by a Microwave Discharge

Yoshio FUKUDA (*Inst. of Phys. and Chem. Res. and IMS*), **Hisaharu HAYASHI** (*Inst. of Phys. and Chem. Res. and IMS*), **and Saburo NAGAKURA**

[*Chem. Phys. Lett.*, in press]

Magnetic field effects on the emission intensity were studied for the NO (B-X) bands in an afterglow produced by a microwave discharge of N_2-O_2 mixture. The (0, v'') bands were remarkably quenched by an external magnetic field below 1.8 T, while the (1, v'') and (2, v'') bands were slightly intensified by the field. On the other hand, the emission of the NO (B-X) bands produced from N (^2D, ^2P) and N_2O was not found to be influenced by the magnetic field. Therefore, the magnetic field effects observed in the former reaction can be considered to be due to some formation processes of NO ($B^2\Pi_r$).

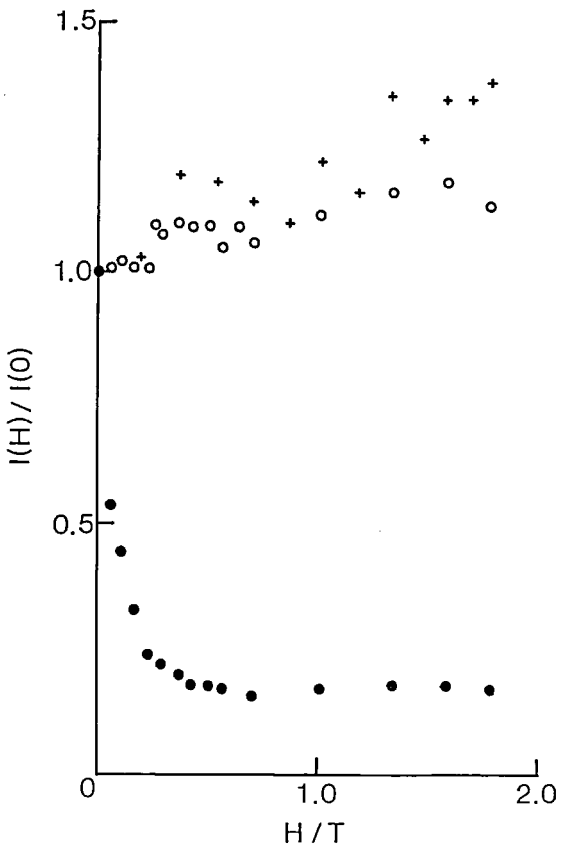

Figure 1. Magnetic field dependence of emission intensity (I (H)/I (0)) observed for N_2 (3.1 Torr) + O_2 (0.4 Torr): •, (0, 9) band at 338.5 nm; ○, (1.13) band at 413.0 nm; +, (2, 14) band at 421.0 nm. Experimental error, ± 0.08.

III-I-2 Magnetic Field Effects on Photoionization of N, N, N′, N′-Tetramethyl-*p*-phenylenediamine in 2-Propanol

Yoshifumi TANIMOTO (*Kanazawa Univ. and IMS*), Takeshi WATANABE, Ryoichi NAKAGAKI, Mitsuo HIRAMATSU (*Hamamatsu Photonics, K.K. and IMS*), and Saburo NAGAKURA

[*Chem. Phys. Lett.*, **116**, 341 (1985)]

Magnetic field effects on the photoionization yield of N, N, N′, N′-tetramethyl-*p*-phenylenediamine (TMPD) in deaerated 2-propanol solution were studied by measuring transient photoconductivity. The photocurrent increases by *ca.* 15% on application of a magnetic field (0.72T). The observed results were interpreted in terms of a radical pair model and it was concluded that the monophotonic photoionization takes place through an excited singlet state.

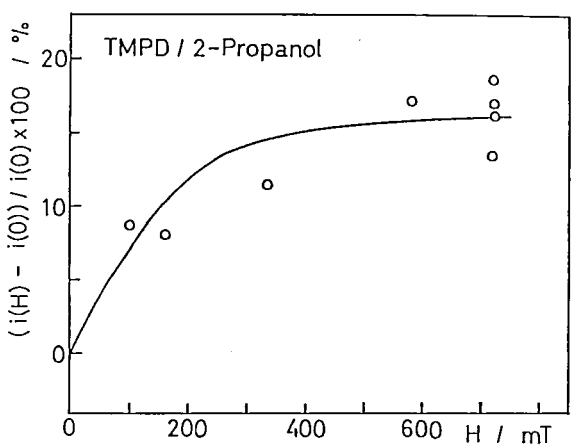

Figure 1. Magnetic field dependence of the maximum photocurrent, *i* for TMPD in deaerated 2-propanol. H and 0 refer to the presence and absence of the magnetic field. Excitation source (XeCl excimer laser, 308 nm).

III-I-3 Photochemistry of Bichromophoric Chain Molecules Containing Electron Donor and Acceptor Moieties. I. Dependence of Reaction Pathways on the Chainlength and Mechanism of Photoredox Reaction of N-[ω-(*p*-Nitrophenoxy) alkyl] anilines.

Ryoichi NAKAGAKI, Mitsuo HIRAMATSU (*Hamamatsu Photonics, K.K. and IMS*), Kiyoshi MUTAI (*Univ. of Tokyo*), and Saburo NAGAKURA

[*Chem. Phys. Lett.*, in press]

Switching of photochemical reaction pathways was found for a series of bichromophoric species, D-$(CH_2)_n$-A, consisting of electron donor (anilino) and acceptor (*p*-nitrophenoxy) moieties by changing the number of methylene groups linking two chromophores. Long-chain molecules ($n \geq 7$) show a photoredox reaction, while short-chain compounds ($n \leq 6$) exhibit the photo-Smiles rearrangement. Difference in photochemical reactivity can be explained in terms of accessibility of the two aromatic reaction centers. The photochemical primary process is concluded to be electron transfer from the donor moiety to the excited acceptor moiety.

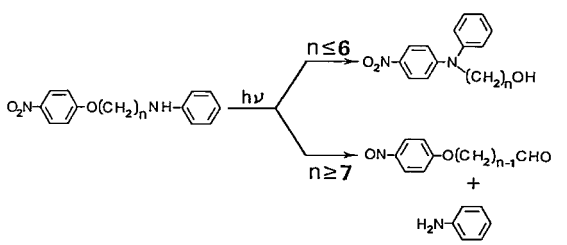

Figure 1. Chainlength effect in bichromophoric photochemistry. Short-chain species ($n \leq 6$) undergo an intramolecular nucleophilic photosubstitution (photo-Smiles rearrangement), while long-chain homologues ($n \geq 7$) exhibit photoinduced oxidative dealkylation of N-alkylanilines.

III-I-4 Photochemistry of Bichromophoric Chain Molecules Containing Electron Donor and Acceptor Moieties. II. External Magnetic Field Effect upon Photoredox Reactions Involving Charge-separated Biradicals.

Ryoichi NAKAGAKI, Mitsuo HIRAMATSU (*Hamamatsu Photonics, K.K. and IMS*), Yoshifumi TANIMOTO (*Kanazawa Univ. and IMS*), Kiyoshi MUTAI (*Univ. of Tokyo*), and Saburo NAGAKURA

The magnetic field effect upon photoredox reactions has been studied for bichromophoric long-chain molecules, D-$(CH_2)_n$-A (where A = *p*-nitrophenoxy, D = anilino or *p*-fluoroanilino, and n =

10, 12 or 16) by means of steady-state photolysis. On application of a magnetic field (0.64T), the yield of photoredox reaction products (*p*-nitrosophenoxy derivatives and aniline) decreases by about 20% compared with the value in the absence of the field. On the other hand, no magnetic field effect is observed in the case of short-chain species (n = 4). Observed results are consistent with Scheme 1, which is based upon the assumption that the charge-separated triplet biradical is involved as a precursor.

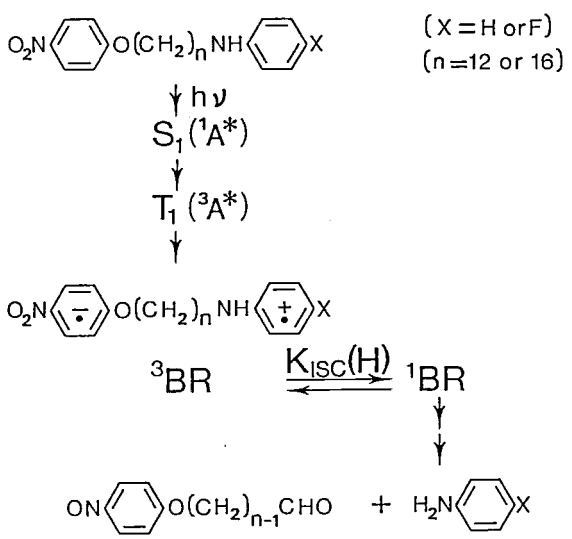

Scheme 1

III-I-5 Magnetic Field Effect on the Intramolecular Hydrogen Abstraction Reaction of *n*-Tetradecyl Anthraquinone-2-carboxylate.

Yoshifumi TANIMOTO (*Kanazawa Univ. and IMS*), **Masanobu TAKASHIMA** (*Kanazawa Univ.*), **Megumu UEHARA** (*Kanazawa Univ.*), **Michiya ITOH** (*Kanazawa Univ.*), **Mitsuo HIRAMATSU** (*Hamamatsu Photonics, K.K. and IMS*), **Ryoichi NAKAGAKI, Takeshi WATANABE, and Saburo NAGAKURA**

[*Chem. Lett.*, **1985**, 15]

The magnetic field effect on photochemistry of *n*-tetradecyl anthraquinone-2-carboxylate (AQC-14) was studied in aerated 1, 1,2-trichlorotrifluoroethane (TCTFE), using steady-state photolysis, two-step laser excitation fluorescence, and laser flash photolysis. The photochemical primary process is an intramolecular hydrogen abstraction by the anthraquinone moiety in the excited triplet state, thus yielding a triplet biradical consisting of the anthrasemiquinone and alkyl radicals. Steady-state photolysis revealed that the yield ϕ for disappearance of AQC-14 decreases by about 10% upon application of magnetic fields (100-200 mT). This can be explained in terms of a decrease in the singlet biradical yield in the presence of magnetic fields.

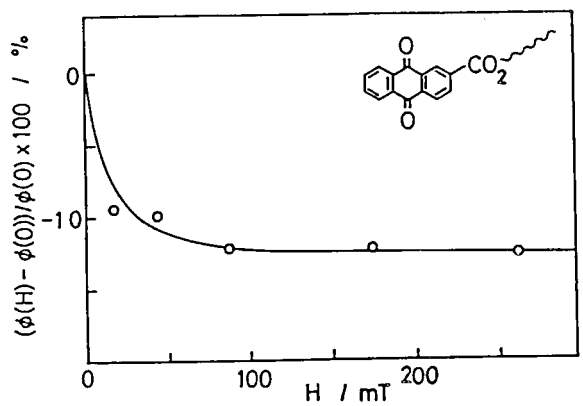

Figure 1. Magnetic field dependence of relative quantum yield ϕ for disappearance of AQC-14 in aerated TCTFE. The yield ϕ was determined by analyzing the absorbance change of the AQC-14 330 nm band induced by steady-state irradiation, and 0 and H refer to the absence and presence of an external magnetic field, respectively.

III-I-6 The Magnetic Field Effects on Electrolysis. II.[1] The Kolbe Oxidation of Phenylacetate.

Takeshi WATANABE, Yoshifumi TANIMOTO (*Kanazawa Univ. and IMS*), **Ryoichi NAKAGAKI, Mitsuo HIRAMATSU** (*Hamamatsu Photonics, K.K. and IMS*), **and Saburo NAGAKURA**

The Kolbe oxidation of phenylacetate has been studied at a platinum anode in the presence of a magnetic field (0.67T). Some of reaction products, toluene and 1, 2-diphenylethane, are derived from the benzyl radical generated by decarboxylation of the phenylacetoxyl radical, and benzaldehyde is an example of highly oxidized products. No magnetic field effect was observed for formation of toluene or 1, 2-diphenylethane, while the yield for benzaldehyde formation is unambiguously influenced

by the external magnetic field. An experiment under Ar purge condition suggests that the magnetic field effect on benzaldehyde formation is attributable to the magnetohydrodynamic effect.

Reference

1) Part I of this series, T. Watanabe, Y. Tanimoto, T. Sakata, R. Nakagaki, M. Hiramatsu, and S. Nagakura, *Bull. Chem. Soc. Jpn.*, 58, 1251 (1985).

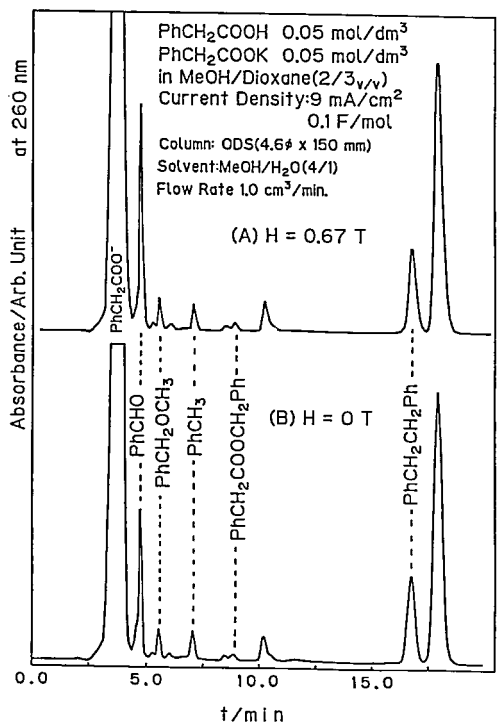

Figure 1. A typical chromatogram recorded after the Kolbe electrolysis in the presence (A) and in the absence (B) of a magnetic field (0.67T).

RESEARCH ACTIVITIES IV
Department of Molecular Assemblies

IV— A Photoelectron Spectroscopy of Organic Solids in Vacuum Ultraviolet Region

Photoelectron spectra of organic solids, carboxylic acid films, and polymers, were observed. A photoelectron spectrometer combined with UVSOR (Ultraviolet Synchrotron Orbital Radiation) light source is being constructed. For this spectrometer, a plane-grating monochromator has been constructed (see VI-).

IV-A-1 An Ultraviolet Photoelectron Spectroscopic Study of Oriented Carboxylic Acid Films Prepared by Vacuum Deposition

Munehisa MITSUYA (*Hitachi Ltd. and IMS*), **Yoshio TANIGUCHI** (*Hitachi Ltd.*), **Naoki SATO** (*Kumamoto Univ.*), **Kazuhiko SEKI, and Hiroo INOKUCHI**

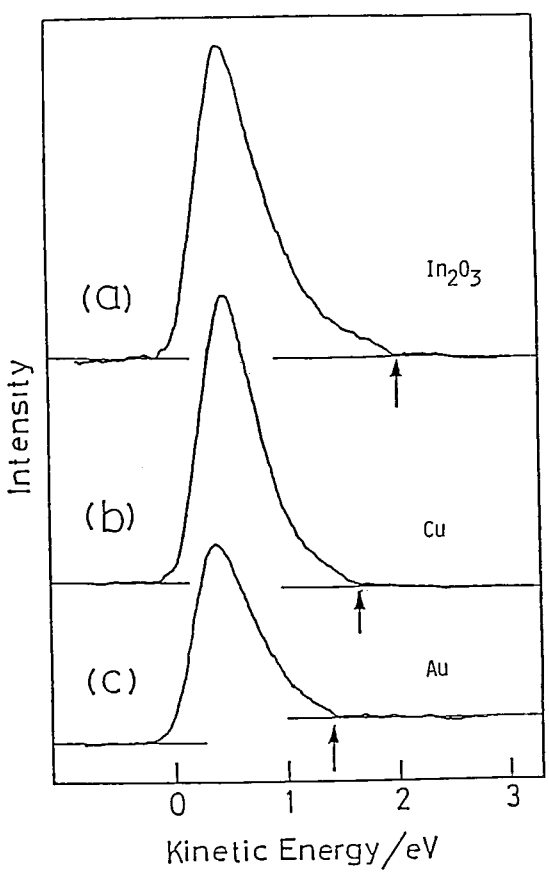

Figure 1. Photoelectron spectra of stearic acid films on the kinetic energy scale. (a) Deposited on indium oxide, (b) copper and (c) gold. Incident photon energy is 9.76 eV. Arrows indicate maximum kinetic energies for photoelectrons.

[*Chem, Phys. Lett.*, 119, 431 (1985)]

Ultraviolet photoelectron spectra were measured for films of aliphatic carboxylic acids made by vacuum deposition. Their threshold ionization potentials varied within 0.6_5 eV according to the measure of molecular orientation. Figure 1 illustrates this effect for stearic acids deposited on various substrates. This variation is explained by the dimer formation in the highly crystalline film.

IV-A-2 Ionization Thresholds of Merocyanine Dyes in the Solid State

Tong B. TANG (*Univ. Cambridge and IMS*), **Kazuhiko SEKI, Hiroo INOKUCHI, and Tadaaki TANI** (*Fuji Photo Film Co., Ltd.*)

[*J. Appl. Phys.*, in press]

The experimental technique of ultraviolet photoelectron spectroscopy (UPS) has been applied to a number of merocyanine dyes related in chemical structure. Their molecular structures are shown in Figure 1. Additionally, polarographic and optical measurements were made on these dyes in solution, and Hückel molecular orbital calculations were carried out for isolated dye molecules. The energy diagrams of the dye solids deduced from UPS and optical measurements are shown in Figure 2. The threshold energy decreases with increasing delocalozation of π-electrons in the compound. With the use of absorption data, we constructed energy band diagrams for the dyes, assuming that these organic materials exist as molecular solids. Our assumption was supported by the observation that their ionization thresholds correlate well with the polarographic

and computatinal results. Photoelectron spectroscopy is deemed to provide a powerful method for studying dyes in practical forms.

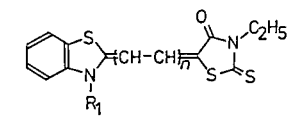

R_1	n	Dye
C_2H_5	0	1
C_2H_5	1	2
C_2H_5	2	3
C_2H_5	3	4
$C_3H_6SO_3H$	2	5

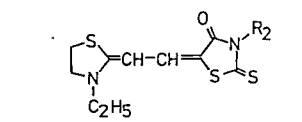

R_2	Dye
C_2H_5	6
CH_2COOH	7

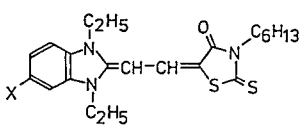

X	Dye
Cl	8
NO_2	9

Figure 1. The merocyanine dyes being studied.

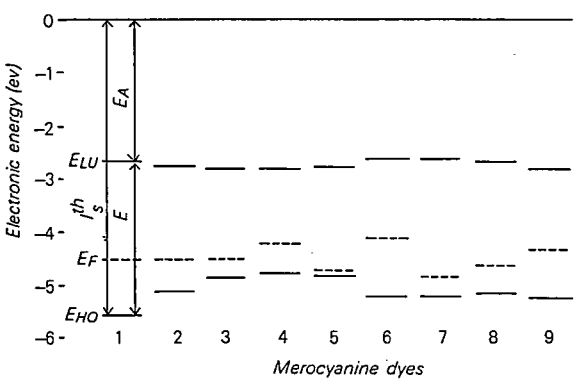

Figure 2. Energy diagrams of merocyanine dye solids. E_{LU} and E_{HO}: energies of the LUMO and HOMO, E_F: Fermi energy of the Fermi level, I_s^{th}: ionization threshold energy, E: excitation energy, and E_A: electron affinity. The origin of the ordinate is the vacuum level.

IV-A-3 Electron Affinities of Polystyrene and Poly(2-vinylpyridine) by Means of Low-Energy Electron Inelastic Scattering

Nobuo UENO*, Kazuyuki SUGITA*, Kazuhiko SEKI, and Hiroo INOKUCHI (**Chiba Univ.*)

[*Jpn. J. Appl. Phys.*, **24**, 1156 (1985)]

Low-energy electon energy loss spectra including secondary electron bands and low-energy electron transmission spectra were measured for polystyrene and poly(2-vinylpyridine) thin films deposited on metal substrates. Almost all features in these spectra were explained by electronic excitations localized iin pendant molecules. The electron affinities of polystyrene and poly(2-vinyl-pyridine) were estimated as 0.4 ± 0.1 eV and 0.3 ± 0.1 eV, respectively, based on the one-to-one correspondence of spectral features in these two types of spectra.

IV—B Electric and Photo-conduction of Organic Solids

As a new type organic semiconductor, a series of uncapped alkyl-substituted tetrathiafulvalenes has been studied.

VI-B-1 Reflection and Photoconduction Spectra of the Single Crystals of Perylene-TCNQ 1:1 and 3:1 Molecular Complexes.

Kikujiro ISHII (*Gakushuin Univ.*), **Kyuya YAKUSHI***, **Haruo KURODA*** and **Hiroo INOKUCHI** (**Univ. Tokuo*)

[*Bull. Chem. Soc. Jpn.*, **57**, 3043 (1984)]

Crystal absorption spectra of the two modifications of the perylene-TCNQ complex were derived from reflection spectra by the Kramers-Kronig transformation and are discussed in relation to the differences in the crystal structures. The spectral

response of photoconduction does not show any efficient photocarrier generation in the lowest charge-transfer band region in either modification. The photoelectrical characters are discussed in connection with the optical spectra and also with the photoelectron emission data.

IV— C Electron Transfer and Electron Transport in Cytochrome c_3

Magnetic susceptibility and magnetic resonance study of hydrogenase and also cytochrome c_3 has been studied. AC conductivity of cytochrome c_3 has been measured. (see VII-G)

IV— D Physics and Chemistry of Graphite and its Intercalation Compounds

The analysis of hydrogen dissociation and chemisorption mechanism on graphite alkali metal intercalation compounds (GIC) is one of the main subjects in this research field. The electron transport and the specific heat measurements in GIC + H_2 ternary system, and also the superconductivity in GIC and GIC + H_2 ternary system are being studied. Further, we are observing the positron-annihilation of GIC and its hydrogen-chemisorbed compounds. (see also VII-K)

IV-D-1 Superconductivity in the First Stage Rubidium Graphite Intercalation Compound C_8Rb

Mototada KOBAYASHI, Toshiaki ENOKI, Hiroo INOKUCHI, Mizuka SANO*, Akihiko SUMIYAMA, Yasukage ODA**, and Hiroshi NAGANO**** (**Kumamoto Univ., **Univ. of Tokyo*)

[*Synthetic Metals* (1985), in press]

The superconductivity in C_8Rb has been observed in AC magnetic susceptibility and magnetization measurements with the external magnetic field applied perpendicularly and parallel to the *c*-plane. The transition temperature T_c is found to be 26 mK. The external magnetic field dependence of AC magnetic susceptibility shows a differential paramagnetic effect and a hysteresis for $H_{ex}//c$-plane and $H_{ex}\perp c$-plane. The superconducting characteristic is type I for both directions. Figure 1 shows the temperature dependence of the thermodynamical critical field H_c and the upper critical field H_{c2}. The $H_{c2}//$ vs T curve has a slightly negative curvature. The observed superconducting properties are compared with those of C_8K. The superconductivity in C_8Rb is concluded to have more three dimensional character than that in C_8K. The difference in T_c between C_8Rb and C_8K is mainly due to the difference in the electron phonon coupling parameter λ between them.

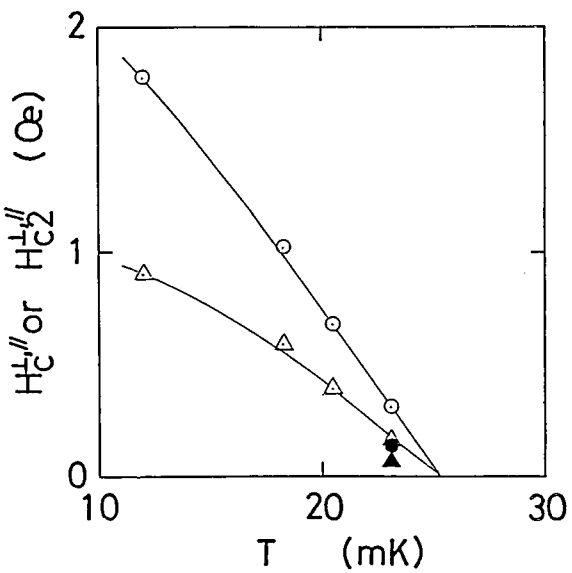

Figure 1. Temperature dependence of $H_c^{\perp}$, $H_c^{//}$, $H_{c2}^{\perp}$ and $H_{c2}^{//}$. The symobols ○ and △ denote $H_c^{//}$ and $H_{c2}^{//}$, respectively, and symbols ● and ▲ $H_c^{\perp}$ and $H_{c2}^{\perp}$, respectively.

IV-D-2 Transport and Superconducting Properties of Potassium Hydride Graphite Intercalation Compounds

Kazuya SUZUKI, Ikuji TSUJIKAWA, Mototada KOBAYASHI, Hiroo INOKUCHI, Yasukage ODA*, Akihiko SUMIYAMA*, Hiroshi NAGANO*, and Yoshihide KIMISHIMA** (*Univ. of Tokyo, **Yokohama National Univ.)

[Synthetic Metals (1985), in press]

Potassium hydride graphite intercalation compounds were prepared by the direct intercalation of potassium hydride into HOPG and their structures were confirmed by (001) X-ray diffraction. The in-plane resistivity of the stage-1 to -3 compounds were measured by the 4-probe technique in the temperature range 4 K - 300 K. The temperature dependence of the resistivity was almost linear except at low temperature regions. The stage-3 $C_{12}KH_x$ exhibited a step-like increase at about 88 K. Superconductivity was examined for the stage-1 and-2 compounds by AC magnetic susceptibility measurement. The stage-1 C_4KH_x was not superconducting down to 70 mK, while the diamagnetism attributed to superconductivity was detected in the stage-2 C_8KH_x, which increased continuously from 360 mK down to 70 mK. Figure 1 shows the temperature dependence of susceptibility for C_8KH_x.

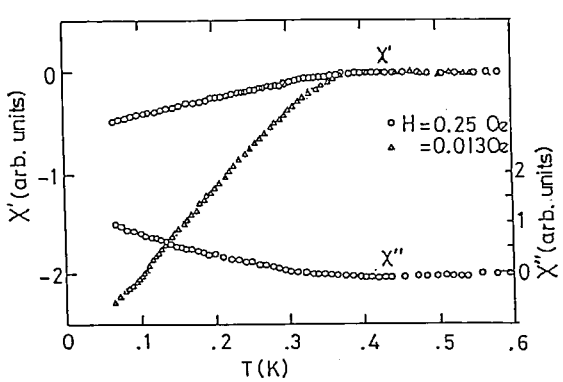

Figure 1. Temperature dependence of susceptibility for C_8KH_x. *H* denotes measuring magnetic field.

IV-D-3 Chemisorption of Hydrogen into a Graphite-Potassium Intercalation Compound C_8K Studied by Means of Positron Annihilation

Hideoki MURAKAMI (*Tokyo Gakugei Univ.*), Mizuka SANO (*Kumamoto Univ.*), Ikuzo KANAZAWA (*Tokyo Gakugei Univ.*), Toshiaki ENOKI, Toshikazu KURIHARA (*Tokyo Gakugei Univ,*), Yoshiharu SAKURAI (*Tokyo Gakugei Univ.*), and Hiroo INOKUCHI.

[*J. Chem. Phys.* 82, 4728 (1985)]

The first stage graphite-potassium intercalation compound C_8K is known to fix hydrogen through a chemisorption process and to become a hydride $C_8KH_{2/3}$. The purpose of the present study is to clarify some aspects of the chemisorption of hydrogen into C_8K by means of positron annihilation. Figure 1 shows the Doppler broadening spectra of positron annihilation for (a) graphite, (b) C_8K and (c) $C_8KH_{2/3}$. The spectrum for C_8K is composed of a narrow band superimposed on a broad band which is mainly attributable to graphite. The narrow band can be explained in terms of the annihilation with the electrons in the interlayer band or the remaining 4s electrons in the potassium layers. When C_8K was exposed to hydrogen gas, the height of the spectrum increased with time and the narrow

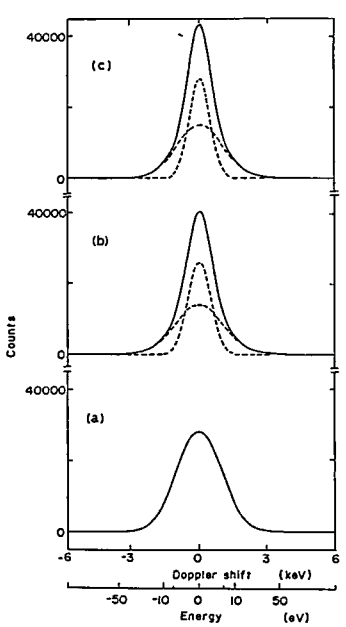

Figure 1. The Doppler-broadened positron-annihilation spectra for (a) graphite ($\gamma \perp c$), (b) C_8K, and (c) $C_8KH_{2/3}$, after deconvolution from the instrumental broadening. The broken lines show the Gaussian bands separated from the spectra.

band was sharpened. These changes of the spectrum by hydrogen uptake indicate a decrease in electronic density on the graphite layers, which is associated with the generation of hydride ions through a charge transfer to hydrogen due to the large electron affinity of hydrogen.

IV— E Organic Metals

Solid charge transfer (CT) complexes including such donors as TMTSF, BEDT-TTF and its derivatives, TTMTTF, and HMTTeF are prepared. Electrical, magnetic, and structural properties of these complexes are studied and discussed on the basis of band structure calculations.

IV-E-1 Chemical and Physical Properties of Cation Radical Salts of BEDT-TTF

Gunzi SAITO, Toshiaki ENOKI, Mototada KOBAYASHI, Kenichi IMAEDA, Naoki SATO, and Hiroo INOKUCHI

[*Mol. Cryst. Liq. Cryst.*, **119**, 393 (1985)]

Extension of TTF skeleton by alkylthio groups makes the donors superior even to TMTSF concerning ionization potential, polarizability, and on-site Coulomb repulsion. Futhermore, due to the presence of the outer sulfur atoms, BEDT-TTF can form two-dimensional network by side-by-side arrangement in the complexes. The balance between the face-to-face and side-by-side interactions results in a variety of polymorphic complexes. We have been studying chemical, physical, structural, and designing works of cation radical salts of BEDT-TTF compounds. $(BEDT\text{-}TTF)_2ClO_4(TCE)_{0.5}$ shows metallic character down to 1.4 K with phase transitions at *ca.* 170 K and 15 K in electrical conductivity. The ESR and static magnetic studies show additional phase transitions. Different temperature dependence of magnetic properties was observed in the relaxed and quenched samples of this salt. A magnetic phase below 20 K was formed by relaxing the salt at high temperature.

IV-E-2 Organic Metals Based on Hexamethylenetetratellura fulvalene (HMTTeF)

Gunzi SAITO, Hiroaki KUMAGAI, (*IMS and Nagoya Univ.*), *Jiro TANAKA, (*Nagoya Univ.*), *Toshiaki ENOKI, and Hiroo INOKUCHI

[*Mol. Cryst. Liq. Cryst.* **120**, 337 (1985)]

Several CT complexes of HMTTeF with TCNQs, quinones, and other acceptors were prepared and electrical and optical properties were examined. A linear correlation between the resistivities and the position of CT bands was observed. In general, 1:1 complexes with strong acceptors ($E_A > 2.60$ eV) show relatively high conductivity with low activation energy as well as strong electronic absorption extending to IR region. Single crystals of TCNQ and 2,5-dimethylTCNQ complexes show metallic character, in which Peierls transition is strongly suppressed.

IV-E-3 The Study of Charge Transfer Complexes of BEDT-TTF Derivatives

Gunzi SAITO, Hitoshi HAYASHI, (*IMS and Nippondenso Co., Ltd*) Toshiaki ENOKI, and Hiroo INOKUCHI

[*Mol. Cryst. Liq. Cryst.*, **120**, 341 (1985)]

Various BEDT-TTF derivatives, which include eight sulfur atoms per molecule, have been synthesized, and their CT complexes with TCNQs, *p*-quinones, and TCNEs have been prepared in order to clarify the steric effect of substituents. Some of the CT complexes revealed high conductivities.

IV-E-4 Crystal Structures and Electrical Properties of Hexacyanobutadiene (HCBD) Charge Transfer Complexes

Gunzi SAITO, Toshiaki ENOKI, Hiroo INOKUCHI, Hiroaki KUMAGAI, * (*IMS and Nagoya Univ.*) Chuji KATAYAMA*, and Jiro TANAKA* (Nagoya Univ.*)**

[*Mol. Cryst. Liq. Cryst.*, **120**, 345 (1985)]

Charge transfer single crystals comprising TTF derivatives and hexacyanobutadiene (HCBD) have been prepared. TMTTF gave two crystals in different stoichiometry, one is 2:1 semiconductor and the other is 1:1 insulator. In the 2:1 complex, TMTTF molecules form face-to-face segregated columns with dimerized manner and HCBD lies perpendicular to the donor columns to form side-by-side segregated columns in the cavity produced by donor columns. The ground state of this complex is antiferromagnetic. The 1:1 complex has face-to-face uniform segregated columns and shows some phase transition at around 150 K. TTMTTF forms a semiconductive 1:1 complex with uniform face-to-face segregated column.

IV-E-5 Organic Conductors Based on Multi-Sulfur π-Donor and/or π-Acceptor Molecules —BEDT-TTF, BMDT-TTF, BPDT-TTF, and M (dmit)$_2$ —

Hayao KOBAYASHI, (*Toho Univ.*), Reizo KATO, (*Toho Univ.*), Takehiko MORI, Akiko KOBAYASHI, (*Univ. Tokyo*) Yukiyoshi SASAKI, (*Univ. Tokyo.*) Gunzi SAITO, and Hiroo INOKUCHI

[*Mol. Cryst, Liq, Cryst.*, **125**, 125 (1985)]

Crystal and electronic structures of various types of molecular metals based on multi-sulfur π-donor and π-acceptor molecules are presented. Band structures of (BEDT-TTF)$_2$ClO$_4$(TCE)$_{0.5}$ and (BEDT-TTF)$_3$ (ClO$_4$)$_2$ indicate their semimetallic (or narrow-gap semiconductive) properties. In β-(BEDT-TTF)$_2$ PF$_6$, BEDT-TTF dimers are arranged along the transverse direction and the Fermi surface is open perpendicular to this direction. The superconducting β-(BEDT-TTF)$_2$I$_3$ has nearly isotropic 2-D Fermi surface. The positive charges in (BMDT-TTF)$_3$ ClO$_4$(DCE) tend to localize and form a Wigner lattice. Similar charge separation makes (BMDT-TTF)$_3$PF$_6$(DCE) a 1-D conductor. (BMDT-TTF) (TCNQ), (DBTTF)[Ni(dmit)$_2$], and (TMTSF)[Ni (dmit)$_2$] are two-chain compounds with high conductivities ($\sigma_{R.T.}$ = 200 – 300 Scm^{-1}). (BMDT-TTF)(TCNQ) has crossing bands, whereas the others have parallel bands. (TMTSF)[Ni(dimit)$_2$] has a periodically modulated superlattice (a, 9b, c).

IV-E-6 Superconducting Tunneling in (TMTSF)$_2$ClO$_4$/a-Si/Pb Junctions

Hiroshi BANDO*, Koji KAJIMURA*, Hiroyuki ANZAI*, Takehiko ISHIGURO*, and Gunzi SAITO (Electrotechnical Lab.*)**

[*Mol. Cryst. Liq. Cryst.*, **119**, 41 (1985)]

(TMTSF)$_2$ClO$_4$/a-Si/Pb junctions using CVD a-Si film as low-potential tunneling barriers have been fabricated. From measurements well below T_c, 3D superconducting transition temperature of (TMTSF)$_2$ClO$_4$, the superconducting energy gap comparable to the BCS theory was detected. At higher temperatures no significant change other than the superconducting transition of Pb was observed. In the quenched crystals much larger gap structure 2Δ = 3 meV was observed, resulting from the SDW state.

IV-E-7 Transverse Magnetoresistance of (TMTSF)$_2$ClO$_4$ in Intermediate Field Region

Keizo MURATA*, Hiroshi BANDO*, Koji KAJIMURA*, Takehiko ISHIGURO*, Hiroyuki ANZAI*, Seiichi KAGOSHIMA, (*Univ. Tokyo*) and Gunzi SAITO (Electrotechnical Lab.*)**

[*Mol. Cryst. Liq. Cryst.*, **119**, 131 (1985)]

The transverse magnetoresistance along the a axis exhibits anomalous angular dependence with respect to the direction of a magnetic field. The behavior varies with the temperature and the field intensity.

IV-E-8 Crystal Structures of Complexes between Hexacyanobutadience (HCBD) and Tetramethyltetrathiafuvalene (TMTTF) and

Tetramethylthiotetrathiafulvalene (TTMTTF)

Chuji KATAYAMA*, Masako HONDA*, Hiroaki KUMAGAI* (*IMS and Nagoya Univ.*), Jiro TANAKA*, Gunzi SAITO (*Univ. Tokyo and IMS*) and Hiroo INOKUCHI (Nagoya Univ.*)**

[*Bull. Chem Soc. Jpn.*, 58, 2272 (1985)]

HCBD forms two molecular complexes with TMTTF, one kind with TTMTTF. In $(TMTTF)_2$ HCBD, TMTTF exists as a dimer cation stacked along the *c*-axis. HCBD anions are included in the cavity of the dimer stack directing their molecular planes parallel to the stacking axis. TMTTF·HCBD has segregated cation and anion stacks. TTMTTF HCBD has a regular segregated column with a partial charge transfer.

IV-E-9 Direct Molecular Imaging of Low Dimensional Solids by High Resolution Electron Microscopy

Natsu UYEDA*, Takashi KOBAYASHI*, Kazuo ISHIZUKA*, Yoshinori FUJIYOSHI*, Hiroo INOKUCHI and Gunzi SAITO (*Univ. Tokyo and IMS*), (Kyoto Univ.*)**

[*Mol. Cryst. Liq. Cryst.*, 125, 103 (1985)]

High resolution electron microscopy was performed to characterize the structure of metal complexes of cyanocompounds formed by solid state reactions. Examples of molecular images are presented to show normal and faulted arrangements in the lattice.

IV— F Studies of Ion-Molecule Reactions by a Threshold Electron-Secondary Ion Coincidence (TESICO) Technique

The knowledge of the microscopic reaction cross sections for evolution of a system in a single reactant quantum state (translational, rotational, vibrational, and electronic) to a single product quantum state is essential for a complete understanding of a chemical reaction. Ion-Molecule reactions are particularly suited for studying such microscopic cross sections since ions can readily be prepared in various internal states in the initial ionization processes, such as photoionization, and the emitted photoelectrons provide information on the distribution among these states.

In this project, we study state-selected ion-molecule reactions by the use of a photoionization technique which utilizes the threshold photoelectron-secondary ion coincidence. The technique allows direct determination of σ (i, v), i.e. the reaction cross section as a function of the internal and collisional energies of reactants. The selection of electronic, vibrational, rotational, and fine-structure states are possible by this technique.

IV-F-1 State Selected Charge Transfer Reactions: O_2^+ ($X^2\Pi_g$, v; $a^4\Pi_u$, v) + $N_2 \rightarrow N_2^+ + O_2$

Kenichiro TANAKA, Tatsuhisa KATO (*Kyoto Univ.*) and Inosuke KOYANO

As a part of our series of investigations on the $(AB + CD)^+$ systems, in which state selected charge transfer reactions are studied for both $AB^+ + CD$ and $CD^+ + AB$, we report here the results on the title reaction. Experimental technique used is the TESICO[1] and the internal state selected are v = 19 and 20 for O_2^+ ($X^2\Pi_g$) and v = 0 – 7 for O_2^+ ($a^4\Pi_u$).

Experimental results are shown in Figure 1. The results clearly show that the charge transfer cross section is extremely small for v = 19 and 20 of the $X^2\Pi_g$ state despite the fact that the vibrational energies of these states well exceed the endoergicity of the $O_2^+ + N_2 \rightarrow N_2^+ + O_2$ reaction, while it is greatly enhanced and, in addition, shows an interesting vibrational state dependence in the $a^4\Pi_u$ state. The solid line curve shows the result of a model calculation based on the energy defects and Franck-Condon factors between each selected reactant state and set of possible product states, normalized to the experimental value at v = 2 of $a^4\Pi_u$. The partial agreement between the experiment and theory would indicate that both long-range electron jump and some intimate collision mechanisms are

involved in this charge transfer process.

Reference

1) I. Koyano and K. Tanaka, *J. Chem. Phys.*, 72, 4858 (1980).

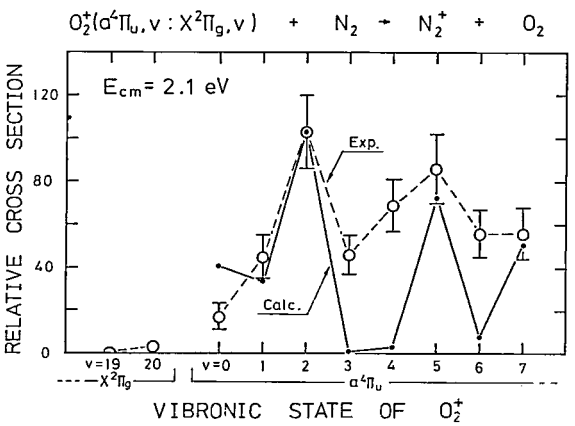

Figure 1. Relative cross sections for the reaction $O_2^+ + N_2 \rightarrow N_2^+ + O_2$ as a function of vibronic state of O_2^+.

IV-F-1 State Selected Charge Transfer Reactions: N_2^+ ($X^2\Sigma_g^+$, v; $A^2\Pi_u$, v) + $O_2 \rightarrow O_2^+ + N_2$

Tatsuhisa KATO (*Kyoto Univ.*), Kenichiro TANAKA and Inosuke KOYANO

The charge transfer reaction reverse to the one reported in the preceeding paper (IV-F-1), *i.e.*, $N_2^+ + O_2 \rightarrow O_2^+ + N_2$, has been studied by selecting internal states of the reactant N_2^+ ion over the v = 0 – 3 of $X^2\Sigma_g^+$ and v = 0 – 3 of $A^2\Pi_u$. Experimental results obtained at a collision energy of 2.1 eV (the same value as that in the preceeding paper) are summarized in Figure 1. Solid line curves connecting small dots again show the results of the model calculation normalized to the expermental value at v = 0 of $A^2\Pi_u$.

It is clearly seen that the N_2^+ ($X^2\Sigma_g^+$) has very small but non-trivial charge transfer cross sections against O_2, independent of the vibrational quantum number from 0 to 3. It is interesting to note that no dramatic change occurs in the cross section between v = 2 and 3, where energetic threshold for the formation of O_2^+ ($a^4\Pi_u$) product occurs. This strongly indicates that the product of the N_2^+ ($X^2\Sigma_g^+$) reaction is not O_2^+ ($a^4\Pi_u$), in spite of the high probability of the reverse reaction for the latter state. When we go to the $A^2\Pi_u$ state, on the other hand, the cross section increases more than one order of magnitude and varies in an interesting manner as a function of vibrational quantum number. The v = 0 and v = 1 cross sections, as well as those for the $X^2\Sigma_g^+$ state, follow the theoretical value fairly well, but the v = 2 and v = 3 cross sections of the $A^2\Pi_u$ state deviate from it considerably. The reason is not straighforwardly clear but it should be noted that the formation of the O_2^+ ($A^2\Pi_u$) product becomes exoergic from this state.

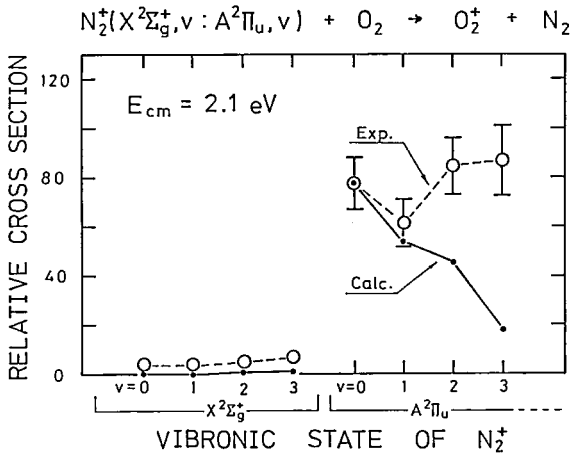

Figure 1. Relative cross sections for the reaction $N_2^+ + O_2 \rightarrow O_2^+ + N_2$ as a function of vibronic state of N_2^+.

IV-F-3 State Selected Ion-Molecule Reactions: H_2^+ (v) + $O_2 \rightarrow O_2H^+ + H$, $O_2^+ + H_2$

Kenichiro TANAKA, Tatsuhisa KATO (*Kyoto Univ.*) and Inosuke KOYANO

In order to elucidate the reaction mechanism of ion-molecule reactions in the $(M + H_2)^+$ system, where at least two potential energy surfaces participate, we have applied the TESICO technique[1] to the vibrational state selection of the primary ions in the reactions

$$H_2^+ (v) + O_2 \rightarrow O_2H^+ + H \quad (1a)$$
$$\rightarrow O_2^+ + H_2 \quad (1b)$$

Experimental results obtained at 1.0 ± 0.4 ev of

collision energy are summarized in Figure 1, where the relative cross sections are plotted as a function of the vibrational quantum number of H_2^+. The broken line curve in the figure shows the results of Anderson et al.[2], *i.e.*, the absolute values of the state selected cross sections for Reactions (1a) and (1b) obtained in rather indirect manner. Our results are normalized to theirs at v = 0 of Reaction (1a). Fairly good agreement is obtained in both experiments. As can be seen from the figure, the cross sections of Reactions (1a) and (1b) show the opposite dependence on the vibrational state, that is, the cross section of Reaction (1a) decreases with increasing vibrational quantum number, while the cross section of Reaction (1b) increases with increasing vibrational quantum number.

We have previously studied Reactions (2a) and (2b) and reported the results in detail elsewhere.[3] Briefly, the results revealed that the cross

$$O_2^+ + H_2 \rightarrow O_2H^+ + H \qquad (2a)$$
$$\rightarrow H_2^+ + O_2 \qquad (2b)$$

sections of Reactions (2a) and (2b) have the same dependence on the internal states of O_2^+.

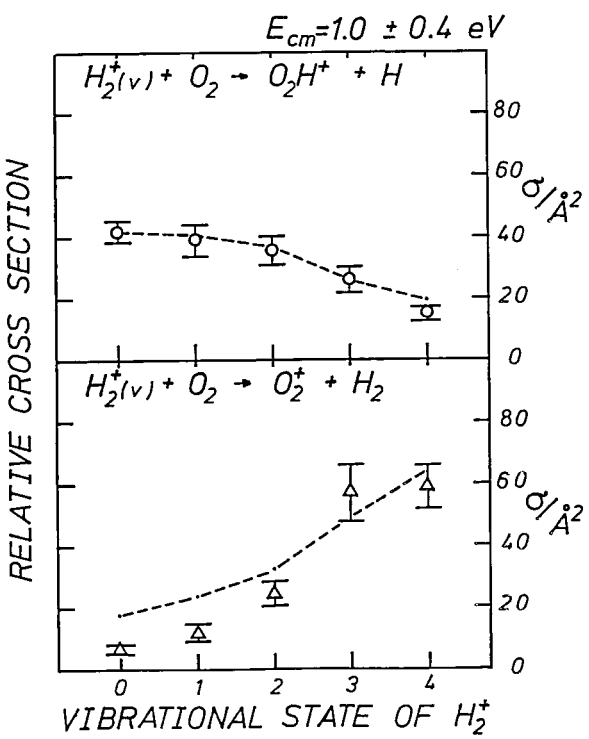

Figure 1. Cross section for Reactions (1a) (upper panel) and (1b) (lower panel) as a function of vibrational quantum number of H_2^+.

From these distinct internal state dependence of the cross sections, we can conclude that Reaction (1a) proceeds adiabatically on a potential energy surface correlating with $H_2^+ + O_2$ at infinite intermolecular separation and, on the contrary, Reaction (2a) proceeds via a nonadiabatic transition from the surface correlating with $O_2^+ + H_2$ to the surface correlating with $H_2^+ + O_2$.

References

1) I. Koyano and K. Tanaka, J. *Chem. Phys.* 72, 4858 (1980).
2) S.L. Anderson, T. Turner, B.H. Hahan, and Y.T. Lee, *J. Chem. Phys.* 77, 1842 (1982).
3) K. Tanaka, T. Kato, P.M. Guyon, and I. Koyano, *J. Chem. Phys.* 77, 4441 (1982).

IV-F-4 Reactions of Vibrational State Selected D_2^+ ions with C_2H_2

Kenji HONMA (*Univ. of Tokyo*), **Kenichiro TANAKA and Inosuke KOYANO**

Vibrational-state selected cross sections have been measured for the reaction of D_2^+ with C_2H_2 by use of the TESICO technique.[1] Although this reaction system possibly has numerous channels, only the products of the following three channels were observed at 1.3 eV of collision energy.

$$D_2^+ + C_2H_2 \rightarrow C_2H_2^+ + D_2 \qquad (1)$$
$$\rightarrow C_2HD^+ + HD \qquad (2)$$
$$\rightarrow C_2H_2D^+ + D \qquad (3)$$

The absence of the channels producing $C_2D_2^+$ and $C_2HD_2^+$ suggests that the reaction proceeds via mainly the direct mechanism.

Reaction cross sections for vibrational states of v = 0 – 7 are summarized in Figure 1, where σ_{26}, σ_{27}, and σ_{28} correspond to the relative cross sections for Reactions 1, 2, and 3, respectively. The charge transfer is the dominant process for all vibrational states. The cross section for Reaction (1) starts to increase at v = 3 and a dramatic increase is also observed in going from v = 4 to v = 5. The increase at v = 5 is also seen in the cross section for Reaction (2). This enhancement of the cross section at v = 5 can be ascribed to the formation of electronically excited product ion: Only the ground state $C_2H_2^+$ (X) ion can be formed from D_2^+ in v = 0 – 4, while the electronically excited $C_2H_2^+$ (A) ion is

possible to be formed with higher vibrational states of the D_2^+ ion. This newly opened channel probably enhances the cross section at v = 5.

The smaller enhancement at v = 3 may be ascribed to the following consecutive path which becomes possible at v = 3.

$$D_2^+ + C_2H_2 \rightarrow C_2H_2D^+ + D \rightarrow C_2H_2^+ + D + D$$

Reference

1) I. Koyano and K. Tanaka, *J. Chem, Phys.* 72, 4858 (1980).

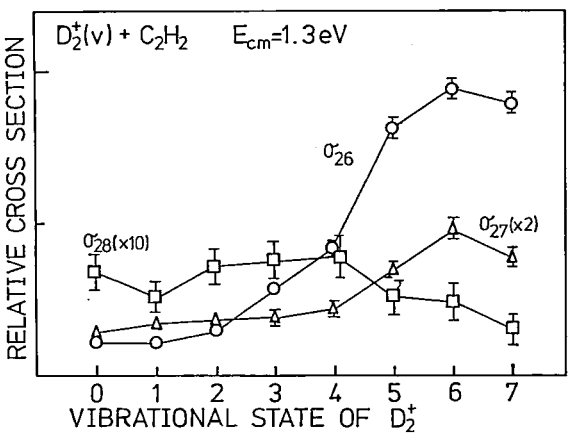

Figure 1. Cross sections for Reactions (1)-(3) as a function of vibrational quantum number of D_2^+.

IV-F-5 Vibrational State Selected Cross Sections for the Reaction of H_2^+ with He and Ne

Kenichiro TANAKA, Shinzo SUZUKI, Zdenek HERMAN (*J. Heyrovsky Inst. of phys. Chem. and Electrochem. and IMS*) **and Inosuke KOYANO**

In order to reveal the role of various forms of energy in promoting the endoergic ion-molecule reaction, the following reactions have been investigated by selecting vibrational and translational energy of H_2^+.

$$H_2^+ + He \rightarrow HeH^+ + H - 0.80\ eV \quad (1)$$
$$H_2^+ + Ne \rightarrow NeH^+ + H - 0.57\ eV \quad (2)$$

Experimental results for Reaction (1) obtained at several collision energies between 0.4 and 3.0 eV are summarized in Figure 1, where relative cross sections are plotted as a function of total energy (sum of the translational and vibrational energy of the reactants). This reaction is one of the simplest ion-molecule reactions for which exact calculation of potential energy surfaces is possible, and thus the reaction has been extensively studied both experimentally and theoretically. The present results give direct and clearer evidence for the previous conclusion that vibrational energy promotes Reaction (1) more efficiently than translational energy, and that reaction proceeds mainly via spectator stripping mechanism at low collision energies. The total energy dependence of the cross sections shown in Figure 1 reproduces the results of trajectory calcultaions[1] remarkably well.

Reaction (2) is an analogue of Reaction (1), but has been much less studied. Experimental results for Reaction (2) obtained have strong resemblance to those in Figure 1, again demonstrating that vibrational energy promotes the reaction more efficiently than translational energy. Thus, we conclude that Reaction (2) also proceeds mainly via spectator stripping mechanism at low collision energies.

Reference

1) W.N. Whitton and P.J. Kuntz, *J. Chem. Phys.* 64, 3624 (1976).

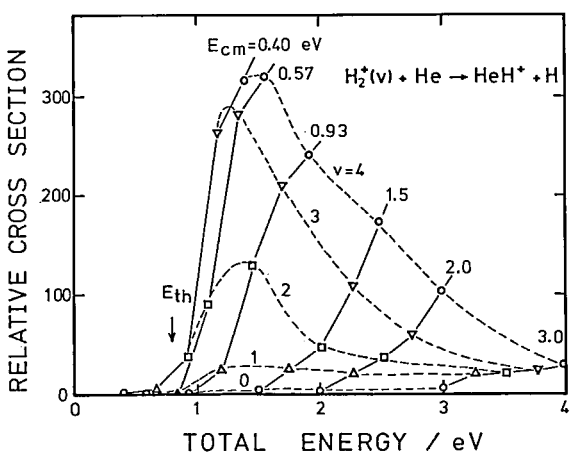

Figure 1. Cross sections for Reaction (1) as a function of total energy of the reactants.

IV— G Photoionization Processes in Small Molecules

Two techniques have generally been used for the study of molecular photoionization processes, i.e., measurements of photoionization efficiency curves (**PIEC**) and photoelectron spectra (**PES**). While **PIEC** yields a wealth of information on the ionization processes and energy levels of ions and neutral molecules, difficulty is often encountered with this technique when autoionization obscures the step structure of the curve. In such a situation, we often resort to **PES** which provides precise locations of ionic states and transition probabilities of these states. However, ionic states that can be studied by the ordinary (constant wavelength) **PES** are largely limited to the states which combine with the ground states of the parent molecule with favorable Franck-Condon factors. Another type of photoelectron spectroscopy is the threshold electron spectroscopy (**TES**) which uses a variable wavelength light source and detects only the zero kinetic energy photoelectrons (threshold electrons). In this method, ionic states which are not favored by direct ionization are often observed through resonance autoionization.

In this project, we study photoionization processes in small molecules by simultaneous measurements of photoionization efficiency curves and threshold electron spectra. Furthermore, we find that the analysis of autoionizing transitions is often possible utilizing charge-transfer processes of the product ions. This technique is also incorporated.

IV-G-1 Threshold Electron Spectra of He and Ne Obtained by Using Synchrotron Radiation

Shizo SUZUKI, Kenichiro TANAKA, Tatsuhisa KATO (*Kyoto Univ.*) **and Inosuke KOYANO**

A new photoionization apparatus, named TEPSICO-II, has been completed and installed in the UVSOR storage ring.[1] It is specially designed for the study of state selected ion-molecule reactions using synchrotron radiation, and consists of a 3 m-normal incidence type of monochromator, a 12 pole ion guide type of reaction chamber, a quadrupole mass spectrometer, and a non-line-of-sight steradiancy type of threshold electron analyzer.

Figure 1 shows threshold electron spectra of He and Ne obtained with this apparatus. As indicated in the figure, threshold electron spectrum of He was taken with the wavelength resolution of the monochromator of 0.05 nm, whereas that of Ne was taken with 0.02 nm. Thus, the difference in the full width of half maximum of the threshold electron spectrum between He and Ne can be ascribed to the difference in the wavelength resolution.

The successful measurement of the threshold electron spectra of He and Ne by using synchrotron radiation encourages us to start the next step to the study of state selected ion-molecule reactions.

Reference

1) K. Tanaka, T. Kato, and I. Koyano, *IMS Ann. Rev.*, 85 (1984).

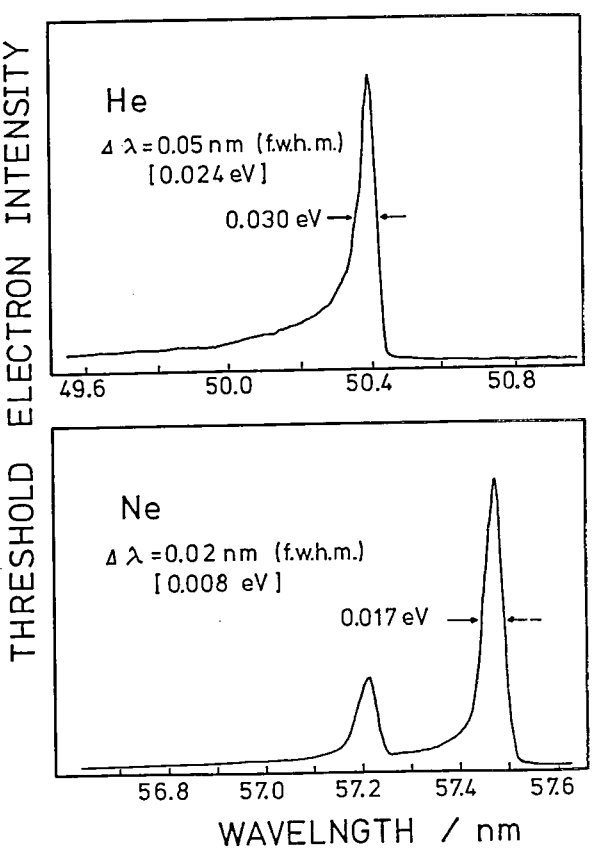

Figure 1. Threshold electron spectra of He and Ne.

IV— H Studies of Unimolecular Decomposition of Complex Molecular Ions

Kenji HONMA (*Univ. of Tokyo*), Kenichiro TANAKA, and Inosuke KOYANO

The TESICO technique which we have developed for the study of state selected ion-molecule reaction (see **IV-F**) is also applicable to the study of unimolecular decomposition of molecular ions. In this technique ions can be prepared with defined amounts of internal energy and their subsequent decomposition investigated. By selecting the parent molecule in this study and comparing its decomposition pattern with the branching ratio of product ions of the corresponding state selected ion-molecule reaction, we can get information on the nature of the intermediate collision complex of ion-molecule reaction. In this project, we are now investigating unimolecular decomposition of $C_2H_2D_2^+$ isomers to get information on the collision complex of the reactions $C_2H_2^+ + D_2$ and $C_2D_2^+ + H_2$.

IV— I VUV Photoelectron Spectroscopic Studies of Gaseous Molecules

Molecular photoelectron spectroscopy with a 58.4-nm HeI resonance source has been used for a long time to determine ionization potentials for a number of organic and inorganic compounds in the gas phase as well as to study their electronic structures in the neutral ground state and various ionic states. Previously, the He I photoelectron spectra measured for about 200 basic compounds in the gas phase under similar experimental conditions have been compiled in a book, together with the theoretical assignments derived from ab initio calculations as well as the MO drawings [Kimura, Katsumata, Achiba, Yamazaki, and Iwata, "Handbook of HeI photoelectron Spectra" (Halsted Press, 1981)].

IV— J Studies of Ionization of Hydrogen-Bonded Dimers and Proton Transfer

Ionization of hydrogen-bonded dimers produced in a supersonic expansion is interesting from the standpoints of both electronic structure and molecular structure, since proton transfer takes place in the ionic states. The observed first two ionization bands in a HeI photoelectron spectrum of the water dimer $(H_2O)_2$ are broad, suggesting that the equilibrium geometry of the water dimer cation considerably differ from that of the neutral water dimer because of proton transfer. This phenomenon is probably common for many other linear hydrogen-bonded dimers. In this sense, the proton transfer of the water dimer cation in the ground state is a typical example. In this project we have been continueing to study hydrogen-bonded dimer cations from both experimental and theoretical points of view.

IV-J-1 Equilibrium Structure and the Two Kinds of Dissociation Energies of the Ammonia Dimer Cation $H_3NH^+ ... NH_2$

Shinji TOMODA (*Osaka Univ.*)
and Katsumi KIMURA

[*Chem. Phys. Lett.*, **121**, 159 (1985)]

From ab initio calculations, the equilibrium structure of the ammonia dimer cation is regarded as a complex between the ammonium ion (NH_4^+) and the aminyl radical (NH_2) with an N...N distance of about 2.8 Å. Two kinds of dissociation energies (D_e's) of this equilibrium cation $(NH_3)_2^+$ (eq) have been evaluated theoretically from the potential energy surface for the two significant dissociation channels into $NH_4^+ + NH_2$ and $NH_3 + NH_3^+$. These theoretical D_e values are found to be about 1.0 eV and 1.7 eV, respectively. A large discrepancy (~1 eV) between these theoretical values and the experimental ones deduced from the appearance energy of $(NH_3)_2^+$ and NH_4^+ [1] has been attributed to the very large

geometrical change (Figure 1) in $(NH_3)_2^+$ by proton transfer as well as the unobservable character of the real adiabatic ionization energy of $(NH_3)_2$ because of the limitation by the Franck-Condon region.

The present value of D_e $[NH_4^+ + NH_2]$ = 1.0 eV seems to be consistent with the experimental solvation energy of NH_4^+ with NH_3 (1.08 eV) obtained in the high-pressure mass spectrometric study. However, the experimental D_e value (0.05 eV) deduced from the appearance energies[1] is certainly too small, compared with the above solvation energy.

Reference

1) S.T. Ceyer, P.W. Tiedemann, B.H. Mahan, and Y.T. Lee, *J. Chem. Phys.*, 70, 14 (1979).

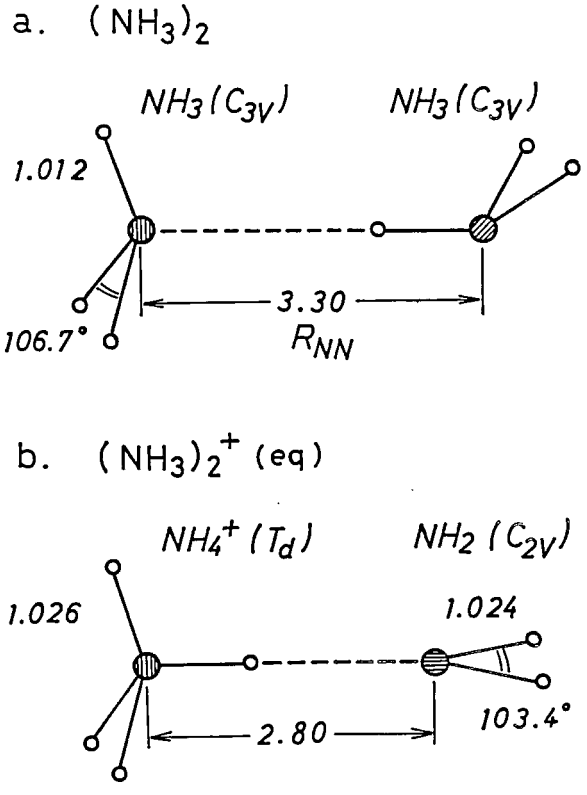

Figure 1. Equilibrium structures of (a) the ammonia dimer $(NH_3)_2$ and (b) its cation $(NH_3)_2^+$, both in their ground electronic states. (a) $(NH_3)_2$: The geometry of the monomer (r_e = 1.012 A, θ_e = 106.7° [11]) is assumed to be conserved in the dimer which has a staggered conformation at the equilibrium N...N distance (R_{NN}) of 3.30 Å. (b) $(NH_3)_2^+$ (eq): The equilibrium cation is regarded as a complex between the ammonium ion (NH_4^+) and the aminyl radical (NH_2). The C_{2v} symmetry axis of NH_2 is coaxial with the N–H...N (hydrogen) bond axis.

IV-J-2 Appearance Energies and Dissociation Energies of Hydrogen-Bonded Dimer Cations: $(H_2O)_2^+$ and $(NH_3)_2^+$

Shinji TOMODA (*Osaka Univ.*) and **Katsumi KIMURA**

[Advances in Mass Spectrometry, in press)]

Ionization energies (IE's) of the simple hydrogen-bonded dimers have been studied experimentally either by photoionization mass spectrometry (PIMS) or by photoelectron spectroscopy (PES). In this paper we characterize the common features in the ionization processes of the water and the ammonia dimer by giving the theoretical appearance energy (AE) and IE values obtained from ab initio potential surface calculations. The experimental AE and IE values are interpreted consistently for both $(H_2O)_2$ and $(NH_3)_2$ by the present theoretical results on the common hypothesis[1, 2] that the real adiabatic ionization energy is not obtained in the experiment because of the Franck-Condon factor limitations.

As is shown in Table 1, the theoretical and the experimental values show reasonable agreement, which suggests strongly the validity of the above hypothesis. Moreover, the hypothesis solves the problem of the unexpectedly small dissociation energies (D_e's) of the ammonia dimer cation deduced from the experimental AE values and requires corrections of the D_e values for both $(H_2O)_2^+$ and $(NH_3)_2^+$. The discrepancy between the theoretical and the apparent experimental D_e value is larger (about 1 eV) for the ammonia dimer cation, probably due to the larger geometrical change in the equilibrium dimer cation.

Table I. TE's and AE's of $(H_2O)_2$ and $(NH_3)_2$ (in eV)

Initial State	Final State	Kind of IE	Theoretical	Experimental
H_2O	$H_2O^+(^2B_1)$	I_v	12.62*	12.62
$(H_2O)_2$	$(H_2O)_2^+(^2A'')$	I_a	10.5	–
		AE	11.1	11.21
		I_v	11.7	12.1
	$H_3O^+(^1A_1)$	AE	11.4	11.73
NH_3	$NH_3^+(^2A''_2)$	I_a	10.16*	10.16
$(NH_3)_2$	$(NH_3)_2^+(^2A')$	I_a	8.4	–
		AE	9.8	9.54
		I_v	10.1	–
	$NH_4^+(^1A_1)$	AE	9.5	9.59

*Reference theoretical value corrected to be equal to the established expermental one.

References
1) S. Tomoda and K. Kimura, *Chem. Phys.*, 82, 215 (1983).
2) S. Tomoda and K. Kimura, *Chem. Phys. Lett.*, **111**, 434 (1984).

IV— K Development and Application of Excited-State Photoelectron Spectroscopy With Resonant Multiphoton Ionization

Excited-State photoelectron spectroscopy by selective excitation/ionization of molecules with UV and visible tunable lasers by means of a resonant multiphoton ionization technique has been developed in this Institute since 1980 [IMS Annual Review (1980-84)]. This new spectroscopy has been found to provide new information about dynamic behavior of excited states that cannot be obtained by other spectroscopic methods. In this sense, such laser photoelectron technique will rapidly develope as a powerful tool for studying photochemical and photophysical behavior of excited states. The technique itself has almost been establashed, although further improvement is desirable. In this project we have been extending our excited-state photoelectron spectroscopic studies to various molecular systems in supersonic jet.

IV-K-1 Photoelectron Spectroscopy of Excited States

Katsumi KIMURA

[*Adv. Chem. Phys.*, **60**, 161 (1985)]

This is the first review paper in the field of laser excited-state photoelectron spectroscopy or multiphoton ionization photoelectron spectroscopy. This review paper is focussed on the following points: (1) characteristics of laser excited-state photoelectron spectroscopy based on resonant multiphoton ionization, (2) related studies published so far in this field, and (3) future applications of this technique to studies of excited states in photochemistry and photophysics.

IV-K-2 Multiphoton Ionization Photoelectron Spectroscopic Study on NO: Autoionization Pathyway through Dissociative Super-Excited Valence States

Yohji ACHIBA Kenji SATO, and Katsumi KIMURA

[*J. Chem. Phys.*, 82, 3959 (1985)]

We have carried out measurements of total ion-current and photoelectrons to study autoionization of NO molecule through the two-photon resonant, valence-excited B $^2\Pi$ state at the $v' = 9$ level (designated as B-9).

From the experimental results, we have deduced the following conclusions. 1) The overall process of producing the normal rotational lines is represented by $X \rightarrow$ B-9 $\rightarrow$ I*$\rightsquigarrow NO^+ + e^-$, where I* means the super-excited valence I $^2\Sigma^+$ state and $\rightsquigarrow$ indicates electronic autoionization forming the ground electronic state of ions. 2) The ionization scheme of producing the intensity-anomalous rotational lines is expressed by $X \rightarrow$ B-9 $\rightarrow$ N-6 $\leftrightarrow$ B'*$\rightsquigarrow NO^+ + e^-$, involving an accidental double resonance, where N is the Rydberg N $(4d\delta)\ ^2\Delta$ state, B'* is the super-excited valence B' $^2\Delta$ state, and $\leftrightarrow$ means an electronic coupling between the Rydberg and the valence states. 3) No photoelectron angular dependence occurs for the $v^+ = 0$ band, probably because of relatively long lifetime of the Rydberg N state.

IV-K-3 Vibrationally Resolved Photoelectron Spectra of Jet-Cooled Naphthalene: Intramolecular Relaxation Processes in S_1 and S_2 States

Atsunari HIRAYA, Yohji ACHIBA, Naohiko MIKAMI (*Tohoku Univ. and IMS*), **and Katsumi KIMURA**

[*J. Chem. Phys.*, 82, 1810 (1985)]

Combining a photoelectron spectroscopic technique with a (1 + 1) resonant ionization method,

we have investigated photoelectron spectra by ionizing naphthalene through single vibronic levels of the S_1 state up to an internal energy (E_{vib}) of about 2500 cm^{-1} as well as through some vibronic levels of the S_2 origin region. The photoelectron spectra thus obtained have been found to show many bands which are interpreted as the vibrational structure of the naphthalene cation. The present photoelectron results also support the available spectroscopic evidence that intramolecular vibrational redistribution occurs at the energy levels higher than 2200 cm^{-1} above the S_1 origin. Intramolecular electronic relaxation from the S_2 to the S_1 state has been found to be faster than ionization under the present laser irradiation conditions, suggesting that the relaxation rate is larger than an order of $10^{11} s^{-1}$.

IV-K-4 Multiphoton Ionization of Triethylamine: Determination of the Vibrationless S_2 Level by Laser Photoelectron Spectroscopy

Masahiro KAWASAKI (*Mie Univ.*), **Kazuo KASATANI** (*Mie Univ.*), **Hiroyasu SATO** (*Mie Univ.*), **Yohji ACHIBA, Kenji SATO, and Katsumi KIMURA**

[*Chem. Phys. Lett.*, 114, 473 (1985)]

Triethylamine was excited to a vibrational level of the S_2 (Rydberg) state and then ionized with a (2 + 1) resonance multiphoton ionization method. One of the important conclusions deduced from this study is that the vibrationless level of the S_2 state is obtainable from a photoelectron spectroscopic point of view. The vibrationless level thus determined is $E_0(S_2) = 41200$ cm^{-1}. It should also be mentioned that only the ionization through the S_2* state is detectable under the present experimental conditions, although the occurence of fast intramolecular electronic relaxation $S_2^* \rightsquigarrow S_1^*$ has so far been reported in the previous fluorescence studies.

IV-K-5 Laser Photoelectron Spectroscopic Determination of Electronic States of Fe Atoms Produced in Multiphoton Dissociation of $Fe(CO)_5$ in the Gas Phase

Yatsuhisa NAGANO, Yohji ACHIBA, and Katsumi KIMURA

Irradiating a gaseous $Fe(CO)_5$ sample by a visible dye laser, we have observed a complicated MPI ion-current spectrum which shows many sharp peaks in the laser wavelength region 446-452 nm, as shown in Figure 1. From mass spectra observed at these ion-current peaks, it has been indicated that Fe atoms are mainly produced. In order to identify the electronic states of Fe atoms produced, we have measured photoelectron kinetic-energy spectra at more than thirty ion-current peaks. Using our photoelectron technique previously described,[1] we have been able to identify the electronic states of the Fe atoms up to the fifth electronic term (a $^3P_2$). In this paper we demonstrate for the first time that the laser photoelectron spectroscopic technique makes it possible to identify electronic states of atomic species produced by photodissociation.

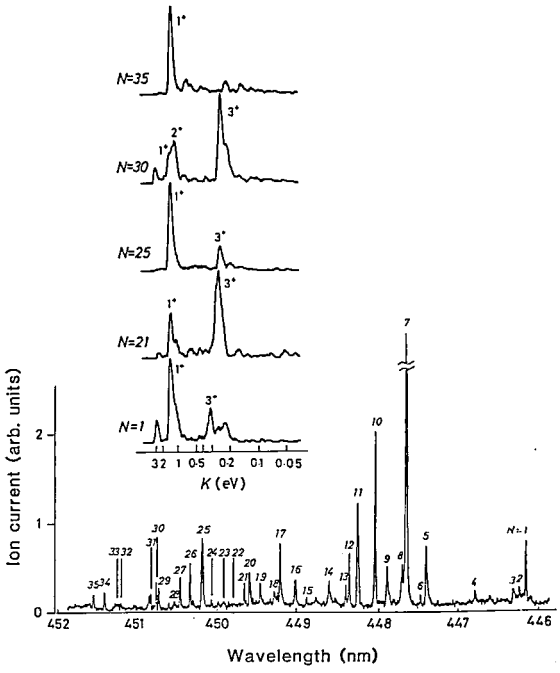

Figure 1. An MPI ion-current spectrum obtained for $Fe(CO)_5$ in the gas phase. The ion-current peaks are numbered by N = 1 – 35. In the upper, five photoelectron spectra are shown, obtained at N = 1, 21, 25, 30, and 35. All these photoelectron spectra originate from the second electronic state of Fe (a ^5F_J). The ionic states are indicated by 1^+, 2^+, 3^+, etc. The photoelectron energy analysis provides unambiguous assignments of MPI ion-current peaks.

Reference

1) Y. Nagano, Y. Achiba, and K. Kimura, *Chem. Phys. Lett.*, 93, 510 (1982).

IV-K-6 Photoelectron Spectroscopic Interpretation on Background Signal Observed in Multiphoton Ionization Ion-Current Spectrum of Iron Pentacarbonyl

Yatsuhisa NAGANO, Yohji ACHIBA, and Katsumi KIMURA

Under moderate laser irradiating conditions, a significant background signal was observed in the MPI ion-current spectra of Fe $(CO)_5$ in the gas phase in the laser wavelength region 360-400 nm as shown in Figure 1. In order to clarify the origin of the ion-current background, photoelectron kinetic-energy measurements were carried out at three laser wavelengths at which only the ion-current background signal is observed. From the photoelectron energy analysis, it is concluded that the background signal of the MPI ion-current spectrum is attributed to two-photon ionizations of various electronic states of Fe atoms produced from Fe $(CO)_5$ by photodissociation.

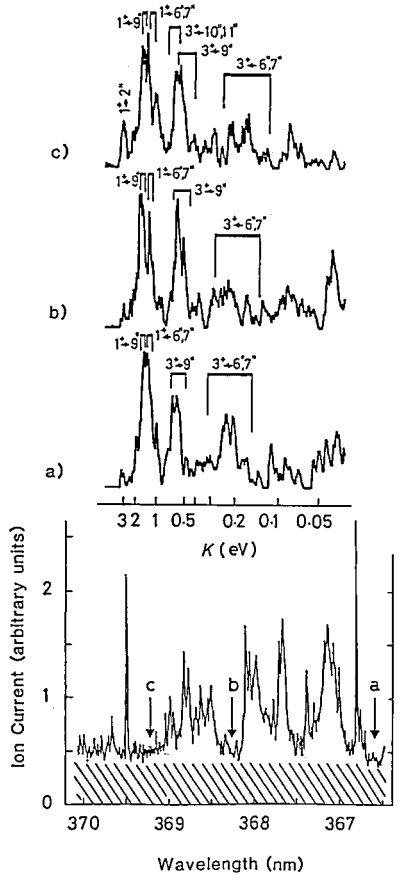

Figure 1. MPI ion-current spectrum obtained for Fe $(CO)_5$ in the 366.5-370.0 nm region. The background signal is shaded. Photoelectron spectra were measured at the three laser wavelengths indicated by arrows a, b, and c. In the upper, photoelectron spectra are shown, which were obtained at the three different laser wavelengths (a, b, and c), where only the background signal appears in the ion-current spectrum. The main photoelectron peaks are interpreted in terms of two-photon ionizations of the excited states (6″, 7″, 9″, 10″ and 11″) of Fe atoms, corresponding to the 1^+ and 3^+ ionic states.

The photoelectron kinetic energies were evaluated by the following relationship: $K_{calc.} = 3h\nu - I + E(i'') - E(j^+)$, where $3h\nu$ is the total photon energy absorbed in the multiphoton ionization, I is the first ionization potential of Fe (7.90 eV), E (i″) and E (j^+) are the internal energies of the initial state i″ and final state j″ of Fe atoms, respectively.

IV-K-7 Rotational State Distributions Observed in UV Photodissociation of the Rare Gas-NO van der Waals Molecules

Kenji SATO, Yohji ACHIBA, and Katsumi KIMURA

Using two-color laser multiphoton ionization technique we have investigated rotational state distributions of photofragments. The electronically excited photofragment NO*(A) was produced by direct UV photodissociation of the rare gas-NO van der Waals molecules. The rotational state distributions of the fragment NO were then determined by a two-photon ionization technique using a visible laser at the same time. The rotational intensity distributions thus obtained are shown in Figure 1.

Experimental results show the following interesting features: 1) Two maxima appear in the rotational state distributions. 2) By changing the excess energy E (corresponding to the energy above the dissociation limit) as well as the rare gas partner, the J number at the two maxima (J_{max}) vary in such a way that $J_{max} \propto \sqrt{E}$ and $J_{max} \propto \sqrt{\mu}$, where μ is the reduced mass of the rare gas-NO complex.

This phenomenon is analogous to the rotational rainbow structure already found in inelastic scattering experiments.[1] Therefore, if the present observation is indeed the case where the rotational state distribution appearing in the photodissociation process is much affected by scattering factors, the present

method would be quite appropriate to understand an anistropic property of a potential surface of a molecular excited state.

Reference

1) R. Schinke and J.M. Bowman, *"Molecular" Collision Dynamics"* ed. by J.M. Bowman, (Springer 1983) pp.61.

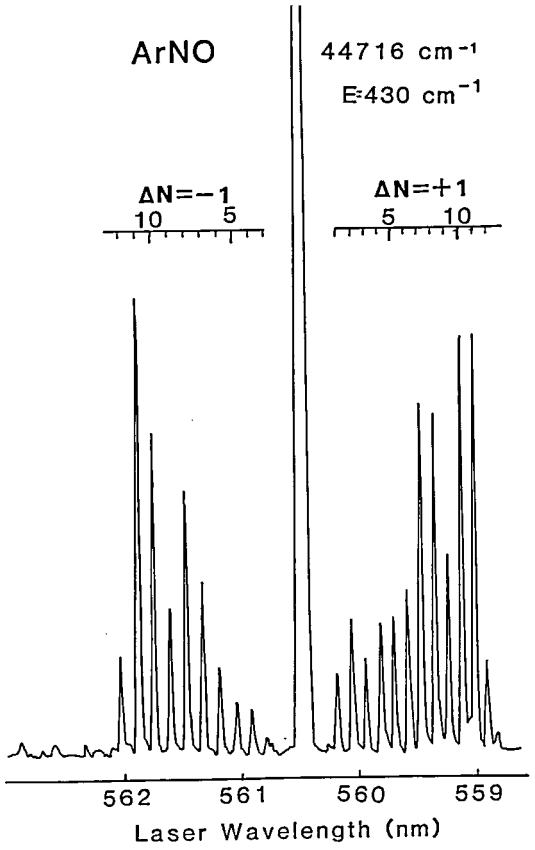

Figure 1. Two-photon ionization spectrum of the A state NO produced by the direct photodissociation of ArNO van der Waals molecule upon excitation at 44300 cm^{-1}. The rotationally resolved spectrum corresponds to the transition of the F ← A, and the intensity of each rotational line reflects the rotational state distributions of the photofragment NO.

IV-K-8 A Rotational Rainbow Approach to Interpret the Rotational State Distributions in Photodissociation

Kenji SATO, Yohji ACHIBA, Hiroki NAKAMURA, and Katsumi KIMURA

Under the assumption of a half-collision approximation, a rotational rainbow approach has been found to be suitable to interpret the rotational state distributions of photofragments produced in the direct photodissociation process of weakly bound van der Waals molecules such as ArNO. In order to reproduce the experimentally observed rotational intensity distribution of the Rydberg A state of the NO photofragment, the photodissociation cross section σ_{if} has been calculated by using the following equation,

$$\sigma_{if} \propto \sum_{JM} \sum_{l_f\ jl} |\Sigma(1+S)^{JM}_{j_f l_f j l}\, W^{JM,\ i}_{jl}|^2$$

where 1 means the unit matrix, S the scattering matrix, and W the Franck Condon factor, J the total angular momentum, M the projection of J, j the rotational quantum number of the photofragment molecule, and l the orbital angular momentum of the dissociated atom and molecule.

Assuming that the van der Waals molecule is very cold; i.e., $j_i = 0$, $M_1 = 0$, $j_i = 0$, and assuming a Lennard-Jones type potential for the NO molecule, we have carried out close coupling calculations for the S matrix associated with the rotational excitation. An example of the calculated J distributions is shown in Figure 1, indicating the two maxima. This pattern is quite similar to those of the experimental ones (see also IV-K-7).

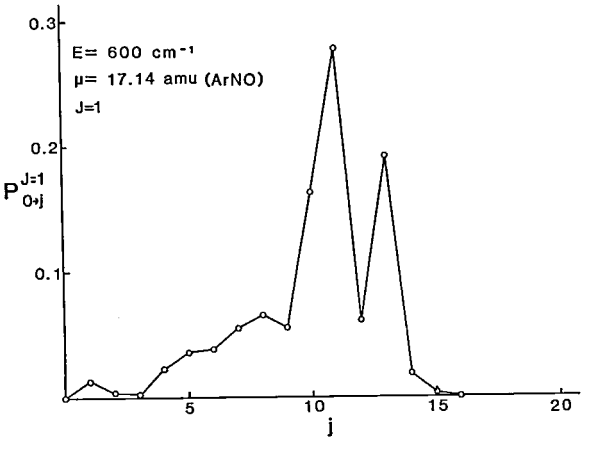

Figure 1. Rotational excitation probability of Ar-NO* (A) collision calculated with close-coupling method using a model potential. The model potential is modified *L-j* (12, 6) potential involving the first and the second order Legendre polynomials. Collision energy is indicated in the figure.

IV-K-9 Evidences for the Formation of Electronically Excited NO in Two-Photon Ionization Process of the NO Dimer

Kenji SATO, Yohji ACHIBA, and Katsumi KIMURA

Two-photon ionization (TPI) mass signals of supersonic expanded NO gas through a pulsed nozzle show only NO^+ formation but not $(NO)_2^+$ at all, while the existence of the NO dimer in the ground state has been confirmed. In order to understand the character of the electronically excited NO dimer, we have studied resonant TPI processes of $(NO)_2$ in detail, especially by measuring photoelectron energy distributions with pulsed UV laser sources around 200 nm.

The present photoelectron measurements have strongly suggested that the UV laser excitation causes a rapid photodissociation of the NO dimer in the excited state, forming the Rydberg A $^2\Sigma^+$ state of free NO and subsequent additional one-photon excitation of the A state then leads to the formation of NO^+.

Actually the photoelectron peak energies obtained at different laser wavelengths shown in Figure 1 are fairly coincident with the energies calculated by the assumption that the NO^+ ion is formed from the A-state NO molecule by a one-photon ionization.

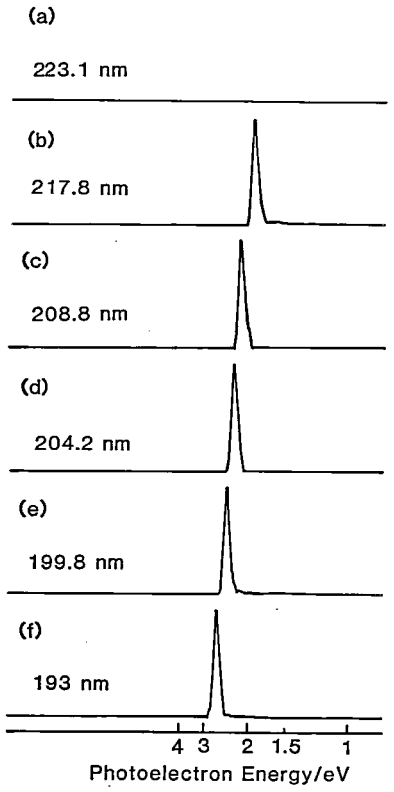

Figure 1. Photoelectron spectra obtained by excitation of the NO dimer using UV laser lights.

The present experimental data suggest the very diffuse absorption spectral feature of the excited NO dimer at around 200 nm and the occurence of rapid predissociation after excitation.

IV-K-10 What is a Precursor for NH_4^+ Production in Two-Photon Ionization of the NH_3 Dimer

Kenji SATO, Yohji ACHIBA, and Katsumi KIMURA

The production of NH_4^+ has been suggested as a dominant ionic species in a two-photon ionization (TPI) process of the NH_3 dimer.[1] Thus the question has arisen why the NH_4^+ is dominant instead of the $(NH_3)_2^+$ parent ion. Since photoelectron spectra always reflect the molecular status produced immediately after the ionization event, measurements of photoelectron energy distributions for TPI of $(NH_3)_2$ must be important to answer to the above question.

So far there have been two possible interpretations to describe such an anomaly. One is that very rapid photodissociation takes place in the excited state of $(NH_3)_2$ prior to the ionization, forming NH_4 and NH_2 neutrals.[2] Subsequent one-photon ionization of the NH_4 radical should result in the formation of NH_4^+. In such a case, the photoelectron spectrum should reflect the ionization of the NH_4 radical. The other one is that at the first stage of the ionization process, the $(NH_3)_2^+$ parent ion is produced as an ionic precursor, and then intramolecular relaxation causes the reaction of $(NH_3)_2^+ \rightsquigarrow NH_4^+ + NH_2$. Therefore, contrary to the former case, the present case necessarily results in a photoelectron spectrum corresponding to the ionization of the parent dimer molecule.

The TPI photoelectron spectra using several different laser wavelengths at around 200 nm are shown in Figure 1, indicating that the electron energy distributions can be interpreted in terms of the formation of the $(NH_3)_2^+$ parent ion at the first ionization stage. It should also be noted that in Figure 1 the photoelectron bands attributable to the polymer ionization are also apparent.

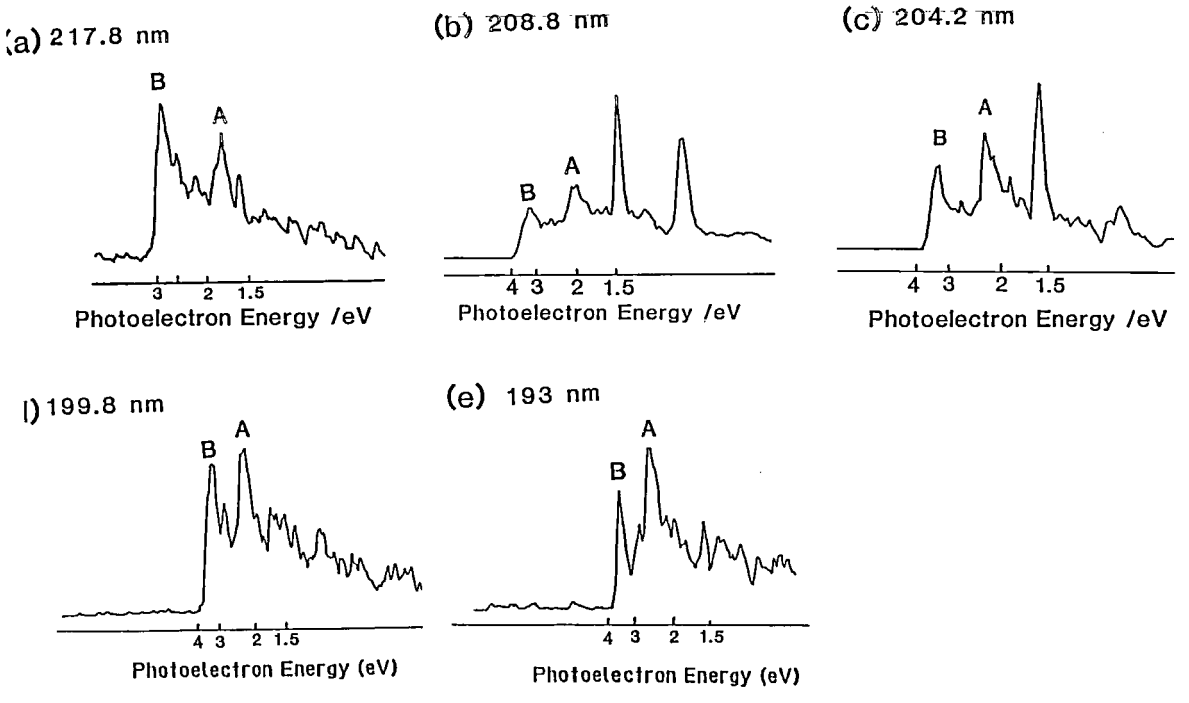

Figure 1. Photoelectron spectra of ammonia dimer and clusters obtained by five different UV laser wavelengths; (a) 217.8 nm, (b) 208.8 nm, (c) 204.2 nm, (d) 199.8 nm, and (e) 193 nm. The photoelectron bands A and B correspond to the ionization of the dimer and the higher order clusters, respectively.

IV— L Synchrotron Radiation Researches of Molecules and Molecular Clusters——Photoionization and Photoelecton Spectroscopy

The use of synchrotron radiation in studies of photoionization and photoelectron spectroscopy in the gas phase is especially attractive for studying high electronic states and various ionic states of molecules and molecular cluster (or van der Waals molecules), because of its continuous character of the light intensity against the wavelength in the whole VUV region. The 600-MeV electron storage fing (UVSOR) is now operating in this Institute (see P. 146).

IV-L-1 Construction of a Supersonic Molecuar Beam Apparatus for Synchrotron Radiation Research

Yohji ACHIBA, Kenji SATO, and katsumi KIMURA

A supersonic molecular beam apparatus for synchrotron radiation experiments has almost been completed. A technique of supersonic beam is apparently suitable and desirable for spectroscopic studies of molecular clusters as well as free molecules. Particularly a combination of this technique with a synchrotron radiation light source would undoubtedly open new aspects in the fields of vacuum UV photophysics and photochemistry.

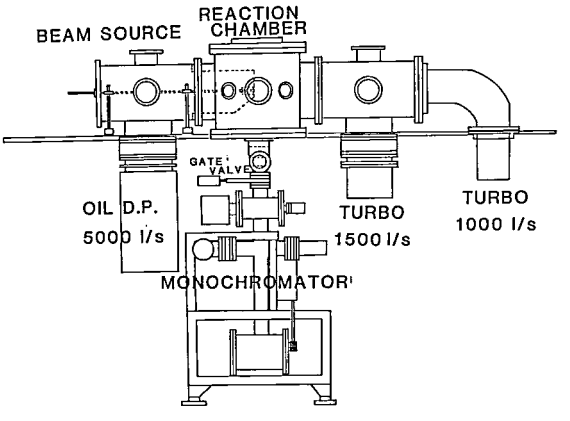

Figure 1. A schematic side view of a supersonic nozzle beam apparatus for sychrotron radiation reserach.

Schematic side view of our molecular beam apparatus is shown in Figure 1. The photon-molecular beam collision chamber is separated from a beam-source chamber with a skimmer, and each chamber is evacuated by two turbo molecular pumps (1500 l/s, 1000 l/s) or an oil diffusion pump (5000 l/s). There is a two-stage differential pumping system between the molecular beam apparatus and a monochromator exit slit to keep the vacuum in the monochromator below 2×10^{-9} Torr under operation. This apparatus would enable us to study; 1) vacuum UV absorption spectra of ultracold free molecules, 2) half collisional reaction processes of superexcited or ionic molecular clusters using a mass selected photoionization technique, and 3) photoelectron energy and angular dependence spectra of molecules and molecular clusters.

IV— M Production, Characterization, and Spectroscopic Studies of Molecular Complexes and Clusters

There are several techniques to investigate physics and chemistry of molecular complexes and clusters. One of the most powerful techniques for producing such weakly bound complexes is the supersonic expansion of a high pressure gas through a small nozzle hole, by which one can produce a very large numbers of exotic molecules. However, characterization of such complexes is hard because of its weak bonding character.

In this project we have applied laser induced fluorescence spectroscopy combined with a nanosecond time resolved fluorescence technique to study the dynamics of electronically excited rare gas clusters and solvated molecules of substituted anthracenes produced in a free jet expansion.

IV-M-1 Lack of Heavy Atom Effect on the Fluorescence Lifetimes of 9-Cyanoanthracene-Rare Gas Clusters in a Supersonic Free Jet

Satoshi HIRAYAMA (*Kyoto Inst. of Tech.*), **Kosuke SHOBATAKE, and Kiyohiko TABAYASHI**

[*Chem. Phys. Lett.* **121**, 228 (1985)]

Fluorescence lifetimes of 9-cyanoanthracene (9CNA) and its rare gas (Ar, Kr, and Xe) clusters have been measured under the supersonic free jet conditions. Figure 1 shows a typical excitation spectrum of 9CNA seeded in Ar at stagnation pressure of 600 Torr. For the bare 9CNA molecule, the lifetime was found to be 28.0 ± 0.2 ns upon 0-0 band excitation and is practically independent of the excess energy within 590 cm^{-1} above the electronic origin. With any kind of rare gas atom, the fluorescence lifetimes of the clusters in the vibrationless states are in the range 26-32 ns, indicating the absence of a heavy atom effect on the energy dissipating path of these clusters, unlike with case of the tetracene-rare gas clusters which were found to show a strong heavy atom effect.[1] On the other hand, in the vibrationally excited states, their lifetimes are greatly shortened. For instance, the 9CNA-Ar and 9CNA-Kr clusters with the excess energy of 214 cm^{-1} decay with the lifetimes of 8.2 ± 0.4 and 10.1 ± 0.3 ns., respectively, while the 9CNA-Xe cluster has a lifetime of 7.4 ± 0.8 ns. The shortening

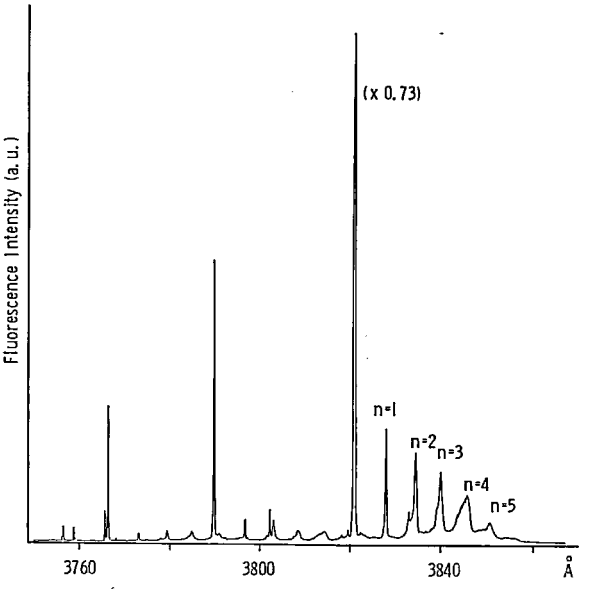

Figure 1. The fluorescence excitation spectra of Ar (p = 600 torr). The fluorescence lifetime for each band and plausible coordination numbers are given on the figures. The bands due to the vibrational excitation of the clusters are also found but their intensities are much lower than those expected.

of lifetimes was explained to be due to enhanced energy relaxation of the electronically excited 9CNA moiety induced by "inter-molecular" collisions in the van der Waals (vdW) vibrational motions between a rare gas atom and 9CNA inside the undissociated vdW molecule subjected to fast intramolecular energy transfer from an intramolecular vibrational mode to vdW modes.

References

1) A. Amirav, U. Even, and J. Jortner, *J. Chem. Phys.*, 75 2489 (1981).

IV— N Molecular Beam Studies of Reaction Dynamics Involving Chemically Reactive Atoms and Free Radicals

In this project we investigate dynamics of the chemical reactions involving reactive species such as N, B, C, CH, etc. using a crossed molecular beams technique. For the production of supersonic nozzle beams of these reactive species, especially for active nitrogen atoms, an arc-heated nozzle beam source has been used. Two molecular beam machines, MBC-I which applies the rotatable mass spectrometer detector and MBC-II with optical spectroscopic detection, are operational.

IV-N-1 Polarization of CN ($B^2\Sigma^+$-$X^2\Sigma^+$) Emission Produced in Collision of Ar ($^3P_{0,2}$) with BrCN

Takashi NAGATA*, Tamotsu KONDOW*, Kozo KUCHITSU* (*Univ. of Tokyo), Kiyohiko TABAYASHI, Shigeru OHSHIMA, and Kosuke SHOBATAKE

[*J. Phys. Chem.* 89, 2916 (1985)]

Rotational alignment in the CN ($B^2\Sigma^+$) fragment was observed by measuring polarization of the CN ($B^2\Sigma^+$-$X^2\Sigma^+$) emission from BrCN excited by Ar ($^3P_{0,2}$) impact. Figure 1 shows the degree of polarization of the CN ($B^2\Sigma^+$-$X^2\Sigma^+$) emission produced from the reaction:

$$Ar\ (^3P_{0,2}) + BrCN \rightarrow Ar\ (^1S_0) + Br + CN\ (B)$$

against the average collision energy. The degree of polarization with respect to the beam axis was 0.023 ± 0.004 at a collision energy of 1.33 eV and decreased with impact energy. This observation indicates that the production of CN (B) fragments is caused primarily by energy transfer from Ar ($^3P_{0,2}$) to BrCN.

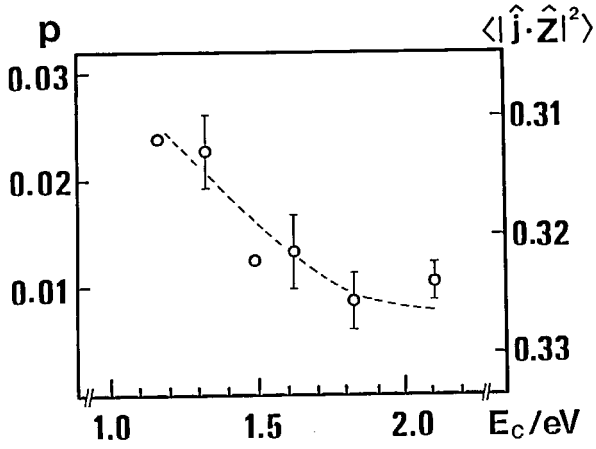

Figure 1. Degree of polarization of the CN ($B^2\Sigma^+$-$X^2\Sigma^+$) emission plotted against the average collision energy of the reactants. The corresponding values for $\langle|j\cdot z|^2\rangle$ are shown on the righthanded ordinate. Error bars represent one standard deviation. The data without error bars, determined by a single measurement, are less accurate than the others.

IV-N-2 Collision Energy Dependence of the Cross Sections for the Dissociative Excitation Reactions: Rg ($^3P_{0,2}$) + NH_3 → Rg + NH ($A^3\Pi$, $c^1\Pi$) + H_2, (Rg = Ar, Kr)

Kiyohiko TABAYASHI and Kosuke SHOBATAKE

[*J. Chem. Phys.* (in press)]

The integral cross sections for the title reactions were determined for relative collision energies between 0.3 and 1.4 eV by applying arc-heated metastable rare gas beams to a crossed molecular beam — TOF energy selection technique[1], in which product fluorescence intensities from both NH ($A^3\Pi$-$X^3\Sigma^-$) and NH ($c^1\Pi$-$a^1\Delta$) bands were monitored. With Ar ($^3P_{0,2}$) excitation, the relative branching fractions of nascent NH ($A^3\Pi$) and NH ($c^1\Pi$) formation

were found to be invariant with the collision energy within the experimental error. With Kr ($^3P_{0,2}$) excitation, however, no apparent NH ($c^1\Pi$-$a^1\Delta$) emission was observed, only emission from NH ($A^3\Pi$) was observed. The absolute cross section for formation of these nascent NH radicals was also determined (Figure 1). Collision energy dependence of the cross section for the reaction Ar ($^3P_{0,2}$) + NH_3 → NH ($A^3\Pi$, $c^1\Pi$) + H_2 was found to be negative, whereas that for the reaction Kr ($^3P_{0,2}$) + NH_3 → NH ($A^3\Pi$) + H_2 showed positive dependence in the collision energy range studied. Possible mechanisms for the formation of NH ($A^3\Pi$, $c^1\Pi$) from Rg ($^3P_{0,2}$) + NH_3 are discussed.

Reference

1) K. Tabayashi and K. Shobatake, *J. Chem. Phys.*, in press.

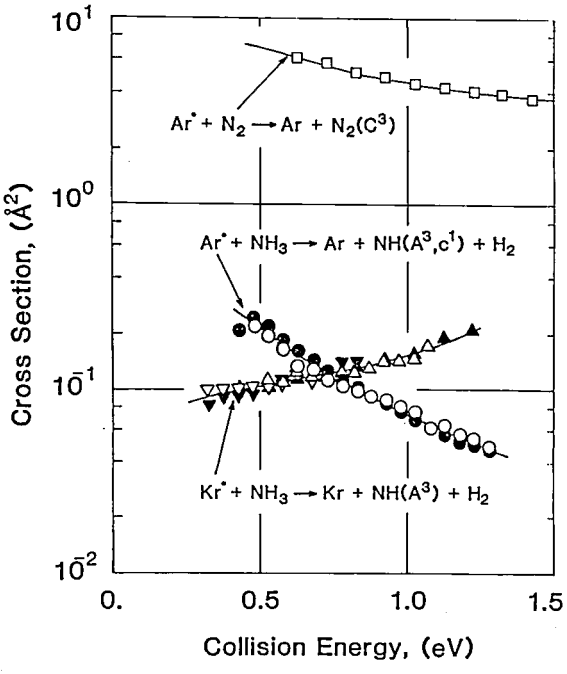

Figure 1. Dissociative excitation cross sections vs collision energy in collisions of Rg* with NH_3. The cross sections for the reference reaction Ar* + N_2 → Ar + N_2 ($C^3\Pi_u$) are also shown. ○, ●: Ar* + NH_3; △, ▲, ▽, ▼: Kr* + NH_3; and □: Ar* + N_2 collisions. Each symbol corresponds to the data obtained under the same Rg* beam stagnation condition.

IV-N-3 Chemiluminescence of NS ($B^2\Pi$) Produced by the Reaction of N* (^2D, ^2P) with COS and CS_2.

Kiyohiko TABAYASHI and Kosuke SHOBATAKE

Despite a large body of kinetic data is available for the quenching processes of metastable N (^2D, ^2P) atoms, it is limitted to near thermal collisions and in only few reactions have the exact reaction channels been identified. Here we have applied an arc-heated N atom beam to crossed molecular beam reactions of N* (^2D, ^2P) with COS and CS_2, and emission from nascent NS ($B^2\Pi$) produced in the reaction was observed.

For both N* + COS and N* + CS_2 reactions, no apparent emissions other than NS ($B^2\Pi$-$X^2\Pi$) band were observed between 2000 and 5200 Å. Typical band emission profiles recorded at average collision energies $\bar{E}$ = 0.78 for COS rection and 0.81 eV for CS_2 are shown in Figure 1. From these spectra one finds that NS ($B^2\Pi$) products from N* + COS are vibrationally excited up to $v' = 12$, whereas those from N* + CS_2 are less populated in the higher vibrational states (up to $v' \cong 5$). According to the correlation diagrams constructed in C_s symmetry, NS ($B^2\Pi$) should be produced only from N (^2D) + COS and N (^2P) + CS_2 reactants, as the exoergic products. If these adiabatic processes are exclusively involved, one can propose the following processes for the present systems:

$$N(^2D) + COS(X^1\Sigma^+) \rightarrow NS(B^2\Pi) + CO(X^1\Sigma^+)$$
$$\Delta H = -0.42 \text{ eV} \quad (1)$$
$$N(^2P) + CS_2(X^1\Sigma^+) \rightarrow NS(B^2\Pi) + CS(X^1\Sigma^+)$$
$$\Delta H = -0.26 \text{ eV} \quad (2)$$

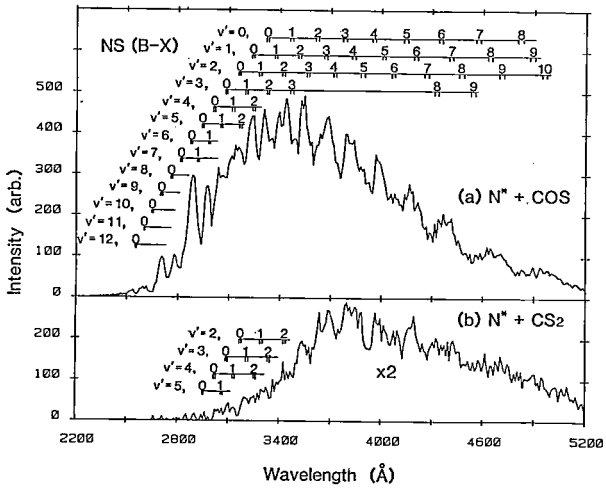

Figure 1. (a) Emission spectrum of NS ($B^2\Pi$-$X^2\Pi$) band recorded from crossed beam reaction of N* + COS at an average collision energy $\bar{E}$ = 0.78 eV (FWHM = 0.80 eV). (b) Emission spectrum of NS ($B^2\Pi$-$X^2\Pi$) band recorded from collisions of N* + CS_2 at $\bar{E}$ = 0.81 eV (FWHM = 0.84 eV).

The behavior of the maximum vibrational excitation in NS ($B^2\Pi$) products are consistent with the present mechanism.

IV— O Vacuum UV Photochemistry of Molecules in the Gas Phase as Studied by Fluorescence Spectroscopy

Photochemistry by vacuum UV (VUV) light has recently become a very active field owing to the rapid progress in and the relatively easy access to the VUV light sources such as synchrotron radiation and VUV laser as well as atomic resonance lines. In the present project we seek to obtain more detailed information about photodissociation dynamics of simple molecules and/or reaction dynamics involving electronically excited atoms and molecules applying fluorescence spectroscopy.

IV-O-1 Construction of a Fluorescence Apparatus for a study of Gas phase Photochemistry Using UVSOR Synchrotron Radiation as a Light Source

Kosuke SHOBATAKE, Sigeru OHSHIMA*, Atsunari HIRAYA, and Kiyohiko TABAYASHI

An apparatus for studies of dynamics of photochemical processes in the gas phase using fluorescence spectroscopy has been constructed on a beam line BL2A of Ultraviolet Synchrotron Orbital Radiation Facility (UVSOR) at IMS. Figure 1 shows a schematic of the apparatus. The optical system has been designed such that (i) synchrotron radiation with horizontal divergence of 40 m radians can be accepted by a 1 m Seya-Namioka monochromator (Hitachi SNM-2), and (ii) final dispersed synchrotron radiation goes upward. This apparatus was designed to use both samples in a gas cell and supercooled molecules or molecular complexes in a free jet. So far gas

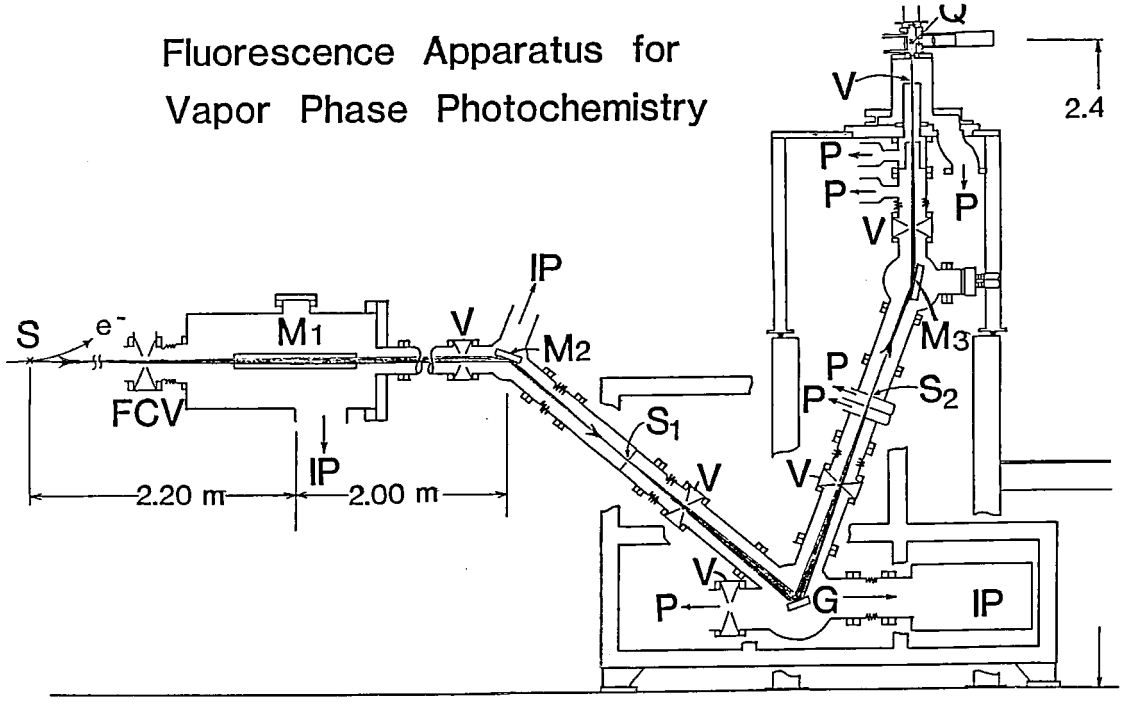

Figure 1. Schematic side view of the fluorescence apparatus for vapor phase photochemistry. From left to right, S: source point of synchrotron radiation. FCV: fast closing valve. M1: first focusing mirror; M2: second focusing mirror; S1: entrance slit into 1 m Seya-Namioka monochromator; G: grating; S2: exit slit; M3: post focusing mirror; Q: synchrotron radiation-molecule interaction region (spot position). IP: ion pump; V: shutoff valve; P: turbomolecular pump.

cell experiments have been done. Dispersed SR, after being focused by a toroidal mirror (M3), enters through a LiF window into a gas cell with a 10.9 cm pass length. Photon flux was monitored by a combination of sodium saliciate converter and photomultiplier (Hamamatsu R585). Fluorescence was detected perpendicularly to the incident light by a photomultiplier tube (Hamamatsu R585). Intensities of the transparent light and fragment fluorescence, the sample pressure, and the electron beam current in the storage ring were concurrently monitored for every stepwise scan of the monochromator wave length, were interfaced into a microcomputer (NEC PC9801) via GP-IB interface, and the photoabsorption and the relative fluorescence cross section were determined vs wave length.

Preliminary results of dispersed fluorescence of CN* (B) photofragments from CD_3CN have also been obtained. Fluorescence polarization measurements and dynamical studies of photochemical processes by means of molecuar beam vacuum UV spectroscopy of molecular complexes are under way.

* Present address: Dept. of Chem., Toho Univ., Funabashi, Chiba, 274, Japan.

IV-O-2 Isotope Effect on the Fluorescence Cross Section for Dissociative Exctation Processes. I. CH_3CN and CD_3CN.

Atsunari HIRAYA, Sigeru OHSHIMA*, Yoshiyasu MATSUMOTO, Kiyohiko TABAYASHI, and Kosuke SHOBATAKE**

The relative cross section and quantum yield of fluorescence from the nascent CN* (B, A) formed by photodissociative excitation of acetonitrile-h_3 and -d_3 were determined in the wave length region of exciting photon between 1050 and 1500 Å on the fluorescence apparatus for vapor phase photochemistry using UVSOR synchrotron radiation as a light source. Figure 1a and 1b show the absortion and the fluorescence cross section againt the excitation photon wave length for CD_3CN and CH_3CN, respectively. The quantum yield for emission from the excited photofragment CN* (B, A) formed by the reaction:[1,2]

$$CX_3CN + h\nu \rightarrow CX_3CN^{**}$$
$$\rightarrow CX_3 + CN^* \text{ (B, A)} \quad (X = H, D)$$

has been found to increase gradually with photon energy. We have also found that the fluorescence quantum yields for two isotopic compounds are almost identical in the valence band region above 1300 Å, while that for the CD_3CN is about a factor of two larger than the one for CH_3CN in the Rydberg transition region below 1250 Å. The present findings are explained in light of the isotope effect of competing dissociation channels involving the motion of hydrogen atoms in the methyl group, such as formation of $CH_2CN + H$, $CHCN + H_2$, $CH_2 + HCN$. Preliminary measurements of the dispersed fluorescence spectra of CD_3CN have been successfully carried out at several peak positions.

* Present address: Dept. of Chem., Toho University Funabashi, Chiba, 274, Japan.

** Present address: Inst. of Chem. & Phys. Research, Wako, Saitama, 351, Japan.

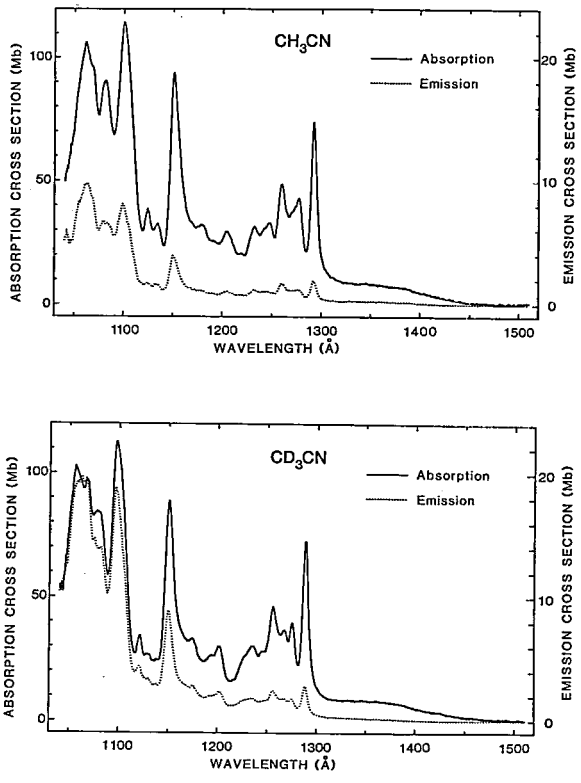

Figure 1. Absorption and fluorescence cross section versus wave length of the exciting photons for CD_3CN (upper) and CH_3CN (lower) in the gas phase. The fluorescence cross section was put on an absolute scale by scaling the fluorescence intensity to that of H_2O whose absolute fluorescence cross section is determined by Lee et al. (J. Phys. **B 11**, 47 (1978)). The resolution of the disperesed synchrotron light was about 5.0 Å.

Reference
1) H. Okabe and V.H. Dibeler, *J. Chem. Phys.* 59, 2430 (1973).
2) M.N.R. Ashfold and J.R. Simons, *J. Chem. Soc. Faraday* 2 74, 1263 (1978).

IV-O-3 Emission Spectra of SiH ($\tilde{A}^2\Delta \rightarrow X^2\Pi$) and $SiCl_2$ ($\tilde{A}^1B_1 \rightarrow \tilde{X}^1A_1$) in the VUV photolyses of Silane and Chlorinated Silanes.

Nobuaki WASHIDA (*Nat, Inst. Environ. Stud., and IMS*), **Yutaka MATSUMI***, **Toshio HAYASHI*** (**ULVAC Co.*), **Tohio IBUKI** (*Kyoto Univ.*) **Atunari HIRAYA, and Kosuke SHOBATAKE**

[*J. Chem. Phys.* 83, 2769 (1985)

Vacuum UV photolyses of silane and chlorinated silanes were investigated by using rare gas resonance lamps. Strong emission from the $A^2\Delta \rightarrow X^2\Pi$ transition of SiH and the $^1P_0 \rightarrow {}^1D_2$ transition of Si were observed in photolysis of SiH_4 by Ar and Kr resonance lamps. It was suggested that the threshold energies for the appearance of both emission were lower than the values obtained by the electron-impact of SiH_4 reported by Perrin et al. A new broad unstructured emission band in the region 300-400 nm was observed in the photolysis of SiH_2Cl_2 and $SiHCl_3$ by Ar, Kr, and Xe lamps. The band was attributed to the $\tilde{A}^1B_1 \rightarrow \tilde{X}^1A_1$ transition of $SiCl_2$ radicals from the measurement of the apperance energy of the emission by using synchrotron orbital radiation.

IV-O-4 Absorption and Emission Cross Section of I_2 Vapor in 105 – 210 nm

Atsunari HIRAYA, Robert J. DONOVAN (*Univ. of Edinburgh*), **and Kosuke SHOBATAKE**

The absorption cross section and the emission cross section of I_2 vapor were measured in the 105 - 210 nm region, using synchrotron radiation produced from UVSOR as a light source. As shown in Figure 1, the absorption spectrum of iodine vapor consists of a broad feature with a maximum at 182.5 nm (D ← X), followed by very sharp band systems assigned to several Rydberg series in shorter wave length region from 178 to 132 nm, and continuous absorption blow the ionization limit at 131.9 nm.

Comparing the absorption cross section with the emission corss section, one finds that the emission yield varies considerably with wave length. Relatively high emission yield of the broad feature peaking at 182.5 nm can be understood as the fluorescence from ion-pair state (s) to the ground and lower excited states. For the Rydberg series, only the bands between 151 nm and 132 nm exhibit fairly high emission yield. The longer wavelength limit of the emission yield corresponds to the threshold for the dissociation into the ground state ($^2P_{3/2}$) and lowest Rydberg state ($^4P_{5/2}$) iodine atoms. The energy level of these fragments is 8.29 eV above the ground state of I_2. Considering the hot-band excitation, the dissociation limit should be located at 151 nm. The observed limit is in good agreement with this value. The shorter wave length limit of the emission yield corresponds to the ionization threshold.

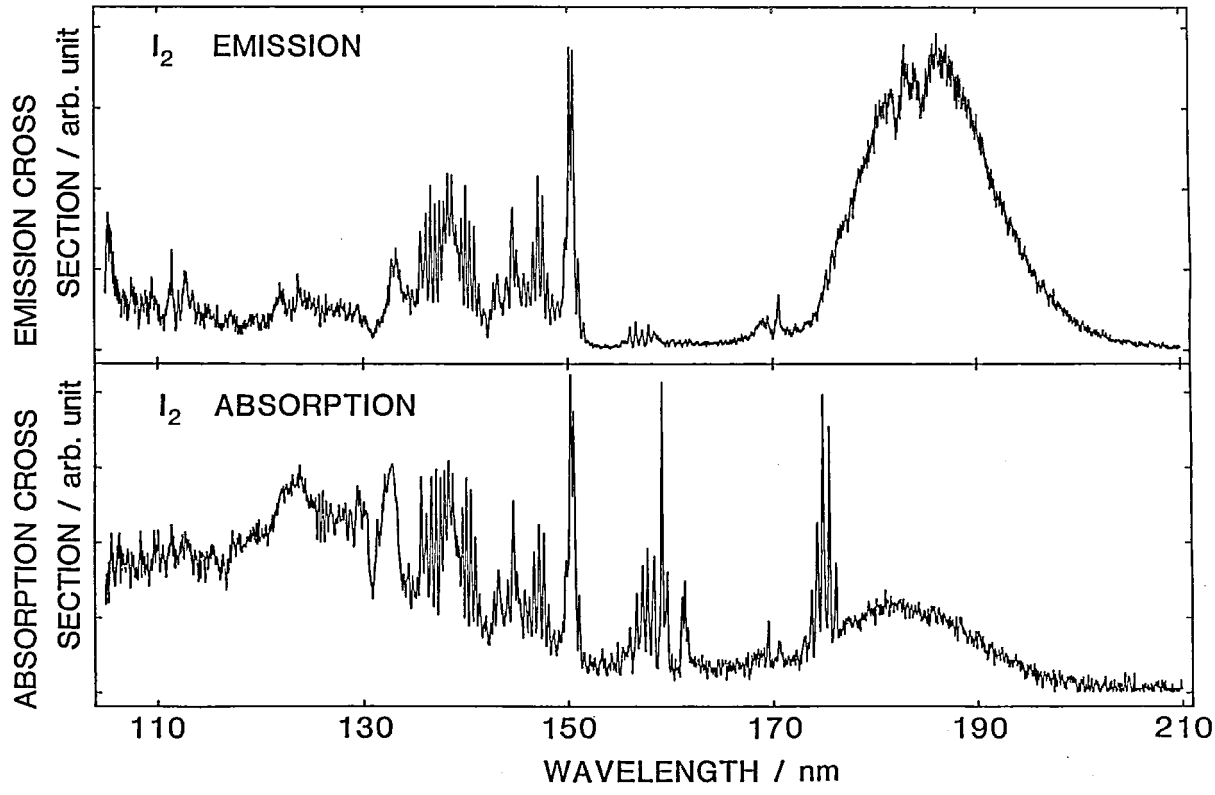

Figure 1. Absorption (lower) and emission (upper) cross section of I_2 vapor. Spectral band width is about 0.2 nm.

IV— P Optical Properties of Organic Liquids

The study on the liquid state of organic compounds which have relatively strong intermolecular interaction is one of the unexplored interesting problems in the field of molecular assemblies dynamics. In this study, the fluorescence spectra, fluorescence life times, absorption spectra and Raman spectra of anthracene and pyrene in the molten state have been observed and analyzed in terms of the excited state dynamics.

IV-P-1 Fluorescence Spectra of Anthracene Liquid

Noriko IWASAKI (*ISSP, Univ. of Tokyo*), **Rumiko HORIGUCHI** (*Ochanomizu Univ. and IMS*) and **Yusei MARUYAMA**

[*Bull. Chem. Soc. Jpn.*, **58**, 2409 (1985)]

The excimer fluorescence of anthracene liquid has been found for the first time. The absorption edge of the liquid shifts to the longer wavelength side compared with that of the crystal. The origin of this absorption could be attributed to the ground state dimers in the liquid. These dimers are essentially responsible for the excimer formation observed in the fluorescence spectra.

IV-P-2 Time Resolved Fluorescence Spectra of Anthracene and Pyrene Liquids

Rumiko HORIGUCHI (*Ochanomizu Univ. and IMS*), **Noriko IWASAKI** (*ISSP, Univ. of Tokyo*) and **Yusei MARUYAMA**

The existence of an excimer in anthracene liquid has been confirmed by the measurement of its fluorescence rise time of less than 100 ps with the use of a subnanosecond time resolved spectroscopy. The life time of the excimer in the liquid anthracene is extraordinary short, i.e. 0.2 - 0.3 ns and almost the same as that of the monomer. Pyrene liquid also shows the excimer fluorescence which extends to longer wavelength side comparing with the crystalline excimer. The life time of pyrene liquid excimer

is 10 ns and it became a little larger in the longer wavelength region.

Many librational modes due to "the liquid phase" are already present in the Raman spectra of the anthracene crystal at the temperature near the melting point, and some of the librational modes due to "the crystal phase" still slightly remain in the spectra of the liquid just above the melting point.

IV— Q Black Phosphorus and Lead Iodide

Black phosphorus and lead iodide are layered structure semiconductors. We have studied the several electronic properties of black phosphorus single crystals and also tried to prepare intercalation compounds based on the black phosphorus. Lead iodide and its family form intercalation compounds with long chain hydrocarbon amines, e.g. $(C_9H_{19}NH_3)_2PbI_4$. Several organic solvents molecules have been found to undergo secondary intercalation to this type of compounds.

IV-Q-1 Negative Magnetoresistance and Anderson Localization in Black Phosphorus Single Crystals

Noriko IWASAKI (*ISSP, Univ. of Tokyo*), **Susumu KURIHARA** (*ISSP, Univ. of Tokyo*), **Ichimin SHIROTANI** (*Muroran Inst. of Technology*), **Minoru KINOSHITA** (*ISSP, Univ. of Tokyo*) **and Yusei MARUYAMA**

[*Chem. Lett.*, 1985, 119]

The electrical resistance of black phosphorus single crystals at low temperatures has been analyzed as functions of temperature and magnetic field. Logarithmic dependence of the conductivity on both variables has been found. This fact, together with the negative magnetoresistance observed at 4.2 K, suggests the existence of the two dimensional Anderson localization of valence-band holes in black phosphorus single crystals at low temperature.

IV-Q-2 Electronic Properties of Black Phosphorus Single Crystals and Intercalation compounds

Setsuko SUZUKI (*Ochanomizu Univ.*), **Tomoko OSAKI** (*Ochanomizu Univ.*), **Hizuru YAMAGUCHI** (*Ochanomizu Univ.*), **Sumiko SAKAI** (*Ochanomizu Univ.*) **Kyoko NAGASATO** (*Ochanomizu Univ.*), **Ichimin SHIROTANI** (*Muroran Inst. of Technology*) **and Yusei MARUYAMA**

[Submitted to *Bull. Chem. Soc. Jpn.*]

An actual procedure for the preparation of black phosphorus single crystals by bismuth solution method has been explored. Electrical and optical properties of obtained crystals and also of crystals which are prepared under high presure have been measured. There is an unsettled question concerning the anisotropy of the electrical conductivities.

Several preliminary attempts for synthesizing black phosphorus intercalation compounds have been carried out for the first time. An evidence for the intercalation by an X-ray analysis is presented.

IV-Q-3 Tunneling Spectroscopic Study on the Electrical Properties of Black Phosphorus— In Relation to the Anderson Localization of Charge Carriers

Noriko IWASAKI (*ISSP, Univ. of Tokyo*), **Ichimin SHIROTANI** (*Muroran Inst. of Technology*) **and Yusei MARUYAMA**

In order to observe the change of the electron density of states in the occurrence of the charge carrier localization, we have measured the temperature dependence of tunneling spectra using the [Black Phosphorus Single Crystal | Aluminum Oxide Ultra-thin Film | Gold Film] type cells. The density of state which is proportional to the dI/dV decreased with lowering the temperature and a sharp dip appeared around the Fermi level below 10 K. This behavior is a clear indication of the localization of charge carriers which are responsible for transport in the black phosphorus crystals.

IV-Q-4 Synthesis and Characterization of Black Phosphorus Intercalation Compounds

Toshifumi NISHII (*Mitsubishi Yuka Co. Ltd. and IMS*), **Ichimin SHIROTANI** (*Muroran Inst. of Technology*) **and Yusei MARUYAMA**

We have tried to intercalate potassium, cesium, lithium or iodine into black phosphorus crystals. The constitutions have been estimated by the weight change during the reaction with the use of a vacuum balance. In the cases of iodine and cesium, new X-ray diffraction lines appeared and could be attributed to new interlayer spacing structures.

IV-Q-5 In situ X-ray Observation on the Intercalation of Weak Interaction Molecules Intercalation into Perovskite-type Layered Crystals $(C_9H_{19}NH_3)_2PbI_4$ and $(C_{10}H_{21}NH_3)_2CdCl_4$

Yuri I. DOLZHENKO (*Kharkov Polytechnical Inst. and IMS*), **Tamotsu INABE and Yusei MARUYAMA**

[*Bull. Chem. Soc. Jpn.* in press]

Intercalation-deintercalation process of weak interaction organic molecules such as α-chloronaphthalene and *o*-dichlorobenzene into highly oriented polycrystalline $(C_{10}H_{21}NH_3)_2CdCl_4$ films and hexane into $(C_9H_{19}NH_3)_2PbI_4$ single crystals has been observed in situ by using X-ray technique. The process is highly reversible. Increasing of interlayer spacing is in reasonable agreement with the size of the intercalated molecules and corresponds to the parallel orientation of aromatic ring planes or hexane chains in between two paraffin layers of the host crystals.

IV— R Synthesis and Electrical Properties of Organic Conductors

Our research activities are focused on the synthesis and characterization of new type of organic conductors including AzaTCNQ, OCNAQ, and phthalocyanine derivatives.

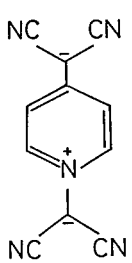

AzaTCNQ⁻

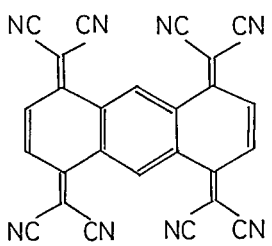

OCNAQ

IV-R-1 Synthesis and Electrical Properties of AzaTCNQ Complexes.

Hatsumi URAYAMA (*Ochanomizu Univ. and IMS*), **Tamotsu INABE, and Yusei MARUYAMA**

Many TCNQ complexes were found to be good organic conductors. AzaTCNQ, which was synthesized by Wudl,[1] has a similar molecular structure to TCNQ but has a different electronic structure. As an electron acceptor the AzaTCNQ is much stronger than TCNQ, and usually the anionic form is very stable. Molecular complexes with TTF families and other donor molecules can be obtained by metathesis or electrochemical reaction. Some of the complexes have been found to have good electrical conductivities. The studies of structures and electrical properties are now in progress.

Reference

1) F. Wudl, "Chemistry and Physics of One-Dimensional Metals", ed. H.J. Keller, *NATO Adv. Study Inst.* 249 (1977).

IV-R-2 Synthesis and Electrical Properties of OCNAQ complexes

Tsutomu MITSUHASHI (*Univ. of Tokyo*), **Tamotsu INABE, and Yusei MARUYAMA**

Two TCNQ units are bound by conjugated system in OCNAQ. The strength as acceptor for first electron is comparable to TCNQ, while second electron

can be accepted easily because of the existence of two TCNQ units. Such property, namely reduced on-site Coulomb repulsion, will affect the electronic structures of solids of charge transfer complexes. TTF-OCNAQ was obtained as powder form and shows resistivity of 6×10^2 S^{-1} cm at room temperature. Single crystals can be grown electrochemically or by slow diffusion. The structures and electrical properties of the complexes will be studied.

IV-R-3 Thermoelectric Power of Phthalocyanine Complexes

Tamotsu INABE, Kenichi IMAEDA, and Tobin J. Marks (*Northwestern Univ.*)

The thermoelectric power (TEP) of conductive phthalocyanine complexes, $M(Pc)X_{1/3}$; where M = H_2 [1] and Ni[2], X = I_3 and BF_4, was measured. As shown in Figure 1 for $H_2(Pc)I$, the TEP in metallic conductive region is linearly correlated with temperature. By assuming a tight-binding band model the bandwidth is estimated as about 1 eV, which is in good agreement with the value obtained from optical method; i.e. 1.3 eV.

References

1) T. Inabe, T.J. Marks, R.L. Burton, J.W. Lyding, W.J. McCarthy, C.R. Kannewurf, G.M. Reisner, and F.H. Herbstein, *Solid State Commun.*, 54; 501 (1985).
2) T.Inabe, S. Nakamura, W.B. Liang, T.J. Marks, R.L. Burton, C.R. Kannewurf, and K. Imaeda, submitted to *J. Am. Chem. Soc.*

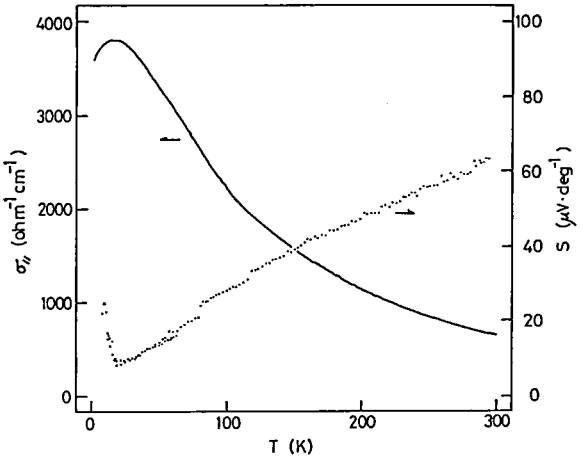

Figure 1. Single crystal conductivity and thermoelectric power of $H_2(Pc)I$.

IV— S Tunable Picosecond Pulses from a Short-Cavity Dye Laser under Ultra-High Pressure using Diamond-Anvil Cell

Yuzo ISHIDA (*ISSP, Univ. of Tokyo*), **Noriko IWASAKI** (*ISSP, Univ. of Tokyo*), **Katsuyuki ASAUMI** (*ISSP, Univ, of Tokyo*), **Tatsuo YAJIMA** (*ISSP, Univ. of Tokyo*) **and Yusei MARUYAMA**

[*Appl. Phys. B* in press]

It is demonstrated that broadly tunable picosecond pulses are generated from a dye laser of very short cavity utilizing a diamond-anvil cell, which operates at pressures up to 10 GPa. The pulses as short as 5 ps are obtained from the rhodamine 6G dye laser pumped by a frequency doubled Q-switched Nd: YAG laser. The way of tuning is based on the pressure induced shift of the emission peak of the dye. The laser is tunable over 20 nm by chaning the pressure of the cell within 4 GPa.

IV— T Ultra-Thin Organic Multi-Layers Films Prepared by Molecular Beam Epitaxy Technique

Yusei MARUYAMA and Tamotsu TANABE

An ultra-high vacuum evaporation system for organic compounds has been constructed. Several testing procedures and improvements are now going on. A schematical view of the system is shown in the Figure.

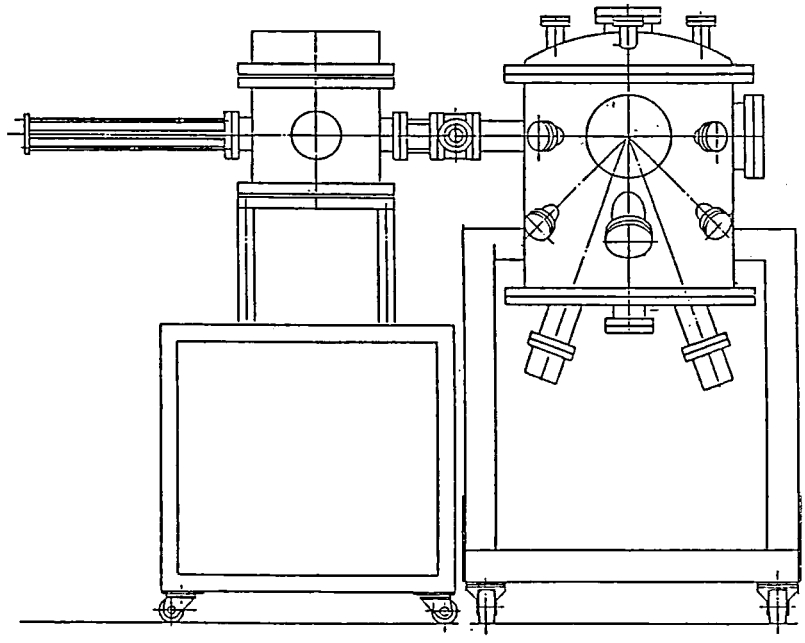

IV— U Charge Density Waves, Spin Peierls Transition and New Type Superconductivity in Bronzes and Other Low Dimensional Conductors

IV-U-1 Charge Density Wave States in Mo_8O_{23}

Masatoshi SATO, Hideshi FUJISHITA*, Shoichi SATO* and Sadao HOSHINO* (**Institute for Solid State Physics*)

[*J. Phys. C* submitted]

By means of neutron and x-ray four circle diffractions, the evidence of the transition in Mo_8O_{23} to the charge density wave (CDW) state has been found. It can give the orgin of the anomalous temperature dependence of the resistivity and the magnetic susceptibility. The incommensurate CDW appears at $T_{c1} \lesssim 360$ K and the incommensurate-commensurate transition takes place at $T_{c2} \simeq 285$ K. Argument on the condensed mode and on the possible coupling mechanism of the distortion with the CDW are presented, based on the results of the structure analysis.

IV-U-2 Charge Density Wave States in Mo_8O_{23} II: Structure Determination

Hideshi FUJISHITA*, Masatoshi SATO, Shoichi SATO* and Sadao HOSHINO* (**Institute for Solid State Physics*)

[*J. Phys. C* submitted]

Crystal Structure of the new low-dimensional conductor Mo_8O_{23} has been determined at 370 K and 100 K using x-ray four circle diffractometer. Mo_8O_{23} has an incommensurate structure between about 320 K and 285 K. The structure at 370 K is essencially the same as that presented by Magneli for room temperature. The structure at 100 K can be described mainly by the inhomogeneous rotations of MoO_6 octahedra. The displacements associated with the dilations or the contraction of the octahedra seem to take place in addition to the rotations.

IV-U-3 NMR Stury of $Rb_{0.3}MoO_3$: Static Structure and Dynamical behavior of the Charge Density Wave

Kazushige NOMURA*, Kiyoshi Kume* and Masatoshi SATO (**Tokyo Metropolitan Univ.*)

[*European Workshop on Charge Density Waves in Solids*, Zagreb 1985]

The so called blue bronzes, which are ternary molybdenum oxides, reveal a quasi one dimensional conduction at room temperature and undergo a Peierls type phase transition at T_c ($\simeq$ 180 K). Below T_c an incommensurate charge density wave (CDW) was observed by x-ray and neutron diffractions. With lowering the temperature, the wave vector of the CDW approaches the commensurate value (0.75b*) at about 100 K and there has been the controversy on the existence of the incommensurate-commensurate transition. As for the dynamical behaviors, the nonlinear conductivity has been observed and attributed to the depinning of the CDW. The narrow band noise was also observed and discussed in connection with the sliding CDW. In order to study these problems, the NMR line of Rb atoms has been observed in this work. The observed line shape clearly shows that the incommensurate phase remains even at 77 K. At the same time, the existence of the discommensuration is discarded. We also observed the NMR line shape with applying current to the crystal. The variation of the line shape with varying current value showed the direct evidence of the sliding CDW.

IV-U-4 X-ray Study of Field Induced Deformation of Sliding CDW in $K_{0.3}MoO_3$

Tsuyoshi TAMEGAI*, Kitomi TSUTSUMI*, Seiichi KAGOSHIMA*, Yasuyuki KANAI* and Masatoshi SATO (**Univ. of Tokyo*)

[*Solid State Commun.* submitted]

A deformation of the CDW is investigated under the electric field whose magnitude is intensionally made inhomogeneous in the one dimensional conductor $K_{0.3}MoO_3$. It is verified that the CDW's deformation, which occurs in the transverse ($2a^*$-c^*)-direction, is caused by the field gradient in the sample. In the sample where the CDW deformation is found without the intensional inhomogeneity of the field, the deformation is not uniform from point to point. Possible relations are discussed between the structural change and the electrical polarization observed in pulse measurements of the conductivity.

IV-U-5 Time-Resolved X-ray Study of Sliding CDW in $K_{0.3}MoO_3$

Tsuyoshi TAMEGAI*, Kitomi TSUTSUMI*, Seiichi KAGOSHIMA*, and Masatoshi SATO (**Univ. of Tokyo*)

[*Proc. Int. Conf. Synchrotron Radiation Instrumentation* Stanford 1985]

In the title compound a superstructure is found to be modified when an electric field exceeding a threshold is applied parallel to the one-dimensional axis. The modification occurs as a rotation of the wave vector specifying the superstructure. The direction of the rotation depends on the polarity of the electric field applied, and the magnitude of the rotation is of the order of 10^{-3} rad. When the electric field is a few times as high as the threshold. The change in the superstructure is measured as a function of time for pulsed electric fields. The superstructure is formed by an ordering of charge-density waves (CDW) characteristic of low-dimensional systems. The experimental results are discussed in relation to the sliding motion of CDWs.

IV-U-6 Interphonon Interactions at the CDW Phase Transitions in $(TaSe_4)_2I$ and $(NbSe_4)_2I$

Shunji SUGAI (*Osaka Univ.*), **Masatoshi SATO and Susumu KURIHARA** (*Institute for Solid State Physics*)

[*Phys. Rev.* **B** submitted]

Lattice vibrations in quasi one dimensional CDW system, $(TaSe_4)_2I$ and $(NbSe_4)_2I$, are investigated by Raman scattering. The existence of three CDW-related TO modes is found in this experiment, and the following model for the CDW transition is proposed. The compound of this system has strong interaction between the Kohn-anomaly TO mode and the TA mode both of which are on the same branch in the extended Brillouin zone of the MSe_4 unit. As a consequence of the interaction, the TA mode condenses prior to the Kohn-anomaly TO mode. The theory of the CDW phase transition in the coupled system is presented.

IV-U-7 Neutron Scattering Study of the Quasi One Dimensional Conductor $(TaSe_4)_2I$

Hideshi FUJISHITA*, Stephan M. SHAPIRO#, Masatoshi SATO and Sadao HOSHINO* (**Institute for Solid State Physics, #Brookhaven National Laboratory*)

Neutron scattering experiments have been carried out on the quasi one dimensional conductor $(TaSe_4)_2I$. At the superlattice point (0.05, 0.05, 0.085) the condensation of the transverse acoustic mode which polarizes in the c plane was observed. This result confirms the previous assignment by the analysis of the x-ray experiments. A 'spoon-like' anomaly on the dispersion curve of the TA branch was observed around the superlattice point. In addition, we found an extremely low-lying TA mode.

IV-U-8 Superconductivity and Charge Density Wave in $(Li_{1-x}K_x)_{0.9}MoO_6O_{17}$ and $(Li_{1-x}Na_x)_{0.9}Mo_6O_{17}$

Yuji MATSUDA, Masashige ONODA and Masatoshi SATO

The so called molybdenum purple bronzes, $A_{0.9}Mo_6O_{17}$ are ternary transition metal oxides, where A is an alkali metal atom. The A atoms are in the planes separated by the stacked layers of the MoO_6 octahedra. As is known from the structural features, these compounds exhibit low dimensional electrical conduction. While $K_{0.9}Mo_6O_{17}$ and $Na_{0.9}Mo_6O_{17}$ undergo the CDW transitions which are typical for two dimensional conductors, the behaviors of $Li_{0.9}Mo_6O_{17}$ are somewhat anomalous; as the temperature is lowered, the temperature derivative of the resistivity ($d\rho/dT$) changes its sign at about 25 K and after the rapid increase of ρ, the superconducting transition takes place at about 1.9 K. In order to clarify the origin of the anomalous behaviors, we have prepared the compound series of $(Li_{1-x}K_x)_{0.9}Mo_6O_{17}$ and $(Li_{1-x}Na_x)_{0.9}Mo_6O_{17}$ by electrolysis. The anomalous increase of the resistivity with decreasing T and the superconductivity are found for all crystals with $x < x_c$. For $x > x_c$, the CDW transitions have been observed. The specific heat measurements indicate that the superconductivity is intrinsic one. The measurements of the magnetic susceptibility show that the anomalous behavior of the resistivity for $T < 25$ K is not due to the CDW formation. The study from the structural view point is also in progress.

IV-U-9 Far Infrared ESR Study of Spin-Peierls Compound MEM $(TCNQ)_2$

Yuji MATSUDA (*Institute for Solid State Phys., IMS*) **Toshiro SAKAKIBARA*, Tsuneaki GOTO*, and Yuji ITO*** (**Institute for Solid State Phys.*)

Electron spin resonance experiments have been performed on spin-Peierls compound MEM $(TCMQ)_2$ at far infrared (H_0 = 255 kOe) and X-band (H_0 = 3.3 kOe) regions, with a special interest on the predicted high field incommensurate phase. The low field ESR revealed a rapid increase in the resonance width below the spin-Peierls transition temperature T_{sp} = 17.8 K while no change has been observed in the high field experiments down to 4.2 K within the present experimental resolution $\Delta H_{res} \simeq 50$ Oe. ($\Delta H_{res}/H \simeq 2 \times 10^{-4}$). It is plausible that the predicted incommensurate phase does not exist, but that the high temperature uniform phase survives at high field region down to the lowest temperature studied.

IV-U-10 X-ray Four Circle Diffractometer and X-ray Rotation Camera for Use at Low Temperatures

Masatoshi SATO and Masashige ONODA

For the studies of the systems with strong electron phonon interaction from the structural point of view, an x-ray four circle diffractometer which can be used at the temperature down to 10 K and an x-ray rotation camera which can be used down to 40 K are under construction. By use of these instruments, the various types of the structural transitions can be studied. Especially, the transition region from superconductors to the bipolaron insulators with varying the electron phonon coupling constant λ will be studied using the transition metal oxides and so called bronzes.

IV—V Intramoleculav Conversion

IV-V-1 Intramolecular Conversion over a Low Barrier. 3. Gas-Phase NMR Studies of an H-Bond Association

S.H. BAUER* (*Cornell Univ. and IMS*), Tomoko YAMAZAKI, K.I. LAZAAR (*Cornell Univ.*) and N.-S. CHIU (*Cornell Univ.*)

[*J. Amer. Chem. Soc.*, **107**, 743 (1985)]

Gas-phase NMR spectra of mixtures of $(CH_3)_2O$ and HCl were recorded for mole ratios 1:1 → 1:4, at total pressures of 400-40 Torr, over the temperature range 300–212K, in order to investigate the kinetics of formation of the $(CH_3)_2O$:HCl complex. The results gave only a lower bound for the dissociation rate constant, in the limiting low-pressure regime, and confirmed the published thermochemical values for association: $\Delta H^0 = -6.9$ kcal/mol and $\Delta S^0 = -25.6$ eu. Two of the low wagging frequencies proposed for the complex had to be raised from 50 to 100 cm^{-1} to obtain agreement between the calculated and observed ΔS^0. The NMR spectra provide a reliable value for the increment in the proton chemical shift due to hydrogen bond formation and enable estimates to be made of equilibrium vapor pressures of $(CH_3)_2O$: HCl at several temperatures (212 → 213 K). The kinetics of dissociation are in the second-order regime, and the activation energy for dissociation cannot be greater than 8.5 kcal/mol.

* Visiting Professoy, Sept. – Dec. 1983

RESEARCH ACTIVITIES V

Department of Applied Mole Cular Science

V— A High-Spin Organic Molecules

We have been engaged in the molecular design, generation and exploration of physicochemical properties, of high-spin organic molecules. The previously reported tetracarbene was found to have the conformational isomers having different zero-field tensors, but their nonet spin multiplicity was kept irrespective of the conformational isomerism. When a pair of triplet species are allowed to interact on each other freely, quintet, triplet and singlet states are generated in a statistical ratio of 5 : 3 : 1. One of the three possible states could be favored by imposing geometrical constraints to the path of the approach. We have been able to show by a model experiment on the [2.2] paracyclophane derivatives that the stacking of the benzene rings of two triplet diphenylcarbene molecules can lead to dimer systems with the ground quintet state when the orientation of the overlap is in pseudoortho or pseudopara relations. In order to see if the principle can be extended to intermolecular interactions, a series of crystalline samples of substituted diphenyldiazomethanes were scrutinized. The intermolecular intereaction between the corresponding diphenylcarbene molecules was found to be ferromagnetic when generated by photolysis of the polycrystalline solid samples of *p*-methoxy-, *p, p'*-dimethoxy and *p, p'*-dioctyloxydiphenyldiazomethanes at 10 K. A study of conformationally fixed triplet nitrenes revealed an interesting loss of stereospecificity.

V-A-1 Preparation and ESR Detection of a Ground-State Nonet Hydrocarbon as a Model for One-Dimensional Organic Ferromagnets

Yoshio TEKI (*Osaka City Univ.*), **Takeji TAKUI** (*Osaka City Univ.*), **Koichi ITOH** (*Osaka City Univ.*), **Hiizu IWAMURA** and **Kazumasa KOBAYASHI**[1)]

[*J. Am. Chem. Soc.*, in press]

When a single crystal of benzophenone doped with *m*-phenylenebis [m-(α-diazobenzyl)phenyldiazomethane] was irradiated in a K-band ESR cavity with the 405-nm Hg line at 4.2 K, the eight-line fine structure due to *m*-phenylenebis [(diphenylmethylen-3-yl)methylene] (**1**) was obtained.[2)] The spectrum showed an irreversible transition at 64 K to give two sets of new nonet signals. Another irreversible spectral change was observed at 92 K to give a fourth set of nonet signals (Figure 1). These changes were ascribed to the molecular conformational effect in the nonet **1**. A semiempirical calculation of the fine-structure tensor has been carried out for the four nonet isomers by assuming that the dipole-dipole interaction between the electron spins and the one-center n-π interactions on the divalent carbon atoms are most important. Further assumptions of molecular geometry led to the calculated fine-structure tensors simulating the observed ones. The low temperature conformer is represented by structure **1'**. The significance of the high-spin state is discussed in relation to the potentiality of organic ferromagnets.

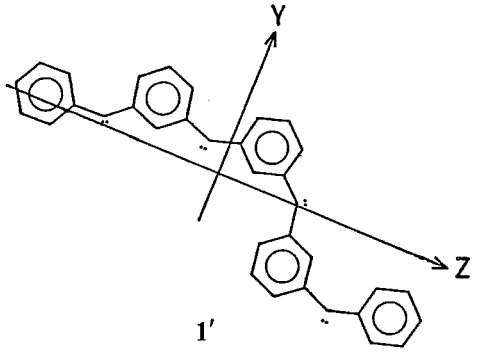

1'

References
1) IMS Graduate Student from Yamaguchi University for 1980.
2) Y. Teki, T. Takui, K. Itoh, H. Iwamura and K. Kobayashi, *J. Am. Chem. Soc.*, **105**, 3722 (1983); *IMS Ann. Rev.*, 112 (1983).

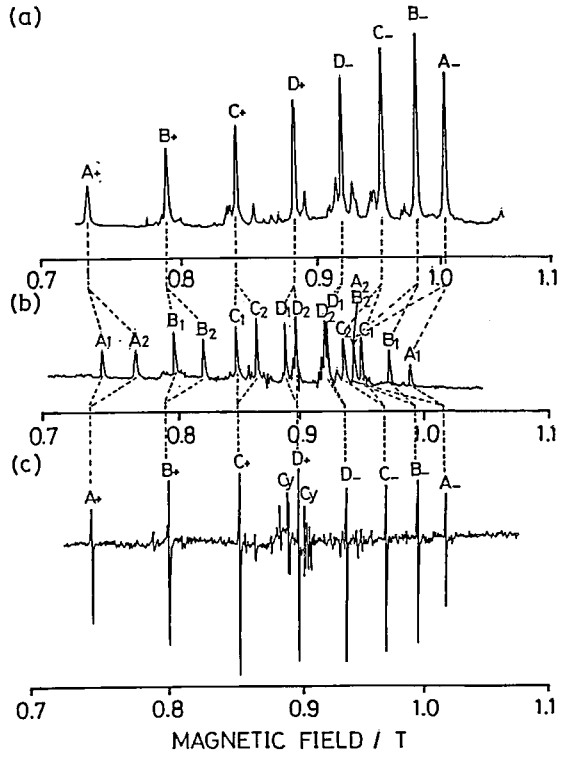

Figure 1. Temperature dependence of the K-band ESR spectrum with the magnetic field along the a axis of the benzophenone crystal. (a) The specturm observed in the dispersion mode at 4.2 K after photolysis and before the conformational changes. (b) The spectrum observed at 77 K after the first conformational change at 64 K. (c) The spectrum obtained in the absorption mode at 77 K after completing the second conformational transition at 92 K.

V-A-2 Preparation of Isomeric Bis(α-diazobenzyl)[2.2]paracyclophanes

Akira IZUOKA, Shigeru MURATA, Tadashi SUGAWARA and Hiizu IWAMURA

In order to study the effect of the stacking orientation on the spin-spin interaction between the two triplet diphenylcarbene molecules, the title compounds have been prepared as precursors of the model dicarbenes. Three isomeric dibromo[2.2]paracyclophanes were prepared and separated according to the literature method.[1] Each isomer was dilithiated by *n*-butyllithium in ether and treated with benzaldehyde to give the corresponding diol, which was then oxidized by pyridinium chlorochromate in dichloromethane to give the dibenzoyl [2.2] paracyclophane. It was converted to the didiazo compound through the bis(hydrazone) by oxidizing with yellow HgO in benzene at room temperature. The crude product was purified by alumina column chromatography by rapid elution with benzene: pseudoortho, mp 107-109°C dec; pseudometa, mp 136–138°C dec; pseudopara, mp 147–148°C dec. All the new compounds gave satisfactory elemental analyses and ^{1}H NMR data as shown in Figure 1.

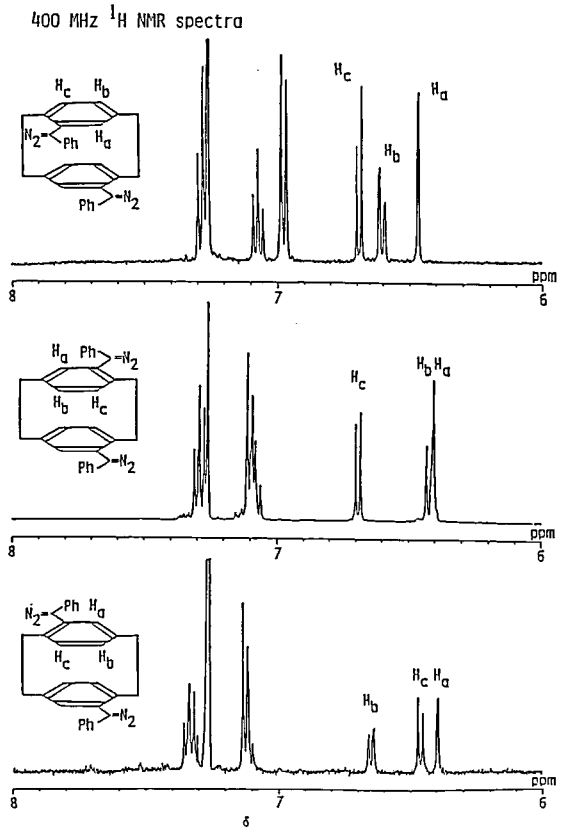

Figure 1. ^{1}H NMR spectra (400 MHz) of isomeric bis(α-diazobenzyl)[2.2]paracyclophanes.

References
1) H. Reich and D.J. Cram, *J. Am. Chem. Soc.*, 91, 3527 (1969).

V-A-3 Ferro- and Antiferromagnetic Interaction between Two Diphenylcarbene Units Incorporated in the [2.2] Paracyclophane Skeleton

Akira IZUOKA, Shigeru MURATA, Tadashi SUGAWARA and Hiizu IWAMURA

[*J. Am. Chem. Soc.*, **107**, 1786 (1985)]

The electron spin-spin interaction between the two triplet diphenylcarbene units incorporated in the [2.2] paracyclophane skeleton has been investigated by ESR spectroscopy. Pseudo-ortho, pseudo-meta and pseudo-parabis(diazo)[2.2] paracyclophanes (**1a** ~**3a**)[1] were photolyzed with pyrex-filtered UV light in a 2-methyltetrahydrofuran glass at11K to give the corresponding dicarbenes (**1b**~**3b**). Intense quintet signals with $|D|$=0.0624 and $|E|$=0.0190 cm^{-1} were obtained from **1a**. Their intensity obeyed the Curie law in the temperature range 11~50K, showing that quintet **1b** was the ground state. A signal at 104.0 mT due to the thermally populated triplet was also detected at temperatures above 20K. Pseudo-meta-bis (phenylmethylenyl)[2.2] paracyclophane (**2b**) did not show any ESR signal at 11K. As the temperature was raised above 20K in the dark, a set of triplet signals with $|D|$=0.1973 and $|E|$=0.0038 cm^{-1} appeared. Thus it was found that **2b** was in the singlet ground state and its triplet was thermally populated. Intense quintet signals were detected at 11K for **3b**, but it was too unstable chemically to study the Curie plots. The McConnell's theory[2] on the intermolecular magnetic interaction between two organic radicals has now been demonstrated and a new strategy for increasing the dimension of the high spin aromatic molecules was found.

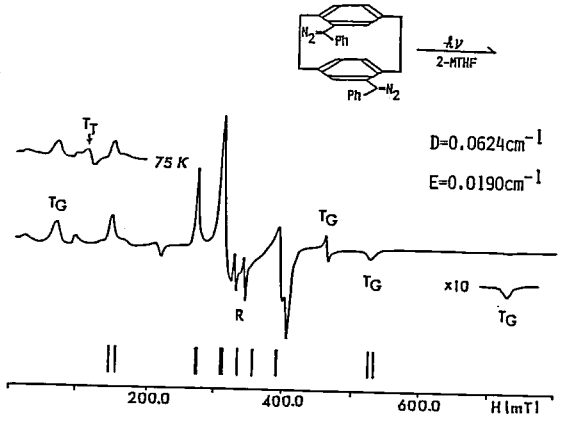

Figure 1. ESR spectrum (9.33098 GHz) obtained after irradiation of 1a in 2-methyltetrahydrofuran at 11 K. Lines indicate the calculated transition of the quintet state based on the third-order perturbation method. T_G is assigned to a monocarbene which presumably was formed by failure in removal of the second diazo group or by further reaction with solvent molecules at one of the carbenic centers. T_T is assinged to the thermally populated triplet species of the dicarbene.

References
1) See the preceding report, V-A-2.
2) H.M. McConnell, *J. Chem. Phys.*, 39, 1910 (1963).

V-A-4 A Pairwise Ferromagnetic Interaction between Substituted Diphenylcarbene Molecules in Crystals

Tadashi SUGAWARA, Hideyuki TUKADA (*The Univ. of Tokyo*), Shigeru MURATA and Hiizu IWAMURA

When polycrystalline solid samples of *p*-methoxy- and *p, p'*-dimethoxydiphenyldiazomethane (**3** and **4**, respectively) were photolyzed in an ESR cavity at 10 K, fine structures due to triplet (T), quintet (Q) and higher multiplet species (M) were observed. The Q signals, e.g., $|D|$=0.136 and $|E|$=0.015 cm^{-1} from **4**, were always most conspicuous and interpreted as arising from the pairwise interaction of the triplet *P,P'*-dimethoxydiphenylcarbenes (**2**) formed in the host crystals of **4**. The Curie plot of the ESR signal intensities (Figure 1) has shown that the T species are isolated from the other species and that there are two sites for Q, one isolated and the other interconverting with the antiferromagnetically coupled pair. The temperature dependence of the para-

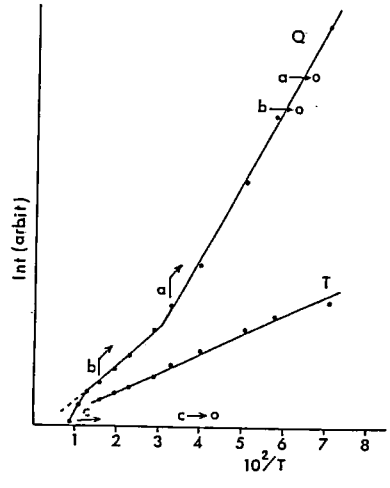

Figure 1. Curie plots of the quintet signals (Q) due to the pairwise interaction between the triplet carbenes and that of the isolated triplet ones (T). Open circles a and b indicate reproducibility of the intensity of Q after warming up to (a) 30 K and (b) 62 K. Point c (o) represents irreversible decomposition of Q after warming up to 110 K.

magnetic susceptibility of the photolyzed sample was also consistent with the Q ground state of the pair of the triplet **2**. From the light intensity dependence, the formation of the Q pair in polycrystalline **4** was found to be one-photonic especially at shorter wavelength. The pairwise ferromagnetic interaction between the T carbenes generated in the crystals of **4** was explained in reference to the crystal packing of the corresponding *p, p'*-dimethoxybenzophenone as a model for that of **2**.

V-A-5 Design of Molecular Assembly of Diphenylcarbenes Having Ferromagnetic Intermolecular Interaction

Tadashi SUGAWARA, Shigeru MURATA, Keisaku KIMURA, Hiizu IWAMURA, Yoko SUGAWARA (*Riken*) **and Hitoshi IWASAKI** (*Riken*)

[*J. Am. Chem. Soc.*, **107**, 5293 (1985)]

In order to stack the benzene rings of diphenylcarbene molecules in a magnetically favorable orientation[1] in crystals, we have taken advantage of the dispersion force of alkyl chains[2] and have introduced octyloxy groups at the para-positions of diphenyldiazomethane. When irradiated in an ESR cavity at 10 K, polycrystalline bis(*p*-octyloxyphenyl)diazomethane (**1**) showed ESR fine structures due to the formation of high-spin species ($S > 4/2$). The magnetization of the sample obtained by photolysis of **1** at 4 K was measured at various temperatures and external magnetic field strengths. The $1/X_p$ vs T plots showed the development of the ferromagnetic molecular field at low temperatures (Figure 1). The field dependence of the magnetization at 4.5 K fitted closely the species with $S = 4/2$ and that at 2.1 K more closer the aggregate with $S = 8/2$. A crystal structure analysis has been carried out on an orthorhombic crystal of *p, p'*-dioctyloxybenzophenone isomorphous to that of **1**. The multi-layered molecular packing is consistent with the observed ferromagnetic interaction between the neighboring molecules.

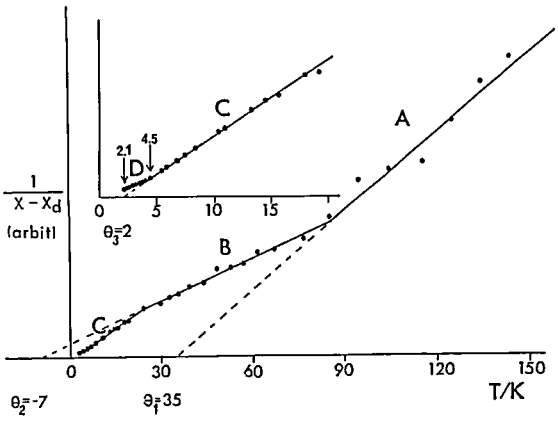

Figure 1. The temperature dependence of the reciprocal paramagnetic susceptibility for cabene species generated in polycrystalline **1**. Inset: The plot at lower temperatures than 20 K is shown in an expanded scale.

References

1) A. Izuoka, S. Murata, T. Sugawara and H. Iwamura, *J. Am. Chem. Soc.*, **107**, 1786 (1985); *IMS Ann. Rev.*, 108 (1985).
2) S. Abrahamsson, *Acta Crystalogr.*, **12**, 301, 304 (1959); U.T. Mueller-Westerhoff, A. Nazzal, R.J. Cox, A.M. Giround, *J. Chem. Soc., Chem. Commun.*, 497 (1980); H. Inokuchi and G. Saito, private communication.

V-A-6 Photochemical Reactivities of Rotameric *ap*- and *sp*- 3, 5-Dimethyl-2-(9-fluorenyl)phenyl Azides in Fluid Methanol Solution

Shigeru MURATA, Tadashi SUGAWARA and Hiizu IWAMURA

[*J. Am. Chem. Soc.*, **107**, 6317 (1985)]

Two conformationally fixed nitrenes **1***ap* and **1***sp* show contrasting chemical and spectroscopic behaviors when generated at cryogenic temperatures from the corresponding rotamers of the title azides (**2***ap* and **2***sp*).[1] We have now studied the products and their distributions in the photoreactions of **2** at room temperature. Azide **2***ap* gave mainly azepine **3** derived from **1***ap* by the internal addition of the nitrene to the fluorene ring, and **2***sp* gave methoxyamine **4** derived from **1***sp* by the hydrogen migration followed by the addition of methanol to the o-quinoid imine intermediate. However, cross-over of products **3** – **5** was observed in the two reactions as shown in Table 1. The loss of the stereospecificity in these reactions was ascribed to the conformational isomerization of the

benzazirine intermediate **6** formed from **1** in fluid solutions.

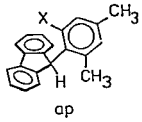

ap

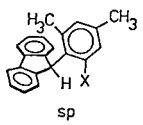

sp

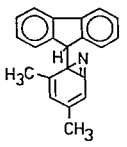

6

1, X = N:
2, X = N_3

Table 1. Product yields (%)

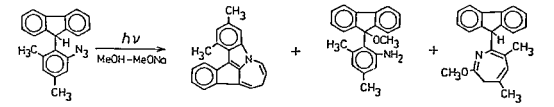

	2	**3**	**4**	**5**
ap		70	9	8
sp		29	40	22

27°C

Reference

1) S. Murata, T. Sugawara and H. Iwamura, *J. Am. Chem. Soc.*, **105**, 3723 (1983); *IMS Ann. Rev.*, 111 (1983); S. Murata, T. Sugawara, N. Nakashima, K. Yoshihara and H. Iwamura, *Tetrahedron Lett.*, **25**, 1933 (1984); *IMS Ann. Rev.*, 108 (1984).

V—B Stereochemical Consequences of the Nonbonded Interactions in Overcrowded Molecules

Disrotatory coupling of the internal rotational degrees of freedom in double rotor molecules has been studied for a series of (9-triptycyl)$_2$X derivatives. These molecules undergo rapid internal rotation (~10^9 s^{-1} at room temperature) in a strictly gear-meshed fashion, giving rise to new stereoisomerism in the *2, 2'*-and *3, 3'*-dichloro-derivatives. The racemic and meso isomers which arise due to different phase relationship between the substituted benzene rings are separated by HPLC. The high energy barrier to the gear-slipping process was now obtained by measuring the temperature dependence of the isomerization rates as 39 kcal mol^{-1} for the *2, 2'*-dicholoroamine (X = NH) and compared with those of the methane (X = CH_2) and ether (X = O). An effort was made to obtain an operational test for determining the transition state structure for the gear-slipping process.

V-B-1 Effect of the Central Atoms on the Tightness of the Molecular Bevel Gear. II[1] Meso- and dl-bis(2-chloro-9-triptycyl)amines

Yuzo KAWADA (*Ibaraki Univ.*), **Hiroshi YAMAZAKI** (*Ibaraki Univ.*), **Gen KOGA** (*Ibaraki Univ.*) and **Hiizu IWAMURA**

2-chloro-9-triptycyl azide (Tp-N_3) (ν_{N3} 2110 cm^{-1}) was obtained in 51% yield by the reaction of 2-chloro-9-triptycyllithium (TpLi) with *p*-toluenesulfonyl azide in anhydrous ether-benzene. Treatment of Tp-N_3 with TpLi at −78°C gave in 56% yield 1, 3-bis(2-chloro-9-triptycyl)triazene (Tp-N=N-NH-Tp). Two hundred mg portions of Tp-N=N-NH-Tp were decomposed at 280°C under nitrogen atmosphere to give bis(2-chloro-9-triptycyl)amine (Tp_2NH) (60% yield). Separation of the phase isomers was effected by HPLC to give meso (mp 425°C) and dl(mp 429°C) isomers. Rates of interconversion of the isomers were determined at 176–275.5°C to give good Arrhenius plots from which the activation energy value was obtained as summarized in Table 1. The results are interpreted in terms of the shorter C-X bond lengths and larger deformation force constants of the C-X-C moieties as we descend the series from X = CH_2 to O. The inversion at the nitrogen atom was found not to contribute to the isomerization process.

Table 1. Activation Parameters for the Gear-Slipping Process in Tp_2X

X in Tp_2X	E_a/kcal mol^{-1}	log A
CH_2 [1)]	32.2 ± 0.1	12.1 ± 0.1
NH	39.1 ± 0.1	12.4 ± 0.2
O[1)]	42.0 ± 0.5	12.3 ± 0.2

Reference

1) Y. Kawada and H. Iwamura, *J. Am. Chem. Soc.*, **105**, 1449 (1983); *IMS Ann. Rev.*, 114 (1981).

V-B-2 *Meso*, *d* and *l* Isomers of Bis(9-triptycyl)methane-2, 2'-dicarboxylic Acids

Yuzo KAWADA (*Ibaraki Univ.*), **Hiroshi YAMAZAKI** (*Ibaraki Univ.*), **Gen KOGA** (*Ibaraki Univ.*) and **Hiizu IWAMURA**

As an operational test for distinguishing between the two possible transition state structures A and B for the gear-slip process in the molecular gear of bis-(9-triptycyl)methanes, the effect of the 2-substituents on the rates of two isomerization processes *meso* ⇌ *dl* and *d* ⇌ *l* was taken into consideration. Bis(2-methyl-9-anthryl)methane was obtained in five steps starting from 2-methylanthraquinone. The addition of benzyne to the anthracene derivative followed by bromination with NBS and alkaline hydrolysis gave the isomeric mixture of the title compound in 1.2% overall yield. The acid was converted into the D(+)-α-phenylethylamide and the diastereomeric mixture was separated into the meso′, *d′* and *l′* isomers by chromatography on silica gel. A preliminary kinetic study has been carried out on these diastereomers to show that the processes meso′→ *d′* + *l′*, *l′*→*d′* + meso′ and *d′*→*l′* + meso′ have quite similar activation parameters. The results are more compatible with the transition state structure A.

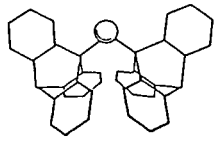

A

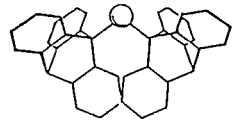

B

V—C Oxidation Reaction Mechanisms and Micellar Effects

Carbonyl oxides are important intermediates in a number of oxidation reactions. As an extension of our spectroscopic study on these reactive intermediates, we have studied their further reaction with triplet oxygen. The absence of their isomerization to dioxiranes was established by an elaborate ^{18}O-labeling experiment. The Fenton-type hydroxylation of aromatic nuclei in the TiO_2-sensitized photooxidation was found to involve ·OH radicals formed by two different mechanisms. Another example of increased efficiency of photochemical reactions in micellar systems was obtained for the photooxidation of 2-propanol. A ^{35}Cl NMR relaxation study continued to be instrumental in disclosing the ionic interactions in micellar systems.

V-C-1 ^{18}O-Tracer Study on the Rearrangement of Carbonyl Oxide Intermediates to Esters

Katsuya ISHIGURO (*Nagoya Univ.*), **Kohtaro TOMIZAWA** (*Nagoya Univ.*), **Yasuhiko SAWAKI** (*Nagoya Univ.*) **and Hiizu IWAMURA**

[*Tetrahedron Lett.*, **26**, 3723 (1985)]

Carbonyl oxides are important reactive intermediates in the ozonolysis of olefins and photooxidation of diazo compounds. As a diagnostic test for the possible interconversion between carbonyl oxides and related intermediates, we studied the rearrangement of propiophenone oxide to ethyl benzoate in the presence of oxygen. When PhC(=N_2)Et was photolyzed in the presence of oxygen ($^{32}O_2$:$^{34}O_2$:$^{36}O_2$= 100:1.17:27.9) and mesotetraphenylporphine, complete scrambling of the oxygen atoms was observed in ethyl benzoate. Whereas retention of the original combination of the oxygen isotopes is required for eq. 1, the observed scrambling is best explained in terms of eq. 2. Carbonyl oxides are concluded not to isomerize to dioxiranes. The radical addition of oxygen to carbonyl oxides to give peroxidic species such as **t** may be responsible for chemiluminescence observed in the reaction of carbenes with oxygen.[1)]

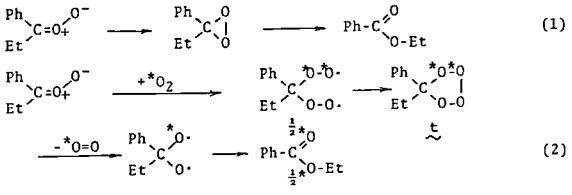

(1)

(2)

References

1) N.J. Turro, J.A. Butcher, Jr., and G.J. Heffron, *Photochem. Photobiol.*, **34**, 517 (1981).

V-C-2 An ^{18}O-Tracer Study on the TiO_2-Sensitized Photooxidation of Aromatic Compounds

Katsuhiko TAKAGI (*Nagoya Univ.*), **Toshio FUJIOKA** (*Nagoya Univ.*), **Yasuhiko SAWAKI** (*Nagoya Univ.*) **and Hiizu IWAMURA**

The TiO_2-sensitized photooxidation of toluene to give cresols (photo-Fenton type reaction) is suggested to involve hydroxyl radical HO· formed by reduction of O_2 with electron in the conduction band of TiO_2 (Eqs. 1 and 2).[1] It is also possible that HO· is formed via the oxidation of water by positive hole h^+ of TiO_2* (Eqs. 1 and 3).[2] An ^{18}O-tracer study using $^{18}O_2$ gas has been carried out to differentiate

$$TiO_2 \xrightarrow{h\nu} h^+ + e^- \quad (1)$$

$$O_2 + e^- \rightarrow O_2^{-\cdot} \rightarrow H_2O_2 \rightarrow HO\cdot \quad (2)$$

$$H_2O + h^+ \rightarrow HO\cdot + H^+ \quad (3a)$$

$$HO^- + h^+ \rightarrow HO\cdot \quad (3b)$$

between the two mechanisms. The incorporation of ^{18}O into phenol for the TiO_2-sensitized oxidation of benzene was now found to be pH-dependent; it increased approximately linearly from 21% at pH2 to 70% at pH12. The results clearly show that, whereas HO·comes mainly from O_2 at higher pH, water is the oxygen source at lower pH. Competitive trapping of electron with proton to give H_2 is considered to be responsible for the reduced contribution of O_2 at lower pH.

References
1) M. Fujihira, Y. Satoh and T. Osa, *Nature*, **293**, 206 (1981); M. Fujihira, Y. Satoh and T. Osa, *Bull. Chem. Soc. Jpn.*, **55**, 666 (1982).
2) Y. Simamura, H. Misawa, T. Oguchi, T. Kanno, H. Sakuragi and K. Tokumaru, *Chemistry Lett.*, 1691 (1983).

V-C-3 Effect of AOT-Reversed Micelle on the Photooxidation of 2-Propanol with Colloidal TiO_2

Katsuhiko TAKAGI (*Nagoya Univ.*), **Toshio FUJIOKA** (*Nagoya Univ.*), **Yasuhiko SAWAKI** (*Nagoya Univ.*) and **Hiizu IWAMURA**

[*Chemistry Lett.* in press]

In an attempt to increase the contact area of organic substrates with TiO_2 colloids as photosensitizers, various micellar systems have been examined. When a hexane solution of 2-propanol containing TiO_2 in an AOT (dioctyl sodium sulfosuccinate) reversed micellar system (AOT: 100 mM, H_2O: 1.1 M) was deaerated and irradiated with a Pyrex-filtered uv lamp, the relative efficiency for the formation of acetone was about 150 times as high as in the aqueous colloidal TiO_2. The more favorable distribution of 2-propanol in aqueous phase is considered to be responsible for making the alcohol in an efficient contact with the excited TiO_2 supported likewise in the water pool. The chemical yield of acetone varied with the size of the water pool as shown in Figure 1, where $\omega = [H_2O]/[AOT]$. Two opposite effects must be contributing to the observed plots. When $\omega < 10$, the TiO_2 particle is surrounded tightly by the negatively charged inner surface of the AOT micelle. These highly anionic environment would enhance the efficiency of positive hole ejection from the excited TiO_2, resulting in the steeper curvature at $\omega < 10$. With increasing water content in the pool ($\omega > 10$), dissolution of larger amounts of the alcohol in the water pool may become significant.

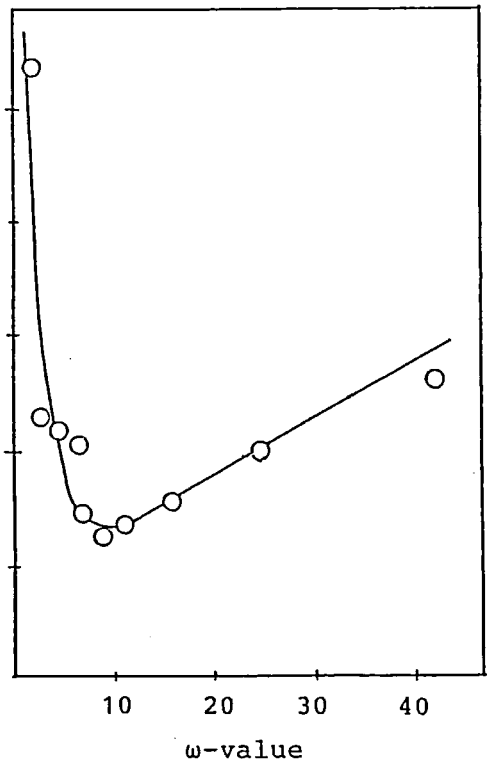

Figure 1. Effect of ω-value on the oxidation of 2-propanol (–O–O–). Initial concentration: 150 mM 2-propanol with 5 mM TiO_2 and 100 mM AOT.

V-C-4 Interaction of Chloride Ions with Nonionic Surfactant as Mediated by Inorganic Cations Incorporated in Surfactant Micelles

Toru NAKANISHI,[1] Tsutomu SEIMIYA (*Tokyo Metropolitan Univ.*), Tadashi SUGAWARA and Hiizu IWAMURA

[*Chemistry Lett.*, 2135 (1985)]

In order to study the role of added salts on the "cloud point" of aqueous nonionic surfactants, the ^{35}Cl NMR line widths[2] ($\Delta\nu^{Cl}$) was determined for the n-$C_{12}H_{25}O(CH_2CH_2O)_pH$ (p = 5, 6, 7 and 8)/water/XCl (X = H, Li and Na) systems. The ^{17}O NMR line width due to the water molecules was also determined to obtain a measure of the microviscosity of the systems. The broadening ($\Delta\nu^{Cl}_{excess}$) of $\Delta\nu^{Cl}$ by introduction of the nonionic surfactant (p = 6,1.2 mol/kg) to aqueous XCl solutions (0.5 mol/kg) was 15.0, 16.5 and 19.3 Hz for NaCl, LiCl and HCl, respectively, at 50°C. The results are explained by a model in which cations X^+ are bound to the polyethylene moiety of the surfactant micelles. The resultant positively charged polyvalent micelles would attract chloride ions on their surface and effect broadening of the ^{35}Cl NMR line width. The salting-in phenomenon caused by the addition of HCl is now ascribed to the enhanced hydration of the surfactant molecules which bind protons more strongly than other cations. Added NaCl seems to weaken the surfactant-water interaction by the strong hydration of the free Na cations.

Reference
1) IMS Graduate Student from Tokyo Metropolitan University for 1982–1984.
2) T. Sugawara, M. Yudasaka, Y. Yokoyama, T. Fujiyama and H. Iwamura, *J. Phys. Chem.*, 86, 2705 (1982).

V—D CO_2 Uptake by Tetraazacycloalkane Complexes

Previously, we reported that zinc (II) complexes of tetraazacycloalkanes with an appropriate cavity size take up CO_2 as $ROCO_2^-$ or $RR'NCO_2^-$. In certain cases (*e.g.*Zn ([14] $aneN_4$)$(ClO_4)_2$ and Zn([15] $aneN_4$)$(ClO_4)_2$), the uptake reaction proceeds so facile that CO_2 is taken up spontaneously from the air. Some of the products were structurally characterized by X-ray analyses. We also observed reversible absorption and desorption of CO_2 in organic solvent. [See M. Kato and T. Ito, *Inorg. Chem.*, 24, 504, 509 (1985); H. Ito and T. Ito, *Bull. Chem. Soc. Jpn.*, 58, 1755 (1985)].

We have continued to study such type of CO_2 uptake chemistry with a particular emphasis on a role of metal ion and factors influencing the efficiency.

V-D-1 Syntheses, Characterization, and Structures of (Monomethyl Carbonato)-nickel (II), -copper(II), and -cobalt(II) Complexes with Tetraazacycloalkanes Obtained from CO_2 Uptake

Masako KATO and Tasuku ITO

A new series of monometyl carbonato complexes of nickel(II), cobalt(II), and copper(II) containing tetraazacycloalkanes (L) have been synthesized and characterized: L = [14] $aneN_4$ (1,4,8,11-tetraazacyclotetradecane), [15] $aneN_4$ (1,4,8,12-tetraazacyclopentadecane, *iso*-[14] $aneN_4$ (1,4,7,11-tetraazacyclotetradecane), and Me_4[14] $aneN_4$ (1,4,8,11-tetramethyl-1,4,8,11-tetraazacyclotetradecane). These compounds have been obtained through CO_2 uptake reaction in basic methanol from corresponding four coordinate complex, [M(L)]-$(ClO_4)_2$. X-ray structures of three compounds, Cu([14] $aneN_4$)$(O_2COCH_3)(ClO_4)$, Ni(Me_4[14]-ane N_4)$(O_2COCH_3)(ClO_4)$, and [Ni(Me_4[14] $aneN_4$)$(O_2COCH_3)_2$]·$HNEt_3$·ClO_4, have been determined. They have different types of structure, I, II and III, respectively. All the monomethyl carbonato complexes synthesized are classified into the three types on the basis of IR and/or electronic spectral data, supplemented with the X-ray results. Efficiency of the CO_2 uptake depends strongly on the coordination structure which is controlled by a combination of metal ion and tetraazacycloalkane. Difference in the reactivity among metal ions and factors influencing the efficiency have been studied in connection with the zinc(II) system which undergoes the most effective CO_2 uptake of this type.

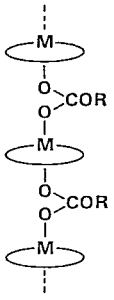

I

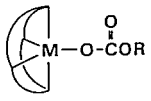

II

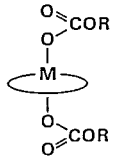

III

V-D-2 Synthesis and Structure of (Nitroacetato) ((7*RS*, 14*RS*)-5,5,7,12,12,14-hexamethyl-1, 4, 8, 11-tetraazacyclotetradecane)-nickel(II), [Ni(na) (Me_6[14] $aneN_4$)]

Haruko ITO (*Aichi Kyoiku Univ.*) **and Tasuku ITO**

[*Bull. Chem. Soc. Jpn.*, 58, 2133 (1985)]

Much attention has been paid to the formation of a new C-C bond using CO_2 as carbon source. α-Nitro acids, for example, were obtained by the treatment of $Mg(OCH_3)_2$[1] or $MgCl_2$ and triethylamine.[2] The driving force of the reaction was attributed to the formation of a stable magnesium(II) chelate of α-nitro carboxylate ion during the reaction, since free anion of α-nitro carboxylate is susceptible to decarboxylation. However, no direct structural evidence has been reported. Aiming at the deeper understanding of the CO_2 uptake chemistry of this type, we prepared and isolated nitroacetato complex and investigated its chemical properties.

The title compound, [Ni(na) (Me_6[14] $aneN_4$)], has been synthesized by the reaction of α-[Ni(Me_6-[14] $aneN_4$] $(ClO_4)_2$ with potassium nitroacetate (K_2na) in water. X-Ray analysis shows that the complex is a *cis*-NiO_2N_4 type with the tetraazamacrocycle folded, and that dianionic nitroacetate (na^{2-}) chelates the nickel(II) with one oxygen atom of the CO_2^- moiety and one oxygen atom of the NO_2^- moiety to form a six-membered chelate ring (Fig. 1).

The nitroacetato ligand in this complex is faily stable toward decarboxylation, especially in methanol. The stability is attributed to the formation of the stable six-membered nitroacetato chelate and to the macrocyclic effect of the ligand Me_6[14] $aneN_4$ that can fold.

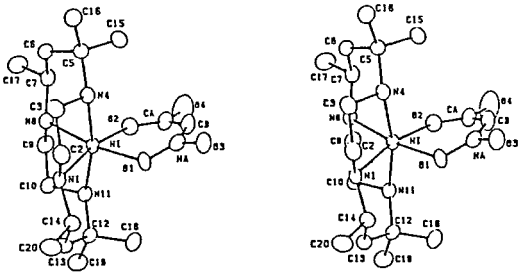

Reference

1) M. Stiles and H.L. Fiukbeiner, *J. Am. Chem. Soc.*, 81, 505 (1959).
2) N. Matsumura, Y. Yagyu and E. Imoto, *Nippon Kagaku Kaishi*, 1801 (1976).

V—E EXAFS Study of Iron Complexes at Spin-Equilibrium

EXAFS method is expected to be a possible means for structural study of metal complexes in solution. Our continued efforts in EXAFS study (*IMS Ann. Rev.*, 117, (1984) are now being directed toward such a problem. Some applications have been already reported for solution systems containing single chemical species. However, difficulties arise in the application to an equilibrium system comprised of two or more components, because structural informations from EXAFS are one-dimensional and, there are problems on the phase shifts. It is necessary to extract structural information associated with a given species from observed EXAFS spectrum.

We are now trying to apply EXAFS to spin equilibrium system of iron complexes both in solid and solution states. The spin equilibrium systems are considered to be the simplest and the most appropriate for our purpose, since they contain only high- and low-spin species which have drastically different Fe-donor distances.

V-E-1 EXAFS Study of Iron(II) and Iron(III) Complexes at Spin-Equilibrium—Solid State Study

Koshiro TORIUMI, Yuji UMETSU (*Kumamoto Univ.*),[1] **Masako KATO, Akira OHYOSHI** (*Kumamoto Univ.*) **and Tasuku ITO**

Fe *K*-edge EXAFS spectra of $[Fe^{II}\{(6\text{-}Rpy)_3tren\}](PF_6)_2$ (R=H, CH_3) at spin-equilibrium of ($^1A \leftrightarrow {}^6T_2$) and those of $[Fe^{III}(Sal_2m,n,m\text{-}tet)]NO_3$ (m,n,m=2,2,2;3,2,3;3,3,3) at ($^2T_2 \leftrightarrow {}^6A_1$) were measured in the temperature range of 80–300K by using SOR-EXAFS facility. As an example, EXAFS spectra of powdered $[Fe\{(6\text{-}Mepy)_3tren\}](PF_6)_2$ are given in Fig. 1, which shows a drastic change in its pattern upon varing temperature. This corresponds to the spin transition between ^1A and $^5T_2$. The spectral change is consistent with reported temperature dependence of magnetic susceptibility.[2] In all the compounds studied, EXAFS waves of high spin complexes attenuated more rapidly than those of low spin complexes. This is attributable to the large difference in Fe-L distances in the former in contrast to the almost equivalent distances in the latter.

Mean coordination bond distances determined by least-squares curve-fitting analyses are in good agreement with averaged distances of X-ray data.[2] Reliable Fe-L distances were obtained by applying the constant E_0 value for all the analyses.

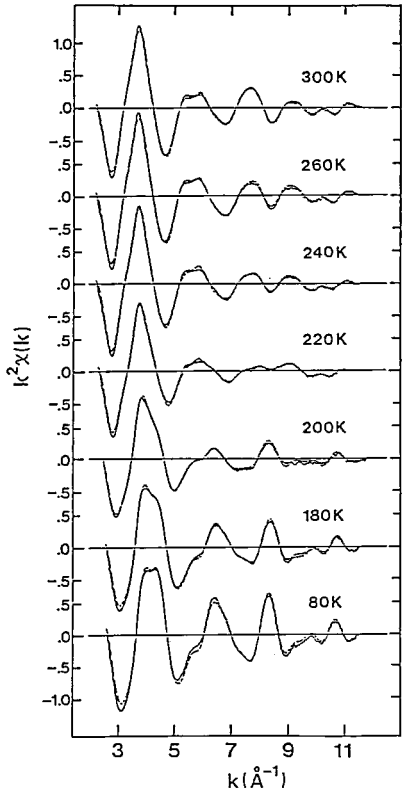

Figure 1. EXAFS spectra of $[Fe\{(6\text{-}Mepy)_3tren\}](PF_6)_2$ crystalline powder at 80–300K.

References

1) IMS graduate student from Kumamoto University for 1984.
2) M.A. Hoselton, L.J. Wilson and R.S. Drago, *J. Am. Chem. Soc.*, 97, 1722 (1975).

V-E-2 EXAFS Study of Iron(II) and Iron(III) Complexes at Spin-Equilibrium—Solution State Study

Koshiro TORIUMI, Yuji UMETSU (*Kumamoto Univ.*),[1] **Masako KATO, Akira OHYOSHI** (*Kumamoto Univ*) **and Tasuku ITO**

Fe *K*-edge EXAFS spectra of the same compounds as in V-E-1 have been measured in solution state at 220–300K. Almost saturated aceton solutions of Fe(II) complexes (0.08–0.3 mol dm^{-3}) and methanol solutions of Fe(III) complexes (0.04–0.14 mol dm^{-3}) were used. Temperature dependence of EXAFS spectra of $[Fe(Sal_2 2,2,2\text{-}tet)]NO_3$ in aceton solution is shown in Fig. 1. The spectral change corresponds to the spin-transition between $^2T_2$ and $^6A_1$. For the complexes at equilibrium in solution, EXAFS curve-fitting analyses gave intermediate coordination bond distances between low-spin and high-spin values obtained from X-ray analysis.[2]

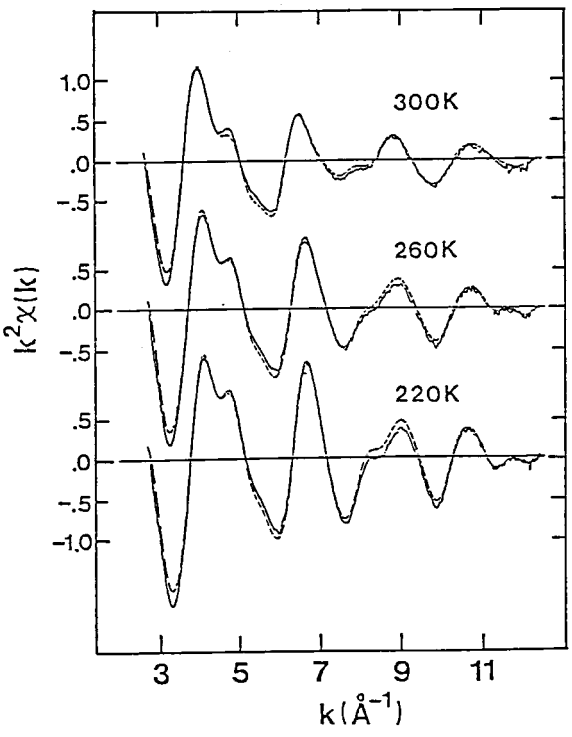

Figure 1. EXAFS spectra of $[Fe(Sal_2 2,2,2\text{-}tet)]NO_3$ 0.14 mol dm^{-3} methanol solution at 220–300K.

References
1) IMS graduate student from Kumamoto University for 1984.
2) T. Ito, M. Sugimoto, H. Ito, K. Toriumi, H. Nakayama, W. Mori and M. Sekizaki, *Chem. Lett.*, 121 (1983).

V—F Organo-Alminum Complexes of Tetaaza Macrocyclic Liqands

Synthesis, structural characterization, and reactivity study of aluminum-tetraazamacrocyclic complexes with Al-carbon bond is the subject of our continued interest [see *IMS Ann. Rev.*, 118 (1984)]. In this year we have studied photochemistry of Al(TPP) (Et) in collaboration with Prof. S. Tero of Coordination Chemistry Laboratory.

V-F-1 Photochemical Cleavage of the Al-C Bond of Al(TPP)(Et) (TPP = tetraphenylporphyrinato). Spin Trapping of the ·Al-(TPP) Radical and Photolysis Quantum Yield

Shozo TERO-KUBOTA, Naomi HOSHINO (*Ochanomizu Univ.*), **Masako KATO, Virgil L. GOEDKEN** (*Florida State Univ. and IMS*) **and Tasuku ITO**

[*J. Chem. Soc. Chem. Commun.*, 959 (1985)]

The Al-C bond of Al(TPP) (Et) is homolytically cleaved upon visible light photolysis in benzene in the presence of an excess of 2,4,6-tri-*t*-butylnitrosobenzene, yielding spin adducts of Al(TPP) and ethyl radicals with a quantum yield of the order of 10^{-3} (See VI-B-1).

V—G One-Dimensional Halogen-Bridged M(II)-M(IV) Mixed-Valence Complexes (M=Pt,Pd,Ni)

Synthesis and characterization of one-dimensional M(II)–M(IV) mixed valence compounds (M=Pt, Pd, Ni) having a linear chain structure remain to be the subject of our activities [See *IMS Ann. Rev.*, 119 (1983) and *ibid.*, 117 (1984)]. We have continued to study chemistry of such type of compounds.

V-G-1 Structure of a Bromo-Bridged One-Dimensional Pd^{II}-Pd^{IV} Mixed Valence Complex, catena-μ-Bromo-bis(ethylenediamine) palladium(II, IV) Diperchlorate, $[Pd(C_2H_8N_2)_2]\,[PdBr_2(C_2H_8N_2)_2]\,(ClO_4)_4$

Masahiro YAMASHITA (*Kyushu Univ.*), **Koshiro TORIUMI and Tasuku ITO**

[*Acta Cryst.*, **C41**, 876 (1985)]

For an understanding of solid state physical properties, structural parameters along the linear chain are of fundamental importance. In this study, the X-ray structure of the titled compound has been determined (Fig. 1): orthorhombic, Imcb, a=10.814 (1), b=13.608(2), c=9.663(4)Å. The crystal comprises linear chains, · · · Pd^{II} · · · Br-Pd^{IV}-Br, parallel to the a axis, where tetragonal $[PdBr_2(en)_2]^{2+}$ and sauare-planar $[Pd(en)_2]^{2+}$ units are

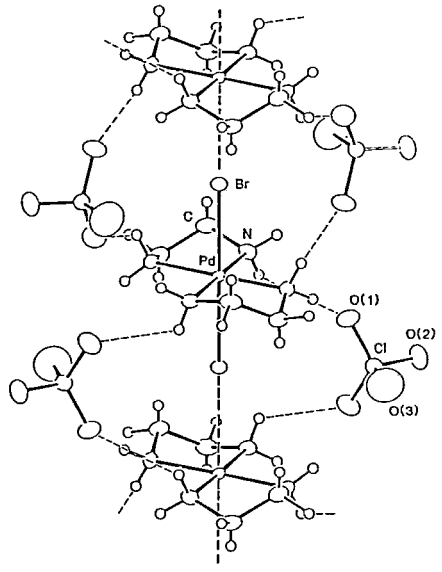

Figure 1. Portion of the infinite chain along a with surrounding ClO_4^- ions. The thick and thin deshed lines represent the Pd^{II} ... Br bond and the hydrogen bond, respectively.

stacked alternately with bromo bridges. The Pd^{IV}-Br and $Pd^{II} \cdots Br$ distances along the chain are 2.496 (1) and 2.911 (1)Å, respectively. The ratio between Pd^{IV}-Br and $Pd^{II} \cdots Br$ distances is 0.86, which is larger than that of the chloro analog (0.77).

V-G-2 The Chloro-Bridged One-Dimensional Nickel(II)-Nickel(IV) Mixed-Valence Complex Obtained from Disproportionation Reaction of the Nickel(III) Complex in (CH_3OCH_3)-(HBF_4)

Masahiro YAMASHITA (*Kyushu Univ.*), **Ichiro MURASE** (*Kyushu Univ.*), **Isao IKEMOTO** (*Tokyo Metropolitan Univ.*) and **Tasuku ITO**

[*Chem. Lett.*, 1133 (1985)]

The chloro-bridged one-dimensional Ni^{II}-Ni^{IV} mixed-valence complex with 3,7-diazanonane-1,9-diamine (L), $[Ni^{II}L]\,[Ni^{IV}Cl_2L](BF_4)_4$, was prepared by the disproportionation reaction of the Ni^{III} complex, $[Ni^{III}Cl_2L]\,Cl$, using $(CH_3OCH_3)(HBF_4)$ as a solvent and reactant. The authenticity was evidenced by the X-ray photoelectron spectra, electric spectrum, and electrical conductivity.

V-G-3 X-ray Photoelectron Spectra and Electrical Conductivities of One-Dimensional Halogen-Bridged Pd(II)–Pt(IV) and Ni(II)–Pt(IV) Mixed-Valence Complexes

Masahiro YAMASHITA (*Kyushu Univ.*), **Ichiro MURASE** (*Kyushu Univ.*), **Tasuku ITO, Yoshiki WADA** (*Univ. of Tokyo*), **Tadaoki MITANI** and **Isao IKEMOTO** (*Tokyo Metropolitan Univ.*)

[*Bull. Chem. Soc. Jpn.*, 58, 2336 (1985)]

The X-ray photoelectron spectra and electrical conductivities have been measured for the one-dimensional halogen-bridged metal-alternated mixed-valence complexes, $[Pd^{II}(en)_2]\,[Pt^{IV}X_2(en)_2]\,(ClO_4)_4$ (X=Cl, Br and I) and $[Ni^{II}(en)_2]\,[Pt^{IV}X_2(en)_2]$-$(ClO_4)_4$ (X=Cl and Br), along with their parent complexes, $[Pd(en)_2]\,Cl_2$, $Ni(en)_2Cl_2$, and $[PtCl_2$-$(en)_2]\,Cl_2$ (See VII-L-4).

V—H Organic Molecules with Characteristic Reactivities and Functionalities

Double- to quadruple-layered metacyclophanes were synthesized and the intramolecular photodimerization between the two benzene units was observed upon UV irradiation. The unique reactivities were rationalized in terms of the strain of the benezene rings in layered cyclophanes. A new sperand azophenol dye was synthesized and found to show the perfect selectivity in coloration toward lithium ions in organic solvents.

V-H-1 Photodimerization of Benzenes in Strained Dihetera[3.3]metacyclophanes

Hiroyuki HIGUCHI, Eiji KOBAYASHI, Yoshiteru SAKATA (*Osaka Univ.*) and **Soichi MISUMI** (*Osaka Univ. and IMS*)

[*Tetrahedron*, 41 (1985) in press]

Double to quadruple-layered dihetera [3.3] metacyclophanes containing O, S and Se atoms in the bridge chains were synthesized by the usual methods. On irradiation, three quadruple-layered cyclophanes **1a-c** undergo a photodimerization of two inner benzenes to give good yields of novel cage compounds **2a-c** which revert thermally to the starting cyclophanes. The driving forces for such intriguing photoreaction were studied with respect to strain of benzene, effect of chalcogen atom species, interfacial

constraint, etc., using several reference cyclophanes. It is concluded that the face-to-face stacking of two fairly strained benzene nuclei is responsible for the photodimerization and the two outer benzenes are required for the effective interconversion between quadruple-layered diheteracyclophanes and their isomeric cage compounds.

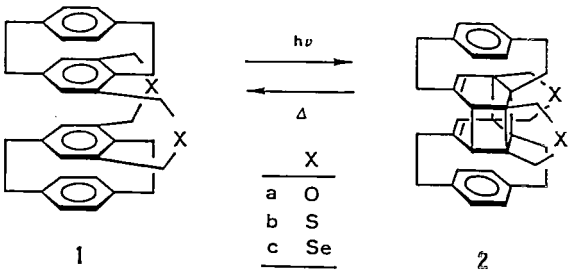

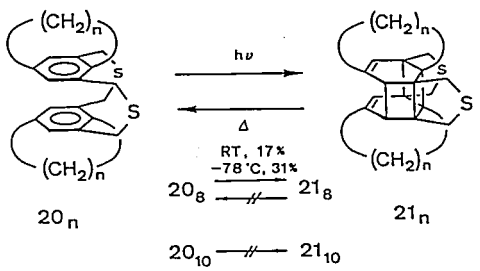

References

1) H. Higuchi, K. Takatsu, T. Otsubo, Y. Sakata and S. Misumi *Tetrahedron Lett.*, **23**, 671 (1982).
2) H. Higuchi, M. Kugimiya, T. Otsubo, Y. Sakata, and S. Misumi, *Tetrahedron Lett.*, **24**, 2593 (1983).

V-H-2 A Spherand Azophenol Dye: Lithium Ion Specific Coloration with "Perfect" Selectivity

Tahahiro KANEDA, Shin'ichi UMEDA, Hisako TANIGAWA (*Osaka Univ.*), Soichi MISUMI (*Osaka Univ. and IMS*), Yasushi KAI, Hisashi MORII, Kunio MIKI and Nobutami KASAI (*Osaka Univ.*)

[*J. Am. Chem. Soc.*, **107**, *4802 (1985)*]

The synthesis of a new spherand azophenol dye, its coloration with perfect lithium selectivity among 63 metal salts, and the crystal structure of a relevant spherand are described. When crystalline lithium salts were added to a yellow solution of the spherand dye in chloroform containing piperidine as a base, dramatic color change to violet took place rapidly. No tendency for interaction was observed with all the other salts.

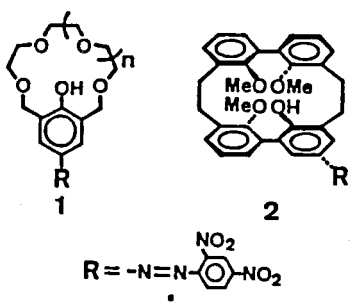

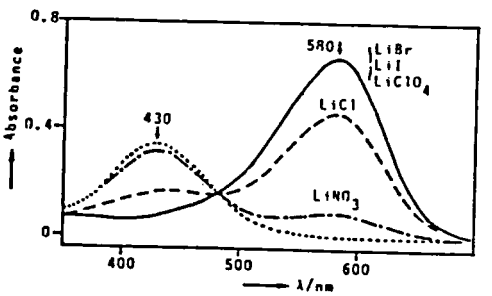

Figure 3. Visible spectra of spherand–metal salt–piperidine systems in $CHCl_3$. (---) salt free, LiF, Li_2SO_4, MX (M=Na, K, Rb, Cs; X=F, Cl, Br, I, ClO_4, NO_3, SO_4), $BeCl_2$, MX_2(M=Mg, Ca, Sr, Ba; X=Cl, Br, ClO_4), MX_2(M=Mn, Co, Ni, Zn, Cd, Sn, Hg; X=Cl, Br), MCl_3(M=Al, Cr, Fe, Sb, Cr, Bi), $Pb(OAc)_2$, $AgClO_4$.

References

1) T. Kaneda, K. Sugihara, H. Kamiya and S. Misumi, *Tetrahedron Lett.*, **22**, 4407 (1981); K. Sugihara, T. Kaneda and S. Misumi, *Heterocycles*, **18**, 57 (1982).
2) K. Nakashima, S. Nakatsuji, S. Akiyama, T. Kaneda and S. Misumi, *Chem. Lett.*, **1982**, 1781; K. Nakashima, Y. Yamawaki, S. Nakatsuji, S. Akiyama, T. Kaneda and S. Misumi, *ibid.*, **1983**, 1415; K. Nakashima, N. Mochizuki, S. Akiyama, T. Kaneda and S. Mizumi, *Chem. Pharm. Bull.*, **32**, 2468 (1984).

V—I Synthesis of a Hetera-annulene and Its Chemical Properties

To test the aromaticity in a hetera-annulene with 10π-electron system, 2, 7-methanothia [9] annulene (**1**) was synthesized. The equilibrium between **1** and its valence isomer **2** was studied by variable temperature ^{13}C NMR and electronic spectra.

V-I 2, 7-Methanothia [9] annulene: Synthesis and Equilibrium with Its Norcaradiene Valence Isomer

Renji OKAZAKI (*Univ. of Tokyo and IMS*), Toshio HASEGAWA and Yoko SHISHIDO (*Univ. of Tokyo*)

[*J. Am. Chem. Soc.*, **106**, 5271 (1984)]

2, 7-Methanothia [9] annulene (**1**) was synthesized from 1, 6-diiodo-1,3,5-cycloheptatriene in 13 steps. Variable-temperature ^{13}C NMR and electronic spectra indicated that **1** is in equilibrium with its valence isomer, 9-thiatricyclo [4.3.1.$0^{1,6}$] deca-2,4,7-triene (**2**). From the ^{13}C NMR spectra, the equilibrium ratio **1**/**2** was estimated as 16/84 in $CDCl_3$-CS_2 (1:1) at 30°C. Comparison of the temperature dependence of ^{13}C chemical shifts of **1** with that of other related systems suggested the presence of some stabilization in **1**, which was attributed to the aromaticity of **1** as a 10π-electron system although direct evidence for the presence of diatropicity in **1** could not be obtained from ^{1}H NMR spectroscopy due to a fast equilibrium even at low temperatures.

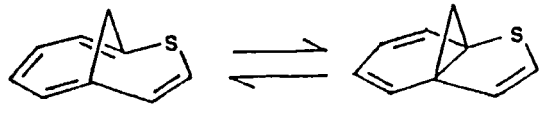

1 **2**

RESEARCH ACTIVITIES VI
Coordination Chemistry Laboratories

Coordination Chemistry Laboratories were established in 1984 to facilitate the studies of coordination compounds in wider sense, particularly in the interdisciplinary region between molecules and a variety of inorganic compounds. They consist of two laboratories. Laboratory of Synthetic Coordination Chemistry was transferred for the period of two years from Research Institute for Iron, Steel and Other Metals, Tohoku University to develop the synthesis of metal cluster complexes with characteristic physical and chemical properties.

Emphasis is also given to novel coordination compounds formed between hard Lewis acid and soft ligands with sulfur and phosphorus. Laboratory of Complex Catalysis aims fundamental studies relevant to complex catalysis including kinetics of elementary reactions of catalytic activity and the relationship between homogeneous and heterogeneous catalysis.

VI-A Synthesis and Crystal Growth of Ternary Transition Metal Cluster Complexes

Humihiko TAKEI, Shin TSUNEKAWA and Syoichi HOSOYA

Single crystals of rare earth molybdenum sulphide $Ho_xMo_6S_8$ ($x \sim 1$) have successfully been prepared using a newly designed high temperature and high pressure furnace. This compound, known as one of the rare earth Chevrel-type compound, has been the subject to clarify the unusual physical property, that is, the cooperation of magnetism and superconductivity. The crystal growth was carried out under such severe condition as up to 100 atm of He gas pressure and up to 2000°C of heating temperature. As this compound was found to melt incongruently above 1600°C, the flux method was introduced: slow cooling of $HoMo_6S_8$-Ho_2S_3 melt in an Mo crucible. As shown in figure 1, the as-grown crystals have the well-developed $(100)_{rhombohedral}$ faces. X-ray analyses revealed that the Ho content x in the crystal was very close to unity.

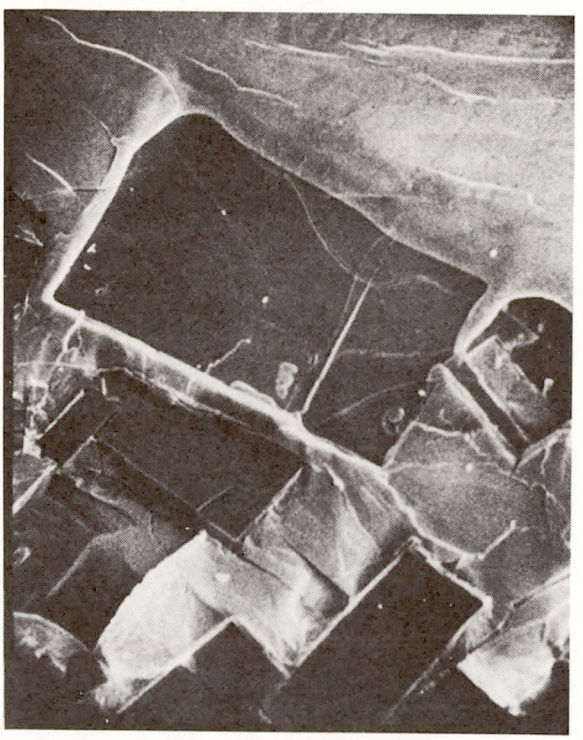

Figure 1 SEM photograph of $HoMo_6S_8$ crystals. The maximum edge length is about 1 mm.

VI—B ESR Studies on the Photochemical Reaction Mechanism and the Excited States of Coordination

VI-B-1 Photochemical Cleavage of the Al-C Bond of Al(TPP)Et (TPP = Tetraphenylporphyrinato). Spin Trapping of the ·Al(TPP) Radical and Photolysis Quantum Yield

Shozo TERO, Naomi HOSHINO, Virgil L. GOEDKEN (*Florida State Univ, and IMS*), **and Tasuku ITO**

[*J. Chem. Soc. Chem. Commun.* (*1985*), *959*]

The ESR study of metalloporphyrin π-cation and anion radicals has made fundamental contribution to our understanding of photosynthetic and metabolic processes, as well as contributing to our theoretical understanding of these systems. In this paper, we reported the spin trapping of a new radical, the neutral ·Al(TPP) species, by 2,4,6-tri-t-butylnitrosobenzene (TBN) together with the photolysis quantum yields.

Photolysis of the degassed benzene solution of Al(TPP)Et with visible light ($\lambda > 550$ nm) in the presence of TBN produced the spin adducts, TBN-Al(TPP) and TBN-Et.

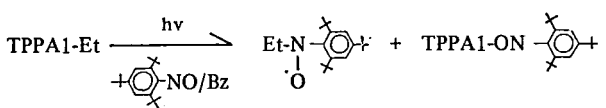

The ESR parameters were determined as a^N = 1.20, a^{Al} = 0.19 mT, and g = 2.0049 for TBN-Al(TPP) and a^N = 1.34, a^H_β = 1.79, a^H_{meta} = 0.08 mT, and g = 2.0061 for TBN-Et, respectively.

The photolysis quantum yields were determined for three different wave lengths, which corresponded to the absorption maxima of the Soret (435 nm), $Q_{0,1}$ (568 nm), $Q_{0,0}$ (612 nm) bands, respectively, of the Al(TPP) Et in chloroform. The reaction was easily followed spectrophotometrically as shown in Figure 1. The results at 20° were as follows: $\phi = (3.1 \pm 0.2) \times 10^{-3}$ (irradiation at 435 nm), $(8.5 \pm 0.5$ nm) $\times 10^{-3}$ (568 nm), and $(4.9 \pm 0.3) \times 10^{-3}$ (612 nm).

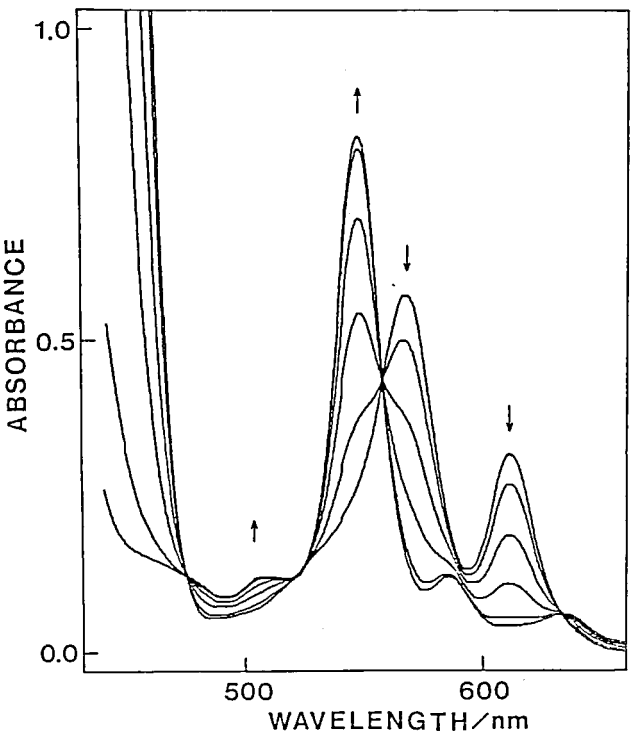

Figure 1. Absorption spectral change upon photolysis of a chloroform solution of Al(TPP)Et at 10°C. Photolysis conditions: λ 430 nm, band width 10 nm, duration 5 × (2 min).

VI-B-2 Time-Resolved ESR Study on the Excited Triplet State of Tetraazamacrocyclic Complex.

Shozo TERO, Tasuku ITO and Jiro HIGUCHI (*Yokohama National Univ.*)

There has been few study on the electronic structure and excited states of metal complexes which have highly conjugated synthetic macrocycles, in contrast to the porphyrins and phthalocyanine complexes. Time-resolved ESR technique has been applied to the observation of the excited triplet (T_1) state of $(C_{22}H_{22}N_4)$AlEt complex. The ESR spectra were obtained with dc detection (no field modulation) method, using JEOL FE2XG ESR spectrometer. The signal was taken into a boxcar integrator (PAR 162) at arbitary times after the N_2 laser pulse (Molectron UV-24).

Figure 1 shows the time-resolved ESR spectrum of $(C_{22}H_{22}N_4)$AlEt in 2-methyltetrahydrofurane (MTHF) observed at 1 μs after the laser pulse at 77 K. The emission signal at 0.16 T is assigned to the $|\Delta m_s| = 2$ transition. The $|\Delta m_s| = 1$ transitions are observed between 0.26 and 0.4 T. The zero-field splitting parameters of D = 0.0618 and E = 0.0058 cm^{-1} were obtained from the spectrum. The Z and X signals of the complex at the low-field $|\Delta m_s| = 1$ transitions are emissive and those at high-field are absorptive. On the other hand, the low-field Y signal is absorptive and the high-field one is emissive. Therefore, we can conclude that the D value is positive and the T_X sublevel of the complex is preferentially populated. The axes were assigned by theoretical calculation using ASMO-CI method in the Paraiser-Parr-Pople approximation.

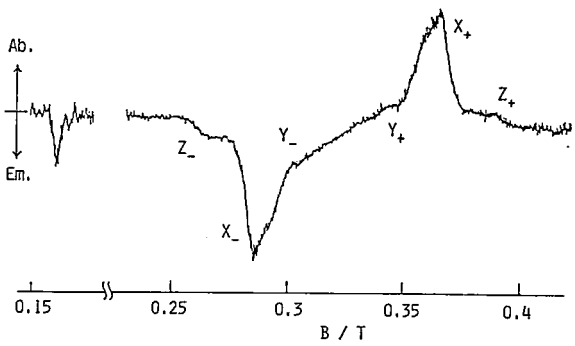

Figure 1. Time resolved ESR spectrum of excited triplet state of $(C_{22}H_{22}N_4)$AlEt in MTHF observed at 1.0 μs after the laser pulse at 77 K.

VI—C Kinetics and Mechanism of Outer-sphere Oxidation of the Oxovanadium(IV) Complexes in Aqueous Solution.

Oxovanadium (IV) complexes give interesting regio-selectivity towards ligand substitution reactions, the cis-site being much more inert than the trans-site to the oxide. Kinetic studies have been performed to elucidate the role of the cis-site towards one electron transfer reactions by use of VO^{2+} complexes with multidentate aminocarboxylates and one-electron oxidants such as hexachloroiridate(IV) and hyperoxo-bridged binuclear complexes of cobalt (III).

VI-C-1 Kinetics and Mechanism of the Outer-sphere Oxidation of *cis*-Aquaoxovanadium (IV) Complexes Containing Quadridentate Amino Carboxylates.

Kazuo SAITO, Yoichi SASAKI* and Masato NISHIZAWA* (**Tohoku Univ.*)

[*Inorg. Chem.*, 24, *767 (1985)*]

cis-Aquaoxovanadium (IV) complexes [VO (pmida) (H_2O)] (pmida = [(2-pyridylmethyl) imino] diacetate (2–)) and [VO (nta) (H_2O)] $^-$(nta = nitrilotriacetate (3–)) were oxidized with $[Ir^{VI}Cl_6]^{2-}$and [(en) Co^{III} (μ–NH_2, $O_2^{(-)}$) Co^{III} $(en)_2]^{4+}$ (en = ethylenediamine) in aqueous solutions of pH 3.5 to 5.0 at ionic strength 0.1 to 1.0 M. Kinetic studies with a stopped flow spectrophotometer gave the kinetic formula $R = (k_{H_2O} + k_{OH}K_a\ [H^+]^{-1})[V^{IV}]$ [oxidant] where K_a is the acid dissociation constants of the aquaoxovanadium(IV) complexes. The entropy of activation rather than enthalpy of activation seems to be responsible for the fact that k_{OH} is ca. 10^3 times bigger than k_{H_2O} for the redox couples. The difference in electronic interaction between the redox couples at the transition state appears to be more important than the Franck-Condon between the aqua and hydroxo complexes. Importance of the solvation is discussed on the basis of the dependence of the activation parameters on the charge product of the redox couple.

VI-C-2 Kinetics of the Oxidation of an Ethylenediaminetetraacetate Complex of the Oxovanadium(IV) Ion with Hexachloroiridate(IV) in Aqueous Solution.

Kazuo SAITO, Yoichi SASAKI*, Masatoshi KANESATO*, Kenichi OKAZAKI* and Akira NAGASAWA* (*Tohoku Univ.*)

[*Inorg. Chem.*, 24, *772 (1985)*]

A new complex Na[$V^{IV}O$(edtaH)] (edta = ethylenediaminetetraacetate (4–)) has a pK_a value 3.22 at 25°C and I = 1.0 M and oxidized to *cis*-dioxovanadium(V)-EDTA complex with $[Ir^{IV}Cl_6]^{2-}$. Kinetic studies with a stopped flow spectrometer showed that there is a steady-state intermediate $V^{V}O$-EDTA complex which is converted into the dioxo complex accompanied by the dissociation of one of the coordinated carboxylate arms. Second order rate constants of the electron transfer process to give the intermediate are 330 and 650 $M^{-1}s^{-1}$ for the protonated and deprotonated EDTA complex, respectively, at 25°C and I = 1.0 M. These values are smaller than those for the one-step oxidation of *cis*-aquaoxo(quadridentate)vanadium (IV) ions with the iridate (IV).

VI—D Catalytic Action of Organoniobium Complexes

Niobium is between zirconium and molybdenum on the periodic table of the elements, but its organometallic complexes have been so far synthesized with only limited variety of ligands. Past studies have been centralized in niobium (V) complexes, but complexes with lower oxidation number of niobium are expected to provide interesting frontier of chemical studies of complex catalysis.

VI-D-1 Catalytic Activity of Organometallic Complexes of Niobium in Lower Oxidation State Containing Cyclopentadienyl and Related Ligands

Akira NAKAMURA (*Osaka Univ. and IMS*), Hajime YASUDA,* Kazuyuki TATSUMI,* and Satoru UENO (**Osaka Univ.*)

[*J. Am. Chem. Soc.*, 107, *2410 (1985)*]

Organometallic complexes of niobium in low valent state have been studied little. We have found that the oxidation state I to IV are stabilized by use of auxiliary ligands such as η^5-cyclodienyl (η^5-C_5H_5) and η^5-[$C_5(CH_3)_5$]. Reaction of [$NbCl_4(C_5R_5)$] (R = H, CH_3) and enediylmagnesium gave highly reactive 1, 3-diene complexes [$NbCl_2$(diene) (C_5R_5)] and [Nb (diene)$_2$(C_5R_5)]. Among them [Nb (C_4H_6)$_2$-(η^5-C_5H_5)] containing 2 moles of 1, 3-butadiene can act as catalyst for the polymerization of acetylene and butadiene. The corresponding tantalum complexes give only very low reactivity, indicating delicate difference in bonding is reflected in the reactivity in an amplified manner. The influence of structure of the auxiliary ligands upon the reactivity and selectivity is now under study.

VI—E Structure and Lewis Acid-Base Reactions of Transition Metal Complexes with Hard Metal Ions and Soft Ligating Atoms.

When soft ligating atoms such as sulfur, selenium, phosphorus and arsenic form chelate complexes with transition metal ions with high electric charges, characteristic structure and chemical properties are observed. New mixed ligand complexes containing aminoalkylphosphine derivatives of cobalt have been synthesized and their crystal structure determined by X-ray diffraction method.

VI-E-1 Preparation and Characterization of $[Co^{III}X_2(edpp)_2]^+$ (edpp = $NH_2CH_2CH_2P(C_6H_5)_2$, X = Cl^-, Br^-, I^-, NCO^-, N_3^-, NO_2^-)and $[CoX_2(en)(dppe)]^+$ (en = ethylenediamine,

dppe = $(C_6H_5)_2PCH_2$-$CH_2P(C_6H_5)_2$, X = Cl^-, Br^-, NCS^-) and Crystal Structure of *trans*-(NCS, NCS), *cis*(P,P) [Co $(NCS)_2$ $(edpp)_2Br \cdot 3H_2O \cdot (CH_3)_2CO$ and *cis*(NCS, NCS), *trans* (P,P)–$[Co(NCS)_2(edpp)_2]$ Br· CH_3OH

Kazuo KASHIWABARA (*Nagoya Univ. and IMS*), Masamichi ATOH,* Haruko ITO, Tasuku ITO and Junnosuke FUJITA* (**Nagoya Univ.*)

[*Bull. Chem. Soc. Jpn.*, 57, *3139 (1984)*]

These complexes were synthesized by the wet method and separated by column chromatography. Depending on the stability of individual isomers only limited varieties of isomers were obtained in pure state. X-Ray crystallography disclosed that Co-N-C-S linkage is always linear and the Co-P distances are similar to one another. The average Co-NH_2 and Co-NCS distances in the trans (NCS, NCS) isomer (2.010 and 1.882 Å) are longer and shorter than those of the cis (NCS, NCS) isomer (1.970, 1.960 Å), respectively. The visible and ultraviolet absorption spectra were compared with those of related dianionocobalt (III) complexes.

VI-E-2 Preparation and Characterization of [Co(acetylacetonato)-diamine or 2,2′-bipyridyl) (aminoalkylphosphine)]$^{2+}$. Crystal Structure of (+) $^{CD}_{531}$-Λ-*fac*(*N*)-(acetylacetonato) [(1*R*, 2*R*)-1, 2-cyclohexanediamine] [(2-aminoethyl)diphenylphosphine] cobalt(III)Perchlorate, [Co $(C_5H_7O_2)(C_6H_{14}N_2)(C_{14}H_{16}NP)]$ $(ClO_4)_2$

Kazuo KASHIWABARA (*Nagoya Univ. and IMS*), Masakazu TAKATA,* Haruko ITO, Tasuku ITO and Junnosuke FUJITA* (**Nagoya Univ.*)

[*Bull. Chem. Soc. Jpn.*, 58, *2247 (1985)*]

Nine new cobalt(III) complexes of the type [Co (acac)(L)(edpp)]$^{2+}$ (L = *R*, *R*-cyclohexanediamine or 2,2′-bipyridyl, [Co(acac)(L′)(empp)]$^{2+}$ (L′ = en and bpy) and structurally related [Co(acac)-(bpy) (en)]$^{2+}$ were prepared and resolved into optical isomers. X-Ray crystallography disclosed that $(+)^{CD}_{531}$-[Co (acac) (*R*, *R*-chxn)(edpp)] $(ClO_4)_2$ is monoclinic, the three N atoms are in facial sites and the absolute configuration is Λ. The structure of other complexes were assigned by comparing the pmr and CD spectra with those of this complex. The complexes with 1, 2-diamine and bipyridine gave exclusively fac(*N*) and mer(*N*) isomers, respectively.

RESEARCH ACTIVITIES VII
Computer Center

VII—A Theoretical Investigatigations of Metalloporphyrins by the Ab Initio SCF MO Method

Metal complexes are interesting polyatomic systems because of their complicated electronic structure and because of their catalytic function. Metalloporphyrins are prominently important as an active center of energy conversion processes in biological systems. In this project the electronic structure and the fundamental functions are studied for several complexes by performing *ab initio* MO computations.

VII-A-1 *Ab initio* MO study on equilibrium bond distance between Fe and pyridine in bis (pyridine) (porphinato) iron for various electronic states

Minoru SAITO (*Nagoya Univ. and IMS*) **and Hiroshi KASHIWAGI**

[*J. Chem. Phys.* 82, *3716 (1985)*]

For bis (pyridine) (porphinato) iron [$FeP(py)_2$], a correlation between the iron electronic state and the equilibrium Fe-N_{py} distance was investigated. Potential energy curves as a function of the Fe-N_{py} distance were calculated for low-spin, intermediate-spin, and high-spin states of the ferric and ferrous ions by the *ab initio* SCF MO method. The potential curves for ferric ions are shown in Fig. 1. The equilibrium Fe-N_{py} distances were obtained from the potential curves.

The values obtained for the ferric low-spin and high-spin states were in good agreement with the experimental values for Fe(III) (OEP) (3-Clpy)[2] within the difference, ± 0.05 Å. It was found that the equilibrium distance satisfies the following inequality.

Fe (III) $(d_{z^2})^0$ < Fe (II) $(d_{z^2})^0$ < Fe (III) $(d_{z^2})^1$ < Fe (II) $(d_{z^2})^1$,

where we used the notations $(d_{z^2})^1$ and $(d_{z^2})^0$ to denote whether the $3d_{z^2}$ orbital is occupied or not.

The following significant features were also found. The distance and the force constant for the symmetrical py-Fe-py stretching are strongly correlated with the overlap population between the $3d_{z^2}$ orbital and pyridine-nitrogen orbitals. This correlation is very similar to that found in the previous investigation [J. Chem. Phys. 82, 848 (1985)] for four-coordinate Fe-porphine.

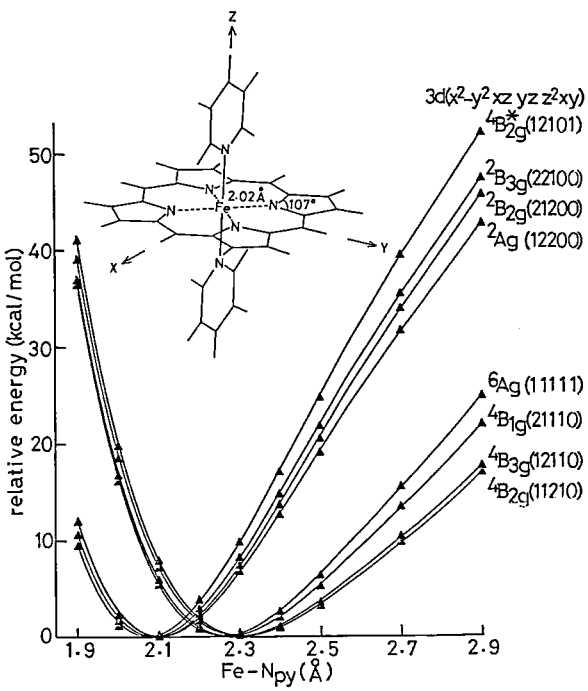

Figure 1. Potential curves as a function of the Fe-N_{py} distance for ferric states of $FeP(py)_2$, where these curves are shifted to be zero energy at their potential minina.

VII-A-2 *Ab Initio* MO Study on Relationship between Oxidation Number and Charge Distribution in Some CoF_6^{n-} (n = 4, 3 and 2) Complexes.

Eisaku MIYOSHI (*Fukuoka Dental College*) and Hiroshi KASHIWAGI

Relationship between the oxidation number of a metal ion and charge distribution around the central metal in some hexafluoro cobaltate complexes, CoF_6^{n-} (n = 4, 3 and 2), is studied by using numerical integration of a charge density obtained by *ab initio* SCF MO calculations. The radial dependence of electron number in a sphere and spherically averaged radial charge distributuion are closely examined. Charge distribution in $Co(II)F_6^{4-}$ is found to be very close to that of an independent ion model of $[Co^{2+} + 6 \times F^-]$. In the ground state of $Co(IV)F_6^{2-}$, which has less electrons than $Co(II)F_6^{4-}$ by two in $d\gamma$ (e_g) formally, about one electron migrates from ligands to the metal atom through a bonding MO ($3e_g$). This type of migration is very small in $Co(II)F_6^{3-}$. This difference between the Co(III) and Co(IV) complexes leads to almost the same charge distributions around the central metal. The oxidation number of the central metal ion can be defined as a difference between the number of valence electrons in the neutral metal atom and the number of electrons in anti-bonding MO's of the complex, which consist mainly of metal d-orbitals. Thus, the number of electrons in the anti-bonding MO's determines the oxidation number of the central metal in transition-metal complexes. On the other hand, metal d electrons in bonding MO's, which consist mainly of ligand orbitals, are out of relation to the oxidation number.

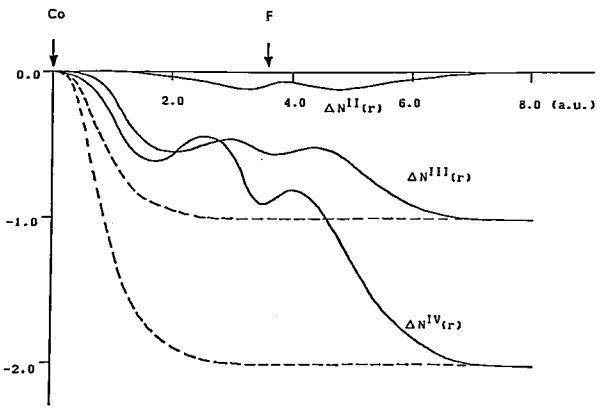

Figure 1. Difference of number of electrons in a sphere, $\Delta N^i(r)$, from an independent ion model (I I M) of $[Co^{2+} + 6 \times F^-]$. "i" is the oxidation number of the cental metal in the $Co(i)F_6^{n-}$ complexes. The broken lines represent radial dependence of decrease in electron number when one and two electrons are removed from a 3d orbital of the Co^{2+} ion.

CHEMICAL MATERIALS CENTER

VII—B Chemistry of New Metallacyclic Compounds

The study on metallacyclic compounds is directly relevant to an understanding of the reaction mechanisms of synthetically important catalyses such as olefin oligomerization, cyclocoupling, metathesis, and so on, and may also provide the basis for developments of new efficient catalyst systems. We have been studying synthesis, isolation, and characterization of new metallacyclic compounds.

VII-B-1 Synthesis of New Fischer-Type Carbene Complexes: Characterization and Reactions of Titanoxycarbene Complexes Derived from the Coupling of $(\eta^5\text{-}C_5Me_5)_2Ti\text{-}(CH_2{=}CH_2)$ and Metal Carbonyls

Kazushi MASHIMA, Kouki JYODOI,* Akira OHYOSHI,* and Hidemasa TAKAYA (*: *Kumamoto Univ.*)

Carbene—metal complexes have been attracting continuous attention because they are important reaction intermediates in transition-metal catalyzed organic reactions such as olefin metathesis and Fischer—Tropsch synthesis. They are also used as versatile reagents for organic synthesis. Fischer-type carbene complexes have been usually prepared by the reaction of metal carbonyls with strong nucleophiles such as alkyllithium and lithium amide followed by alkylation. This time, we synthesized new titanoxycarbene complexes **3** by the cyclocoupling of **1** with metal carbonyls of group 6 (eq

(1)). The present synthetic route is also applicable to bimetallic carbonyls of group 7 transition metals (eq (2)). The structure of **5b** was established by X-ray structure determination. Interesting thermal behaviors of these new titanoxycarbene complexes have been elucidated.

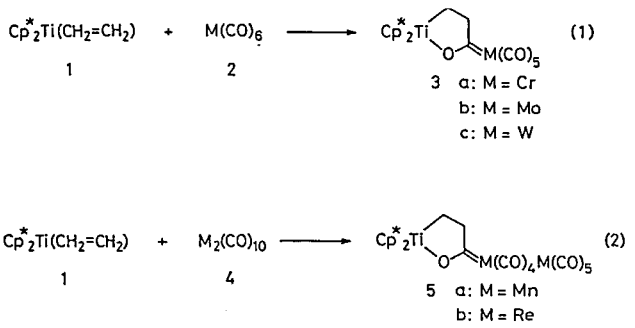

VII—C Synthesis of New Chiral Diphosphines and Their Use in Homogeneous Asymmetric Catalysis

The molecular designing and synthesis of new effective chiral ligands are the most important requirements for developing synthetically useful asymmetric catalysis. Our attention has been focussed on the subjects of developments of new effective homogeneous asymmetric catalysts, investigation, and elucidation of the reaction mechanisms and factors controlling the asymmetric induction.

VII-C-1 Synthesis of New Optically Active Diphosphines Bearing 1,1′-Binaphthyl Group

Hidemasa TAKAYA, Tetsuo OHTA, Kinko KOYANO and Ryoji NOYORI (*Nagoya Univ.*)

[in part, *J. Org. Chem.*, in press]

Recently numerous chiral di-*tert*-phosphines have been devised as ligands for transition-metal catalyzed asymmetric syntheses in homogeneous phase. We reported (*R*)- or (*S*)-2, 2′-bis(diphenylphosphino)-1, 1′-binaphthyl (**1**) (R = C_6H_5, abbreviated to BINAP), a new atropisomeric bis(triaryl)phosphine. By virtue of the C_2 chirality, molecular pliancy, and electronic characteristics, BINAP exhibits excellent chiral recognition ability in various asymmetric reactions and is now becoming, among others, one of the most important phosphine ligand.[1,2] We have developed a new practical rout to optically pure BINAP (**1a**) and its derivatives **1b**—**1f** which stems on the preparation of racemic dioxides of BINAP and its derivatives followed by optical resolution by use of readily available optically active organic acids. Investigation of new types of asymmetric catalysis are in progress by use of these ligands.

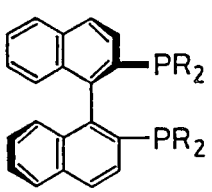

1

a: R=C_6H_5 b: R=*p*-$CH_3C_6H_4$
c: R=*p*-*tert*-BuC_6H_4 d: R=*p*-$CH_3OC_6H_4$
e: R=cyclohexyl f: R=isopropyl

References
1) A. Miyashita, A, Yasuda, H. Takaya, K. Toriumi, T. Ito, T. Souchi and R. Noyori, *J. Am. Chem. Soc.*, **102**, 7932 (1980).
2) R. Noyori and H. Takaya, *Chemica Scripta*, 83, 25 (1985).

VII-C-2 Asymmetric Hydrogenation of Allyl Alcohols Catalyzed by BINAP—Rh(I) Complexes

Shin-ichi INOUE,* Masato OSADA,* Kinko KOYANO, Hidemasa TAKAYA and Ryoji NOYORI* (*: *Nagoya Univ.*)

[*Chem. Lett.*, 1007 (1085)]

Homogeneous asymmetric hydrogenation of olefins using chiral phosphine—Rh(I) complex catalysts has been extensively investigated. Usually, however, high enantioselection has been achieved only with α-acylaminoacrylic acids or related substrates. In the course of exploring utility of our BINAP ligand **1**, we found that geraniol (**4**) and nerol (**5**) can be hydrogenated in the presence of the Rh(I) complexes to citronellol (**6**) of up to 66% optical purity. Original BINAP (**1**) and newly synthesized TolBINAP (**2**) and CyBINAP (**3**) were used.

Although further efforts should be exerted to improve the conditions to be of practical value, the present reaction is important in that this is one of the limited number of examples of asymmetric olefin hydrogenation of non-enamide substrates accomplished in fair optical yields. Interesting features of this asymmetric hydrogenation has been demonstrated.

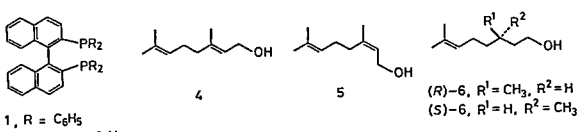

1, R = C_6H_5
2, R = p-$CH_3C_6H_4$
3, R = cyclohexyl

4 5

(*R*)-6, $R^1 = CH_3$, $R^2 = H$
(*S*)-6, $R^1 = H$, $R^2 = CH_3$

Scheme II

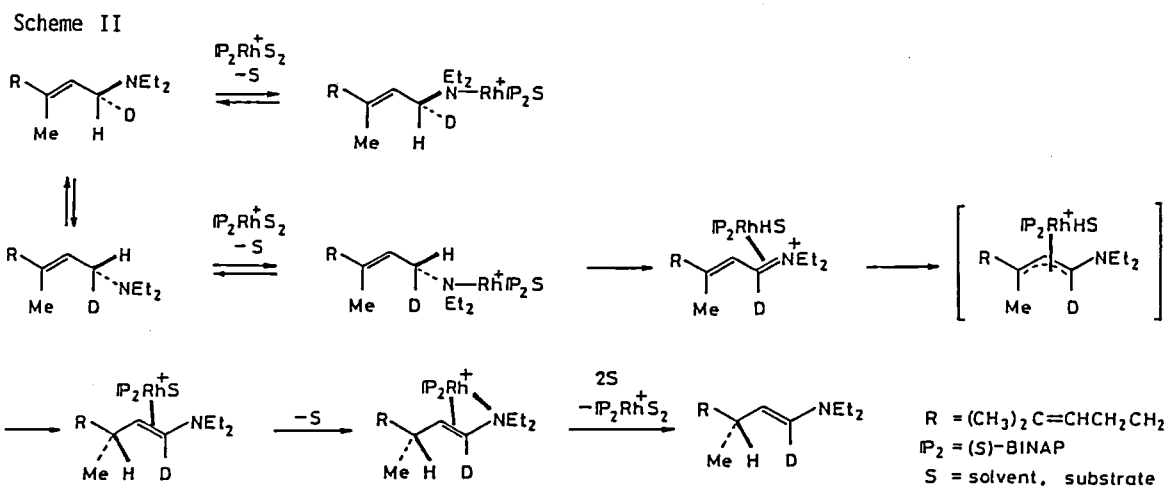

R = $(CH_3)_2C{=}CHCH_2CH_2$
IP$_2$ = (*S*)-BINAP
S = solvent, substrate or product

VII-C-3 Mechanism of the BINAP—Rh(I) Catalyzed Asymmetric Isomerization of Allylamines

Hidemasa TAKAYA, Shin-ichi INOUE,* Tsuneo SATO,* Ryoji NOYORI,* Kazuhide TANI and Sei OTSUKA**** (*: *Nagoya Univ.* **: *Osaka Univ.*)

The successful designing and synthesis of BINAP ligand has brought about many important transition metal asymmetric synthesis.[1] The cationic (*R*)- or (*S*)-BINAP—Rh(I) complexes cause highly enantioselective 1, 3-hydrogen migration of allylamines into enamines in 95—99% optical yields.[2] This time, we have revealed the stereochemical course of the isomerization by use of chiral deuterium labeled substrate **1** (Scheme I). On the basis of ^1H and ^{31}P NMR study, we have proposed the mechanism of the isomertization which is shown in Scheme II.

Scheme I

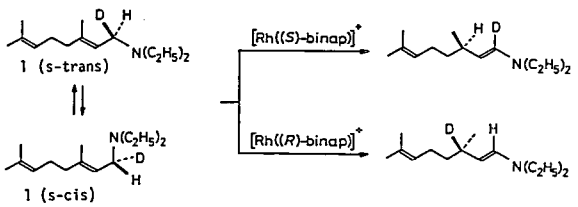

References

1) A. Miyashita, H. Takaya, T. Souchi, and R. Noyori, *Tetrahedron*, 40, 1245 (1984).
2) K. Tani, T. Yamagata, S. Akutagawa, H. Kumobayashi, T. Taketomi, H. Takaya, A. Miyashita, R. Noyori, and S. Otsuka, *J. Am. Chem. Soc.*, 106, 5208 (1984).

Instrument Center

VII—D Excitation-Energy Transport in Organized Molecular Assemblies

Langmuir-Blodgett multilayers and phospholipid bilayers are typical examples of organized molecular assemblies. In molecular assemblies, photons are absorbed to produce excited species, which then engage in an excitation energy transfer to reaction centers. In the reaction center, photochemical reactions including excimer formation and charge separation take place under the specifically organized molecular arrangement. In this research project, we are concerned with Langmuir-Blodgett films and vesicles in which the long-distance excitation energy transport (Förster type) takes place in two- and three-dimensional architectures. The dynamical characteristics are investigated by means of a picosecond time-resolved fluorescence spectrophotometer.[1] The focus has been directed to (1) fundamentals of energy migration and collection in multilayered architectures and (2) photochemical reactions under the highly-ordered molecular assemblies. The goal of our work is to develop new electrooptic devices capable of spatial control and switching of photonic-energy transport.

Reference

1) I. Yamazaki, N. Tamai, H. Kume, H. Tsuchiya and K. Oba, *Rev. Sci. Instrum.*, 56, 1187 (1985).

VII-D-1 Sequential Excitation-Energy Transport in Stacked Multilayers of Langmuir-Blodgett Type

Iwao YAMAZAKI, Naoto TAMAI and Tomoko YAMAZAKI

The Langmuir-Blodgett (LB) film is a multilayered molecular assembly in which one can build up in a desired structure from different kinds of monolayers. The LB film is prepared by transferring a monolayer spread on a water surface onto a quartz substarate. By dipping and raising a substrate through the compact monolayer, different kinds of monolayers are deposited successively on each excursion. The present study has been initiated with a view to investigating kinetics of Förster-type excitation-energy transfer in multilayered architechtures. Figure 1 shows a structure of the LB films which we are concerned with. In a sequence of the energy transfer, donor and acceptor layers are stacked with the distance between the layers being changed. When the inner surface layer containing thiacarbocyanine is excited at 540-nm laser pulses, photonic energy is transferred sequentially among the layers of various kinds of cyanine dyes. The fluorescence time behaviors of each layer are measured by means of a picosecond time-resolved spectrophotometer to deduce a kinetics of sequential energy transport as a function of distance between the layers.

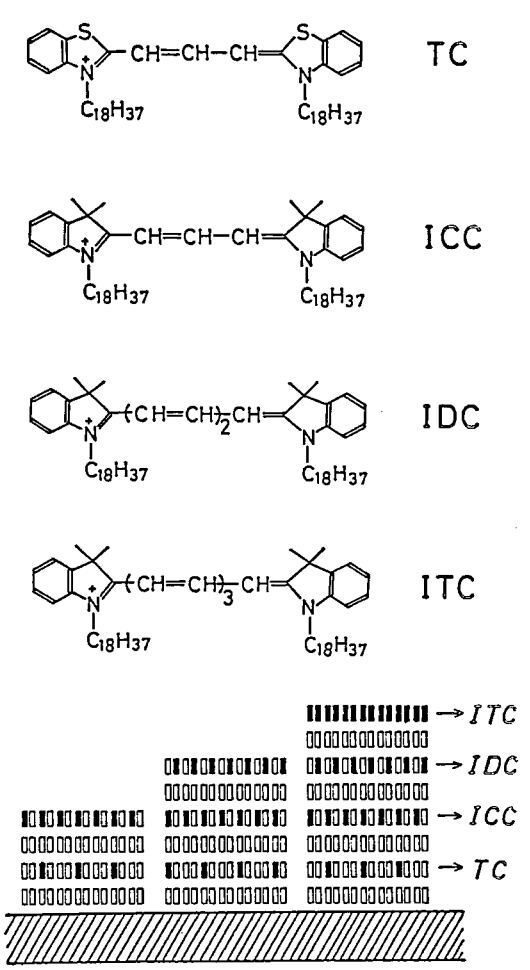

Figure 1. Langmuir-Blodgett films containing different kinds of cyanine dyes in each monolayer: thiacarbocyanine (TC), indocarbocyanine (ICC), indodicarbocyanine (IDC) and indotricarbocyanine (ITC).

VII-D-2 Two-Dimensional Excitation-Energy Transfer in Langmuir-Blodgett Monolayer

Naoto TAMAI, Tomoko YAMAZAKI and Iwao YAMAZAKI

The two-dimensional excitation-energy transfer of Förster type has been studied with Langmuir-Blodgett monolayers containing 11-(N-carbazolyl) undecanoic acid (CU) and 16-(9-anthroyloxy) parmitic acid (AP).

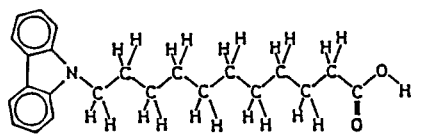

CU

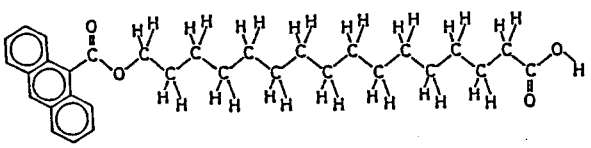

AP

The kinetics of the energy transfer from CU (donor) to AP (acceptor) in the LB monolayer was examined by monitoring the donor fluorescence by using a picosecond time-resolved spectrophotometer. The decay curves of CU are shown in Figure 1 for the various concentrations of AP. These decay curves were analyzed in terms of a superposition of an exponential decay term and a two-dimensional energy transfer equation developed by Hauser et al.[1] as follows:

$$\rho(t) = A_1 \exp[-t/\tau_D - 2\gamma_A (t/\tau_D)^{1/3}] + A_2 \exp(-t/\tau_D).$$

This may suggest an irregularity in the structure of LB film. The critical transfer distance from a carbazole to an anthracene chromophore was estimated to be 20–30 Å in accordance with the value calculated from the spectroscopic data.

Reference

1) M. Hauser, U.K.A. Klein and U. Gösele, *Z. Physik. Chem. NF*, **101**, S255 (1976).

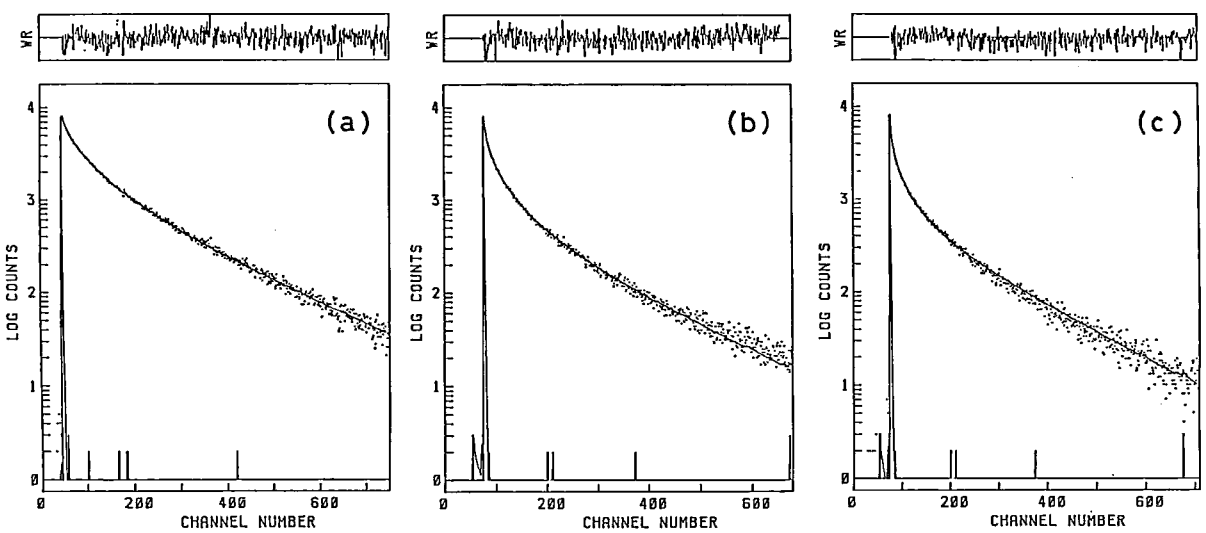

Figure 1. Fluorescence decay curves of the donor CU in the LB film in the presence of the acceptor AP of (a) 0 mol%, (b) 2.87 mol% and (c) 5.58 mol%. The solid curves are the best-fit curves calculated on the basis of Eq. (1).

VII-D-3 Fractal Behaviors of Excitation-Energy Transfer in Two-Dimensional Molecular Organizates

Naoto TAMAI, Tomoko YAMAZAKI, Iwao YAMAZAKI and Noboru MATAGA (*Osaka Univ.*)

Statistical self-similar structures, which are referred to as fractals, are emerging as an essential concept underlying the behavior of disordered systems.[1] In cases of the Förster-type energy transfer, the decay function of the donor fluorescence is given by a equation characterized by the fractal dimension, $\bar{d}$, which generally differs from the dimension of the embedding Euclidian space.[2] We have studied on the two-dimensional excitation energy transfer with vesicles

and Langmuir-Blodgett films on the basis of the fractal analysis as well as the classical statistics.

Figure 1 shows the fractal analysis of the fluorescence decays of rhodamine 6G (donor) in the presence of malachite green (acceptor) adsorbed on anionic DHP vesicle surface. The analysis gives the fractal dimension $\bar{d} = 1.31 \pm 0.087$ which is constant irrespective of the acceptor concentration. In a different pair of donor and acceptor, rhodamine B and malachite green, the same fractal dimension as above was obtained. The results indicate that the dye molecules are not randomly adsorbed on the vesicle surface, and its distribution forms a fractal structure. The fractal structure was also shown in the energy transfer in the Langmuir-Blodgett film.

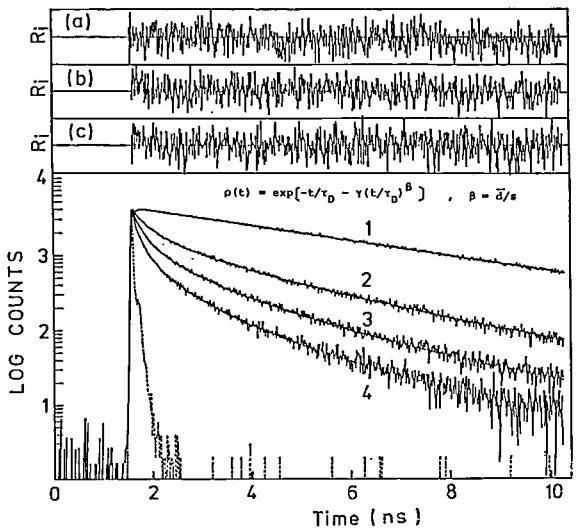

Figure 1. Curve fitting for the fluorescence decays of the donor (rhodamine 6G) in the two-dimensional energy transfer on vesicle surface in terms of the fractal kinetics. The concentrations of malachite green are (1) 0 M, (2) 2.17×10^{-6} M, (3) 3.32×10^{-6} M and (4) 4.40×10^{-6} M.

References

1) B.B. Mandelbrot, "The Fractal Geometry of Nature", Freeman, San Francisco, 1982.
2) J. Klafter and A. Blumen, *J. Chem. Phys.* 80, 875 (1984).

VII—E Picosecond Time-Resolved Fluorescence Spectroscopy on Photophysical Processes in Organized Molecular Assemblies

In highly-ordered molecular assemblies such as Langmuir-Blodgett films and oriented vapor-deposited films, one can expect to observe new aspects of photochemical and photophysical processes because uniform thin layers with the two-dimensional order might show configurational and dynamical behaviors quite different from those of homogeneous solution or from the bulk properties of crystals. In this research project, excimer formation and ground-state molecular association in the highly anisotropic media are investigated by means of a picosecond time-resolved fluorescence spectroscopy. To examine the layered structures with a spatial resolution, we have developed a new experimental technique capable of monitoring selectively the emission at particular depth in the multilayered structure.

VII-E-1 Molecular Association in Langmuir-Blodgett Multilayers

Tomoko YAMAZAKI, Naoto TAMAI and Iwao YAMAZAKI

Molecular association of pyrene chromophores in the Langmuir-Blodgett (LB) film was investigated by means of a picosecond time-resolved fluorescence spectroscopy. Three types of LB films were prepared with different layered structures as shown below. In the figure, the solid and open circles stand for pyrene ring and carboxyl group, respectively. The time-resolved fluorescence spectra for 2L type are

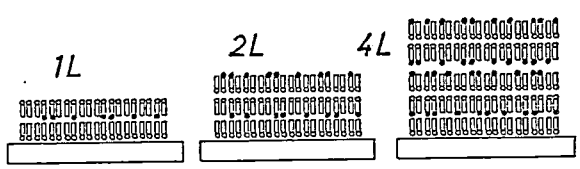

shown in Figure 1. Four types of fluorescence bands were resolved depending on the time region: (1) F_1, a ground-state dimer band with three peaks at 381, 401 and 422 nm (0 – 200 ps), (2) E_1, a new type of excimer band with a peak at 420 nm (0 – 10 ns), (3) F_2, a well-known excimer band at 470 nm (after

2 ns) and (4) F_2, an isolated monomer band with three peaks at 377, 397 and 421 nm (after 10 ns). The absorption and the fluorescence excitation spectrum also reveal that the pyrene rings form the ground-state dimer in the LB film. On going from 1L to 4L, intensities of the excimer bands (E_1 and E_2) increase twofold.

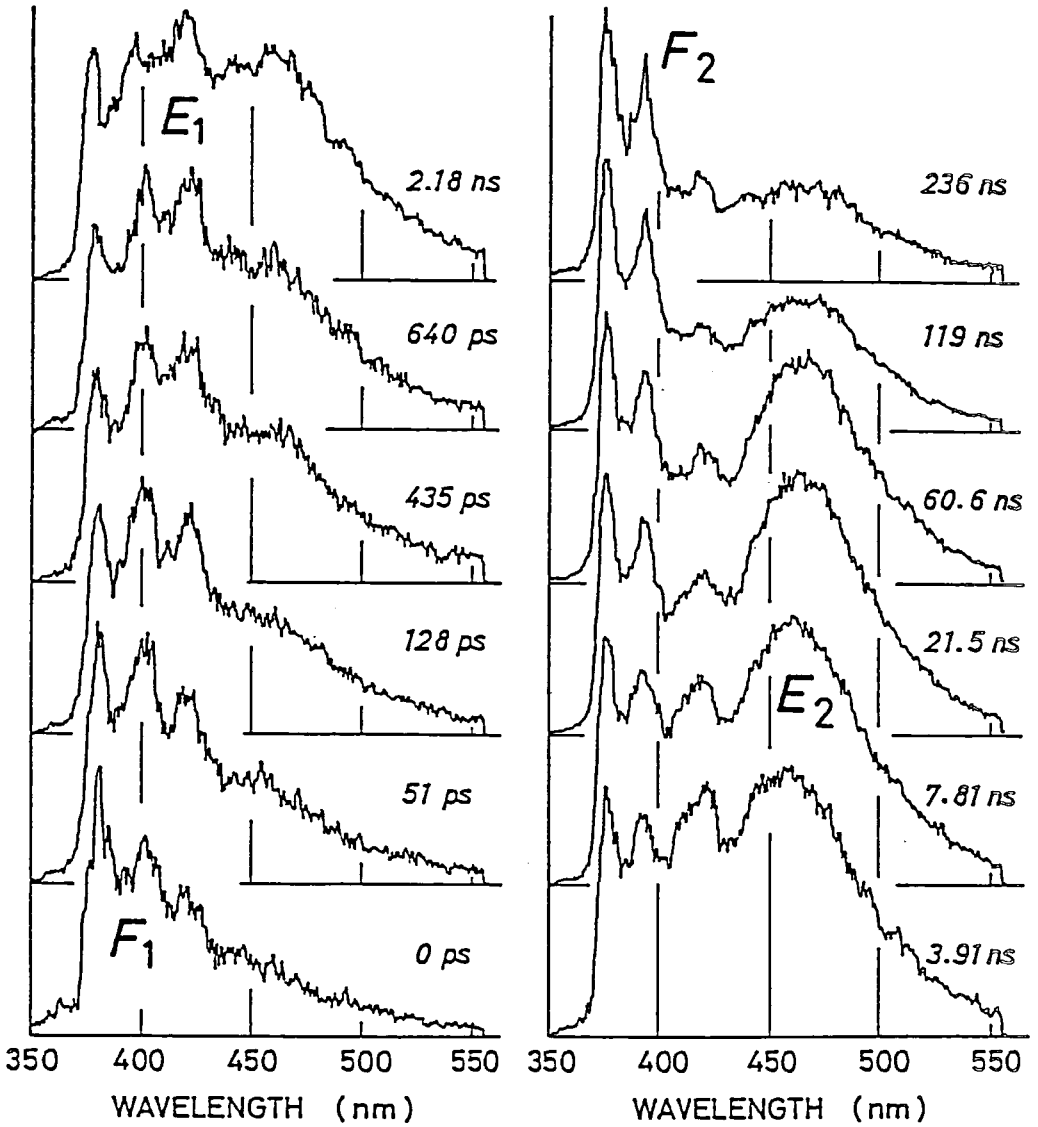

Figure 1. Time-resolved fluorescence spectra of the LB multilayer (2L type) consisting of stearic acid and 16-(1-pyrenyl) hexadecanoic acid (13.9 mol%). The excitation wavelength is 315 nm.

VII-E-2 Vacuum-Deposited Films of 12-(1-Pyrenyl)dodecanoic Acid Analyzed by Fluorescence Spectroscopy

Munehisa MITSUYA and Yoshio TANIGUCHI (*Hitachi Adv. Res. Lab.*), **Naoto TAMAI, Iwao YAMAZAKI and Hiroshi MASUHARA** (*Kyoto Inst. Tech.*)

[*Thin Solid Films*, in press (1985)]

Compared to aromatic hydrocarbons, the present

compound is more easily deposited at room temperature and the formed thin film is more stable. The fluorescence spectrum and behavior are quite different from those of its powders, dilute solutions, and films prepared by evaporating the solvent. The fluorescence bands were observed at 423, 448, 478 and 510 nm in addition to the pyrene monomer fluorescence. Co-depositions of this molecule and stearic acid change the relative intensity of these new bands and monomer fluorescence. Analyzing ps time-resolved spectra of these films, microscopic structures around the pyrenyl chromophore and their dynamics were discussed.

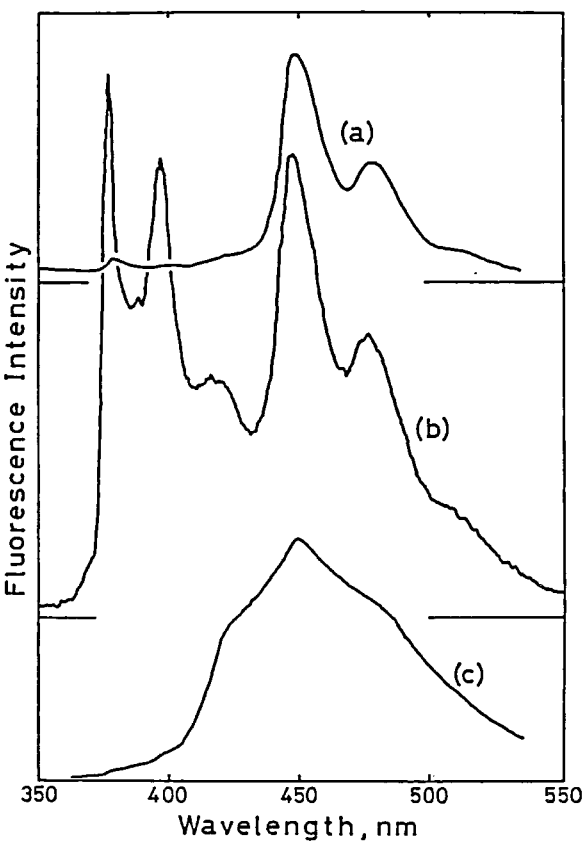

Figure 1. Fluorescence spectra of 12-(1-pyrenyl) dodecanoic acid systems. (a) A vacuum-deposited film. (b) A vacuum-deposited film containing 96 weight % of stearic acid. (c) A film formed by evaporating the solvent slowly from its benzene solution.

VII-E-3 Time- and Depth-Resolved Fluorescence Spectra of Layered Organic Films Prepared by Vacuum-Deposition

Yoshio TANIGUCHI and Munehisa MITSUYA (*Hitachi Adv. Res. Lab.*) **Naoto TAMAI, Iwao YAMAZAKI and Hiroshi MASUHARA** (*Kyoto Inst. Tech.*)

[*J. Colloid Interface Sci.*, **104**, 596 (1985)]

A time-resolved total internal reflection fluorescence spectroscopy makes it possible to measure photoprocesses and molecular motions in the surface of organic solids. In order to demonstrate this possibility, a triple-layered model film was prepared by depositing successively 12(1-pyrenyl)dodecanoic acid (15 nm thickness), stearic acid (150 nm) and perylene (100 nm) on a sapphire. Two peaks below 480 nm in

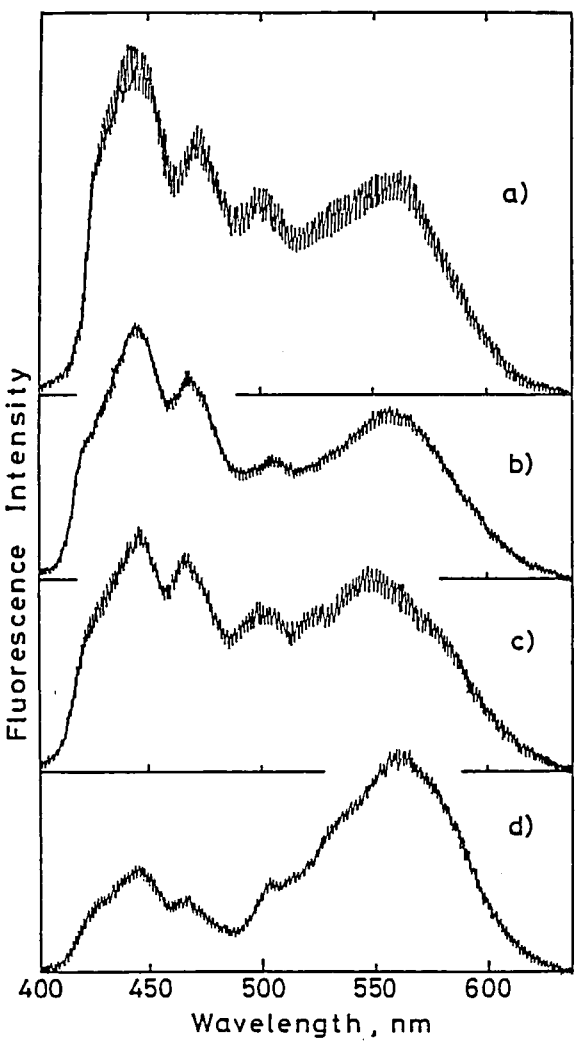

Figure 1. Fluorescence spectra of the triple-layered model film as a function of an incident angle of the exciting laser pulse. Incident angles are (a) 70.0°, (b) 65.8°, (c) 61.8° and (d) 55.9°.

fluorescence spectra are ascribed to the 12-(1-pyrenyl) dodecanoic acid layer, while a broad emission around 560 nm is to the perylene layer. The relative intensity of both bands is a function of the incident angle

of an excitation beam, as shown in Figure 1. The contribution of the surface layer is increased under total internal reflection condition. Since rise and decay behavior of the surface layer is different from that of other layers, a surface fluorescence can be more enhanced by choosing an appropriate gate-time.

VII—F Photonic Energy Transport and Primary Reaction in Biological Photoreceptors

A tetrapyrrolic chromoprotein plays a vital role as the red-light photoreceptor in accessory pigments and phytochrome of plants. Photosynthetic organisms have evolved a light harvesting antenna system for light absorption and energy transfer to the reaction center. In blue-green and red algae, the system consists of several kinds of phycobiliproteins which contain phycocyanobilin and phycoerythrobilin as chromophores (Figure 1). In the course of the energy transfer processes, fluorescence is emitted from each pigment, and is used as a probe for investigating the energy transfer mechanism. Phytochrome is also a tetrapyrrolic chromoprotein (Figure 1) quite similar to phycobilins, and acts as a photoreceptor controlling several diverse morphogenetic and developmental responses in plants. In the present study, excitation-energy transport and primary reactions in the tetrapyrrolic photoreceptors are investigated with a picosecond time-resolved spectroscopic technique.

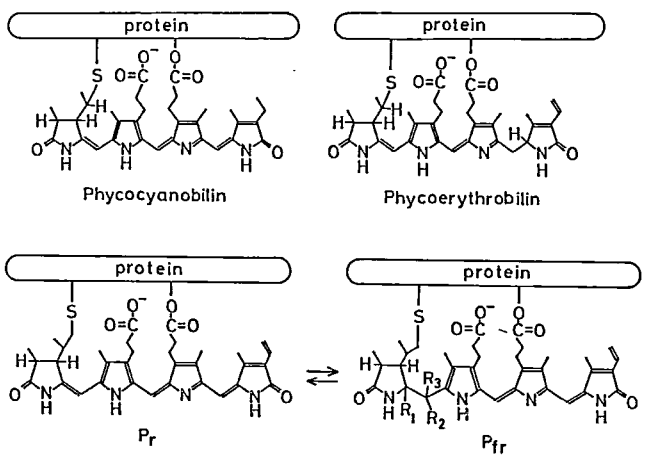

Figure 1. Structural formula of the four tetrapyrrolic chromophores which are included in phycobilins and phytochrome. Phycocyanobilin and phycoerythyrobilin are chromophores in the photosynthetic accesory pigments. Phytochrome of the red-light absorbing type (Pr) is photochemically transformed to the far-red-light absorbing type (Pfr).

VII-F-1 Excitation-Energy Transfer Kinetics in the Chromatically Adapted Systems

Mamoru MIMURO (*NIBB*), **Iwao YAMAZAKI, Tomoko YAMAZAKI, Naoto TAMAI, Akio MURAKAMI** (*NIBB*) **and Yoshihiko FUJITA** (*NIBB*)

[*Photochem. Photobiol.*, **41**, 597 (1985)]

Excitation energy transfer in chromatically adapted phycobilin system was investigated with the blue-green algae *Tolypothrix tenuis* and *Fremyella diplosiphon* by using a time-resolved spectroscopic technique.[1] Special attention was paid to the energy migration at the phycocyanin (PC) level in the phycoerythrin (PE)-rich and PE excited system and in the PE-less and PC excited system (Figure 1). The energy transfer from PC to allophycocyanine was far faster in the former than in the latter in both organisms. Such feature was the same as our previous observation for PE-rich system of *Porphyridium cruentum* and PE-less system of *Anacystis nidulans*.[2]

Thus the difference in phycobilisome structure is not a cause for such difference. Based on simulation analysis, we interpreted our observation as that (1) all PC chromophores do not equally participate to the energy migration within PC compartment but (2) a short transfer path through PC compartment is formed probably by f-type chromophores and (3) the difference in the "length" of this path is a main determinant for kinetic difference between PE-rich and PE-less systems.

References

1) I. Yamazaki, N. Tamai, H. Kume, H. Tsuchiya and K. Oba, *Rev. Sci. Instrum.*, 56, 1187 (1985).
2) I. Yamazaki, M. Mimuro, T. Murao, T. Yamazaki, K. Yoshihara and Y. Fujita, *Photochem. Photobiol.*, 39, 233 (1984).

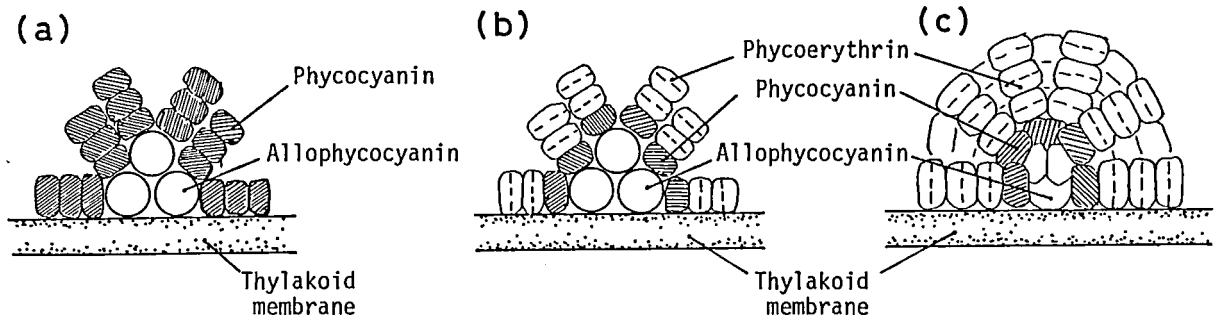

Figure 1. Schematic representation of three types of phycobilisomes: (a) PE-less and (b) PE-rich hemidiscoidal phycobilisomes (PBS) in red-grown and green-grown *Flemyella diplosiphon*, respectively, (c) a PE-rich hemispherical PBS in *Porphyridium cruentum*.

VII-F-2 Primary Photoprocess of 124 kDalton Phytochrome

P.-S. SONG (*Texas Tech Univ.*), **Naoto TAMAI and Iwao YAMAZAKI**

To characterize the nature of primary photoprocesses of phytochrome which serves as the red-far red reversible photoreceptor for photomorphogenesis in plants, viscosity dependence of the fluorescence lifetimes of phytochrome isolated from etiolated oat seedling (*Avena sativa* L.) has been investigated. As is shown in Figure 1, the fluorescence decay of phytochrome exhibited approximately two components; one with lifetimes in the range of 50–70 ps and another with 1.1–1.2 ns in phosphate buffer with or without 40–67% glycerol. However, relative amplitudes of these decay components were found to be strongly viscosity dependent (Fig. 1). Thus, the longer decay component increased from 2–5% in phosphate buffer to about 20% in 67% glycerol-phosphate buffer. These results have been interpreted in terms of primary reaction from the excited singlet state of phytochrome, yielding a photoreversible intermediate whose rates of formation and decay were apparently viscosity-dependent. Further, the viscosity dependence is consistent with the primary reaction involving conformational changes of the chromophore and its apoprotein environment.

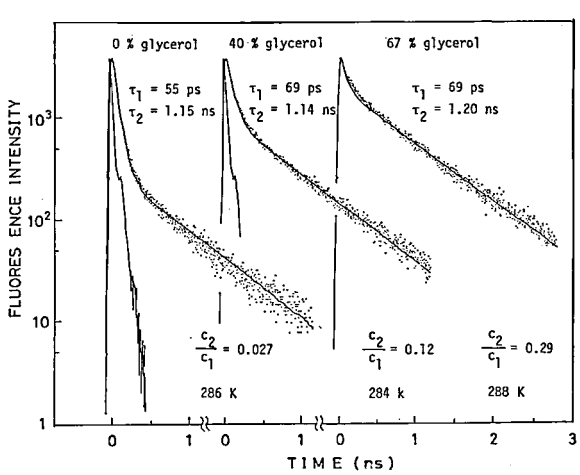

Figure 1. Fluorescence decay curves (.....) and best-fit curves (——) calculated by convolution with the instrumental response function for phytochrome (Pr) in glycerol-buffer mixture at ca. 288 K. Concentrations: (a) 1.8 M; (b) 1.2 M, (c) 0.7 M. Excitation pulse wavelength, 636 nm, and emission wavelength monitored, 680 nm.

VII—G Electron Transfer in Hydrogenase and Cytochrome c_3

Hydrogenase is an enzyme for hydrogen cleaverage reaction and cytochrome c_3 having four hemes in a single polypeptide chain is a native electron carrier in this reaction. The active center and the mechanism of the reaction for these molecules have been studied by magnetic and electrical measurements.

VII-G-1 Magnetic Susceptibility of Hydrogenase

Keisaku KIMURA, Hiroo INOKUCHI, Hitoko NANAMI (*Shizuoka Univ.*), **and Tatsuhiko YAGI** (*Shizuoka Univ.*) (*J. Biochem.* 97, *1831* (*1985*))

Magnetization and magnetic susceptibility measurements revealed that the hydrogenase from *Desulfovibrio vulgaris* Miyazaki, strain F, has an independent unpaired electron in its iron-sulfur cluster. Figure 1 shows the saturation of the magnetization plotted against the temperature-normalized field strength, H/T, where H stands for the magnetic field strength, and T, temperature. As shown, the plots for saturation coincided with the theoretical curve given by the Brillouin function for $S = 1/2$. The paramagnetic center of the *Desulfovibrio* hydrogenase was found to be different from that in the *Chromatium* hydrogenase which interacts with another paramagnetic center, probably nickel.

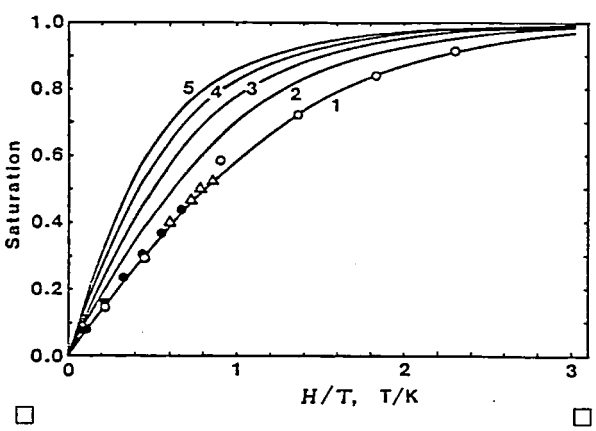

Figure 1. Plot of magnetization of hydrogenase vs temperature-normalized field strength, H/T.
Theoretical curves are given by the Brillouin function for S = 1/2 (curve 1), S = 1 (curve 2), S = 3/2 (curve 3), S = 2 (curve 4), and S = 5/2 (curve 5). The saturation value was normalized to 1.0. Plots with open circles: at 2.2 K with the magnetic field between 0.5 T and 5.0 T, solid circles: at 4.4 K with the magnetic field between 0.5 T and 3.0 T, and triangles: between 2.2 K and 4.4 K with the constant magnetic field of 1.98 T.

VII-G-2 AC Electrical Conductivity of Anhydrous Cytochrome c_3 Film

Yusuke NAKAHARA (*Miyakonojo Nat. Col. Tech.*), **Keisaku KIMURA, Tatsuhiko YAGI** (*Shizuoka Univ.*), **and Hiroo INOKUCHI**

The ac conductivity of anhydrous ferrocytochrome c_3 film was measured as functions of frequency (500 Hz – 13 MHz) and temperature (250 – 300 K) under a hydrogen pressure of 290 kPa. The admittance, Y, was given by

$$Y = G_{dc1} + G_{dc2} + G_{ac} + j\omega(C_{ac} + C_{\infty})$$

where G_{dc1} and G_{dc2} correspond to two semiconduction dc components with different activation energy and G_{ac} and C_{ac} are ac components of admittance. The temperature dependence of conductance is shown in Figure 1. The dc contribution was obtained

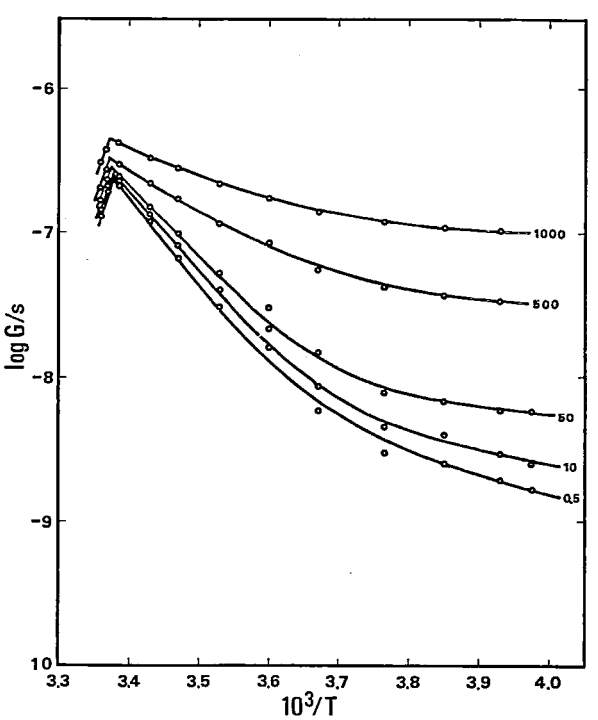

Figure 1. The temperature dependence of the conductance. The figures on the right side of the curves present a frequency. The maximum conductance was observed at 296 K.

by extraporating ω to be 0. The activation energy of G_{ac}, 0.2 eV, was in agreement with that of G_{dc2}. G_{ac} is suggested to be owing to the carrier hopping among several sites with the potential barrier of 0.2 eV.

VII—H The Study of Metal Fine Paricles by Means of Gas Evaporation Technique

Fine particles whose sizes are less than ten nm, are characterized by the quantum size effect, surface effect on the bulk properties and also a fluctuation of a thermodynamical properties by its low dimensionality. These effects were studied as functions of metal species and organic solvents.

VII-H-1 Size Effect in CESR of Mg and Ca Small Particles

Sanshiro SAKO (*Mie Univ.*), **and Keisaku KIMURA** (*Surf. Sci.*, **156**, *511* (*1985*))

The conduction electron spin resonance (CESR) of Mg and Ca particles was measured. An anomalous narrow line was found in the CESR of Mg small particles, overapping with the normal bulk-like broad line. This anomalous line was originated from the smallness of the particles. In Ca sample, only an anomalous line was detected as shown in Figure 1. Several characteristics were withdrawn as: 1) The line results from the smallness of the particles, 2) The linewidth is approximately proportional to the frequency, 3) The linewidth becomes narrow when the size becomes small, 4) The intensity of the line shows a low temperature increase. 5) The line appears in lower field than the bulk line. This line was explained by the quantum size effect.

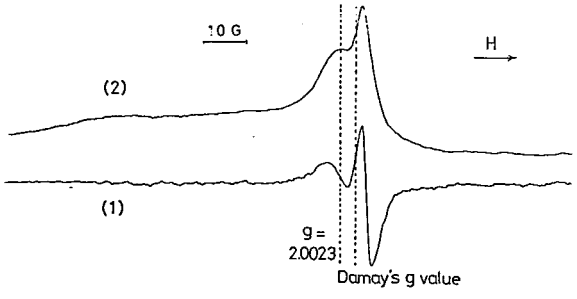

Figure 1. CESR spectra of Ca small particles (average size 88 nm) at X band, room temperature. (2) is the integral of (1).

Reference
1) P. Damay, T. David and M.J. Sienko, *J. Chem. Phys.*, **61**, 4369 (1974).

VII-H-2 Dispersibility and Electron Spin Resonance in the Colloidal System of Metal/Organic Solvent Prepared by Means of Gas Evaporation Technique.

Shunji BANDOW and Keisaku KIMURA (*Nippon Kagaku Kaishi, 1360* (*1985*))

A highly pure colloidal system, composed of metal ultrafine particles and an organic solvent, was produced by means of modified gas evaporation method. This sytem is free from colloidal stabilizers and is good for the study of the interface of a simple colloidal system. The surface state of metal ultrafine particles dispersed in organic solvents and the dispersibility of the colloids thus prepared were examined as a function of kinds of metal species and solvents. A strong correlation between the state of the colloids and a dipole moment of a solvent was found. In a solvent with a large dipole moment, many metal particles were well dispersed. On the other hand, none of metal particles was dispersed in the solvent with a small dipole moment, resulting in coagulation. This was discussed in connection with the formation of the electric double layer on the surface of metal fine particles. Detailed studies of the dependence of particle dispersibility on the dipole moment of the solvent were made in lead colloidal systems.

Electron spin resonance (ESR) was detected in the colloidal system of zinc particles in hexane (Zn/hexane) at 3 K. The Lorentzian ESR signal was observed at g = 1.97. This line was reasonably attributed to the Zn^+ ion localized in the surface layer of Zn ultrafine particles but not to the conduction electrons of Zn metal. The ESR signal was affected by the introduction of oxygen gas and it depended both on the type of solvent and on a state of colloid:

In the Zn/hexane system, ESR signal disappeared after the introduction of oxygen, but not in Zn/1-butanol system, indicating that the magnitude of the dipole moment of the solvents, hexane (0.085D) and l-butanol (1.50D), also affects ESR activity.

VII-H-3 Construction of the Preparation Chamber for Ultrafine Particles under Ultra-high Vacuum

Keisaku KIMURA

A surface effect is enhanced in the ultrafine particles, especially in divalent metals in which the surface of metal particles is easily oxidized and reacts with solvents under the normal vacuum. Therefore, a high vacuum chamber aiming the working pressure of 10^{-8} Torr, has been constructed in the Equipment Development Center. This chamber is equipped with a quadruple mass spectrometer, film thickness guage, and with an inlet-outlet of organic solvent, and is connected to the 150 l turbo molecular pump system which guarantees the vacuum of nano Torr. Both the preparation of ultrafine particles and the formation of metal/organic colloids are conducted in this chamber giving in situ surface modification of the particles.

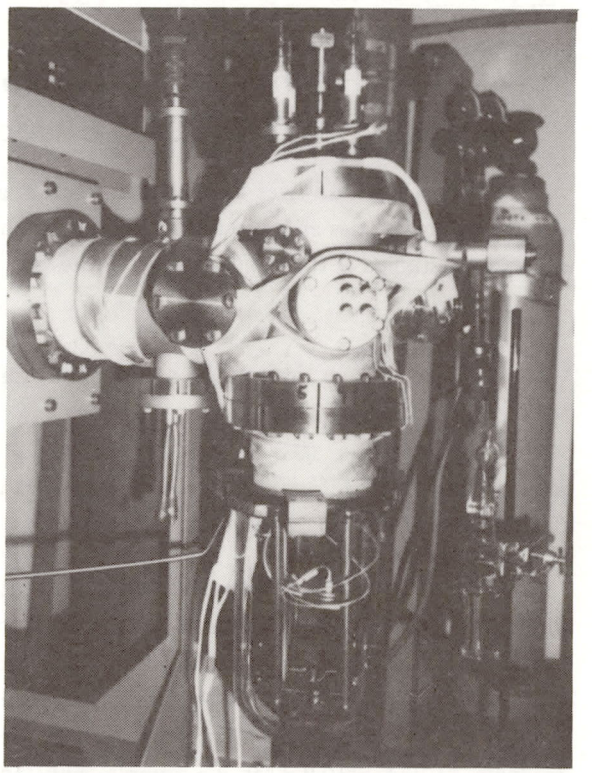

Figure 1. The preparation chamber for ultrafine particles connected to the turbo molecular pump.

VII—I Development of Experimental Devices and Techniques

The Instrument Center is equipped with various types of instruments for molecular spectroscopy, solid-state chemistry and magnetic spectroscopy.[1] All of them are opened widely for researchers in universities and institutions as well as staffs in IMS. In view of efficient use of these instruments, the Center staffs are concerned with development of new experimental devices and techniques.

Reference
1) List of Instruments, No. 5, IMS Instrument Center (1985)

VII-I-1 Application of the Time-Correlated, Single-Photon Counting Technique to the UVSOR Vacuum-UV Spectrophotometer

Takaya YAMANAKA, Mitsukazu SUZUI, Toshio HORIGOME, Tadaoki MITANI and Iwao YAMAZAKI

A time-correlated, single-photon counting system has been constructed as an emission detection system for a vacuum-UV spectrophotometer in UVSOR. Figure 1 shows a schematic diagram of the instrument. The pulsed light from the UVSOR beam line (repetition rate 90 MHz; pulse width (fwhm) 0.5 ns) is dispersed with a Seya-Namioka type monochromator.[1] The luminescence from the sample is detected by a microchannel-plate photomultiplier with a MgF_2 window (Hamamatsu R1564U). The output pulses are fed into the time-to-amplitude converter to obtain fluorescence decay curves on a multichannel pulse-height analyzer and a 8K-words multichannel scaler

which are controlled by a microcomputer system.[2] Time-resolved luminescence measurements, i.e , decay curves and time-resolved spectra, can be made in wavelengths ranging from vacuum-UV to visible region.

Reference

1) T. Horigome, K. Hayakawa, M. Suzui, N. Okada, H. Toshida, N. Mizutani, S. Kato, M. Nagata, K. Sakai and T. Mitani, *Ann. Rev. IMS*, 1984, p.140.
2) Y. Shindo, *Bull. Res. Inst. Appl. Elec., Hokkaido Univ.*, No. 3, 1 (1984).

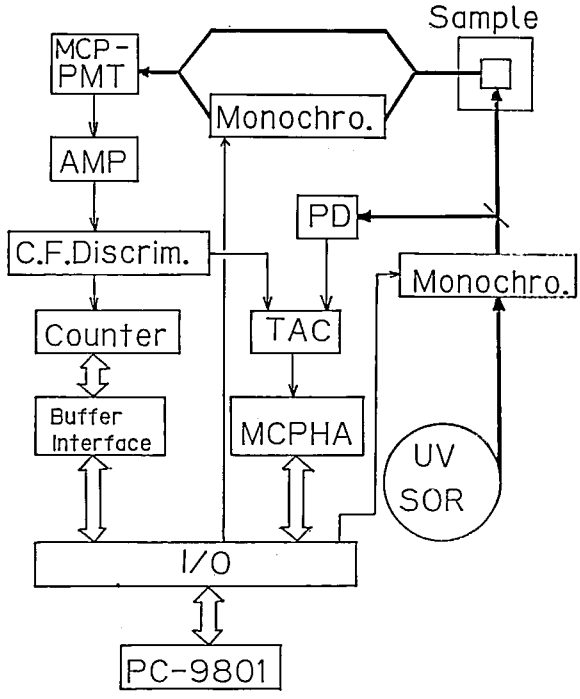

Figure 1. Schematic diagram of the time-correlated, single-photon counting apparatus designed for the UVSOR vacuum-UV spectrophotomter. PD, photodiode; TAC, time-to-amplitude converter; MCPHA, multichannel pulse-height analyzer; MCP-PMT, microchannel-plate photomultiplier.

LOW TEMPERATURE CENTER

VII—J Development of a Dynamic Seal

VII-J Development of a Dynamic Seal

Kiyonori KATO and Keiichi HAYASAKA

A Wilson seal and a silicon tube are widely used for the connection between a liquid helium container and a transfer tube. The tightness, however, is not sufficient on moving the transfer tube.

We have developed a "dynamic seal", which is tightly sealed when we insert a transfer tube into a container. The principle of the dynamic seal is as follows: When the container is pressurized, the internal pressure P working against the O-ring is balanced by the counter forces arising at the O-ring, so that the seal is sealed tightly without any leakage shown in Figure 1-a. On moving a transfer tube slowly, a frictional force F works in addition to the internal pressure P. On evacuating a helium container, the situation is similar to that for a pressurized container, because of the symmetrical structure of the seal.

The dynamic seal is also available for a supporting rod of a sample which position is changed in a cryostat. Figure 1-b shows the application of the dynamic seal for the connection between a transfer tube and a liquid helium container. No leak was detected between 760 mmHg and 0.5 kg/cm^{2}G on moving the transfer tube.

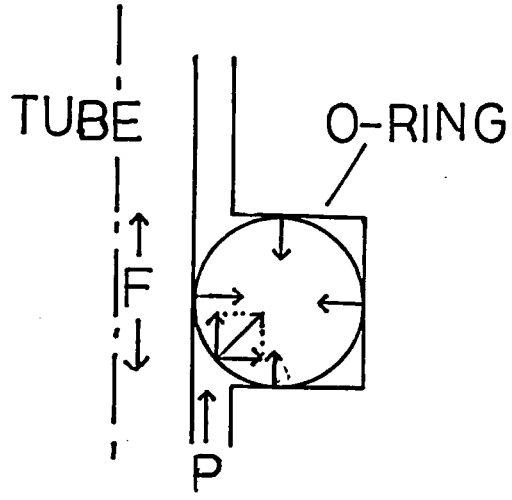

FIGURE 1-a

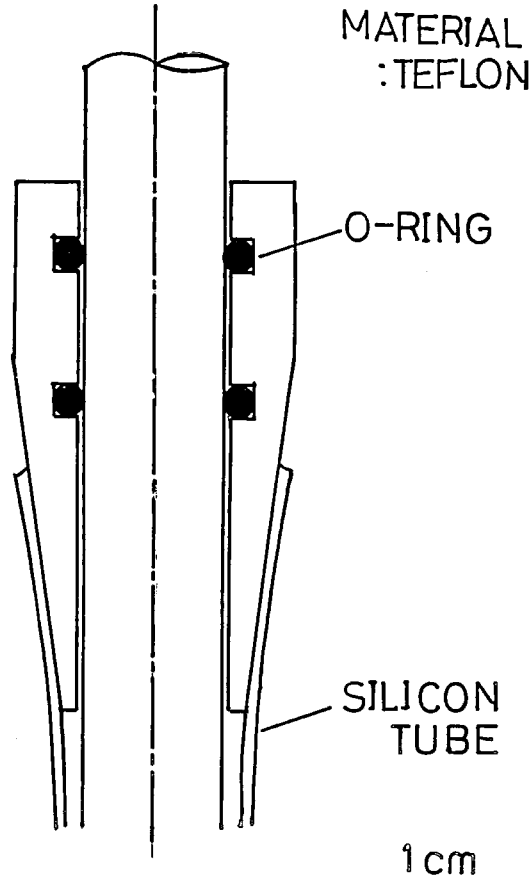

FIGURE 1-b

VII—K Hydrogen Absorption in Graphite Intercalation Compounds

Graphite-alkali metal intercalation compounds absorb hydrogen chemisorptively, leading to the occlusion of hydrogen in intercalate layers. The introduction of hydrogen gives effects on the electronic and the lattice vibrational properties of the compounds due to the large electron affinity of hydrogen and the occupation of the sites by hydrogen species in the intercalate layers.

We investigate the properties of the hydrogen-absorbed graphite intercalation compounds by means of specific heat and superconductivity measurements. (See also IV-D).

VII-K-1 Enhanced Superconductivity in Hydrogenated Potassium-Mercury-Graphite Intercalation Compounds

Gerhard ROTH(MIT), Alison CHAIKEN(MIT), Toshiaki ENOKI, Nai Chang YEH(MIT), Gene DRESSELHAUS(MIT) and P. M. Tedrow(MIT).
Toshiaki ENOKI, Mizuka SANO (*Kumamoto*

Stage-1 potassium-mercury graphite intercalation compounds with markedly different superconducting transition temperatures T_c and transition widths ΔT_c are found to have uniformly high T_c and narrow transitions after exposure to hydrogen, as shown in Fig. 1. These hydrogen-doping experiments suggest a schematic model for the density of states in stage-1

potassium-mercury-graphite intercalation compounds.
[*Phys. Rev.* **B32**, 533 (1985)]

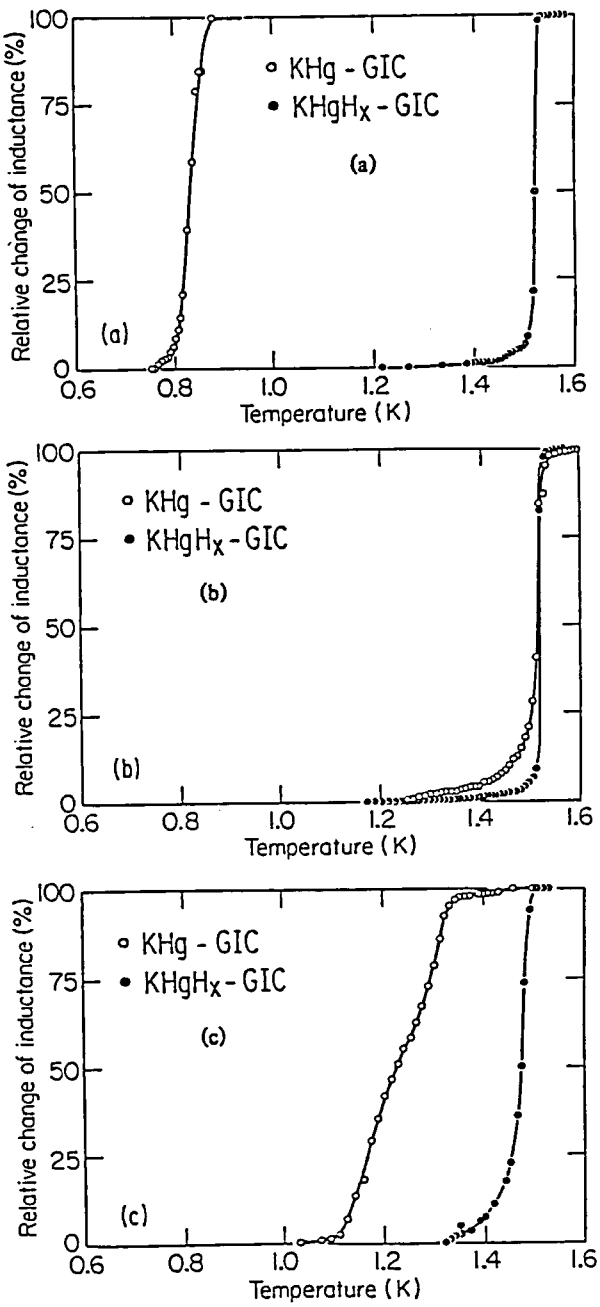

Figure 1. Effect of hydrogen doping on the superconducting transitions of three types of stage-1 KHg-GIC's. (1) T_c increases from 0.85 to 1.51 K, and ΔT_c decreases from 0.035 to 0.011 K. (b) T_c remains constant at 1.53 K, and ΔT_c decreases the same amount as in (a). (c) Tc increases from 1.32 to 1.49 K, and ΔT_c decreases from 0.25 to 0.03 K.

VII-K-2 Low-Temperature Specific Heat of Hydrogen-Chemisorbed Graphite-Alkali Metal Intercalation Compounds

Toshiaki ENOKI, Mizuka SANO (*Kumamoto Univ.*) and Hiroo INOKUCHI

The results of low-temperature specific-heat measurements are presented for hydrogen-chemisorbed C_8M(M=K, Rb), to clarify the effects of dissolved hydrogen on its electronic and lattice vibrational properties. As shown in Fig. 1, the density of states at the Fermi level $N(E_F)$ is suppressed through a charge transfer from C_8M to hydrogen which is stabilized in interstitial sites in the intercalate layers. This finding is consistent with the results of ESR and position-annihilation measurements. The introduction of hydrogen increases the acoustic and optic phonon energies for C_8KH_x ($x<0.1$). The electronic effects of dissolved hydrogen are considered to be the cause of the increase. At the hydrogen-saturated concentration ($C_8KH_{2/3}$), the phonon energies are lowered by an increase in the effective mass of the intercalants due to the strong ionic coupling between K and H through bondings with hydrogen. In the case of the C_8Rb system, the acoustic-phonon energies increase while the optic phonon ones decrease through the introduction of small concentrations of hydrogen ($x<0.1$). The effects of dissolved hydrogen on the superconductivity of C_8KH_x are discussed using the specific-heat results.

[*Phys. Rev.* B32, 2497 (1985).]

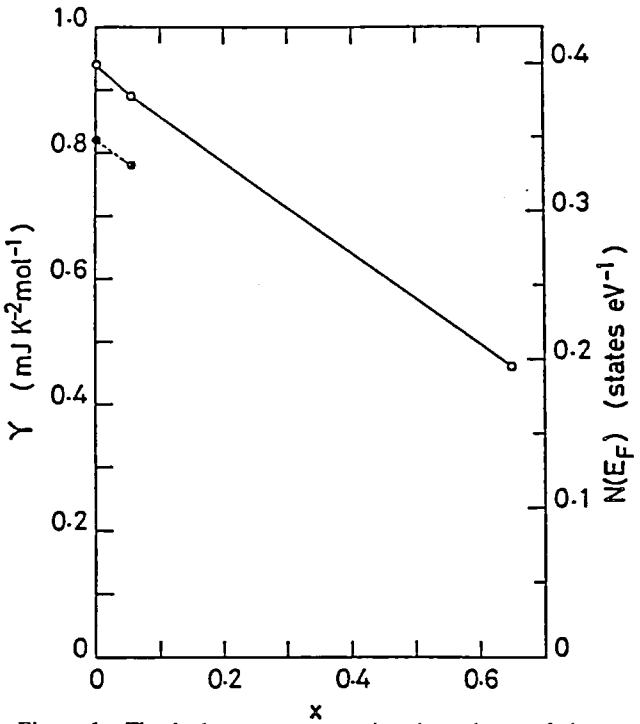

Figure 1. The hydrogen concentration dependence of the electronic specific heat parameter γ and N (E_F) for C_8KH_X and C_8RbH_X. Open circles denote the results of C_8KH_X and solid circles C_8RbH_X. Solid and dashed lines are guides for the eye.

EQUIPMENT DEVELOPMENT CENTER

VII—L Studies of Quasi-One-Dimensional Materials

VII-L-1 The Phase Diagram of the Neutral-Ionic Phase Transition of the Mixed-Stacked Charge Transfer Complex TTF-p-Chloranil

Tadaoki MITANI, Yoshio KANEKO,* Yoshinori TOKURA,* Gunji SAITO* and Takao KODA* (*Univ. of Tokyo*)

The neutral-to-ionic (NI) phase transition observed in tetrathiafulvalene-p-chloranil charge-transfer complex has been investigated by the DC conductivity measurements as a function of temperatures and hydrostatic pressures. In a neutral phase, a remarkable increase of the conductivity was observed by applying pressure. This is attributable to a creation of charged domain-walls due to collective excitations of ionic molecules in the neutral lattice. While, the ionic phase, being accompanied with dimerization of donor and acceptor pairs, was found to be fairly stable against applied pressure. These peculiar features of the conductivities provided the phase diagram of the NI transition, in which the discontinuous NI transition previously observed at an atmospheric pressure changes[1] into a continuous transition at a critical pressure, P_c = 220 Mpa.

Reference

1) T. Mitani, G. Saito, Y. Tokura and T. Koda, *Phys. Rev. Lett.*, 53, 842 (1984).

VII-L-2 Charge Transfer Exciton in Halogen-Bridged Mixed-Valent Pt and Pd Complexes: Analysis Based on the Peierls-Hubbard Model

Yoshiki WADA, Tadaoki MITANI and Masahiro YAMASHITA (*Kyushu Univ.*)

[*J. Phys. Soc. Jpn.* **54**, 3143 (1985)]

Polarized reflection and luminescence have been measured for the single crystals of $[MA_2]$ $[MX_2A_2]$ $(ClO_4)_4$ (M=Pt, Pd, X=Cl, Br, I and A=ethylenediamine, cyclohexanediamine). The strong absorption bands due to the charge-transfer (CT) exciton transition between the mixed-valent metal ion have been investigated in detail in the visible or infrared energy region. The dependence of the CT excitation energies on the species M and X is shown to be consistent with the prediction by the Peierls-Hubbard model which incorporates the effect of the electron-electron correlation on inter-metal sites. The oscillator strength of the CT excitons are observed to be enhanced by substituting heavier halogen ions. This enhancement is interpreted by a halogen-linked super-transfer mechanism. The unusually large values of the oscillator strength can be qualitatively explained in terms of the trimer CT model.

VII-L-3 New Quasi-One-dimensional Materials: Halogen-Bridged Binuclear Platinum Mixed Valent Complexes, $K_4[Pt_2A_4X_2]$ (X=Cl, Br and I, A=$(HO_2P)_2O$, CH_3CS_2)

Tadaoki MITANI, Yoshiki WADA and Masahiro YAMASHITA (*Kyushu Univ.*)

Reflectivity, luminescence, magmetic susceptibility and electric conductivity measurements have been made on the linear-chain halogen-bridged binuclear platinum mixed valent complexes, $K_4[Pt_2A_4X]$ (X=Cl, Br and I, A=$(HO_2P)_2O$, CH_3CS_2). The temperature dependences of their electric conductivity show semiconducting behaviours, indicating existence of a finite energy gap in their half filled conduction bands. Their magnitudes are in order of Cl>Br>I for X in consistent with those obtained from the optical spectra. The results of magnetic susceptibility measurements indicate that they are diamagnetic from R.T. down to 4 K. In addition to these experimental results, the observation of a broad luminescence band in $K_4[Pt_2P((HO_2P)_2O)_4Cl]$ single crystals with the large Stokes shift suggests that the origin of the gap is due to the existence of the charge density wave in the quasi-one dimensional crystals.

VII-L-4 Spectroscopic Study of the Neutral-to-Ionic Phase Transition in TTF-Chloranil

Yoshinori TOKURA,* Yoshiki KANEKO,* Hiroshi OKAMOTO,* Seiji TANUMA,* Takao KODA,* Tadaoki MITANI and Gunji SAITO* (**Univ. of Tokyo*)

[*Mol. Cryst. Liq. Cryst.*, **125**, 71 (1985)]

Infrared reflectance spectra have been investigated on TTF-chloranil single crystals near the neutral-to-ionic phase transition temperature T_c. It was confirmed that abrupt changes in the ionisity and the stack dimerization take place simultaneously at T_c. The effect of an external electric field and light irradiation upon the dimerized lattice below T_c has been investigated by reflectance measurements.

VII-L-5 X-Ray Photoelectron Spectra and Electrical Conductivities of One-Dimensional Halogen-Bridged Pd(II)–Pt(IV) and Ni(II)–Pt(IV) Mixed-Valence Complexes

Masahiro YAMASHITA,* Ichiro MURASE (**Kyushu Univ.*), **Tasuku ITO, Yoshiki WADA, Tadaoki MITANI and Isao IKEMOTO** (*Tokyo Metropolitan Univ.*)

[*Bull. Chem. Soc. Jpn.*, **58**, 2336 (1985)]

X-ray photoelectron spectra have been measured for the one-dimensional halogen-bridged metal-alternated mixed-valence complexes, $[M(en)_2]$ $[PtX_2(en)_2]$ $(ClO_4)_4$ (M=Pd or Ni, X=Cl, Br and I). Comparing the binding energies of the Pt(IV)4f levels in these hetero-metal complexes with those previously reported for the homo-metal halogen bridged Pt(II)–Pt(IV) mixed-valence complexes, the reductive trend of the oxidation of Pt(IV) is found to be significantly

suppressed by the metal alternation. In accord this results, the magnitudes of the activation energy obtained from the electrical conductivities are in order of Pd(II)–Pt(IV)>Ni(II)–Pt(IV)>Pt(II)–Pt(IV), suggesting that the electron-electron repulsive energy on M(II) ions plays an important role on the mixed-valent states.

VII—M Study of Optical Pumping in Solids and Liquids

VII-M-1 Optical Spin Orientation in Ruby by Zeeman-Selective U-Band Absorption

Yoshihiro TAKAGI, Yukio FUKUDA,* and Tsuneo HASHI* (**Kyoto Univ.*)

[*Opt. Commun.*, **55**, 115 (1985)]

Optically induced magnetization (OIM) in ruby at room temperature has been observed by excitation of the U-absorption band. Optically induced Zeeman Coherence associated with different pairs of Zeeman sublevels has been also observed as free induction decay signals. Zeeman-selectivity in the U-band transition is derived by assuming a spin-orbit coupling which provides a small fraction of the intensity of the U-band. Calculation of the relative transition probability yields different Zeeman population distributions depending on the types of irreducible representations used for the spin-orbit coupling. Observations of OIM due to excitation of the Y-band and OIM in KCr-alum were made and differences in the sign of the OIM were discussed group-theoretically.

VII-M-2 Excitation Spectra of Optical Spin Orientation in Ruby and KCr Alum

Yoshihiro TAKAGI

Excitation spectra of optical spin orientation (OSO) in ruby and KCr alum have been observed in the visible spectral region at room temperature and 77K. Ruby has a variety of d-d absorption lines and bands corresponding to spin-forbidden and spin-allowed transitions, respectively. Observation of OSO due to absorption of circularly polarized light has revealed a dependence of the sign of OSO on the absorption lines or bands as shown in Figure 1. The sharp lines (spin-forbidden) with the intensities comparable to or rather higher than that for the broad bands (spin-allowed) suggest that OSO is given in such a way that the spin-orbit coupling, which shares the angular momentum into orbital and spin systems, gives the intensity preferebly rather than the spin-independent odd-parity crystalline field does. According to this model, relative transition probabilities between Zeeman sublevels of the ground and excited states were calculated. In the calculation the spin-orbit coupling was represented by a sum of ungerade irreducible representations generated from a product of the irreducible representations of the spin-orbit coupling (T_{1g}) and the odd-parity crystalline field (T_{1u}). The result agreed well with the observed spectral dependence of OSO. The detail will be reported elsewhere.

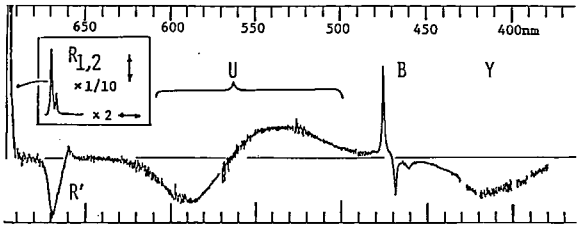

Figure 1. Excitation spectrum of OSO in ruby at room temperature. The OSO was observed as an optically induced magnetization detected with a pickup coil using an excimer laser-pumped dye laser (twelve dye solutions were separately used).

VII-M-3 Direct Measurement of Optical Spin Orientation in the Excited Triplet State of Aromatic Hydrocarbons at Room Temperature

Yoshihiro TAKAGI

[*Chem. Phys. Lett.*, **119**, 5 (1985)]

Optically induced magnetization has been observed in polycrystals and solutions of various aro-

matic carbonyls, quinons, and aza-aromatics at room temperature using a simple pickup coil detector. The magnetic-field dependence of the magnitude of the induced magnetization provided clear evidence of the creation of a spin polarization in the photo-excited triplet state. The sign of the magnetization coincides with the sign of the zero-field splitting parameter, D. The origin of the spin polarization is a spin-state selectivity in the intersystem crossing rate from the excited singlet state to the triplet state. The relaxation times of the magnetization varied from 1 to 100 ns depending on the materials and the strength of the external magnetic field. Use of a picosecond laser as the excitation source and the fast signal processing provided a high time-resolution.

VII—N Development of Experimental Devices

VII-N-1 Construction of a Vacuum-UV Spectrophotometer

Toshio HORIGOME, Kazuo HAYAKAWA, Mitsukazu SUZUI, Takaya YAMANAKA, Iwao YAMAZAKI and Tadaoki MITANI

A Seya-Namioka-type vacuum-UV monochromator was constructed by the members of the Equipment Development Center last year and installed in the UVSOR beam line for common use. A vacuum-UV spectrophotometer using this monochromator have been constructed in close collaboration with the staff of the Instrument Center. A time-correlated, single-photon counting system was employed as a detection method of the pulsed light from the UVSOR beam line (see VII-I-1). In Figure 1, we show a typical example of output signals measured by this spectrophotometer; (A) a fluorescence decay curve of anthracene single crystals at liq. N_2 temperature, excited by the synchrotron radiation at 1500 Å, (B) a pulse shape of the synchrotron radiation. We confirmed that this apparatus is a powerful tool to investigate energy transfer mechanisms in organic crystals in a wide energy region from 2 eV to 40 eV.

VII-N-2 Construction of a High Pressure ESR Spectrometer Using a Helix Resonator

Hisashi YOSHIOKA,* Shunsuke KAZAMA* (*Shizuoka College of Parmacy), Toshio HORIGOME and Tadaoki MITANI

[*Ana. Chem.* 57, No. 12 (1985)]

High pressure ESR spectrometer was constructed. A Helix was used as the resonator in place of the conventional cavity. The various maching systems between the herix resonator and the coaxial line were investigated in order to obtain the spectra of high signal-to-noise ratio. For the first application of the apparatus, the spectra of a spin label in lipid bilayer were measured under the pressure up to about three thousands atoms.

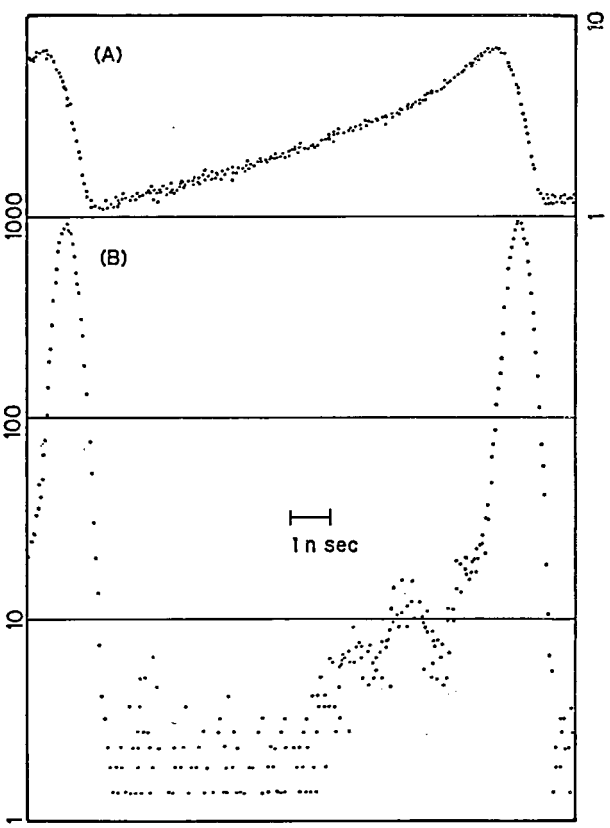

Figure 1. A typical example of output signals from a vacuum-UV spectrophotometer (see text).

VII-N-3 CAMAC Crate Controller with DMA Mode

Hisashi YOSHIDA, Kazuo HAYAKAWA, Yoshihiro TAKAGI and Tadaoki MITANI

The CAMAC interface has been combined with a personal comupter (NEC, PC-9801) for a standard data acquisition system in UVSOR facility. We have developed a crate controller consisting of 16 Command Registers and Data Registers as well as the basic control circuits. Data is bidirectionally transfered between CAMAC modules and the controller with these registers. All of the registers are controlled by i/o instructions in PC-9801. A schematic diagram is shown in Figure 1. A high data-transfer rate was obtained by using a DMA mode in the controller. A typical value of the dataway cycle is 2.5 microseconds, which is about 7 times higher than those in the usual program transfer modes In addition. many types of data transfer can be made in the DMA mode by preprogramming multi-functions.

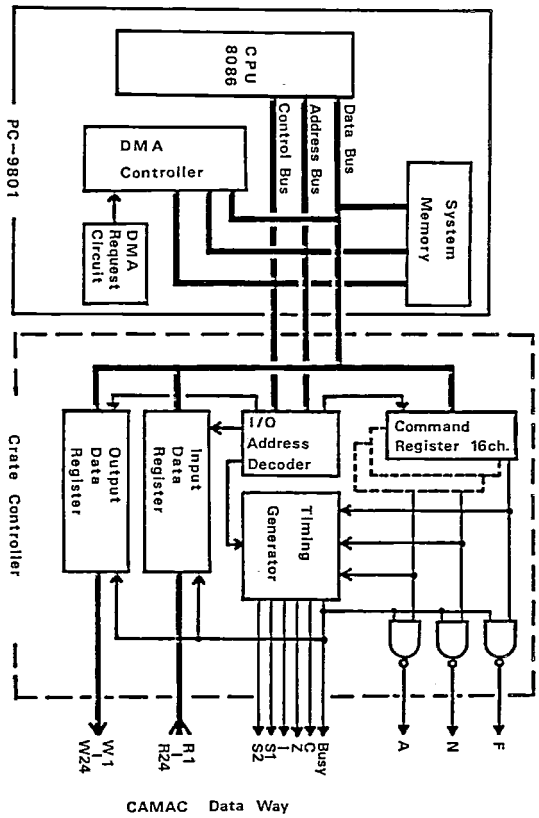

Figure 1. System diagram

ULTRAVIOLET SYNCHROTRON ORBITAL RADIATION FACILITY

VII—P Construction of UVSOR Light Source

VII-P-1 Ion-Trapping Effect in UVSOR Storage Ring

Toshio KASUGA, Hiroto YONEHARA, Toshio KINOSHITA and Masami HASUMOTO

[*J.J.A.P.*, 24, 1212 (1985)]

UVSOR is an electron-storage ring dedicated to vacuum ultraviolet synchrotron radiation research. The first beam was stored in the ring in November 1983, and from that time on, efforts have been devoted to improving the performance of the ring. Some inconvenient phenomena have been found during the accelerator studies. One of the most serious problems is the growth of the vertical size of the electron beam. This phenomenon is explained by the ion-trapping effect, in which the ions trapped in the electron beam change the operating point of the storage ring and enhance the coupling between horizontal and vertical oscillations, resulting in a considerable increase in the vertical beam size. This ion-trapping was successfully cured by the RF knockout method, which excited the betatron oscillation.

VII—Q Construction of Measurement Systems for UVSOR

At the end of August 1985, eight beam lines are working and six beam lines are under construction. The list of monochromators is given in Table I in "Ultraviolet Synchrotron Orbital Radiation Facility" and several measurement systems are described in IV-L-1, IV-O-1, VII-I-1 and VII-M-1 in this issue.

VII-Q-1 Performance of Plane-Grating Monochromators for 2 eV $< h\nu <$ 150 eV.

Kazuhiko SEKI (*Dept. of Molecular Assemblies*), **Hideyuki NAKAGAWA** (*Fukui Univ. and IMS*), **Kazutoshi FUKUI** (*Fukui Univ.*), **Eiji ISHIGURO** (*Osaka City Univ.*), **Riso KATO** (*Kyoto Univ.*), **Takehiko MORI** (*Dept. of Molecular Assemblies*), **Kusuo SAKAI and Makoto WATANABE**

[*Nucl. Instrum. Methods Phys. Res.*, in press]

Two plane-grating monochromators were constructed. Their design was reported previously.[1] Each has two plane gratings and five mirrors for focusing the diffracted light onto the exit slit, which are interchangeable in the vacuum according to the used wavelength region. One of the monochromators was installed at the beamline BL6A2 for optical studies of solids at low temperature, and the other at BL8B2 for angle-resolved UV photoelectorn spectroscopy of solids. The observed intensity distribution of the output at a slit width of 500 μm is shown in Figure 1. The unit of the ordinate can be normalized for an absolute value of 2×10^{11} photons/s at a ring current of 27 mA, by measuring the photoemission from an Al-foil and using a reported value of photoemission yield.[2] The resolution at a slit width of 300 μm was found to be 0.015 – 0.3 eV in the wavelength region from 230 to 13.5 nm, and the spot size of the zeroth-order visible light at the sample position is $\leq 1 \times 1$ mm^2, as designed.

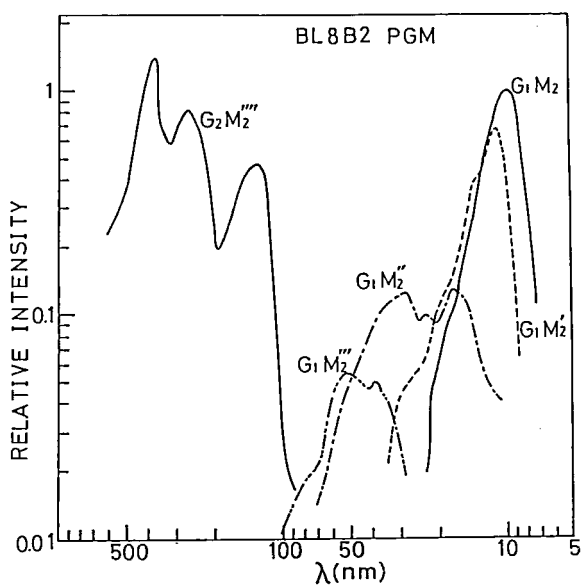

Figure 1. The relative intensity distribution of the output from the PGM monochromator at a slit width 500 μm measured using a photomultiplier with a sodium salicglate energy converter.

References

1) K. Seki, M. Watanabe, E. Ishiguro and R. Kato, *IMS Ann. Rev.* 118 (1982).
2) E. B. Solomon, *Nucl. Instrum. Methods* 172 79. (1980).

VII-Q-2 Performance of the Constant Offset Two Crystal Monochromator for BL7A

Takatoshi MURATA,* Tokuo MATSUKAWA, Masahiro MORI,** Masayoshi OBASHI,** Shunichi NAOE,*** Hikaru TERAUCHI,**** Yasuo NISHIHATA,**** Osamu MATSUDO, Jun-ichiro YAMAZAKI** (*Kyoto Univ. of Education,* Osaka Univ.,** Kanazawa Univ., *** Kwansei-Gakuin Univ.*****)

A performance test of the constant offset two crystal monochromator constructed last year, has been made with monochromating crystals of KAP, Mica, and Beryl whose 2d value is 26.64 Å, 19.80 Å and 15.98 Å respectively for x-ray emitted from UVSOR.

Mechanical movement of the monochromator was found to be very smooth, and the constant offset was successfully achieved.

Reflection intensity and resolving power of KAP diminished gradually due to radiation damage on the first crystal surface while both Mica and Beryl were found to be very stable to the radiation. However in the spectra with both these crystals several strong glitches mainly due to Na and Al were observed.

In Figure 1 is shown an example of near edge absorption spectrum of Na K-edge of NaCl at room temperature evaporated *in situ* on collodion film measured with KAP monochromating crystal. In this case the resolution is not enough due to radiation damage of the KAP crystal.

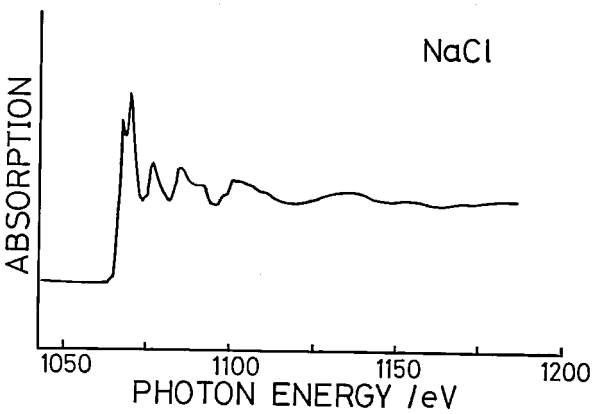

Figure 1. Near edge absorption spectrum of Na K-edge of NaCl at room temperature evaporated *in site* on collodion film.

VII-Q-3 Design of Rowland Circle Grazing Incidence Monochromator

Kusuo SAKAI, Eiji ISHIGURO (*Osaka City Univ.*), **Shichiro MITANI** (*Osaka City Univ.*) **and Makoto WATANABE**

A 2.2 m grazing incidence monochromator with a fixed entrance slit, a fixed grating and an exit slit moving on a Rowland circle, was designed for the wavelength region between 440 Å and 20 Å. After the exit slit, two mirrors are installed so that the direction of the monochromatized light is in horizontal plane and does not change with wavelength scanning. The beam size at the sample is 4(h) x 2(v) mm^2. The drawing of the monochromator is shown in Figure 1. This monochromator will be installed at BL8B1, which has three pre-mirrors. Horizontal acceptance angle of synchrotron radiation is 10 mrad.

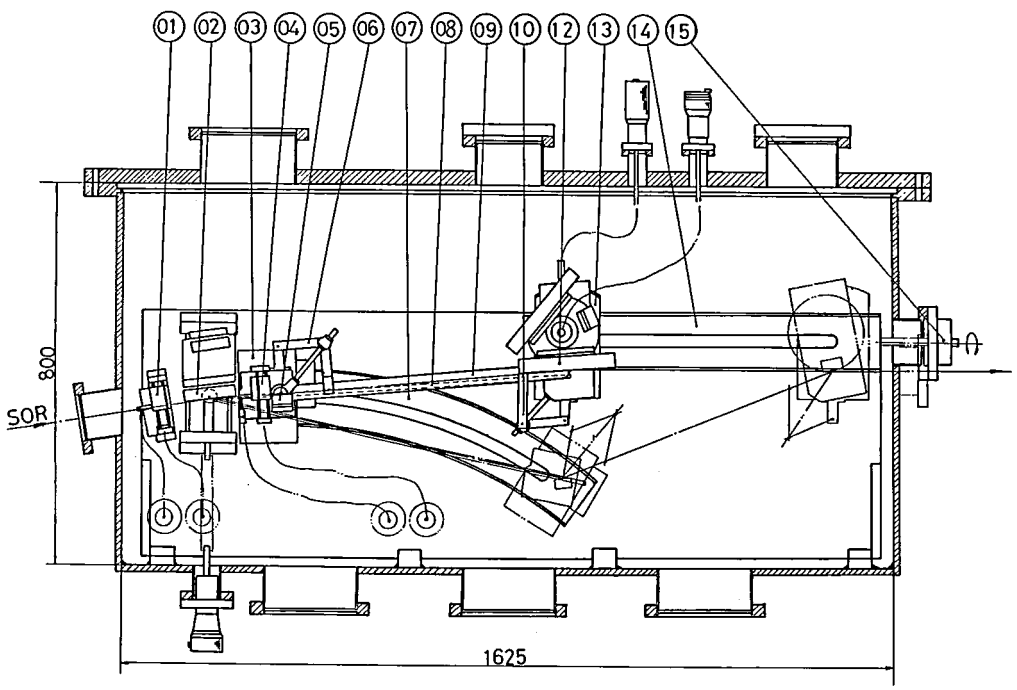

Figure 1. The 2.2 m Rowland circle grazing incidence monochromator. 01: entrance slit, 02: grating, 04: exit slit, 05 and 12: post-mirrors.

VII—R Researches by the Use of UVSOR

Researches of IMS staffs using UVSOR are reported in IV-G-1, IV-O-2, IV-O-3 and IV-O-4 in this issue. Details of researches made by outside users as well as IMS staffs will be reported in Activity Report of UVSOR (1984/1985).

RESEARCH FACILITIES

Fro the sake of brevity of the present issue are included only the newly installed facilities and the acitivities since September 1984. Concerning the activities and facilities before September 1984, please refer to IMS Annual Review (1978 ~ 1984).

Computer Center

The main facilities of the Computer Center are two HITAC M-200H computers, which have a processing capacity of over 10 million instructions per second. They have 32 mega byte main memory and 32 giga byte disk memory. The computers are used not only by the research staff at IMS but also by the staff at nearby National Institute as well as by scientists outside the Institutes in the related fields. As of March 1985, the number of project groups was 220 consisting of 604 users. In the twelve month period ending March 1985, 226727 jobs were processed with 8508 hours of the CPU time.

In December, 1985, the Computer Center will introduce a new computer system consisting of HITAC M-680H and S-810/10 computers produced by Hitachi. The former is a sequential processor which is about 4.5 times as fast as M-200H. The latter is a supercomputer whose maximum speed is about 80 times as fast as M-200H. The Computer Center will begin the service of the new system in January, 1986.

Chemical Materials Center

The Chemical Materials Center plays an important role in the synthesis and purification of chemical substances in IMS. The scientists and technical associates of this facility support other people in IMS to carry out the above works. They also carry out their own researches on synthesis of new interesting compounds, developments of new selective chemical transformations, elucidation of reaction mechanisms, and application of new methodologies developed in IMS to the analysis of chemical substances and reactions. Parts of the scientific activities are presented in the Section VI.

Instrument Center

For the efficient use of instruments, the Center is equipped with various types of instruments for general use.[1] Following instrument has been newly installed in 1985.

Automatic Four-Circle Single-Crystal Diffractometer (Rigaku AFC-5R)

This system consists of a high precision four-circle goniometer, a high power rotating anode X-ray generator (Rigaku RU-200), a minicomputer PANAFACOM U-1200II, and associated electronic measuring equipment. Rotating anode X-ray generator provides high intensity X-ray beam 7 – 10 times stronger than a sealed type X-ray tube. It reduces data collection time to a great extent and enables to use much smaller crystal specimen. A low temperature unit using a cold nitrogen gas stream allows investigations at constant temperatures between –170°C and +200°C over long periods of time.

Reference
1) *List of Instruments*, No. 5, IMS Instrument Center (1985)

Low Temperature Center

In October 1984, Mr. K. Kato moved to this center from the Cryogenic Center of the Univ. of Tokyo. The amount of liquid helium supplied in 1984 was about 12000 ℓ. A helium compressor with a capacity of 90 m^3/h and a helium gas reservoir with a volume of 480 m^3 have been equipped in May 1985 for increasing supply of liquid helium.

Equipment Development Center

A number of research instruments have been designed and constructed by making use of the mechanical, electric and glass-blowing technologies available at this Facility. Representative instruments developed during this fiscal year of 1984 are listed below.

- o In-situ cell for catalyst study by EXAFS spectroscopy. (II-E-1)
- o X-ray Raman spectrometer with variable scattering angle. (Special research project)
- o Ultraviolet photoelectron Spectrometer for reactive solids.
- o A Hinteregger-type discharge lamp.
- o A conventional ultraviolet photoelectron spectrometer for studying molecular crystals and polymers.
- o Cryostat for positron annihilation measurements.
- o Cryostat for NMR measurements.
- o Preparation chamber for Ultrafine particles. (VII-H-3)
- o AC magnetic susceptibility probe.
- o Construction of Metal Beam Source.
- o CAMAC Module (real time clock)
- o Interface for transient digitizer
- o Interface for photoelectron spectrometer
- o Microampere constant current source
- o High-speed pulse counter
- o Computer controlled photo-emission-spectrometer
- o Controller for Double Crystal Monocromator
- o Glass sublimation system
- o Pyrex cell with Pt electrode
- o Quartz cell

Ultraviolet Synchrotron Orbital Radiation Facility

Since August 1985, the UVSOR light source can be operated at the electron energy of 750 MeV. The maximum current attained so far is 330 mA. The lifetime at 100 mA is 2 hours. At present, eight beam lines are opened to users. The list of monochromators in operation and under construction is given in Table I. BL2A, BL2B2, BL3B and BL8B2 are mainly used by staffs of Department of Molecular Assemblies in IMS. The others are for users from universities and the UVSOR Facility is responsible for construction, maintainance and development of these beam lines. In the case of users outside IMS, 4 experiments were made in the fiscal year 1984 and more than 20 experiments will be performed in the fiscal year 1985.

Table I. Monochromators at UVSOR

Beam Line	Monochromator, Spectrometer	Wavelength Region	Acceptance Angle (mrad) Horiz.	Vert.	Experiment
BL1B*	1 m Seya-Namioka	2000-300 Å	60	6	Gas & Solid
BL2A	1 m Seya-Namioka	4000-300 Å	40	6	Gas
BL2B1*	2.2 m Rowland Circle Grazing Incidence	220-20 Å	10	2	Gas
BL2B2	1 m Seya-Namioka	2000-300 Å	20	6	Gas
BL3A1*	None (Filter, Mirror)		(U) 0.3	0.3	Gas & Solid
BL3A2*	2 m Constant Deviation Grazing Incidence	1000-100 Å	10	4	Gas & Solid
			(U) 0.3	0.3	
BL3B	3 m Normal Incidence	4000-300 Å	20	6	Gas
BL6A1*	Martin-Puplett	5 mm-50μm	80	60	Solid
BL6A2	Plane Grating	6500-80 Å	10	6	Solid
BL7A	Double Crystal	15-8 Å	2	0.3	Solid
		15-2 Å	(W) 1	0.15	
BL7B	1 m Seya-Namioka	6500-300 Å	40	8	Solid
BL8A	None		25	8	Irradiation, User's Instrum.
BL8B1*	2.2 m Rowland Circle Grazing Incidence	440-20 Å	10	2	Solid
BL8B2	Plane Grating	6500-80 Å	10	6	Solid

*: under construction. U: with an undulator. W: with a wiggler.

SPECIAL RESEARCH PROJECTS

IMS has special research projects supported by national funds. The following two projects based on the second five year plan (1980–1985) have just finished.

(1) The development and control of molecular functions.

(2) Energy transfer and energy conversion through molecular processes.

The third special research project started in the fiscal year 1982 is:

(3) Molecular science of primordial chemical evolution.

These projects are carried out with close collaboration between research divisions and facilities. Collaborators from outside also make important contributions. Research fellows join these projects. In this report, the results in 1984 are reviewed.

The following two special research projects have started in the fiscal year 1985 under another five year plan, and the results will be reported in near future.

(1) Development and evaluation of molecular synergistic systems and their application to chemical energy conversion.

(2) Fundamental research of molecular devices.

(1) The Development and Control of Molecular Functions.

Dynamical Molecular Structure and Control of Reactive Molecules

Eizi HIROTA,* Shuji SAITO, Chikashi YAMADA, Yasuki ENDO, Kentarou KAWAGUCHI, Tetsuo SUZUKI, Hideto KANAMORI, Tatsuya MINOWA, J. E. BUTLER (*NRL and IMS*), **and J. T. HOUGEN** (*NBS and IMS*)

The generation of transient species by excimer-laser photolysis of appropriate precursors has been successfully applied to more than 10 systems including $SO_2 \rightarrow SO\ (X^3\Sigma^-) + O\ (^3P)$, $CS_2 \rightarrow CS\ (X^1\Sigma^+) + S\ (^3P \text{ or } ^1D)$, and $NH_3 \rightarrow NH_2\ (\tilde{X}^2B_1 \text{ or } \tilde{A}^2A_1) + H\ (^2S)$, as mentioned in II-A-II and II-A-12.

To employ this technique for a wider range of transient molecules, a new spectroscopic system has been designed and constructed. It is essentially an infrared diode laser spectrometer with a supersonic jet nozzle, except that it is combined with multiple photon ionization (MPI) to improve the sensitivity. An excimer-laser-pumped pulsed dye laser has been installed to induce MPI. As a preliminary experiment a gas cell of simple design has been set up to observe MPI signals of NO, and it has been confirmed that these signals changed intensity when NO was pumped by the infrared diode laser beam simultaneously. The beam apparatus constructed has been tested by observing straight infrared absorption and also MPI signals of CH_3I.

Design, Construction and Analyses of High-Spin Organic Molecules and Molecular Assemblies

Hiizu IWAMURA,* Tadashi SUGAWARA, Akira IZUOKA, and Shigeru MURATA

High-spin polycarbenes $C_6H_5\ddot{C}[(m\text{-}C_6H_4)\ddot{C}]_{n-1}C_6H_5$ (1; n = 3, 4 and 6) have been found to have $S = n$ and the spin multiplicity of $2n + 1$ in the ground state. The magnetization of 1 (n = 4) at various temperatures and field strengths shows that the carbene may be regarded as superparamagnetic and that the intermolecular interaction in the fortuitously formed molecular aggregates is antiferromagnetic. In order to design the spin ordering in the molecular assemblies of high-spin organic molecules, the effect of the orientation of the two stacking benzene rings has been studied for the two overlapping molecules of 1 (n = 1). The pseudoortho and

pseudopara orientations were found to be effective for this purpose (V-A-2 and V-A-3). Therefore, if we are able to arrange the appropriate molecular stacking of 1 so that the intermolecular exchange interaction might become ferromagnetic, the polycarbene molecules could serve as a magnetic domain and exhibit ferromagnetism as a macroscopic property. Crystal structures of appropriately substituted diphenyldiazomethanes proved to be partly successful models. When irradiated at 10 K, polycrystalline samples of bis(*p*-octyloxyphenyl)-diazomethane showed the formation of high-spin species ($S > 4/2$) due to the ferromagnetic interaction between the corresponding carbene molecules generated in the crystal lattice (V-A-4 and V-A-5).

Molecular Design of Systems with Correlated Internal Rotation

Hiizu IWAMURA* and Noboru KOGA

Disrotatory coupling of the internal rotational degrees of freedom in double rotor molecules has been studied for bis(9-triptycyl) amines (Tp_2NH) and bis(9-triptycyl) ethers (Tp_2O). These molecules undergo rapid internal rotation in a strictly gear-meshed fashion, giving rise to new stereoisomerism in the derivatives in which one of the benzene rings on each Tp unit is labeled. The racemic and meso isomers which arise due to different phase relationship between the substituted benzene rings were separated by HPLC. The high energy barrier to the gear-slipping process was obtained as 39 kcal mol^{-1} for Tp_2NH carrying the 3, 3′-dichloro substituents by the isomerization study (V-B-1). The low energy barrier to the gear-meshing process was determined to be ca. 4.5 kcal mol^{-1} by analyzing the rise and decay rates of the exciplex fluorescence for a Tp_2O derivative carrying the naphthalene chromophore on one Tp unit and the *tert*-amino group on the other.

Synthesis of Highly Functional Transition Metal Complexes and Their Use in Catalytic Reactions

Hidemasa TAKAYA,* Kazushi MASHIMA, and Tetsuo OHTA

We have been investigating synthesis of various chiral transition metal complexes and their use in asymmetric organic reactions. We have prepared 2, 2′-bis(diphenylphosphino)-1,1′-binaphthyl (BINAP) and several new derivatives of BINAP. A variety of asymmetric catalytic reactions such as hydrogenation of olefinic substrates and carbonyl compounds have been investigated by use of these ligands.

We have also been studying the chemistry of metallacyclic compounds which are important as reaction intermediates in many transition-metal catalyzed reactions. We have prepared new titanoxycarbene complexes of group 6 and 7 metal carbonyls and revealed their interesting chemical properties. Parts of these results are presented in the Section VII-B and C.

Construction of an X-ray Raman Spectrometer with Variable Scattering Angle

Kazuyuki TOHJI, Nobuo MIZUTANI, Toshio HORIGOME and Yasuo UDAGAWA

Existence of inelastic Ramna scattering in the x-ray region has been known for over 20 years. Chemical information contained in the scattering, however, has not been fully utilized so far, because of the difficulty in obtaining spectra with good enough quality. In this project, a spectrometer for x-ray Raman spectroscopy shown in Figure 1 was constructed in order to get x-ray Raman spectra as well as its angle dependence. The main features of this spectrometer are the following;

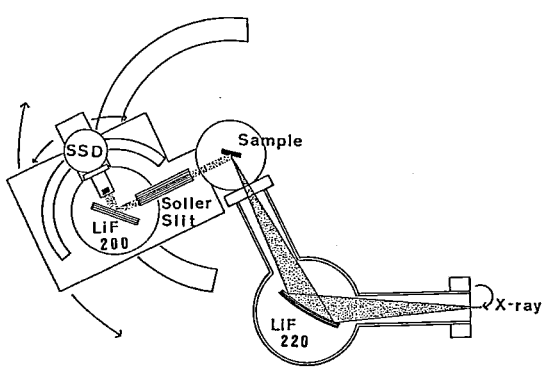

Figure 1. A schematic diagram of the x-ray Raman spectrometer.

1. a curved crystal monochromator to select a characteristic line from an anode to obtain a sharp, intense excitation.
2. variable scattering angle to obtain angle dependence of the seattering intensity.

Control of Molecular Function in Charge-Transfer Complexes

Tadaoki MITANI

If the Madelung energy are closely balanced with the site-energy difference of donor and acceptor molecules in mixed-stacked charge-transfer (CT) complexes, the neutral-to-ionic phase transition will take place and their physical properties is expected drastically to change near the phase transition. It was found that such a critical change in some CT complexes, such as TTF-p-chloranil, is not only due to a change of the degree of the ionisity but also due to changes in the electron-lattice and the electron spin system.[1] This is a starting point to investigate how to control functions of CT complexes in this project. Optical, electrical conductivity, photoconductivity and ESR of TTF-p-chloranil have been investigated as a function of hydrostatic pressure and temperature down to liq. helium temperature. It has been revealed that there exists a new phase under a relatively low pressure where neutral and ionic molecules coexist (see VII-L-1). As a further extension of this study, the investigations of the optically induced ESR and the transient spectra of reflectivity are in progress.

Reference
1) T. Mitani, G. Saito, Y. Tokura and T. Koda, *Phys. Rev. Lett.*, 53, 842 (1984).

Oxidation of Molybdenum Cluster Compound $Cu_2Mo_6S_8$

Humihiko TAKEI, Shin TSUNEKAWA and Syoichi HOSOYA

The copper molybdenum sulphides known as Cu-Chévrel compounds exhibit the high temperature superconductivity under a high magnetic field. Recently, we found oxygen atoms in these compounds have a remarkable role in changing physical properties. The present study was planned to clarify the oxidation of $Cu_2Mo_6S_8$ on calcination in air. Figure 1 shows the result of DTA (Differential Thermal Analysis) and TG (Thermogravimetry), in which two peaks are apparent in the DTA curve. The first peak which corresponds to the rapid increase in the TG curve is due to the oxidation of one copper atom to CuO. At the same time, a partial oxidation of Cu-Chévrel occurred. X-ray and chemical analyses showed that the oxidized Chévrel phase was $Cu_{\sim 1}Mo_6S_8O_y$ and was stable between 350 and 400°C. This compound tends to change into CuO, MoO_3 and SO_2 with further heating. The peak at 510°C (DTA) corresponds to the formation of these oxides. The magnetic measurements indicated that the superconducting transition temperature of the oxidized Chévrel $Cu_{\sim 1}Mo_6S_8O_y$ was about 5.5K which was very close to that of $Cu_{1.0}Mo_6S_8$. This means that oxygen atoms in Cu-Chévrel do not disturb the superconducting coupling among the Mo_6 clusters.

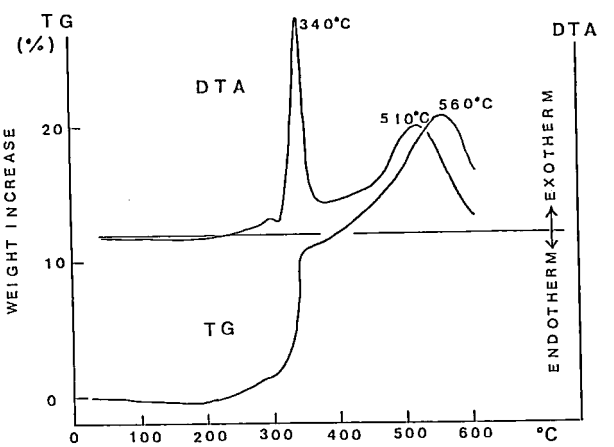

Figure 1. DTA-TG curves of $Cu_2Mo_6S_8$ between room temperature and 600°C in air.

Catalytic Action of Boron-Platinum Group Element Clusters as Heterogeneous Catalysis

Akira NAKAMURA (*Osaka Univ. and IMS*), **Humihiko TAKEI, Kazuo SAITO and Bateel WANG**

Novel cluster complexes of the type $LnPt_XB_y$ (Ln, Lanthanoid elements; Pt, Platinum group ele-

ments) were examined in suspension in organic solvents to find possible catalytic activity as heterogeneous catalysis. Provskite type $PrRh_3B$ and Rock-salt type $Pr[Rh_4B_4]$ gave significant catalytic activity on the hydrogenation of hexenes and hexadienes at room temperature and atmospheric pressure. The activity is substrate selective so that 1-hexene gives n-hexane at a much higher rate than other isomers do. It seems as if hydrogen is absorbed and then transferred to the substrate in benzene solution.

(2) Energy Transfer and Energy Conversion through Molecular Processes

Photocatalytic Effects of Semiconductors and Dyes:
(i) Application to Water Decomposition and Organic Reactions, and
(ii) Dynamic Process of Electron Transfer Through Semiconductor Interface.

Kazuhito HASHIMOTO, Masahiro HIRAMOTO and Tadayoshi SAKATA*

A new type of semiconductor electrodes which are prepared by a photolithography technique has been applied to water splitting, especially to process of oxygen evolution. We have obtained efficient oxygen production on Si electrodes with either a *p-n* junction or an MIS junction. The quantum yield of oxygen evolution was about 45% over the whole visible region. The stability of electrodes exceeds 100 hours of operation.

The strong semiconductor dependence was observed for the photoanodic decomposition of lactic acid. The photocatalytic reactions of organic compounds depended on the morphology of a semiconductor photocatalyst and on the oxidation potential of dye photocatalyst at the excited state.

The electron transfer from an adsorbed dye to a semiconductor substrate is one of the fundamental processes in the dye sensitization of semiconductor. We have measured luminescence decay curves and time resolved spectra of adsorbed dye molecules. The effects of water vapor, solvents, temperature and energy levels of both dyes and semiconductors was investigated.

The mechanism for photocurrent generation in an organic dye photodiode was studied by measuring both transient photocurrents and luminescence decays.

A part of these results is presented in III-D.

Activation Mechanism of Molecular Oxygen by Heme Enzymes

Teizo KITAGAWA, Takashi OGURA, Shinji HASHIMOTO, Shinya YOSHIKAWA (*Konan Univ.*) **and Yoshitaka TATSUNO** (*Osaka Univ.*)

Activation of molecular oxygen by heme enzymes is specific to each group of proteins. We have categorized the iron coordination environments inherent to each group of the proteins using resonance Raman spectroscopy. This year we succeeded in identifying the $Fe^{IV}=O$ stretching Raman line in the reaction intermediates of peroxidase called Compound II. Unexpectedly, the oxygen of the oxyferry heme was exchanged with oxygen of bulk water at neutral pH but not at alkaline pH. The midpoint pH for the acid/alkaline transition was 8.8 which agreed closely with the pK_a value of the heme-linked ionization of Compound II obtained with different techniques. The $Fe^{IV}=O$ stretching frequency was lower at neutral form and exhibited appreciable H/D dependence, suggesting the presence of hydrogen bond to the oxo-ligand from an amino acid residue having pK_a = 8.8. This hydrogen bond presumably plays a key role in the enzymatic catalysis of horseradish peroxidase. We developed an apparatus to measure a transient Raman spectra of reaction intermediates with further shorter life time (10 – 100 μs) and applied it to measure the resonance Raman spectra of Compound I of the peroxidase and an oxygenated intermediate of cytochorme *c* oxidase.

Hot Molecule Mechanism in the VUV Photochemistries

Nobuaki NAKASHIMA, Noriaki IKEDA and Keitaro YOSHIHARA

Primary intermediates of photochemistries of gaseous benzenes were found to be hot molecule (S_0**: highly excited vibrational states in the ground electronic state) by nanosecond laser flash photolysis.[1] The same mechanism was effective for dissociation of olefins and alkylbenzenes. The dissociation rates were measured directly from S_0** of these molecules for the first time.[1,2] This process is quenched by foreign gases, because the energy of the intermediate S_0** transfers to foreign gases. Pressure independent processes were also observed as minor paths.

The rate constants obtained are the specific dissociation rates in the thermal reaction. They can be explained in terms of thermal reaction (RRKM) theory. Olefins and alkylbenzenes are suitable for a study of the dissociation rates, because a wide variety of derivatives are readily available. The present results will give a new aspect on the mechanism of the UVU photochemistries. Related studies are discussed in Sec. III-A.

References

1) N. Nakashima and K. Yoshihara, *J. Chem. Phys.*, 79, 2727 (1983).
2) N. Nakashima, N. Shimo, N. Ikeda and K. Yoshihara, *J. Chem. Phys.*, 81, 3738 (1984).
3) N. Ikeda, N. Nakashima and K. Yoshihara, *J. Chem. Phys.*, 82, 5285 (1985).

Picosecond Dynamics of Excitation-Energy Transport in Organized Molecular Assemblies

Iwao YAMAZAKI, Naoto TAMAI and Tomoko YAMAZAKI

Dynamics of two- and three-dimensional excitation energy transports are investigated with several kinds of multilayered architechtures of Langmuir-Blodgett type by means of a picosecond time-resolved fluorescence spectrophotometer. In the multilayer systems in which different cyanine-dye monolayers are stacked (Fig. 1 (a)), the light energy absorbed by the outer surface is transferred sequentially among the layers, and finally trapped to the reaction center. In the course of the energy transfer, fluorescence is emitted from each cyanine dye, and is used as a probe for investigating kinetics.

Such an artificial multilayer is analogous to the so-called "antenna pigment" system in the photosynthetic organisms, in particular, the accessary pigment system in blue-green and red algae, in which different kinds of phycobiliproteins are stacked like multilayer (Fig. 1 (b)). The final goal of our study is to develop a electrooptic device in molecular scale that controls the light energy transport in the two- and three-dimensional architectures.

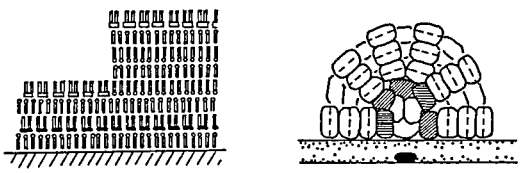

Figure 1. Schematic representation of the stacking multilayers in (a) Langmuir-Brodgett film and (b) phycobilisome. Details of their structures are presented in other places in this text.

External Magnetic Field Effects Upon Chemical Reactions

Hisaharu HAYASHI (*Inst. of Phys. and Chem. Res. and IMS*), **Yoshifumi TANIMOTO** (*Kanazawa Univ. and IMS*), **Ryoichi NAKAGAKI, Takeshi WATANABE, Mitsuo HIRAMATSU** (*Hamamatsu Photonics K.K. and IMS*), **Yoshio FUKUDA** (*Inst. of Phys. and Chem. Res. and IMS*) **and Saburo NAGAKURA**

In order to extend the study of magnetic field effects on chemical reactions to those in the gas phase, we have recently constructed an apparatus for aftergrows using a microwave discharge. The emission of generated aftergrows is measured in the presence of an external magnetic field below 1.8T. Using this apparatus, we have found a remarkable magnetic field effect on the emission of the NO (B-X) bands (see III-I-1). We have also continued to study magnetic field effects on photochemical (see III-I-2 to 5) and electrochemical (see III-I-6) reactions in solution.

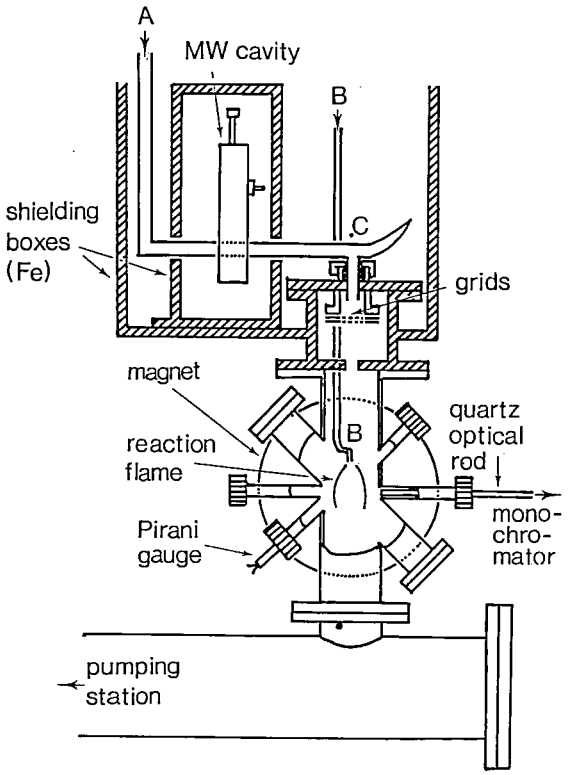

Figure 1. Apparatus for the discharge-flow system and magnet. Gases are introduced through inlets A and B. When the maximum field (1.8T) is applied to the apparatus, the field strength measured within the outer shielding box (C) is below 0.2 mT.

Applications of Excited-State Photoelectron Spectroscopy to Molecules and van der Waals Molecules Produced in Supersonic Jet

Katsumi KIMURA,* Yohji ACHIBA, Kenji SATO, Haruo SHIROMARU

A combination of excited-state photoelectron spectroscopy using nanosecond pulse lasers (UV and visible) and a supersonic molecular beam technique has been developed in this Institute since 1979 (IMS Annual Review, 1980–84). This method has made it possible to study dynamic behavior of atomic and molecular excited states including those which do not fluorescence, from a photoelectron spectroscopic point of view. Photoelectrons emitted from various atomic and molecular excited states have been investigated to clarify what kinds of information can be deduced from excited-state photoelectron spectra.

In this Project, not only single molecules but also van der Waals molecules produced in supersonic jet have been studied with this technique, and several typical applications of this technique have been demonstrated in the fields of (1) ionization selectivity, (2) autoionization, (3) intramolecular vibrational redistribution, (4) photodissociation, (5) excited states of van der Waals molecules (See IV-).

Molecular Beams Study of Photoassisted Surface Reactions

Kosuke SHOBATAKE, Shigeru OHSHIMA, Kiyohiko TABAYASHI and Atsunari HIRAYA

In order to study photoassisted surface reactions using a molecular beams technique, the rotatary mass spectrometer detector of a molecular beam chemistry apparatus (Model MBC-I) has been modified so that higher vacuum can be attained in the ionizer region. The third detector chamber in which an electron bombardment ionizer is housed is also pumped by a clean magnetically suspended turbomolecular pump (SEIKO PRECISION Model STP 300) and a high vacuum (5×10^{-11} Torr) can be attained even when rare gas is used as a sample and/or carrier gas.

The effect of irradiation of excimer laser at 308 nm upon etching reactions of solid Si by F_2 molecules has been studied using the molecular beam chemistry apparatus (Model MBC-I) with a modified rotatary mass spectrometer detector described above. Preliminary results show that (1) the prosses which has been observed is essentially sputtering by laser irradiation, but (2) the etching process is greatly enhanced by surface collision of F_2 molecules on solid Si.

(3) Molecular Science of Primordial Chemical Evolution

Laboratory Observations of U45.379: HCCCCCN, ν_{11}= 1, 1^+, J = 17 – 16 ?

Masatoshi OHISHI (*University of Tokyo*), **Shuji SAITO,*** **Kentarou KAWAGUCHI, Hiroko SUZUKI** (*Tokyo Astronomical Observatory*), **Takashi KASUGA** (*Tokyo Astronomical Observatory*) **and Norio KAIFU** (*Tokyo Astronomical Observatory*)

The U45.379 line, which was detected during the 40 GHz band molecular line survey with the 45 m radio telescope of Nobeyama Radio Observatory,[1] has the highest intensity among those of unidentified interstellar lines ever reported, $T_r \sim 4.2$ K in TMCl. It has no harmonically related lines and shows no fine and hyperfine structures.

After long efforts to identify the source molecule of U45.379, we recently observed a line at 45379.039 (4) MHz by using dc glow discharge in a mixture of acetylene and nitrogen in the free space absorption cell with the source modulation microwave spectrometer. The astronomically determined frequency of the U line is 45379.03 (2) MHz.[1] Based on the chemical behaviors of the line and a speculating survey in the 40 – 50 GHz region, we concluded that the line observed in laboratory is the 1^+, J = 17 –16 transition of ν_{11} = 1 for HCCCCCN, whose frequency is calculated to be 45379.10 MHz from the laboratory microwave spectroscopic study.[2] Since the ν_{11} bending frequency of HCCCCCN is estimated to be 104 cm^{-1},[3] and no interstellar line was detected at the predicted frequency of the 1^-, J = 17 – 16, ν_{11} = 1 transition, it may not be straightforward to identify the 1^+, J = 17 – 16, ν_{11} = 1 line to be the U45.379 which has been observed in the dark TMC1 molecular cloud of 10 to 20 K. A selective pumping mechanism such as an optical pumping may be necessary to reconcile the U45.379 line with the HCCCCCN line.

References
1) H. Suzuki, N. Kaifu, T. Miyaji, M. Morimoto, M. Ohishi and S. Saito, *Astrophys. J.* 282, 197 (1984).
2) M. Hutchinson, H. W. Kroto and D. R. M. Walton, *J. Mol. Spectrosc.* 82, 394 (1980).
3) S. Deguchi and M. Uyemura, *Astrophys, J.* 285, 153 (1984).

Study on Condensation of Interstellar Molecules to Clusters and their Reactions Induced by Photons and Electrons

Nobuyuki NISHI, Hisanori SHINOHARA, Tohru OKUYAMA and Kazunori YAMAMOTO

For the investigation of chemical reactions induced by UV photons, cosmic ray, or electrons on the surface of icy dusts and cometary objects in space, it is necessary to know how molecules forms co-condensates in such circumstances. This is highly related to the intermolecular interaction forces acting on the adsorbate and the surface molecules. This fundamental problem has been studied by investigating the stability of molecular clusters cooled by the expansion of gas mixtures of liquid droplets into high vacuum for the systems of hydrate clusters and other polar molecule clusters.

As found by the rocket-borne and balloon-borne mass spectrometric observation of the earth stratosphere,[1] the acetonitrile hydrate clusters are expected to exist dominantly in interstellar space. The structure or the composition of this binary cluster is found to be dependent on the relative abundance of the two molecular species. In a low CH_3CN concentration, almost all of acetonitrile molecules are captured by water molecules. Inclusion of an acetonitrile molecules in water clusters has been found to enhance the cluster stability and resulting in the growth of clusters. This tendency has been found in HCOOH-H_2O binary clusters and may be found in many other systems with polar molecules. On the ionization by VUV light or low energy electron impact, these clusters exhibit intra-cluster ion-molecules reactions. Typical one is proton transfer reactions producing a protonated cluster ion and a dissociating radical as seen in hydrogen bonding clusters. This ionization will induce radical reactions of the ice surface when the ice surface has a composition similar to the cluser. Acetonitrile forms also binary clusters with ammonia as proved by gas phase expansion, and this indicates that the our previous study on the photochemistry of the mixed solid containing CH_3CN+NH_3 is likely to occur on the icy objects formed in a nitrogen rich molecular cloud.

Reference
1) E. Arijs, D. Nevejans and J. Ingels, Nature, 28, 684 (1980).

Experimental Contribution to the Ion-Molecule Reaction Model for the Formation of Interstellar Molecules

Inosuke KOYANO, Kenichiro TANAKA and Shinzo SUZUKI

It is more than ten years since the first ion-molecule reaction model was proposed as a most probable mechanism for the formation of interstellar molecules. While various refined models have been elaborated since then, most of these models are critically based on several assumptions concerning the individual processes involved in them. In order to experimentally contribute to this problem, we are studying internal and collisional energy dependence of elementary ion-molecule reactions using a novel coincidence technique which we have developed recently.[1] This year, the reactions of vibrationally excited H_2^+ ions (which are supposed to be abundant in the interstellar clouds) with He and Ne have been investigated in particular detail. Relative reaction cross sections have been determind as a function of both vibrational and collisional energy. Preferential effectiveness of vibratilnal energy over collisional energy in promoting these endoergic reactions has been shown quantitatively.

In addition to these, construction of an apparatus which enables the measurements of energy disposal in ion-molecule reactions, such as radiative association, is going on toward the same objectives as the above experiments.

Reference
1) I. Koyano and K. Tanaka, *J. Chem. Phys.* **72**, 4858 (1980).

OKAZAKI CONFERENCES

"Okazaki Conferences" are principal symposia at IMS, which are held on the subjects related to the "Special Research Projects." They are held two or three times a year, with a moderate number of participants around 50, including several invited foreign speakers. The formal language for the conference is English. Outlines of the twenty-first to twenty-third conferences are as follows.

The Twenty-first Okazaki Conference

"Physicochemical Properties of Metalloporphyrins and Hemoproteins with Unusual Electronic States"

(January 29–31, 1985)

Organizers. H. Kobayashi (*Tokyo Inst. Tech.*), **T. Kitagawa** (*IMS*)
Invited Speakers. D.A. Reed (*Univ. of South. Calif.*), **T. Yonetani** (*Univ. of Pennsylvania*), **J.W. Buchler** (*Tech. Hochschule Darmstadt*), **A. Dedieu** (*Univ. of L. Pasteur*), **J. Fajer** (*Brookhaven Natl. Lab.*) **and B.M. Hoffman** (*Northwestern Univ.*)

This Symposium was undertaken to offer physical chemists, spectroscopists, biochemists, organometallic chemists and theoretical chemists an opportunity to get together and discuss their common interests, metalloporphyrins having unusual electronic states; the Fe(IV) state, Fe(V) state [or Fe(IV) cation radical], Fe(VI) state [Fe(II) dioxygen adduct], Fe(I) state [or Fe(II) anion radical], and the corresponding states of other metalloporphyrins.

The actual oxidation state of the metal deduced from theoretical calculations and the formal oxidation number are different, but they are occasionally confused. The oxidation number is a useful concept for experimentalists and indeed used by heme chemists, but its reality still remains to be elucidated. Therefore, a special discussion on "What is the oxidation number?" was hold as a night session. Profs. K. Saito and Y. Hosoya gave basic lectures which were

followed by active discussion between experimentalists and theoreticians.

Profs. A.C. Albrecht (Cornel Univ.) and G.L. Closs (Univ. of Chicago) joined in the symposium as a chairman. Unfortunately, Drs. Fajer and Hoffman could not come to Japan due to some accident. The ordinary session began with the lectures about the properties and significance of unusual redox states of hemeproteins and metalloporphyrins by Prof. I. Yamazaki and H. Kobayashi, respectively. Then the property of radical state was discussed by Drs. C.A. Reed and others. The subject of the second day was the Fe(IV) and Fe(I) porphyrins which were discussed by Drs. T. Yonetani, T. Kitagawa, J. Zimmer, and others. Then the session about theoretical calculations followed it. Drs. A. Dedieu, H. Kashiwagi and K. Tatsumi contributed to the session. The subject of the third day included the property and reactivity of metalloporphyrins. Drs. J.W. Buchler, H. Ogoshi and others gave lectures in this session. Since participants usually present their results in different scientific meetings, they acknowledged importance of this kind of meeting including wide variety of chemists for advancing on another step of their studies.

The Twenty-second Okazaki Conference

EXAFS and its Application to Materials Science

(March 18–20)

Organizers: H. Kuroda (*Univ. of Tokyo*) **and Y. Udagawa** (*IMS*)

Invited Speakers: E.A. Stern (*Univ. of Washington*), **F.W. Lytle** (*Boeing Aerospace Co.*), **P.H. Citrin** (*AT & T Bell Lab.*), **and D.C. Koningsberger** (*Technische Hogeschool Eindhoven*)

This conference was held to discuss about EXAFS (Extended X-ray Absorption Fine Structure) Spectroscopy and its application to materials science. The topics included are the following; (1) Theoretical, (2) Instrumentation, especially laboratory facillities, (3) Structure determination of surface, catalyst, amorphous solid, and inorganic complex compound in solution.

Twenty five talks were presented and about 50 people participated in discussion about various aspects of this still under developing spectroscopy. This is the second conference held in Japan concern-

ing EXAFS spectroscopy, following the first one at IMS on December 1984, and has given stimula to the researchers in this field especially by the attendence of and discussion with the founders of this spectroscopy.

The Twenty-third Okazaki Conference

Ten Years in Molecular Science: Progress and Opportunities
(May 7–8, 1985)

Organizers: **H. Inokuchi** (*IMS*), **E. Hirota** (*IMS*)
Invited Speakers: **G. Herzberg** (*NRC*), **W. Klemperer** (*Harvard Univ.*), **G.C. Pimentel** (*Univ. California, Berkeley*), **S.A. Rice** (*Univ. Chicago*), **A. Weller** (*Max Planck Inst., Göttingen*), **H.C. Wolf** (*Univ. Stuttgart*), **R.G. Parr** (*Univ. North Carolina*), **P.O. Löwdin** (*Univ. Florida*)

This Conference was organized primarily to review the developments in molecular science for past ten years and to discuss opportunities in future. Besides the invited speakers listed above, the following domestic participants also gave talks: M. Tsuboi (Univ. Tokyo), M. Ito (Tohoku Univ.), H. Baba (Hokkaido Univ.), N. Mataga (Osaka Univ.), G.L. Closs (Univ. Chicago and IMS), K. Kuchitsu (Univ. Tokyo), I. Tanaka (Tokyo Inst. Tech.), S. Nagakura (IMS), K. Yoshihara (IMS), H. Tsubomura (Osaka Univ.), Y. Toyozawa (Univ. Tokyo), G.G. Hall (kyoto Univ.), H. Inokuchi (IMS), H. Iwamura (IMS), K. Morokuma (IMS) and E. Hirota (IMS). Each talk summarizes recent developments in the field of the speaker with some historical perspectives for future trends.

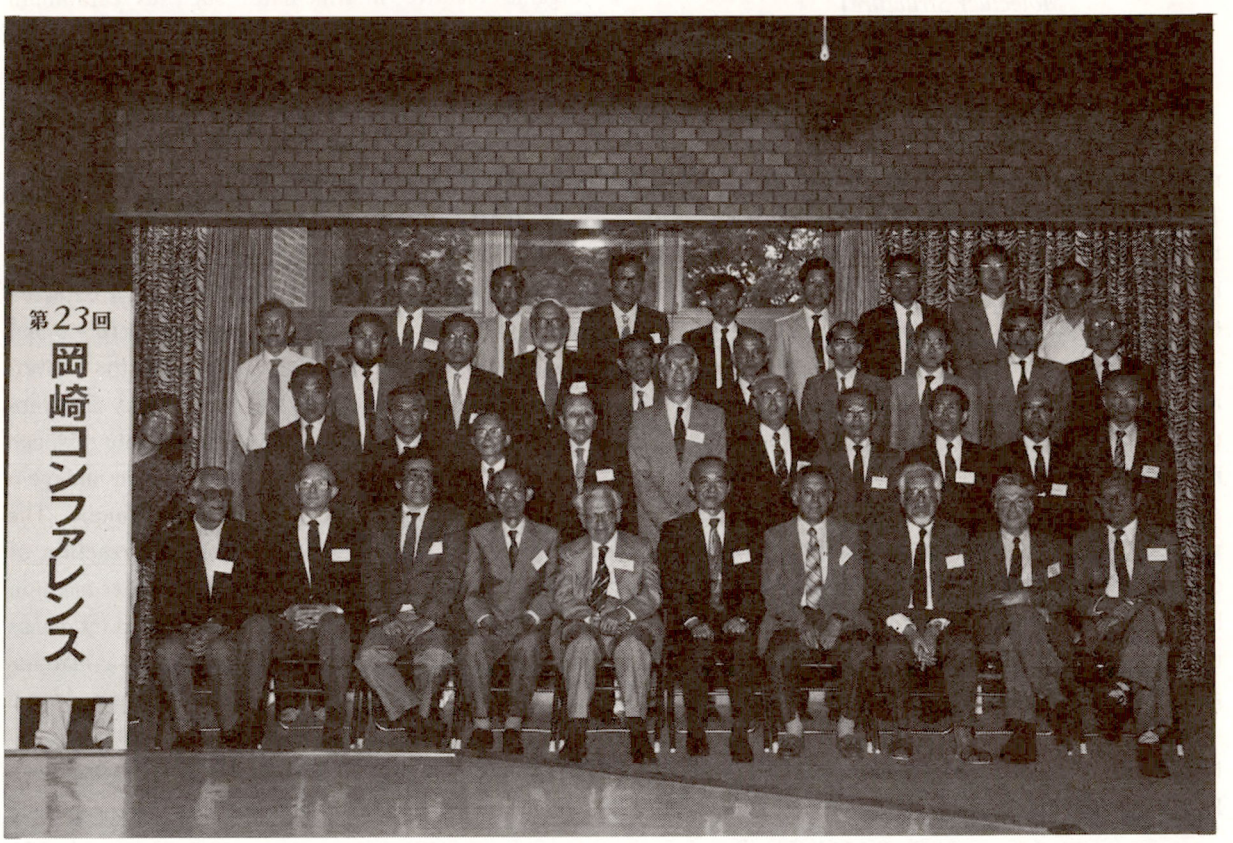

JOINT STUDIES PROGRAMS

As one of the important functions of an inter-university research institution, IMS undertakes joint studies programs for which funds are available to cover research expenses as well as travel and living expenses of individuals. The proposals from domestic scientists are reviewed and controlled by the inter-university committee. The programs are carried out under one of four categories:

1) Joint Studies on special projects (a special project of significant relevance to the advancement of molecular science can be carried out by a team of several groups of scientists).
2) Research Symposia (on timely topics in collaboration with both outside and IMS scientists).
3) Cooperative Research (carried out in collaboration with both outside and IMS scientists).
4) Use of Facility (the Computer Center, Instrument Center and other research facilities at IMS are open to all researchers throughout the country).
5) Joint studies programs using UVSOR facilities have started in the fiscal year 1985.

In the fiscal year 1984, numbers of joint studies programs accepted amounted to 4, 11, 170 and 191 for categories 1) – 4), respectively.

1) Joint Studies

Studies on the Dynamics of Excited Molecules in the Gas Phase Produced by Collisions with Metastable Atoms

Coordinators: **Kozo KUCHITSU** (*Univ. Tokyo*)
Eizi HIROTA (*Department of Molecular Structure*)
Kosuke SHOBATAKE (*Department of Molecular Assembly*)

This project aims at exploring characteristic reactions of molecules induced by metastable atoms. The excitation energies of these atoms correspond to those of VUV radiation, but reaction processes caused by them can be quite different from ordinary photochemical processes. Spectroscopic techniques of various kinds will be applied to unravel reaction mechanisms and to determine structures of reaction products. Particular attention will be paid to the CN radical, which may be prepared in the electronic states that are forbidden to reach from the ground state by dipole transitions. An apparatus is being constructed which prepares metastable rare gases in beam with specified energy in a range from thermal up to 1 eV and lets them collide with cyanides to generate CN radicals in "dark" states.

Collaborators include T. Kondow (Univ. Tokyo), K. Suzuki (Univ. Tokyo), T. Nagata (univ. Tokyo), H. Uehara (Josai Univ.) and H. Nakamura (IMS).

Molecular Design and Construction of New Organic Reactive Intermediates

Coordinator: **Hiizu IWAMURA** (*Department of Applied Molecular Science*)

The joint study has been carried out since 1983 with the aim of constructing and characterizing new organic reactive intermediates such as carbonium ions, carbanions, carbenes and nitrenes of molecular scientific interest. In close collaboration with the scientists of Osaka City University, we generated polycarbenes $C_6H_5\ddot{C}[(m\text{-}C_6H_4)\ddot{C}]_{n-1}C_6H_5$ (n = 3, 4, 5 and 6) that had the ground multiplet states ($2n$ + 1) and therefore the potentiality of organic ferromagnets. A number of conformational isomers that have different zero-field tensors have been detected and analyzed for the tri- and tetracarbenes (n = 3 and 4) (see V-A-1). In a second project with the University of Tokyo group, we designed a series of orthoester anhydrides in which the rates of ionic dissociation and ion-pair return were determined independently by the ^1H and ^{17}O DNR technique. The formation of carbonyl oxides from the reaction of diazo compounds with oxygen and a further reaction to give tetraoxolanes have been established by means of ^{18}O-labeling experiments carried out in collaboration with the Nagoya University group (see V-C-1). Merits and demerits of our ^{17}O-labeling-NMR determination method in reference to the classical ^{18}O-labeling-mass spectral determination method were

critically evaluated.

Control of Molecular Function under Hydrostatic Pressure

Coordinators: **Tadaoki MITANI** (*Equipment Development Center*)
Takao KODA (*univ. of Tokyo*)

This program started in 1984 with aim of creating a new molecular function of organic complexes under high pressure, which are not expected to be observable at ambient pressure. We have designed and constructed an assembly of high-pressure cells for optical, electrical and magnetic measurements under hydrostatic pressure. Among various attempts using these cells, optical reflection and conductivity measurements on mixed-stacked charge-transfer complexes, such as TTF-p-chloranil, have been successfully made to observe a new phase of the neutral-to-ionic transition at a low temperature (see VII-L-1). These results suggest a possibility to control electrical properties of charge-transfer complexes by utilizing the critical phenomena near the phase transition. Further, we have improved a high pressure technique in the ESR measurements, which provides a unique tool to investigate magnetic properties under pressure in detail (see VII-M-2). A extension of these measurements to lower temperatures down to liquid Helium temperature are in progress.

The members of the program are T. Koda, Y. Tokura, Y. Kaneko (Univ. of Tokyo), I. Shirotani (Muroran Inst. of Tech.), T. Takahashi, Y. Maniwa (Gakushuin Univ.), A. Matsui, K. Mizuno (Konan Univ.), H. Nishimura (Osaka City Univ.), H. Yoshioka, S. Kazama (Sizuoka College of Pharmacy) and T. Mitani (Equipment Development Center).

Magnetic Field Effects Upon Dynamic Behavior of Excited Species

Coordinators: **Hisaharu HAYASHI** (*Insitute of Physical and Chemical Research and IMS*)
Hajime KATO (*Kobe University*)
Yoshifumi TANIMOTO (*Kanazawa University*)

Recently, magnetic field effects have been found in many chemical reactions and many energy transfer processes. The effects have provided us with new aspects in dynamic behavior of excited species. However, for some of the effects which have hitherto been found, their mechanisms have not yet been clarified well. Therefore, one of the aims of this joint study is to study the mechanisms of the effects on the gas-phase-emission of CS_2, alkali molecules, and some intermediates in combustion (OH, NO, CH, HPO, etc.) with pulsed lasers. On the other hand, we would like to challenge to discover new magnetic field effects, extending our studies to the reactions of excited species generated by microwave discharge in the gas phase and the intra-molecular hydrogen-abstraction and electron-transfer reactions in solution. This joint study was started on the first of April, 1985.

The other members of the program are H. Sakuragi (*Univ. of Tsukuba and IMS*), H. Abe (*Institute of Physical and Chemical Research*), I. Yamazaki (*Instrument Center*), and R. Nakagaki (*Electronic Structure*).

2) Research Symposia

1. Symposium on Frontier Raman Spectroscopy.
   (September 3rd – 4th, 1984)
   Organizer: T. Kitagawa (IMS)
2. Future and Present Aspects of Magnetic Field Effects upon Chemical Reactions and Biological Phenomena.
   (January 8th – 10th, 1985)
   Organizer: H. Hayashi (IMS)
3. Elemental Reactions in Homogeneous Catalysis.
   (January 17th – 18th, 1985)
   Organizer: K. Ito (Toyohashi Univ.)
4. Preparation and characterization of ultrafine particles.
   (February 16th – 17th, 1985)
   Organizer: N. Wada (Nagoya Univ.)
5. Formation, Structure and Dynamic Behavior of Molecular Clusters.
   (March 11th – 12th, 1985)
   Organizer: K. Kaya (Keio Univ.)
6. Development of Laser Pulse Technique in the Infrared Energy Region.
   (March 22th – 23th, 1985)

Organizer: T. Mitani (IMS)

7. For the Sake of Effective and Creative Use of Supercomputer.
   (March 26th – 27th, 1985)
   Organizer: H. Kashiwagi (IMS)
8. Hydrogen Physisorption and Chemisorption in Graphite, Alkalimetal in Intercalation Compounds.
   (June 2nd – 3rd, 1985)
   Organizer: T. Enoki (IMS)
9. Design and Functions of Organic Thin Films.
   (June 4th – 5th, 1985)
   Organizer: M. Okada (Hiroshima Univ.)
10. Structure and Photo-energy Relaxation in Molecular Assemblies.
    (July 16th – 17th, 1985)
    Organizer: Y. Maruyama (IMS)
11. New Aspects of Laser Chemistry and Dynamics of Excited Molecules.
    (August 2nd – 3rd, 1985)
    Organizer: N. Nishi (IMS)

3) Cooperative Research

This is one of the most important programs IMS undertakes for conducting its own research of the common interest to both outside and IMS scientists by using the facilities at IMS. During the first half of fiscal year of 1984 ending on September 30, 88 outside scientists including 8 invited collaborated with IMS scientists; and during the second half of the fiscal year, 82 outside scientists including 4 invited worked in collaboration with IMS scientists, the names and the affiliations of these collaborators are found in the Research Activities.

4) Use of Facility

The number of projects accepted for the Use of Facility Program of the Computer Center during the fiscal year of 1984 amounted to 142 (407 user), and the computer time spent for these projects is 4140 hours (50% of the total annual CPU time).

Forty nine projects (66 users) were accepted for the Use of Facility Program of the Instrument Center during the fiscal year of 1984.

FOREIGN SCHOLARS

Visitors from abroad play an important role in research activities and are always welcome at IMS. The following is the list of foreign scientists who visited IMS in the past year (Aug. 1984 – July 1985). The sign *1 indicates an attendant to an Okazaki Conference, *2 an IMS Invited Foreign Scholar, *3 an IMS councillor, *4 an IMS visiting scientist and *5 an IMS adjunct professor from abroad.

Prof. A.E. Beylich	Tech. Hochschule, Areher	(FRG)	Aug. 1984
Dr. K. Szczepaniak*4	Inst. Phys. Polish Acad. Sci.	(Poland)	Aug. – Oct. 1984
Prof. W.B. Person*5	Univ. of Florida	(USA)	Aug. 1984 – Jan. 1985
Prof. M. Grätzel*1	Inst. Chim-Phys. EPF	(Switzerland)	Aug. 1984
Prof. P. Shie-Ming	Nat. Taiwan Univ.	(Taiwan)	Aug. 1984
Dr. G. Hodes*1	Weizmann Inst. Sci.	(Israel)	Aug. 1984
Dr. M.G. Kinnaird*1	Kyoto Univ. (Univ. North)	(USA)	Aug. 1984
Dr. J.L. Sessler*1	Kyoto Univ. (Stanford Univ.)	(USA)	Aug. 1984
Prof. M.A. Fox*1	Univ. of Texas	(USA)	Aug. 1984
Dr. A. Hellar*1	Bell Lab.	(USA)	Aug. 1984
Dr. A. Mackor*1	Inst. Applied Chem. TNO	(Netherlands)	Aug. 1984
Prof. T.J. Meyer*1	Univ. of North Carolina	(USA)	Aug. 1984
Dr. A.J. Nozik*1	SERI	(USA)	Aug. 1984
Dr. F. Willig*1	Fritz Haber Inst.	(FEG)	Aug. 1984
Dr. A.J. Frank*1	SERI	(USA)	Aug. 1984
Prof. J. Rabani	The Hebrew Univ. of Jerusalem	(Israel)	Aug. 1984
Prof. S. Huzinaga	Univ. of Alberta	(Canada)	Aug. 1984
Dr. A. Weber	NBS. Washington	(USA)	Aug. 1984
Prof. T. Oka	Univ. of Chicago	(USA)	Aug. 1984
Prof. M. Schwöerer	Univ. Bayreuth	(FRG)	Aug. 1984
Prof. S.C. Shim	KAIST	(Korea)	Aug. 1984
Dr. M.M. Martin	CNRS	(France)	Aug. 1984
Prof. S.B. Costa	Inst. Superior Tecnico	(Portugal)	Sep. 1984
Dr. R.H. Wilson	General Electric	(USA)	Sep. 1984
Dr. P. Carey	Nat. Research Council	(Canada)	Sep. 1984
Dr. V. Hizhnyakov	Inst. Phys. Estonian SSR Acad. Sci.	(USSR)	Sep. 1984
Prof. R.M. Hochstrasser	Univ. of Pennsylvania	(USA)	Sep. 1984
Prof. A.D. Bandrauk	Univ. of Sherbrooke	(Canada)	Sep. 1984
Dr. T.L. Gustafson	Standard Oil Co. Corporate Researach Center	(USA)	Sep. 1984
Prof. S.A. Asher	Univ. of Pittsburgh	(USA)	Sep. 1984
Dr. R.G. Snyder	Univ. of California, Berkely	(USA)	Sep. 1984
Prof. T.G. Spiro	Princeton Univ.	(USA)	Sep. 1984
Prof. W. Hub	Technische Univ., München	(FRG)	Sep. 1984
Prof. E.J. Heller	Univ. of Washington	(USA)	Sep. 1984
Prof. W.L. Peticolas	Univ. of Oregon	(USA)	Sep. 1984
Prof. A.C. Albrecht	Cornell Univ.	(USA)	Sep. 1984, Jan. – Feb. 1985
Prof. H.D. Bist	Indian Inst. Tech., Kanpur	(India)	Sep. 1984
Prof. R.E. Hester	Univ. of York	(UK)	Sep. 1984

Prof. G. Zerbi*[2]	Politecnico Milano	(Italy)	Sep. 1984
Prof. C.H. Wang	Univ. of Utah	(USA)	Sep. 1984
Dr. J.-L Bribes	Place Eugene Bataillon	(France)	Sep. 1984
Prof. B. Venkataraman	Tata Inst. Fundamental Research	(India)	Sep. 1984
Prof. H. Tributsch	Hahn Meitner Inst.	(FRG)	Sep. 1984
Dr. P. Avouris	I.B.M.	(USA)	Sep. 1984
Prof. M. Y. M. Iha	Univ. of Sas Paulo	(Brazil)	Sep. 1984
Prof. L.M. Jackman	The Pennsylvania State Univ.	(USA)	Sep. 1984
Prof. Y. Lu	Chinese Academy of Science	(China)	Sep. 1984
Prof. Dr. D.M. Goodall	Univ. of York	(UK)	Sep. 1984
Dr. Z. Herman	J. Heyrovsky Inst. of Physical Chem. and Elec. Czechoslovak Acad. of Sci.	(CSSR)	Sep. – Dec. 1984
Dr. B.A. Parkinson	Solar Energy Research Inst.	(USA)	Sep. 1984
Prof. M. Winnewisser	Univ. Giessen	(FRG)	Sep. 1984
Dr. B.P. Winnewisser	Univ. Giessen	(FRG)	Sep. 1984
Dr. Y.I. Dolzhenko	Kharkov Polytechnical Inst.	(USSR)	Sep. 1984 – Jun. 1985
Prof. C.B. Harris	Univ. of California	(USA)	Sep. 1984
Prof. M. Kasha*[3]	Florida State Univ.	(USA)	Sep. – Oct. 1984
Dr. M. Gress	DOE	(USA)	Sep. 1984
Prof. C. Llaguno	Univ. of the Philippines	(Philippines)	Oct. 1984
Prof. E.R. Grant	Cornell Univ.	(USA)	Oct. 1984
Mr. Y. Li*[2]	Changchun Institute of Optics and Fine Mechanics, Chinese Academy of Sciences	(China)	Oct. – Nov. 1984
Mr. B. Wang*[2]	Changchun Institute of Optics and Fine Mechanics, Chinese Academy of Sciences	(China)	Oct. – Nov. 1984
Prof. B.R. Henry*[2]	Univ. of Manitoba	(Canada)	Oct. 1984
Prof. J. Koutecky	Freie Univ. Berlin	(FRG)	Oct. 1984
Prof. R.S. Berry	Univ. of Chicago	(USA)	Oct. 1984
Dr. P.A. Hackett	NRC	(Canada)	Oct. 1984
Dr. E. Feller	NSF	(USA	Oct. 1984
Prof. G. Gordon	Miami Univ.	(USA)	Nov. 1984
Dr. P.-M. Guyon	LURE. Laboratoire CNRS	(France)	Nov. 1984
Dr. Y. Lin*[4]	Tsinghua Univ. of Beijing	(China)	Nov. – Dec. 1984
Prof. T. Jiahe*[4]	Tsinghua Univ. of Beijing	(China)	Nov. – Dec. 1984
Prof. N. Liu	Tsinghua Univ. of Beijing	(China)	Nov. 1984
Dr. Y. Xu	Tsinghua Univ. of Beijing	(China)	Nov. 1984
Dr. R.M. Lyer*[2]	Bhabha Atomic Research Centre	(India)	Nov. 1984
Prof. J.K.S. Wan*[2]	Queen's Univ.	(Canada)	Nov. 1984
Dr. J.B. West*[2]	Daresbury Lab.	(UK)	Nov. – Dec. 1984
Prof. R.B. Cundall	Univ. of Salford	(UK)	Nov. – Dec. 1984
Prof. V.B. Koutecky	Freie Univ. Berlin	(FRG)	Nov. 1984
Dr. E. Clementi	IBM	(USA)	Nov. 1984
Dr. A.M. Hellwege	Landolt-Börnstein, Springer	(FRG)	Nov. 1984
Dr. R. Green	NSF	(USA)	Dec. 1984
Prof. Z. Reihnan*[2]	Changchun Inst. Applied Chem.	(China)	Dec. 1984

	Scinica		
Prof. K.L. Kompa	Max-Planck-Inst. fuer Quantenoptik	(FRG)	Dec. 1984
Mr. C.T. Owens	NSF	(USA)	Dec. 1984
Dr. R. Green	NSF	(USA)	Dec. 1984
Prof. G.L. Closs*[5]	Univ. of Chicago	(USA)	Jan. – Jul. 1985
Prof. L.F. Phillips*[2]	Univ. of Canterbury	(New Zealand)	Jan. – Feb. 1985
Prof. M.-H. Lee	Kyungpook National Univ.	(Korea)	Jan. 1985
Prof. Y.H. Kim	The Korea Advanced Inst. Sci.	(Korea)	Jan. 1985
Prof. E. Lippert*[5]	Tech. Univ. Berlin	(FRG)	Jan. – Jul. 1985
Dr. M. Schreiber	Univ. Dortmund	(FRG)	Jan. – Feb. 1985
Dr. S. Watanabe	Observatoire de Paris	(France)	Jan. 1985
Prof. B. Alpert	Univ. Paris VII	(France)	Jan. 1985
Prof. G.P. Panigrahi	Univ. of Berhampur	(India)	Feb. 1985
Dr. K. Albert	Univ. of Tubingen	(FRG)	Feb. 1985
Prof. U. Kim	Yonsei Univ.	(Korea)	Feb. 1985
Prof. P.-S. Song	Texas Tech. Univ.	(USA)	Feb. 1985
Prof. A.C. Albrecht	Cornell Univ.	(USA)	Feb. 1985
Prof. S. Mukamel	Univ. of Rochester	(USA)	Mar. 1985
Prof. A.W. Castleman. Jr.	The Pennsylvania State Univ.	(USA)	Mar. 1985
Dr. A.R.W. McKellar*[2]	Herzberg Institute of Astrophysics	(Canada)	Mar. – May 1985
Prof. H. Kessler	Johan Wilhelm Goethe Univ.	(FRG)	Mar. 1985
Dr. H. Petek	Univ. of California, Berkley	(USA)	Mar. 1985
Prof. E.A. Stern*[1]	Univ. of Washington	(USA)	Mar. 1985
Dr. F.W. Lytle*[1]	Boeing Aerospace	(USA)	Mar. 1985
Dr. P. Citrin*[1]	ATT Bell Lab.	(USA)	Mar. 1985
Prof. D.C. Koningsberger*[1]	Technische Hogeshool Eindhoven	(Netherlands)	Mar. 1985
Dr. Z. Latajka*[2]	Univ. of Wroclaw	(Poland)	Mar. 1984 – Mar. 1985
Prof. W.T. Borden*[4]	Univ. of Washington	(USA)	Mar. – Jul. 1985
Dr. T.B. Tang*[2]	Univ. of Cambridge	(UK)	Mar. 1984 – Feb. 1985
Prof. A.D. Buckingham	Univ. of Cambridge	(UK)	Mar. 1985
Prof. K.A. McLauchlan	Univ. of Oxford	(UK)	Mar. 1985
Prof. J. Moseley	Univ. of Oregon	(USA)	Apr. 1985
Dr. Y. Yan	National Synchrotron Radiation Laboratory, Hefei	(P.R. China)	Apr. 1985
Dr. K. Doblhofer	Fritz-Haber Inst.	(FRG)	Apr. – May 1985
Prof. P. Laszlo*[2]	Univ. of Liège	(Belgium)	Apr. – May, Aug. – Oct. 1985
Prof. X.-Y. Fu*[4]	Peking Normal Univ.	(China)	May – Aug. 1985
Mr. J.-G. Yu*[4]	Peking Normal Univ.	(China)	May – Aug. 1985
Mr. J. Han*[4]	Peking Normal Univ.	(China)	May – Aug. 1985
Prof. K.S. Song	Univ. of Ottawa	(Canada)	May 1985
Prof. D.M. Hanson*[2]	State Univ. of New York at Stony Brook	(USA)	May – Aug. 1985
Prof. D.T. Canvin	Queen's Univ.	(Canada)	May 1985
Dr. R. Rabson	DOE	(USA)	May 1985
Prof. A. San Pietro	Univ. of Indiana	(USA)	May 1985
Prof. G. Porter	Royal Inst.	(UK)	May 1985

Prof. P.O. Lowdin	Univ. of Florida	(USA)	May 1985
Prof. S.A. Rice*[1]	Univ. of Chicago	(USA)	May 1985
Dr. G. Herzberg*[1]	National Research Council	(Canada)	May 1985
Prof. G.G. Hall*[1]	Kyoto Univ.		May 1985
Prof. G.C. Pimentel*[1]	Univ. of California, Berkeley	(USA)	May 1985
Prof. H.C. Wolf*[1]	Univ. of Stuttgart	(FRG)	May 1985
Prof. R.G. Parr*[1]	Univ. of North Carolina	(USA)	May 1985
Prof. M.S. Jhon*[1]	Korea Adv. Inst. of Sci. and Tech.	(Korea)	May 1985
Prof. W. Klemperer*[1]	Harvard Univ.	(USA)	May 1985
Prof. S.H. Such Salk	Univ. of Missouri-Rolla	(USA)	May 1985
Prof. A. Weller*[1]	Max-Planck-Inst., Göettingen	(FRG)	May 1985
Dr. Z.R. Shi	Inst. Chem. Academia Sinica	(China)	May 1984
Dr. M. Stuke	Max-Planck-Inst., Göettingen	(FRG)	Jun. 1985
Prof. I. Miyagawa	Univ. of Alabama	(USA)	Jun. 1985
Dr. G. Dresselhaus	Massachusetts Inst. of Tech.	(USA)	Jun. 1985
Prof. M.S. Dresselhaus	Massachusetts Inst. of Tech.	(USA)	Jun. 1985
Prof. P.C. Eklund	Univ. of Kentucky	(USA)	Jun. 1985
Dr. J.R. Gaier	Lewis Research Center, NASA	(USA)	Jun. 1985
Prof. W.A. Kamitakahara	Iowa State Univ.	(USA)	Jun. 1985
Prof. H. Zabel	Univ. of Illinois	(USA)	Jun. 1985
Dr. H. Resing	Naval Research Center	(USA)	Jun. 1985
Dr. F. Beguin	CNRS, Orléans	(France)	Jun. 1985
Dr. O. Guérard	Univ. Naney	(France)	Jun. 1985
Prof. A. Herold	Univ. Naney	(France)	Jun. 1985
Dr. M.A. West	Roy, Inst.	(UK)	Jun, 1985
Prof. Kyung-H. Jung*[2]	KAIST	(Korea)	Jun. – Aug. 1985
Prof. B.S. Lee*[2]	Inha Univ.	(Korea)	Jul. – Aug. 1985
Prof. B.J. Yoon*[4]	Kangreung Nat. Univ.	(Korea)	Jul. – Aug. 1985
Prof. K.T. No*[4]	Soong Jun Univ.	(Korea)	Jul. – Aug. 1985
Prof. J.A. Herman	Laval Univ.	(Canada)	Jul. 1985
Dr. N. Boens	Leuven Katholic Univ.	(Belgium)	Jul. – Aug. 1985
Prof. L.M. Venanzi	ETH, Zurich	(Switzerland)	Jul. – Aug. 1985
Dr. M.C. Chang*[2]	Sun Cheon Natl. Univ.	(Korea)	Jul. – Aug. 1985
Prof. B.T. Newbold	l'Université de Moncton	(Canada)	Jul. 1985
Dr. Y. Cao	Inst. Chem. Academia Sinica	(China)	Jul. – Aug. 1985
Dr. R.J. Rest	Univ. of Southanpton	(UK)	Jul. – Aug. 1985
Prof. H. Okabe	Haward Univ.	(USA)	Jul. – Sep. 1985
Prof. V.S. Letokhov	U.S.S.R. Academy of Science	(USSR)	Jul. – Aug. 1985
Prof. P. Stang	Univ. of Utah	(USA)	Jul. 1985
Prof. T.Y. Luh	Chinese Univ. Hong Kong	(Hong Kong)	Jul. 1985
Prof. R.J. Donovan	Univ. of Edinburgh	(UK)	Jul. 1985

LIST OF PUBLICATIONS

S. OBARA, N. KOGA and K. MOROKUMA, "Intramolecular CH·····M Interaction: Ab Initio MO Study of the Structure of Ti (CH_3) $(PH_3)_2(X)_2Y$.", *J. Organometallic Chem.* **270**, C33 (1984).

K.D. SEN, K. OHTA and K. KOROKUMA, "Relative Conformer Stability of Diphosphine and Phosphino-difluorophosphine: An ab Initio Study.", *Theochem* **18**, 287 (1984).

K. MOROKUMA, M. HANAMURA and K. AKIBA, "Role of Sulfur d Orbitals in the S·····N Bond Stability of Ammonioalkylsulfuranes.", *Chem. Lett.* 1557 (1984).

Y. OSAMURA, W.T. BORDEN and K. MOROKUMA, "Structure and Stability of Oxyallyl. An MCSCF Study.", *J. Am. Chem. Soc.* **106**, 5112 (1984).

Z. LATAJKA, S. SAKAI, K. MOROKUMA and H. RATAJCZAK, "Possible Gas-Phase Ion Pairs in Amine-HCl Complexes. An ab Initio Theoretical Study.', *Chem. Phys. Lett.* **110**, 464 (1984).

E.R. DAVIDSON and K. MOROKUMA, "On the Proton Field Gradient of Ice Ih.", *Chem. Phys. Lett.* **111**, 7 (1984).

E.R. DAVIDSON and K. MOROKUMA, "A Proposed Antiferroelectric Structure for Proton Ordered Ice Ih.", *J. Chem. Phys.* **81**, 3741 (1984).

S. OBARA, K. KITAURA and K. MOROKUMA, "Reaction Mechanisms of Oxidative Addition $[H_2 + Pt^0(PH_3)_2 \rightarrow Pt^{II}(H)_2(PH_3)_2]$ and Reductive Elimination $[Pt^{II}(H)(CH_3)(PH_3)_2 \rightarrow CH_4 + Pt^0(PH_3)_2]$. Ab Initio MO Study.", *J. Am. Chem. Soc.* **106**, 7482 (1984).

L.L. LOHR, H.B. SCHLEGEL and K. MOROKUMA, "Theoretical Studies of the Gas-Phase Proton Affinities of Molecules Containing Phosphorus-Carbon Multiple Bonds.", *J. Phys. Chem.* **88**, 1981 (1984).

Y. NISHIMURA, M. TSUBOI, S. KATO and K. MOROKUMA, "In-Plane Vibrational Modes of Guanine from an ab Initio MO Calculation.", *Bull. Chem. Soc. Jpn.*, **58**, 638 (1985).

K. MOROKUMA, "Molecular Orbital Studies of Structure and Reactivity of Organosilicon Compounds.", in H. Sakurai Ed., "Organosilicon and Bioorganosilicon Chemistry," Ellis Harwood Ltd., Chichester, p.33 (1985).

S. SAKAKI, K. MOROKUMA and K. OHKUBO, "Ab Initio MO Study of the Coordination Modes and Bonding Nature in Rh^I-N_2 Complexes.", *J. Am. Chem. Soc.* **107**, 2686 (1985).

K. OHTA, E.R. DAVIDSON and K. MOROKUMA, "Dimerization Paths of CH_2 and SiH_2 Fragments to Ethylene, Disilene and Silaethylene: MCSCF and MR-CI Study of Least and Non-Least Motion Paths.", *J. Am. Chem. Soc.* **107**, 3466 (1985).

B.J. YOON, K. MOROKUMA and E.R. DAVIDSON, "Structure of Ice Ih. Ab Initio Two- and Three-Body Water-Water Potentials and Geometry Optimization", *J. Chem. Phys.* **83**, 1223 (1985).

K. TAKATSUKA and H. NAKAMURA, "A Semiclassical Theory in Phase Space for Molecular Processes: Formalism Based on the Dynamical Characteristic Function', *J. Chem. Phys.* **82**, 2573 (1985).

H. NAKAMURA and A. OHSAKI, "Dynamics of Collinear Asymmetric Light Atom Transfer Reactions", *J. Chem. Phys.* **83**, 1599 (1985).

H. ITO, K. TAKATSUKA, H. NAKAMURA and Y. OSAMURA, Y. OZAKI, T. NAGATA, T. KONDOW, K. KUCHITSU, "Calculation of the Potential Energy Curves for the Low-lying Doublet and Quartet States of the CN Radical", *Chem. Phys.* **98**, 81 (1985).

K. NASU, "Many-Polaron Theory for CDW, SDW and Superconducting Phases in One-Domensional N-Sites N-Electrons System—Quantum-Classic Crossover—", *J. Phys. Soc. Jpn.* **54**, 1933 (1985).

S. MURAMATSU and K. NASU, "Depolarization Dynamics of Hot Luminescence in F Centre", *J. Phys. C: Solid State Phys.* **18**, 3729 (1985).

T. TAKEUCHI, S. UENO, M. YAMAMOTO, T. MATSUSHITA and K. NISHIMOTO, "Theoretical Study of Electron Impact Mass Spectrometry II, Ab Initio MO Study of the Fragmentation of 1-Propanol", *Int. J. Mass. Spec. Ion Proc.* **64**, 33 (1985).

K. KAWAGUCHI, T. SUZUKI, S. SAITO, E. HIROTA, and T. KASUYA, "Dye Laser Excitation Spectroscopy of the CCN Radical: The $\tilde{A}^2\Delta_i$–$\tilde{X}^2\Pi_r$ (0,1,0)–(0,1,0) and (0,2,0)–(0,2,0) Bands.", *J. Mol. Spectrosc.*, **106**, 320 (1984).

K. KAWAGUCHI and E. HIROTA, "Far-Infrared Laser Magnetic Resonance Spectrum of the AsH Radical in $X^3\Sigma^-$.", *J. Mol. Spectrosc.*, **106**, 423 (1984).

S. SAITO, K. KAWACUCHI, and E. HIROTA, "Generation, Reaction and High-Resolution Spectroscopy of Short-Lived Molecules and Free Radicals.", *J. Chem. Soc. Jpn., Chem. & Ind. Chem.* (in Japanese), No. 10, 1542 (1984).

K.G. LUBIC, T. AMANO, H. UEHARA, K. KAWAGUCHI, and E. HIROTA, "The ν_1 Band of the DO_2 Radical by Difference Frequency Laser and Diode Laser Spectroscopy: The Equilibrium Structure of the Hydroperoxyl Radical.", *J. Chem. Phys.*, **81**, 4826 (1984).

T. SUZUKI, S. SAITO, and E. HIROTA, "Rotational Perturbations and the Zeeman Effect in the $\tilde{A}^1A''$ (010)–$\tilde{X}^1A'$ (000) Band of HCF.", *Can. J. Phys.*, **62**, 1328 (1984).

Y. ENDO, S. SAITO, and E. HIROTA, "The Microwave Spectrum of the Chloromethyl Radical, CH_2Cl.", *Can. J. Phys.*, **62**, 1347 (1984).

H. SUZUKI, N. KAIFU, T. MIYAJI, M. MORIMOTO, M. OHISHI, and S. SAITO, "Detection of U45.379: An Intense, Peculiar Unidentified Line.", *Astrophys. J.*, **282**, 197 (1984).

S. SAITO, K. KAWAGUCHI, and E. HIROTA, "The Microwave Spectrum of the H_2D^+ Ion: The 2_{20}←2_{21} Transition.", *J. Chem. Phys.*, **82**, 45 (1985).

C. YAMADA, S. SAITO, H. KANAMORI, and E. HIROTA, "Millimeter-Wave Spectrum of the CCO Radical.", *Astrophys. J.*, **290**, L65 (1985).

K. KAWAGUCHI, C. YAMADA, and E. HIROTA, "Diode Laser Spectroscopy of the CO_2^+ ν_3 Band Using Magnetic Field Modulation of the Discharge Plasma.", *J. Chem. Phys.*, **82**, 1174 (1985).

K. KAWAGUCHI, C. YAMADA, S. SAITO, and E. HIROTA, "Magnetic Field Modulated Infrared Laser Spectroscopy of Molecular Ions: The ν_2 Band of HCO^+.", *J. Chem. Phys.*, **82**, 1750 (1985).

T.B. TANG, H. INOKUCHI, S. SAITO, C. YAMADA, and E. HIROTA, "CCCO: Generation by dc Glow Discharge in Carbon Suboxide, and Microwave Spectrum.", *Chem. Phys. Lett.*, **116**, 83 (1985).

T. ISHIWATA, I. TANAKA, K. KAWAGUCHI, and E. HIROTA, "Infrared Diode Laser Spectroscopy of the NO_3 ν_3 Band.", *J. Chem. Phys.*, **82**, 2196 (1985).

C. YAMADA and E. HIROTA, "The $A(^2\Pi_i)$–$X(^2\Sigma^+)$ Transition of the SiN Radical by Infrared Diode Laser Spectroscopy.", *J. Chem. Phys.*, **82**, 2547 (1985).

S. SAITO, Y. ENDO, and E. HIROTA, "The Microwave Spectrum of the PF Radical in the Ground $X^3\Sigma^-$ Electronic State.", *J. Chem. Phys.*, **82**, 2947 (1985).

T. SUZUKI, K. HAKUTA, S. SAITO, and E. HIROTA' "Doppler-Limited Dye Laser Excitation Spectroscopy of the $\tilde{A}^1A''(000)$–$\tilde{X}^1A'(000)$ Band of HSiF.", *J. Chem. Phys.*, **82**, 3580 (1985).

T. SUZUKI, S. SAITO, and E. HIROTA, "Dipole Moments of H_2CS in the $\tilde{A}^1A_2$ (v=0) and $\tilde{a}^3A_2$ (ν_3=1) States by MODR Spectroscopy.", *J. Mol. Spectrosc.*, **111**, 54 (1985).

K. OHNO, H. MATSUURA, Y. ENDO, and E. HIROTA, "The Microwave Spectra of Deuterated Silanes: SiH_3D, SiH_2D_2, and $SiHD_3$.", *J. Mol. Spectrosc.*, **111**, 73 (1985).

K. KAWAGUCHI, S. SAITO, E. HIROTA, and N. OHASHI, "Far-Infrared Laser Magnetic Resonance Detection and Microwave Spectroscopy of the PO_2 Radical.", *J. Chem. Phys.*, **82**, 4893 (1985).

K. TAKAGI, T. SUZUKI, S. SAITO, and E. HIROTA, "Microwave Optical Double Resonance of HNO: Dipole Moment of HNO in $\tilde{A}^1A''(100)$.", *J. Chem. Phys.*, **83**, 535 (1985).

C. YAMADA, H. KANAMORI, and E. HIROTA, "Direct Observation of the Fine Structure Transitions in the Ne^+ and Ar^+ Ions with Diode Lasers.", *J. Chem. Phys.*, **83**, 552 (1985).

H. KANAMORI, J.E. BUTLER, K. KAWAGUCHI, C. YAMADA, and E. HIROTA, "Spin Polarization in SO Photochemically Generated from SO_2.", *J. Chem. Phys.*, **83**, 611 (1985).

K. KAWAGUCHI and E. HIROTA, "Diode Laser Spectroscopy of CF^+.", *J. Chem. Phys.*, **83**, 1437 (1985).

S. HASHIMOTO, Y. TATSUNO and T. KITAGAWA, "Resonance Raman Evidence for the Presence of the Fe^{IV}=0 Bond in Horseradish Peroxidase Compound II", *Proc. Japan Acad.* **60** Ser. B, 345 (1984).

S. MATSUKAWA, K. MAWATARI, Y. YONEYAMA and T. KITAGAWA, "Correlation between the Iron-Histidine Stretching Frequencies and Oxygen Affinity of Hemoglobins; A Continuous Strain Model", *J. Am. Chem. Soc.* **107**, 1108 (1985).

K. KAMOGAWA and T. KITAGAWA, "Solute/Solvent and Solvent/Solvent Interactions in Methanol Solutions: Quantitative Separation by Raman Difference Spectroscopy", *J. Phys. Chem.* **89**, 1531 (1985).

A. MAEDA, T. OGURUSU, T. YOSHIZAWA and T. KITAGAWA, "Resonance Raman Study on Binding of Chloride to the Chromophore of Halorhodopsin", *Biochemistry* **24**, 2517 (1985).

Y. OZAKI, T. KITAGAWA, H. OGOSHI, T. OCHIAI and K. IRIYAMA, "Comparative Study of Metallochlorins and Metalloporphyrins by Resonance Raman Spectroscopy", *Rev. Port. Cuim.* **27**, 340 (1985).

K. TOHJI, Y. UDAGAWA, S. TANABE, T. IDA and A. UENO, "Catalyst Preparation Procedure Probed by EXAFS Spectroscopy II. Cobalt on Titania", *J. Am. Chem. Soc.* **106**, 5178 (1984).

S. TANABE, T. IDA, A. UENO, Y. KOTERA, K. TOHJI and Y. UDAGAWA, "Size Control of Iron Particles Dispersed in SiO_2 Support", *Chem. Lett.*, 1567, (1984).

Y. UDAGAWA, K. TOHJI, A. UENO and T. IDA, "Catalyst Preparation Procedures Probed by EXAFS Spectroscopy", *EXAFS and Near Edge Structure III.* 206 (Springer, 1984).

Y. UDAGAWA and K. TOHJI, "Laboratory EXAFS Spectrometer and a Fast Detection System", *EXAFS and Near Edge Structure III.* 520 (Springer, 1984).

Y. UDAGAWA and K. TOHJI, "EXAFS Measurement by Bent Crystal Monochromators (in Japanese)", *J. Cryst. Soc. Jpn.* 27, 205 (1985).

H. NOMURA, K. MURASAWA, N. ITO, F. IIDA and Y. UDAGAWA, "Pressure Effects on Conformational Equilibria of 1, 2-dichloroethane and 1, 2-dibromoethane by means of Raman Spectroscopy", *Bull. Chem. Soc. Jpn.* 57, 3321 (1984).

H. NOMURA, Y. UDAGAWA and K. MURASAWA, "Pressure and Temperature Effects of the Conformational Equilibria between the Rotational Isomers of sec- and iso-butyl halide", *J. Mol. Structure* **126**, 229 (1985).

K. YOSHIHARA, D.V. O'CONNOR, M. SUMITANI, Y. TAKAGI and N. NAKASHIMA' "Single Vibrational Level Dependence of Picosecond Fluorescence in the Channel 3 Region of Benzene", in *"Application of Picosecond Spectroscopy to Chemistry", NATO ASI Series C, Mathematical and Physical Sciences* Vol. 127, p. 261, Ed. K. B. Eisenthal, D. Reidel, Dordrecht, (1984).

K. YOSHIHARA, M. SUMITANI, D. V. O'CONNOR, Y. TAKAGI and N. NAKASHIMA, "Intramolecular Electronic and Vibrational Redistribution and Chemical Transformation in Isolated Large Molecules—S_1 Benzene", in *"Ultrafast Phenomena IV"*, p.345, Ed. D. H. Auston and K. B. Eisenthal, Springer, New York, (1984).

T. ICHIMURA, Y. MORI, N. NAKASHIMA and K. YOSHIHARA, "Formation of Hot Hexafluorobenzene in the 193 nm Photolysis", *Chem. Phys. Lett.*, **104**, 533 (1984).

N. NAKASHIMA, N. SHIMO, N. IKEDA and K. YOSHIHARA, "Direct Measurements of Formation Rates of Allylic Radicals from Ethylene Derivatives", *J. Chem. Phys.*, **81**, 3738 (1984).

N. IKEDA, N. NAKASHIMA and K. YOSHIHARA, "Formation and Relaxation of Hot Benzyl Radical in the Gas Phase", *J. Phys. Chem.*, 88, 5803 (1984).

Y. FUJIMURA, M. ARAI, N. NAKASHIMA and K. YOSHIHARA, "Theory of Time-Resolved Photon Absorption by Molecules after Radiationless Transition: Application to Benzene after $S_2 \rightarrow S_0$", *Bull. Chem. Soc. Jpn.*, 57, 2947 (1984).

H. SHIZUKA, K. OKAZAKI, M. TANAKA, M. ISHIKAWA, M. SUMITANI and K. YOSHIHARA, "Intramolecular $2p\pi^* \rightarrow 3d\pi$ Charge Transfer in the Excited State of Phenyldisilane Studied by Picosecond and Nanosecond Laser Spectroscopy", *Chem. Phys. Lett.*, **113**, 89 (1985).

M. SUMITANI, D. V. O'CONNOR, Y. TAKAGI, N. NAKASHIMA, K. KAMOGAWA, Y. UDAGAWA and K. YOSHIHARA, "Channel Three Decay in Benzene: A Picosecond Fluorescence Investigation", *Chem.*

Phys., **93**, 359 (1985).

D. V. O'CONNOR, M. SUMITANI, Y. TAKAGI, N. NAKASHIMA, K. KAMOGAWA, Y. UDAGAWA and K. YOSHIHARA, "Channel Three Decay in C_6D_6", *Chem. Phys.*, **93**, 373 (1985).

Y. KAIZU, K. MIYAKAWA, K. OKADA, H. KOBAYASHI, M. SUMITANI and K. YOSHIHARA, "Aqualigand Dissociation of $[Ce(OH_2)_9]^{3+}$ in the 5d ← 4f Excited State", *J. Am. Chem. Soc.*, **107**, 2622 (1985).

T. ICHIMURA, K. NAHARA, Y. MORI, M. SUMITANI and K. YOSHIHARA, "Triplet Lifetime of Chlorotoluenes in the Vapor Phase Studied by Time-Resolved and Stationary Photosensitized Phosphorescence", *Chem. Phys.*, **95**, 9 (1985).

M. NODA, N. HIROTA, M. SUMITANI and K. YOSHIHARA, "Proton Transfer Tautomerism in the Excited State of Indazole in Acetic Acid: Tautomerization via Double Proton Switching", *J. Phys. Chem.*, **89**, 399 (1985).

N. IKEDA, N. NAKASHIMA and K. YOSHIHARA, "Photochemistry of Toluene Vapor at 193 nm. Direct Measurements of Formation and Dissociation Rate", *J. Chem. Phys.*, **82**, 5285 (1985).

N. IKEDA, N. NAKASHIMA and K. YOSHIHARA, "Observation of the Ultraviolet Absorption Spectrum of Phenyl Radical in the Gas Phase", *J. Am. Chem. Soc.*, **107**, 3381 (1985).

K. KASATANI, M. KAWASAKI, H. SATO and N. NAKASHIMA, "Micellized Sites of Dyes in Sodium Dodecyl Sulfate Micelles as Revealed by Time-Resolved Energy-Transfer Studies", *J. Phys. Chem.*, **89**, 542 (1985).

I. ICHIMURA, Y. MORI, N. NAKASHIMA and K. YOSHIHARA, "ArF Laser Photolysis of Hexafluorobenzene Vapor: Formation of Hot Molecules and Their Collisional Relaxation", *J. Chem. Phys.*, **83**, 117 (1985).

T. SAKATA, K. HASHIMOTO and T. KAWAI, "Catalytic Properties of Ruthenium Oxide on n-Type Semiconductors under Illumination", *J. Phys. Chem.*, **88**, 5214 (1984).

T. SAKATA, "Photocatalysis of Irradiated Semiconductor Surfaces: Its Application to Water Splitting and Some Organic Reactions", *J. Photochem.*, **29**, 205 (1985).

K. HASHIMOTO, T. KAWAI and T. SAKATA, "The Mechanism of Photocatalytic Hydrogen Production with Halogenated Fluorescein Derivatives", *Nouv. J. Chim.*, **8**, 693 (1984).

K. HASHIMOTO, T. SAKATA, Y. OZAKI, M. YOSHIURA and K. IRIYAMA, "Transient Photocurrent and Luminescence Lifetime in the Photodiode of Merocyanine Dye Thin Film", *Nippon Kagaku Kaishi*, 1178 (1985).

R.H. WILSON, T. SAKATA, T. KAWAI and K. HASHIMOTO, "Analysis of the Transient Response of a Semiconductor-Electrolyte Circuit to a Short Light Pulse: Application to CdSe Electrodes", *J. Electrochem Soc.*, **132**, 1082 (1985).

H. HARADA, T. SAKATA and T. UEDA, "Effect of Semiconductor on Photocatalytic Decomposition of Lactic Acid", *J. Am. Chem. Soc.*, **107**, 1773 (1985).

W. JAEGERMANN, T. SAKATA, E. JANATA and H. TRIBUTSCH, "Laser-Pulse Photocurrent Transient Measurements at Oxygen Evolving n-PtS_2", *J. Electroanal. Chem.*, **189**, 65 (1985).

M. BABA and I. HANAZAKI, "The $S_1(n, \pi^*)$ States of Cyclopentanone and Cyclobutanone in Supersonic Nozzle Beam", *J. Chem. Phys.*, **81**, 5426 (1984).

M. BABA, U. NAGASHIMA and I. HANAZAKI, "Barrier Height to Inversion of Aliphatic Carbonyl Compounds in the $S_1(n, \pi^*)$ State; *Ab initio* Study of Formaldehyde", *Chem. Phys.*, **93**, 425 (1985).

M. BABA, I. HANAZAKI and U. NAGASHIMA, "The $S_1(n, \pi^*)$ States of Acetaldehyde and Acetone in Supersonic Nozzle Beam; Methyl Internal Rotation and C=O Out-of-plane Wagging", *J. Chem. Phys.*, **82**, 3938 (1985).

I. NISHIYAMA and I. HANAZAKI, "Infrared Photodissociation of Benzene Dimer; Translational Energy Distribution of Dissociation Fragment", *Chem. Phys. Lett.*, **117**, 99 (1985).

T. OKUYAMA and N. NISHI, "Photochemical Reactions in Molecular Solids Containing CH_3CN and NH_3 Studied by UV Laser Photodesorption of Surface Molecules", *Nippon Kagaku Kaishi*, 1506 (1984).

M. KAWASAKI, K. KASATANI, H. SATO, H. SHINOHARA and N. NISHI, "Photodissociation of Cl_2SO at 248 and 193 nm in a Molecular Beam", *Chem. Phys.*, **91**, 285 (1984).

M. UMEMOTO, K. SEKI, H. SHINOHARA, U. NAGASHIMA, N. NISHI, M. KINOSHITA and R. SHIMADA, "Photofragmentation of Mono- and Dichloroethylenes: Translational Energy Measurement of Recoiling Cl and HCl Fragments", *J. Chem. Phys.*, 83, 1657.

A. NISHIYA, N. HIROTA, H. SHINOHARA and N. NISHI, "Identification of Ammonia Clusters in Low Temperature Matrices Using FTIR Short-Pulsed Matrix Isolation Technique", *J. Phys. Chem.*, 89, 2260 (1985).

H. SHINOHARA, N. NISHI and N. WASHIDA, "Photoionization of Unprotonated Cluster Ions $(NH_3)_n^+$, n= 2–25", *J. Chem. Phys.*, 83, 1939 (1985).

R.J. DONOVAN and N. NISHI, "Time-of-flight Photofragmentation Study of IBr", *Chem. Phys. Lett.*, 117, 286 (1985).

Y. TANIMOTO, M. TAKASHIMA, M. UEHARA, M. ITOH, M. HIRAMATSU, R. NAKAGAKI, T. WATANABE and S. NAGAKURA, "Magnetic Field Effect on the Intramolecular Hydrogen Abstraction Reaction of *n*-Tetradecyl Anthraquinone-2-carboxylate.", *Chem. Lett.* 1985, 15.

T. WATANABE, Y. TANIMOTO, T. SAKATA, R. NAKAGAKI, M. HIRAMATSU and S. NAGAKURA, "The Magnetic Field Effects on the Electrolysis of Hexacyanoferate (II) Oxidation and Hexacyanoferate (III) Reduction.", *Bull. Chem. Soc. Jpn.*, 58, 1251 (1985).

Y. TANIMOTO, T. WATANABE, R. NAKAGAKI, M. HIRAMATSU and S. NAGAKURA, "Magnetic Field Effects on Photoionization of N,N,N',N'-Tetramethyl-*p*-phenylenediamine in 2-Propanol.", *Chem. Phys. Lett.*, 116, 341 (1985).

S. NAGAKURA, "Mulliken's Charge-Transfer Theory and Its Application to Chemical Reactions.", *Mol. Cryst. Liq. Cryst.*, 126, 9 (1985).

R. NAKAGAKI, M. HIRAMATSU, K. MUTAI and S. NAGAKURA, "Photo-Smiles Rearrangement (IV) Electron-Transfer Mechanism of an Intramolecular Aromatic Nucleophilic Substitution.", *Mol. Cryst. Liq. Cryst.*, 126, 69 (1985).

R. NAKAGAKI, M. HIRAMATSU, T. WATANABE, Y. TANIMOTO and S. NAGAKURA, "Magnetic Isotope and External Magnetic Field Effects upon the Photo-Fries Rearrangement of 1-Naphthyl Acetate.", *J. Phys. Chem.*, 89, 3222 (1985).

K. SEKI, U.O. KARLSSON, R. ENGERLHARDT and E.E. KOCH, "Intramolecular Band Mapping of Poly (p-phenylene) via UV Photoelectron Spectroscopy of Finite Polyphenyls", *Chem. Phys.* 91, 459 (1984).

S.X. CHEN, K. SEKI, H. INOKUCHI, S. HASHIMOTO, N. UENO and K. SUGITA, "Ultraviolet Photoelectron Spectroscopy of Some Fundamental Vinyl Polymers and the Evolution of Their Electronic Structures", *Bull. Chem. Soc. Jpn.*, 58, 890 (1985).

H. PULM, B. MARQUARDT, H. -J. FREUND, R. ENGELHARDT, K. SEKI, U. KARLSSON, E.E. KOCH and W. von NIESSEN, "Photoionization Study of the CN-anion: A study of the NaCN(001) Surface in Comparison with CO and N_2", *Chem. Phys.*, 92, 457 (1985).

K. ISHII, K. YAKUSHI, H. KURODA and H. INOKUCHI, "Reflection and Photoconduction Spectra of the Single Crystals of Perylene-TCNQ 1:1 and 3:1 Molecular Complexes", *Bull. Chem. Soc. Jpn.*, 57, 3043 (1984).

T.B. TANG, H. INOKUCHI, S. SAITO, C. YAMADA and E. HIROTA, "CCCO Generation by DC Glow Discharge in Carbon Suboxide and Microwave Spectrum", *Chem. Phys. Lett.*, 116, 83 (1985).

K. KIMURA, H. INOKUCHI, H. NANAMI and T. YAGI, "Magnetic Susceptibility of Hydrogenase from Desulfovibrio vulgaris", *J. Biochem.*, 97, 1831 (1985).

K. KIMURA, S. NAKAJIMA, K. NIKI and H. INOKUCHI, "Determination of Formal Potentials of Multihemoprotein, Cytochrome c_3 by ^1H Nuclear Magnetic Resonance", *Bull. Chem. Soc. Jpn.*, 58, 1010 (1985).

T. YAGI, K. KIMURA and H. INOKUCHI, "Analysis of the Active Center of Hydrogenase from Desulfovibrio vulgaris Miyazaki by Magnetic Measurements", *J. Biochem.*, 97, 181 (1985).

H. MURAKAMI, M. SANO, I. KANAZAWA, T. ENOKI, T. KURIHARA, Y. SAKURAI and H. INOKUCHI, "Chemisorption of Hydrogen into a Graphite-Potassium Intercalation Compound C_8K Studied by Means of Positron-Annihilation", *J. Chem. Phys.*, 85, 4728 (1985).

M. KOBAYASHI, T. ENOKI, H. INOKUCHI, M. SANO, A. SUMIYAMA, Y. ODA and H. NAGANO, "Superconductivity in the First Stage Rubidium Graphite Intercalation Compound C_8Rb", *J. Phys. Soc. Jpn.*, **54**, 2359 (1985).

H. BANDOW, K. KAJIMURA, H. ANZAI, T. ISHIGURO and G. SAITO, "Superconducting Tunneling in $(TMTSF)_2ClO_4$/α-Si/Pb Junctions", *Mol. Cryst. Liq. Cryst.*, **119**, 41 (1985).

K. MURATA, H. BANDO, K. KAJIMURA, T. ISHIGURAO, H. ANZAI, S. KAGOSHIMA and G. SAITO, "Transverse Magnetoresistanse of $(TMTSF)_2C10_4$ in Intermediate Field Region", *Mol. Cryst. Liq. Cryst.*, **119**, 131 (1985).

G. SAITO, T. ENOKI, M. KOBAYASHI, K. IMAEDA, N. SATO and H. INOKUCHI, "Chemical and Physical Properties of Cation Radical Salts of BEDT-TTF", *Mol. Cryst. Liq. Cryst.*, **119**, 393 (1985).

G. SAITO, H. KUMAGAI, J. TANAKA, T. ENOKI and H. INOKUCHI, "Organic Metals Based on Hexamethylenetetratellurafulvalene (HMTTeF)", *Mol. Cryst. Liq. Cryst.*, **120**, 337 (1985).

G. SAITO, H. HAYASHI, T. ENOKI and H. INOKUCHI, "The Study of Charge Transfer Complexes of BEDT-TTF Derivatives", *Mol. Cryst. Liq. Cryst.*, **120**, 341 (1985).

G. SAITO, T. ENOKI, H. INOKUCHI, H. KUMAGAI, C. KATAYAMA and J. TANAKA, "Crystal Structures and Electrical Properties of Hexacyanobutadine (HCBD) Charge Transfer Complexes", *Mol. Cryst. Liq. Cryst.*, **120**, 345 (1985).

N. UYEDA, T. KOBAYASHI, K. ISHIZUKA, Y. FUJIYOSHI, H. INOKUCHI and G. SAITO, "Direct Molecular Imaging of Low Dimensional Solids by High Resolution Electron Microscopy", *Mol. Cryst. Liq. Cryst.*, **125**, 103 (1985).

H. KOBAYASHI, R. KATO, T. MORI, A. KOBAYASHI, Y. SASAKI, G. SAITO and H. INOKUCHI, "Organic Conductors Based on Multi-Sulfur -Donor and/or -Acceptor Molecules—BEDT-TTF, BMDT-TTF, BPDT-TTF, and $M(dmit)_2$—", *Mol. Cryst. Liq. Cryst.*, **125**, 125 (1985).

C. KATAYAMA, M. HONDA, H. KUMAGAI, J. TANAKA, G. SAITO and H. INOKUCHI, "Crystal Structures of Complexes between Hexacyanobutadiene and Tetramethyltetrathiafulvalene and Tetramethylthiotetrathiafulvalene", *Bull. Chem. Soc. Jpn.*, **58**, 2272 (1985).

K. HONMA, T. KATO, K. TANAKA and I. KOYANO, "State Selected Ion-Molecule Reactions by a TESICO Technique. IX. Vibrational State Dependence of the Cross Sections in the Reaction $C_2H_2^+(v_2) + D_2(H_2)$.", *J. Chem. Phys.* **81**, 5666 (1984).

K. TANAKA, T. KATO and I. KOYANO, "Mode Specificity in the Reaction $C_2H_4^+(v_2, v_4) + C_2H_4 \rightarrow C_3H_5^+ + CH_3$.", *85h Int. Sym. on Gas Kinet.* (nottingham, 1984) L2.

K. TANAKA, T. KATO, I. KOYANO, N. TAKAHASHI, T. MORIYA and K. TESHIMA, "Velocity Distribution and Velocity Slip in Supersonic Rare Gas Beams. Atoms from Binary and Clusters from Pure Sources.", *Rarefied Gas Dynamics,* H. Oguchi Ed., Univ. of Tokyo Press, pp.751–758 (1984).

Y. ACHIBA and K. KIMURA, "Photoelectron Spectroscopy on Dynamic Behavior of Excited Molecules", *Nippon Kagaku Kaishi* (The Chemical Society of Japan; in Japanese), 1529 (1984).

A. HIRAYA, Y. ACHIBA, K. KIMURA and E.C. Lim, "Identification of the Lowest Energy $n\pi^*$ States in Polycyclic Monoazines: Quinoline and Isoquinoline", *J. Chem. Phys.*, **81**, 3345 (1984).

A. HIRAYA, Y. ACHIBA, N. MIKAMI and K. KIMURA, "Multiphoton Ionization Photoelectron Spectroscopic Study on Intramolecular Relaxation Processes of Naphthalene", *J. Chem. Phys.*, **82**, 1810 (1985).

M. KAWASAKI, K. KASATANI, H. SATO, Y. ACHIBA, K. SATO and K. KIMURA, "Multiphoton Ionization of Triethylamine: Determination of the Vibrationless S_2 Level by Laser Photoelectron Spectroscopy", *Chem. Phys. Lett.*, **114**, 473 (1985).

Y. ACHIBA, K. SATO and K. KIMURA, "Multiphoton Ionization Photoelectron Spectroscopic Study on NO: Autoionization Pathway through Dissociative Super-Excited Valence States", *J. Chem. Phys.*, **82**, 3959 (1985).

S. TOMODA and K. KIMURA, "Do We Observe the "Adiabatic" Ionizations of the Water Dimer?—An Interpretation of the Threshold Ionization Energy and the Nature of the Ionic States", *Chem. Phys. Lett.*, **111**, 434 (1984).

K. TABAYASHI, S. OHSHIMA and K. SHOBATAKE, "Arc-Heated Atomic Nitrogen Beam Source for Crossed Molecular Beam Experiments", *Proceedings of the 14th Int. Symp. on Rarefied Gas Dynamics*, **14**, 635 (1984).

T. FUJIMOTO, S. KATO, and K. SHOBATAKE, "An Experimental Study of Translational Exchange on a Ceramic Surface by the Method of Argon Molecular Beam", *Trans. Jpn. Soc. Mech. Eng.* (in Japanese), **B51** 356 (1985).

T. NAGATA, T. KONDOW, K. KUCHITSU, K. TABAYASHI, S. OHSHIMA and K. SHOBATAKE, "Polarization of $CN(B^2\Sigma^+-X^2\Sigma^+)$ Emission Produced in Collision of $Ar(^3P_{0,2})$ with BrCN", *J. Phys. Chem.*, **89**, 2916 (1985).

N. WASHIDA, Y. MATSUMI, T. HAYASHI, T. IBUKI, A. HIRAYA and K. SHOBATAKE, "Emission Spectra of $SiH(A^2\Delta \rightarrow X^2\Pi)$ and $SiCl_2(\tilde{A}^1B_1 \rightarrow \tilde{X}^1A_1)$ in the VUV Photolyses of Silane and Chlorinated Silanes." *J. Chem. Phys.*, **83**, 2769 (1985).

N. IWASAKI, S. KURIHARA, I. SHIROTANI, M. KINOSHITA and Y. MARUYAMA, "Negative Magnetoresistance and Anderson Localization in Black Phosphorus Single Crystals.", *Chem. Lett.*, **1985**, 119.

N. IWASAKI, R. HORIGUCHI and Y. MARUYAMA, "Fluorescence Spectra of Anthracene Liquid.", *Bull. Chem. Soc. Jpn.*, **58**, 2409 (1985).

T. INABE, T.J. MARKS, R.L. BURTON, J.W. LYDING, W.J. McCARTHY, C.R. KANNEWURE, G.M. REISNER and F.H. HERBSTEIN, "Highly Conductive Metallophthalocyanine Assemblies. Structure, Charge Transport, and Anisotropy in the Metal-Free Molecular Metal $H_2(Pc)I$.", *Solid State Commun.*, **54**, 501 (1985).

S.H. BAUER, T. YAMAZAKI, K.I. LAZAAR and N.-S. CHIU, "Intramolecular Conversion over a Low Barrier. 3. Gas-Phase NMR Studies of an H-Bond Association", *J. Amer. Chem. Soc.*, **107**, 743 (1985).

T. SUGAWARA, S. BANDOW, K. KIMURA, H. IWAMURA and K. ITOH, "Magnetic Behavior of Nonet Tetracarbene, *m*-Phenylenebis ((diphenylmethylen-3-yl) methylene)", *J. Am. Chem. Soc.*, **106**, 6449 (1984).

S. NAGAOKA, N. HIROTA, M. SUMITANI, K. YOSHIHARA, E. LIPCZYNSKA-KOCHANY and H. IWAMURA, "Investigation of the Dynamic Processes of the Excited States of o-Hydroxybenzaldehyde and Its Derivatives. II. Effects of Structural Changes and Solvent", *J. Am. Chem. Soc.*, **106**, 6913 (1984).

A. IZUOKA, S. MURATA and H. IWAMURA, "7-Diazo-7*H*-benz[*de*]anthracene and 7*H*-Benz[*de*]anthracen-7-ylidene", *Bull. Chem. Soc. Jpn.*, **57**, 3526 (1984).

T. NAKANISHI, T. SEIMIYA, T. SUGAWARA and H. IWAMURA, "Interaction of Chloride Ions with Nonionic Surfactant as Mediated by Inorganic Cations Incorporated in Surfactant Micelles", *Chemistry Lett.*, 2135 (1984).

K. TAKAGI, K. AOSHIMA, Y. SAWAKI and H. IWAMURA, "Electron-Relay Chain Mechanism in the Sensitized Photoisomerization of Stilbazole Salts in Aqueous Anionic Micelles", *J. Am. Chem. Soc.*, **107**, 47 (1985).

T. SUGAWARA and H. IWAMURA, "Photochemistry of 1-Azatriptycene", *J. Am. Chem. Soc.*, **107**, 1329 (1985).

N. KOGA and H. IWAMURA, "Barrier to Coupled Internal Rotation in Di-9-triptycyl Ether. Kinetics of Intramolecular Exciplex Formation in racemic 2,3-Benzo-9-triptycyl 2-[(Dimethylamino)-methyl]-9- triptcyl Ether", *J. Am. Chem. Soc.*, **107**, 1426 (1985).

A. IZUOKA, S. MURATA, T. SUGAWARA and H. IWAMURA, "Ferro- and Antiferromagnetic Interaction between Two Diphenylcarbene Units Incorporated in the [2.2]Paracyclophane Skeleton", *J. Am. Chem. Soc.*, **107**, 1786 (1985).

R.D. McKELVEY, T. SUGAWARA and H. IWAMURA, "Structure at the Anomeric Center in 2-Alkoxytetrahydropyrans and Their Radicals, Studied by ^{13}C Coupling in NMR and ESR Spectra", *Magn. Reson. Chem.*, **23**, 330 (1985).

R.D. McKELVEY and H. IWAMURA, "Anomeric Effect in Hydrogen Abstraction Reactions of Conformationally Fixed 2-Alkoxytetrahydropyrans", *J. Org. Chem.*, **50**, 402 (1985).

H. IWAMURA, T. SUGAWARA, K. ITOH and T. TAKUI, "High-spin Polycarbenes as a Model for Organic Ferromagnets", *Mol. Cryst. Liq. Cryst.* **125**, 251 (1985).

Y. TEKI, T. TAKUI, H. YAGI, K. ITOH and H. IWAMURA, "Electron Spin Resonance Line Shapes of Randomly Oriented Molecules in Septet and Nonet States by Perturbation Approach", *J. Chem. Phys.*, 83, 539 (1985).

K. TAKAGI, T. FUJIOKA, Y. SAWAKI and H. IWAMURA, "An ^{18}O-Tracer Study on the TiO_2-Sensitized Photooxidation of Aromatic Compounds", *Chemistry Lett.*, 913 (1985).

K. ISHIGURO, K. TOMIZAWA, Y. SAWAKI and H. IWAMURA, "^{18}O-Tracer Study on the Rearrangement of Carbonyl Oxide Intermediates to Esters", *Tetrahedron Lett.*, **26**, 3723 (1985).

Y. KITAMURA, T. ITO and M. KATO, "Piezochromism of Nickel(II) Complexes with Tetraaza Macrocyclic Ligands in Water", *Inorg. Chem.*, **23**, 3836 (1984).

V. GOEDKEN, H. ITO and T. ITO, "An Unusually Stable Al-Alkyl Bond: Synthesis and Reactivity Studies of the Macrocyclic $Al(C_{22}H_{22}N_4)C_2H_5$ Complex", *J. Chem. Soc., Chem. Commun.*, **1984**, 1453.

S. YANO, Y. SAKAI, K. TORIUMI, T. ITO, H. ITO and S. YOSHIKAWA, "Reaction of Metal Complexes with Carbohydrates: Isolation and Characterization of Novel Nickel(II) Complexes Containing N-Glycoside Ligands Derived from Amino Sugars." *Inorg. Chem.*, **24**, 498 (1985).

M. KATO and T. ITO, "Facile CO_2 Uptake by Zn(II)-tetraazacycloalkane Complexes. 1. Syntheses, Characterizations and Chemical Properties of Monoalkylcarbonato(tetraazacycloalkane)zinc(II) Complexes. *Inorg. Chem.*, **24**, 504 (1985).

M. KATO and T. ITO, "Facile CO_2 Uptake by Zn(II)-tetraazacycloalkane Complexes. 2. X-ray Structural Studies of μ-Monomethylcarbonato(1,4,8,11-tetraazacyclotetradecane)zinc(II) Perchlorate, $Zn(O_2COCH_3)([14]aneN_4)(ClO_4)$, Di-$\mu$-monomethylcarbonato-tris [(1,4,8,12-tetraazacyclopentadecane)zinc(II)] Perchlorate, $[\{Zn([15]aneN_4)\}_3(O_2COCH_3)_2](ClO_4)_4$, and (Monomethylcarbonato)(1,4,8,11-tetramethyl-1,4,8,11-tetraazacyclotetradecane)zinc(II) Perchlorate, $[Zn(O_2COCH_3)(Me_4[14]aneN_4)](ClO_4)$", *Inorg. Chem.*, **24**, 509 (1985).

M. MIKURIYA, K. TORIUMI, T. ITO and S. KIDA, "Temperature Dependence of Structure and Magnetic Interaction in a Dialkoxo-bridged Binuclear Copper(II) Complex, Dichloro-bis$\{\mu$-$\{$2-[2-(dipropylamino)-ethylthio] ethanolato$\}$ –N, S, μ-O$\}$ dicopper (II)", *Inorg. Chem.*, **24**, 629 (1985).

S. ONAKA, Y. KONDO, M. YAMASHITA, Y. TATEMATSU, Y. KATO, M. GOTO and T. ITO, "Metal-Metal Bonds Extended over a Porphyrin Ring. 1. Syntheses of (TPP)Sn-$M(CO)_{n-1}$-Hg-$M(CO)_n$ and (TPP)In-$M(CO)_n$ ($M(CO)_n$=$Mn(CO)_5$, $Co(CO)_4$) and X-ray Molecular Structure Analysis of (TPP)Sn-$Mn(CO)_4$-Hg-$Mn(CO)_5 \cdot 1/2CH_2Cl_2$", *Inorg. Chem.*, **24**, 1070 (1985).

H. ITO and T. ITO, "Dialkylcarbamato Complexes of Ni(II), Zn(II) and Cd(II)-tetraazacycloalkanes Obtained from CO_2-Uptake, and X-ray Structure of Diethylcarbamato-7RS,14RS-5,5,7,12,12,14-hexamethyl-1,4,8,11-tetraazacyclotetradecanenickel(II) Perchlorate", *Bull. Chem. Soc. Jpn.*, **58**, 1755 (1985).

H. ITO and T. ITO, "Synthesis and Structure of (Nitroacetato) ((7RS, 14RS)-5,5,7,12,12,14-hexamethyl-1,4,8,11-tetraazacyclotetradecane)nickel(II), $[Ni(na)(Me_6[14]aneN_4]$", *Bull. Chem. Soc. Jpn.*, **58**, 2133 (1985).

M. YAMASHITA, I. MURASE, T. ITO, Y. WADA, T. MITANI and I. IKEMOTOTO, "X-Ray Photoelectron Spectra and Electrical Conductivities of One-dimensional Halogen-bridged Pd(II)–Pt(IV) and Ni(II)–Pt(IV) Mixed-valence Complexes", *Bull. Chem. Soc. Jpn.*, **58**, 2236 (1985).

M. YAMASHITA, I. MURASE, I. IKEMOTO and T. ITO, "The Chloro-bridged One-dimensional Nickel(II)-Nickel(IV) Mixed-valence Complex Obtained from Disproportionation Reaction of the Nickel(III) Complex in $(CH_3OCH_3)(HBF_4)$", *Chem. Lett.*, **1985**, 1133.

H. ITO and T. ITO, "Syntheses, Characterization, and Moleclar Structures of Nitroalkanato Nickel(II), Zinc(II), and Cadmium(II) Complexes with Tetraazacycloalkanes", *Chem. Lett.*, **1985**, 1251.

Y. MORIOKA, K. TORIUMI, T. ITO, A. SAITO and I. NAKAGAWA, "Crystal Structures of the Room- and Low-Temperature Phases of Monoclinic Potassium Ferricyanide", *J. Phys. Soc. Jpn.*, **54**, 2184 (1095).

M. GOTO, K. MORI, Y. KURODA, T. SAKAI and T. ITO, "Isolation of a Novel Oxygenated Dimer of 3-Methylindole, 5aβ(H),11aα(H)-12β-Hydroxy-10bβ,12α-dimethyl-5a,10b,11a,12-tetrahydro-6H-oxazolo [3,2-a:4,5-b'] diindole, and Structure Determination of Its Acethylated Derivative", *Chem. Pharm. Bull.*, **33**, 1878 (1985).

K. TORIUMI, T. KANAO, M. YAMASHITA, Y. UMETSU, M. KATO, A. OHYOSHI and T. ITO, "Structural Study of One-Dimensional Ni(II)-Ni(IV) Mixed Valence Complexes by Means of EXAFS", *Photon Factory Activity Report*, VI-68 (1983/84).

M. YAMASHITA, K. TORIUMI and T. ITO, "Structure of a Bromo-Bridged One-Dimensional Pd^{II}-Pd^{IV} Mixed-Valence Complex, catena-μ-Bromo-bis(ethylenediamine)palladium(II, IV) Diperchlorate, $[Pd(C_2H_8N_2)_2][PdBr_2(C_2H_8N_2)_2](ClO_4)_4$", *Acta Cryst.*, C41, 876 (1985).

H. WATANABE, H. IWASAKI and H. TAKEI, "Structure of the Primitive Tetragonal $ErRh_4B_4$", *Acta Cryst.*, C40, 1644 (1984).

M. KIKUCHI, K. HIRAGA, Y. SHONO and H. TAKEI, "Observation of Shocked and Unshocked $BaZnGeO_4$ by Means of Electron Microscopy", *Solid State Chem.*, 51, 390 (1985).

S. TERO-KUBOTA, N. HOSHINO, M. KATO, V.L. GOEDKEN and T. ITO, "Photochemical Cleavage of the Al-C Bond of Al(TPP)(Et) (TPP = tetraphenylporphyrinato). Spin Trapping of the ·Al(TPP) Radical and Photolysis Quantum Yield", *J. Chem. Soc. Chem. Commun.*, 959 (1985).

M. NISHIZAWA, Y. SASAKI and K. SAITO, "Kinetics and Mechanisms of the Outer-Sphere Oxidation of *cis*-Aquaoxovanadium(IV) Complexes Containing Quadridentate Amino Polycarboxylates. Interpretation of the Difference in Activation Parameters with the Charge Type of Reactants", *Inorg. Chem.* 24, 767 (1985).

Y. SASAKI, M. KANESATO, K. OKAZAKI, A. NAGASAWA and K. SAITO, "Kinetics of the Oxidation of an Ethylenediaminetetraacetate Complex of the Oxovanadium(IV) Ion with Hexachloroiridate(IV) in Aqueous Solution", *Inorg. Chem.* 24, 772 (1985).

M. ATOH, K. KASHIWABARA, H. ITO, T. ITO and J. FUJITA, "Preparation and Characterization of $[CoX_2(edpp)_2]^+$ (edpp = $NH_2CH_2CH_2P(C_6H_5)_2$, X = Cl^-, Br^-, I^-, NCO^-, NCS^-, N_3^-, NO_2^-) and $[CoX_2(en)(dppe)]^+$ (en = $NH_2CH_2CH_2NH_2$, dppe = $(C_6H_5)_2PCH_2CH_2P(C_6H_5)_2$, X = Cl^-, Br^-, NCS^-). Crystal Structures of *trans*(NCS, NCS), *cis*(P, P)–$[Co(NCS)_2(edpp)_2]$ $Br \cdot 3H_2O \cdot (CH_3)_2CO$ and *cis*(NCS, NCS), *trans*(P, P)–$[Co(NCS)_2(edpp)_2]$ $Br \cdot CH_3OH$", *Bull. Chem. Soc. Jpn.*, 57, 3139 (1984).

M. TAKATA, K. KASHIWABARA, H. ITO, T. ITO and J. FUJITA, "Preparation and Characterization of [Co (acetylacetonato) (diamine or 2, 2'-bipyridyl) (aminoalkylphosphine)]$^{2+}$. Crystal Structure of $(+)_{531}^{CD}$ - Λ - *fac*(N)-(Acetylacetonato)[(1*R*, 2*R*)-1, 2-cyclohexanedimaine] [(2-aminoethyl) diphenylphosphine] cobalt(III)perchlorate, $[Co(C_5H_7O_2)(C_6H_{14}N_2)(C_{14}H_{16}NP)](ClO_4)_2$", *Bull. Chem. Soc. Jpn.*, 58, 2247 (1985).

M. SAITO and H. KASHIWAGI, "*Ab initio* MO Study on Relationships between the Electronic State and Out-of-plane Displacement of the Iron Atom in Four-coordinate Fe-porphine", *J. Chem. Phys.*, 82, 848–855 (1985).

M. SAITO and H. KASHIWAGI, "*Ab initio* MO Study on Equilibrium Bond Distance between Fe and Pyridine in bis(pyridine) (porphinato)iron for Various Electronic States", *J. Chem. Phys.*, 82, 3716–3721 (1985).

I. YAMAZAKI, N. TAMAI, T. YAMAZAKI, M. MIMURO and Y. FUJITA, "Excitation Energy Transfer in Phycobilin-Chlorophyll a System of Algal Intact Cells", *Ultrafast Phenomena IV* (ed. D. H. Auston and K. B. Eisenthal) 490 (1984).

N. TAMAI, I. YAMAZAKI, H. MASUHARA and N. MATAGA, "Picosecond Time-Resolved Fluorescence Spectra of Liquid Crystal: Cyanooctyloxybiphenyl", *Ultrafast Phenomena IV* (ed. D. H. Auston and K. B. Eisenthal) 355 (1984).

N. TAMAI, T. YAMAZAKI, I. YAMAZAKI and N. MATAGA, "Diffusion Effect on Excitation Energy Transfer in Solution: Analyses by Means of Picosecond Time-Resolved Fluorimeter", *Chem. Phys. Letters*, 120, 24 (1985).

I. YAMAZAKI, M. MIMURO, N. TAMAI, T. YAMAZAKI and Y. FUJITA, "Picosecond Time-Resolved Fluorescence Spectra of Photosystems I and II Chlorella pyrenoidosa", *FEBS Letters*, 179, 65 (1985).

I. YAMAZAKI, N. TAMAI, H. KUME, H. TSUCHIYA and K. OBA, "Microchannel-Plate Photomultiplier Applicability to the Time-Correlated Photon-Counting Method", *Rev. Sci. Instrum.*, 56, 1187 (1985).

M. MIMURO, I. YAMAZAKI, T. YAMAZAKI and Y. FUJITA, "Excitation Energy Transfer in the Chromatically

Adapted Phycobilin Systems of Blue-Green Algae: Difference in the Energy Transfer Kinetics at Phycocyanin Level", *Photochem. Photobiol.* **41**, 597 (1985).

I. HATTA, Y. NAGAI, N. TAMAI and I. YAMAZAKI, "Two Kinds of State in the Smectic Ad Phase of Octyloxycyanobiphenyl (8OCB) and Octylcyanobiphenyl (8CB)", *Mol. Cryst. Liq. Cryst.*, **123**, 295 (1985).

Y. TANIGUCHI, M. MITSUYA, N. TAMAI, I. YAMAZAKI and H. MASUHARA, "Time- and Depth-Resolved Fluorescence Spectra of Layered Organic Films Prepared by Vacuum-Deposition", *J. Colloid Interface Sci.*, **104**, 596 (1985).

A. FUJIMOTO, J. NAKAMURA, I. YAMAZAKI, T. MURAO and K. INUZUKA, "Proton Transfer in the Excited State of 1- and 2-Methyl-4-amino-5H-[1] benzopyrano [3, 4-c] pyridin-5-one Dimers and Complexes", *Bull. Chem. Soc. Japan*, **58**, 88 (1985).

T. YAGI, K. KIMURA and H. INOKUCHI, "Analysis of the Active Center of Hydrogenase from *Desulfovibrio vulgaris* Miyazaki by Magnetic Measurements", *J. Biochem.*, **97**, 181 (1985).

K. KIMURA, S. NAKAJIMA, K. NIKI and H. INOKUCHI, "Determination of Formal Potentials of Multihemo-protein, Cytochrome c_3 by ^{1}H Nuclear Magnetic Resonance", *Bull. Chem. Soc. Jpn.*, **58**, 1010 (1985).

K. KIMURA, H. INOKUCHI, H. NANAMI and T. YAGI, "Magnetic Susceptibility of Hydrogenase from *Desulfovibrio vulgaris*", *J. Biochem.*, **97**, 1831 (1985).

S. SAKO and K. KIMURA, "Size Effect in CESR of Magnesium and Calcium Small Particles". *Surf. Sci.*, **156**, 511 (1985).

K. KIMURA, S. BANDOW and S. SAKO, "Magnetic Susceptibilities of Small Particles of Magnesium and Beryllium" *Surf. Sci.*, **156**, *883 (1985).*

S. BANDOW and K. KIMURA, "Dispersibility and Electron Spin Resonance in the Colloidal System of Metal/Organic Solvent Prepared by Means of Gas Evaporation Technique", *Nippon Kagaku Kaishi*, 1360 (1985).

G. ROTH, A. CHAIKEN, T. ENOKI, N.C. YEH, G. DRESSELHAUS and P.M. TEDROW, "Enhanced Superconductivity in Hydrogenated Potassium-Mercury-Graphite Intercalation Compounds.", *Phys. Rev.* **B32**, 533 (1985).

T. ENOKI, M. SANO and H. INOKUCHI, "Low-Temperature Specific Heat of Hydrogen-Chemisorbed Graphite-Alkali Metal Intercalation Compounds", *Phys. Rev.*, **B32**, 2497 (1985).

R. NOYORI and H. TAKAYA, "Binaphthyls: The Beauty and Chiral Uses," *Chemica Scripta*, **25**, 83 (1985).

S. INOUE, M. OSADA, K. KOYANO, H. TAKAYA and R. NOYORI, "Asymmetric Hydrogenation of Geraniol and Nerol Catalyzed by BINAP—Rhodium(I) Complexes", *Chem. Lett.*, 1007 (1985).

K. MASHIMA and H. TAKAYA, "Stable Titanacyclopentanes: Isolation, Characterization, and Reaction of 5, 5-Bis(pentamethylcyclopentadienyl)-5-titanaspiro [2.4] heptanes Derived from $(\eta^5\text{-}C_5Me_5)_2Ti(CH_2{=}CH_2)$ and Methylenecyclopropanes," *Organometallics*, 4, 1464 (1985).

Y. WADA, T. MITANI, M. YAMASHITA and T. KODA, "Charge Transfer Exciton in Harogen-Bridged Mixed-Valent Pt and Pd Complexes: Analysis Based on the Peiels-Hubbard Model", *J. Phys. Soc. Jpn.*, **54**, 3134 (1985).

Y. TOKURA, Y. KANEKO, H. OKAMOTO, S. TANUMA, T. KODA, T. MITANI and G. SAITO, "Spectroscopic Study of the Neutral-to-Ionic Phase Transition in TTF-Chloranil", *Mol. Cryst. Liq. Cryst.*, **125**, 71 (1985).

M. YAMASHITA, I. MURASE, T. ITO, Y. WADA, T. MITANI and I. IKEMOTO, "X-Ray Photoelectron Spectra and Electrical Conductivities of One-Dimensional Halogen-Bridged Pd(II)–Pt(IV) and Ni(II)–Pt(IV) Mixed-Valence Complexes", *Bull. Chem. Soc. Jpn.*, **58**, 2336 (1985).

Y. TAKAGI, M. SUMITANI, N. NAKASHIMA and K. YOSHIHARA, "Efficient Generation of Picosecond Coherent Tunable Radiation between 190 and 212 nm by Sum-Frequency Mixing from Raman and Optical Parametric Radiations", *IEEE J. Quantum Electron.*, **QE-21**, 193 (1985).

Y. TAKAGI, "Direct Measurement of Optical Spin Orientation in the Excited Triplet State of Aromatic Hydrocarbons at Room Temperature", *Chem. Phys. Lett.*, **119**, 5 (1985).

Y. TAKAGI, Y. FUKUDA and T. HASHI, "Optical Spin Orientation in Ruby by Zeeman-Selective U-Band

Absorption", *Opt. Commun.*, **55**, 115 (1985).

T. KASUGA, H. YONEHARA, T. KINOSHITA and M. HASUMOTO, "Ion-Trapping Effect in UVSOR Storage Ring", *J.J.A.P.*, **24**, 1212 (1985).

Review Articles and Textbooks

C. SATOKO, "Application of Force Analysis to Interactions between Oxygen Atoms and Surface Atoms on the Al(111) and Mg(0001) Surfaces", *Solid-State Sciences*, **59** edited by A. Yoshimori and M. Tsukada, Springer-Verlag, pp.104–112 (1985).

C. SATOKO, "Electronic Structure of Microclusters", *Solid-State-Physics* (in Jpanese), Vol. 19, 705 (1984).

K. NISHIMOTO, "Ab initio MO study of the Redox Function of Flavin", in "Biomolecules-Electronic Aspects", C. Nagata et al. Ed., Japan Sci. Soc. Press, Tokyo, pp. 9–19 (1985).

S. KAWAGUCHI and K. NISHIMOTO, "Introduction to Physical Chemistry", Kagakudojin, Kyoto, 1985.

E. HIROTA, "Rotational Isomerism as a Dynamical Molecular Process.", *J. Mol. Structure*, **126**, 25 (1985).

E. HIROTA, "Infrared Laser Kinetic Spectroscopy.", *Chemistry* (in Japanese), **40**, 408 (1985).

E. HIROTA, "High-Resolution Spectroscopy of Transient Molecules.", Springer, Heidelberg, 1985.

E. HIROTA, "Microwave Spectroscopy of Isotope-Substituted Nonpolar Molecules.", in "Molecular Spectroscopy: Modern Research.", Vol. III, K. Narahari Rao ed., Academic Press, Florida, 1985, pp.297–319.

H. SUZUKI, M. OHISHI, M. MORIMOTO, N. KAIFU, P. FRIBERG, W.M. IRVINE, H.E. MATHEWS, and S. SAITO, "Recent Observations of Organic Molecules in Nearby Cold, Dark Interstellar Clouds.", *Proc. IAU Symp.*, 112 (1985).

T. KITAGAWA, "Resonance Raman Study on Enzyme-Substrate Interactions of Heme- and Flavo-enzymes" in "Biomolecules, Electronic Aspects" C Nagata, M. Hatano, J. Tanaka and H. Suzuki eds. Japan Sci. Soc. Press/Elsevier, Amsterdam pp.205–223 (1985).

K. YOSHIHARA, "Energy Redistribution and Chemical Transformation in Isolated S_1 Benzene", *Prog. Chem. Chem. Indust. (in Korean)*, **24**, 675 (1984).

T. SAKATA, "Organic Synthesis with Photocatalysts", *Denki Kagaku* (in Japanese), **53**, 15 (1985).

K. SEKI, "Electronic Energy Structure of Aromatic Rings in Polymers", *Kobunshi* (in Japanese), **33**, 773 (1984).

I. KOYANO, K. TANAKA and T. KATO, "State Selected Ion-Molecule Reactions" (in Japanese) *Mass Spectros.* **32**, 397R (1984).

K. TANAKA, T. KATO and I. KOYANO, "State Selected Ion-Molecule Reactions: Low Energy Charge-Transfer Reactions" (in Japanese) *Mass Spectros.* **32**, 401R (1984).

I. KOYANO and H. INOKUCHI, "Studies in Molecular Science Using Extreme Ultraviolet" (in Japanese) *SUT Bulletin*, 2, 35 (1985).

K. KIMURA, "Ionization Photoelectron Spectroscopy for Excited-State Atoms and Molecules", in "Multiphoton Processes" ed. by P. Lambropoulos and S. J. Smith, Springer-Velag, Berlin, p. 164 (1984).

Y. MARUYAMA, "Black Phosphorus and Its Intercalation Compounds.", *Physics*, (in Japanese), **6**, No. 8 (1985).

H. IWAMURA, "Molecular Design of Correlated Internal Rotation", *J. Mol. Structure*, **126**, 401 (1985).

S. TERO-KUBOTA, Y. IKEGAMI and M. NAKANO, "Spin Trapping of Active Oxygen Radicals for Medical and Biological Scientists", *Japanese J. Inflamation* (in Japanese) **5**, 3 (1985).

H. KASHIWAGI, "Expectation of Supercomputer in Molecular Science" (in Japanese), Johoshori, Vol. 26, No. 1, 57–58 (1985).

H. KASHIWAGI and M. SAITO, "Ligand Bonds in Metal Complexes from the Viewpoint of Molecular Orbital Theory—Existence of Higher Animals Depends on the Electronic Configuration of Fe Ion—" (in Japanese), Kagakuzokan, **106**, 205 (Kagakudozin, 1985).

H. KASHIWAGI, "Oxidation State and Electron Distribution in Fe-Porphyrin Complexes", pp.31–50 (Biomolecules—Electronic Aspects—, Chikayoshi Nagata et al. eds. Japan Sci. Soc. Press, Tokyo/Elsevier,

Amsterdam, 1985).
T. ENOKI, H. INOKUCHI and M. SANO, "Hydrogen Absorption in Graphite-Alkali-Metal Intercalation Compounds.", *Kotai Butsuri* (in Japanese) **20**, 405 (1985).
I. YAMAZAKI, H. KUME, N. TAMAI, H. TSUCHIYA and K. OBA, "Microchannel-Plate Photomultiplier and Its Application to the Time-Correlated Single-Photon Counting Method", *Oyo Butsuri.*, **54**, 702 (1985).
H. MASUHARA, Y. TANIGUCHI and I. YAMAZAKI, "Characterization of Organic Thin Films by Means of Fluorescence Spectroscopy", *Zairyo Gijutu*, **3**, 40 (1985).
K. KIMURA, "The Preparation of Metal Ultrafine Particles and the Surface State in the Light of Magnetic Properties", *Hyoumen* (in Japanese), **22**, 613 (1984).
K. KIMURA, "The Solid State Properties and the Function of Ultrafine Particles", *Kagaku to Kogyo* (in Japanese), **38**, 760 (1985).
G. SAXON, "Free Electron Lasers – A Survey", *Rev. Laser Eng.* **13**, 398 (1985).
M. WATANABE, H. KITAMURA and M. KIHARA, "Synchrotron Light Source", *Physics Monthly* (in Japanese) **5**, 711 (1984).
K. SAKAI and M. WATANABE, "Vacuum System of UVSOR", *Ionics* (in Japanese) **11**, 109 (1985).

Institute for Molecular Science, Myodaiji, Okazaki 444, Japan